Crosstalk Between Transforming Growth Factor-Beta And Wnt Signalling Pathways In Dermal Fibroblasts

Justin Gillespie

Submitted in accordance with the requirements for the degree of Doctor of Philosophy

The University of Leeds
School of Medicine and Health

January 2015

The candidate confirms that the work submitted is his own and that appropriate credit has been given where reference has been made to the work of others.

Acknowledgements

I would like to thank Ass. Prof. Francesco Del Galdo for the opportunity to undertake a part-time PhD in his lab as apart of my post. I would also like to thank my co-supervisors Prof. Michael M. McDermott and Dr. Gina Doody. As a late edition to my supervisory team, Gina's discussions with me helped make the project more exciting towards the end of my study. I would like to express my gratitude to those involved within the wider remit of my studies including Dr. Elena Jones, Dr. Ai Lyn Tan and Dr. Thomas Hughes. As part of this work I acknowledge Prof. Christopher Denton and Dr. Emma Derrett-Smith for their contribution as external collaborators. Thanks are also due to everybody who took an interest in this work at national/international conferences or as part of an article submission review process, which opened up much needed critical discussion of the work. I would like to express my sincere gratitude towards Prof. Graham Cook and Prof. David Abraham both of who have agreed to be my independent assessors prior to the submission of this thesis.

Thanks to Sarah Kreuz who, apart from being an understanding friend, provided helpful scientific discussions and support. A special thanks to my dear friends Sheetal, Katie, Kostas, Ula, Jamie, Annemarie, Orla, Giusy, Kasia, James, Ruth and Penelope, without whom this process would have been a lot harder and a lot less interesting.

Finally I would like to thank my parents who have supported me through my studies.

Abstract

Activation of the transforming growth factor-beta (TGFβ) and Wnt/β-catenin signalling pathways have been linked to the pathogenesis of tissue fibrosis in systemic sclerosis (SSc) and crosstalk between the pathways is considered to be significant. Indeed, TGFβ upregulated secreted frizzled-related protein 4 (SFRP4), a putative Wnt signalling antagonist; however, rhSFRP4 had no regulatory effects upon Wnt/TGFβ signalling in dermal fibroblasts from healthy control (HC) or SSc patients. This was irrespective of caveolin-1 (CAV-1) expression, an important component of caveolae, which is known to selectively regulate receptor-mediated signalling potential. Primarily, SSc fibroblasts displayed an inherent increase in responsiveness to canonical Wnt activation compared to HC. Consistently, the basal expression of AXIN2, a primary target and critical regulator of the canonical Wnt signalling pathway, was reduced in SSc fibroblasts. TGFβ was able to induce a quantitatively similar reduction in AXIN2 expression in HC fibroblasts that was initially mediated by an increase in the rate of mRNA decay. Concurrently, decreased Axin-2 expression was also evident in the TβRIIΔk-fib transgenic mouse model, which has a constitutive and fibroblast-specific activation of the TGFβ signalling pathway. Functional studies demonstrated that TGFβ-primed HC fibroblasts displayed an enhanced canonical Wnt signalling amplitude equivalent to that of SSc fibroblasts. Mechanistically, gain or loss of AXIN2 bioavailability suppressed or reproduced the TGFβ-mediated increase in canonical Wnt signalling amplitude, respectively.

Overall, this study demonstrates that TGFβ signalling can sensitise

fibroblasts to canonical Wnt signalling through AXIN2 depletion and reproduce the activation observed in SSc fibroblasts. However, this did not lead to the profibrotic activation of fibroblasts in two independent models of canonical Wnt signalling hyperactivation. Therefore further evaluation of processes associated with fibrosis including proliferation, migration and cell survival, might resolve the anti-fibrotic outcomes observed for therapeutics targeting the Wnt/β-catenin pathway in models of experimental fibrosis.

Table of contents

List of tables

List of figures

Abbreviations

3′UTR	3′ untranslated region
ACA	Anti-centromere antibodies
ACE	Angiotensin-converting enzyme
ACR	American College of Rheumatology
AII	Angiotensin II
AKT	Protein kinase B
ANA	Anti-nuclear antibody
AP-1	Activator protein-1
APC	Adenomatous polyposis coli
ARE	Adenosine and uridine (AU)-rich elements
AUF1	AU-rich element RNA-binding protein 1
BCA	Bicinchoninic acid
BMP	Bone morphogenetic proteins
BSA	Bovine serum albumin
CAMKII	Calmodulin-dependent protein kinase II
CAV-1	Caveolin-1
CBP	CREB-binding protein
CK1	Casein kinase-1
CN	Calcineurin
Co-SMAD	Common-SMAD
CO_2	Carbon dioxide
COX-2	Cyclooxegenase-2
CRD	Cysteine rich domain
CREB	C-AMP-responsive element binding protein

CSD	Caveolin scaffolding domain
CTGF	Connective tissue growth factor
DACT	Dapper
DAG	1,2-diacylglycerol
DAMPs	Damage associated molecular patterns
DAPI	4', 6-diamidino-2-phenylindole
dcSSc	Diffuse cutaneous systemic sclerosis
DKK	Dickopff proteins
DMEM	Dubecco’s Modified Eagle’s Medium
DNA	Deoxyribonucleic acid
Dvl	Dishevelled
DZ	Dizygotic
ECM	Extracellular matrix
ED-A	Extradomain A
EEA-1	Early endosome antigen 1
ER	Endoplasmic reticulum
ERK	Extracellular signal-regulated kinase
ET-1	Endothelin-1
FGF	Fibroblast Growth Factor 5
Fz	Frizzled receptor
GDFs	Growth and differentiation factors
GSK-3β	Glycogen synthase kinase-3β
HC	Healthy control
HPRT1	Hypoxanthine phosphoribosyltransferase 1
HRP	Horseradish peroxidase enzyme
hTERT	Human telomerase reverse transcriptase
I-SMADS	Inhibitory SMADS

IDF	Integrated density of fluorescence
IL-1	Interleukin
ILD	Interstitial lung disease
IP3	Inositol 1,4,5-triphosphate
JNK	JUN N-terminal kinase
LAP	Latency associated peptide
lcSSc	Limited cutaneous systemic sclerosis
LDS	Lithium dodecyl sulfate
LLC	Large latent complex
LRP-6	Low-density lipoprotein receptor-related protein-6
LTBP	Latent TGFβ binding protein
m7G	7-methylguanosine cap
MEK	Mitogen-activated protein kinase
MHC	Major histocompatibility complex
MKK	MAP kinase kinases
MMPs	Matrix metaloproteinases
mRSS	Modified Rodnan skin score
MTT	(3-(4,5-Dimethylthiazol-2-yl)-2,5-Diphenyltetrazolium Bromide)
MZ	Monozygotic
NF-κB	Nuclear factor kappa-beta
NFAT	Nuclear factor of activated T cells
NLS	Nuclear localisation signal
NTR	Netrin-like domains
OCP	Optic cup periphery
P38 MAPK	P38 mitogen-activated protein kinase
PABP	Poly(A)-binding protein
PAH	Pulmonary arterial hypertension

PBS	Phosphate buffered saline
PCOLCES	Type I procollagen C-proteinase enhancer proteins
PCP	Planar-cell-polarity
PDGF	Platelet-derived growth factor
PI3K	Phosphoinositide-3-kinase
PKC	Protein kinase-C
PLC	Phospholipase-C
POL	Polymerase
poly(A)	Polyadenosine
PORCN	Porcupine
PVDF	Polyvinylidene difluoride membrane
qRT-PCR	Quantitative real-time polymerase chain reaction
R-SMADS	Receptor-regulated SMADS
RGS	Regulators of G-protein signalling domain
RNA	Ribonucleic acid
ROR	Receptor tyrosine kinase-like orphan receptor
ROS	Reactive oxygen species
RYK	Receptor tryrosine kinase
SBE	SMAD binding element
Scl-GVHD	Sclerodermoid graft versus host disease
SFRP	Secreted frizzled-related protein
SNP	Single nucleotide polymorphism
SRC	Scleroderma renal crisis
SSc	Systemic sclerosis
TAK1	TGFβ-activated kinase 1
TGFβ	Transforming growth factor-beta
TIMP-1	Tissue inhibitor of metalloproteinase-1

TNF	Tumour necrosis factor
TNFRSF12A	Tumour Necrosis Factor Receptor Superfamily member 12A
TRAF	TNF receptor-associated factor 4
TRIP	TRAF interacting protein
TTP-1	Tristetraprolin
TβRI	Type I serine-threonine receptor kinase
TβRII	Type II serine-threonine receptor kinases
VEGF	Vascular endothelial growth factor
VSMC	Vascular smooth muscle cells
WIF-1	Wnt inhibitory factor-1
WT	Wild-type
ZFP36	Zinc finger protein 36 homolog
α-SMA	Alpha-smooth muscle actin
β-TRCP	Beta-transducin repeat-containing protein

1 Introduction

1.1 Systemic sclerosis

Systemic sclerosis (SSc) is a rare and highly heterogeneous disease that affects between 75,000–100,000 individuals in the United States (Varga & Abraham, 2007). The etiology of the disease includes autoimmunity, inflammation, vasculopathy (blood vessel damage and reduced capillary density that leads to decreased blood flow and impaired tissue oxygenation) and fibrosis through excessive synthesis and deposition of collagens and other extracellular matrix (ECM) proteins (Varga & Abraham, 2007; Katsumoto et al., 2011).

A number of clinical disease classifications have been proposed to better define SSc patient subsets, including SSc sine scleroderma (no skin involvement), limited (skin tightness distal to metacarpophalangeal joints), intermediate (skin tightness affecting whole arm, but no involvement of the trunk) and diffuse (skin tightness involving both extremities and trunk) (van den Hoogen et al., 2013). A revised classification in 2013 was reached, through a collaborative effort by members of the ACR and EULAR, which included standardised criteria for disease classification such as skin thickening, fingertip lesions, telangiectasia, nailfold capillary abnormalities, Raynaud's phenomenon, SSc-specific autoantibodies (anti-topoisomerase I, anti-centromere, anti-RNA polymerase III), interstitial lung disease and pulmonary arterial hyperptension (van den Hoogen et al., 2013).

1.2 SSc pathology

1.2.1 Skin

SSc patients are commonly divided into two key clinical subsets according to their level of skin involvement; the limited cutaneous subset (lcSSc) and the diffuse cutaneous subset (dcSSc) (LeRoy et al., 1988). The former is characterised by a skin involvement proximal to elbows and knees, affecting the trunk whereas the lcSSc subset has skin involvement that is limited to the distal extremities and face (Eisenberg et al., 2008). Additionally, the lcSSc subset is characterised by prominent vasculopathy whereas the dcSSc subset is associated with a higher risk of internal organ fibrosis. Indeed, the dcSSc subset is most active within the first 3 years from onset, and within this time severe complications in the lung, kidney and heart can develop (Quillinan & Denton, 2009). Skin thickening in this subset is often preceded by hyperpigmentation, giving a pathognomonic ‘salt and pepper’ appearance. During the fibrotic phase, the skin becomes more thickened, losing its elasticity, hair follicles and sweat glands. This stage can be followed by a clinical resolution as a result of skin atrophy, which typically softens the skin but does not completely recover its elasticity or lost annexes (Eisenberg et al., 2008).

Clinically, skin involvement is readily detectable and quantified by physicians using the modified Rodnan skin score (mRSS). This method was first described in 1979, and takes into account 17 skin areas (Rodnan et al., 1979). These areas are pinched between two fingers and scored from 0 (no thickening) to 3 (severe thickening) up to a maximum score of 51 (Rodnan et al., 1979). While this method suffers from a certain amount of inter-observer

variability, it is a sufficient reflection of diffuse cutaneous disease severity owing to the fact that patient survival has been directly correlated to the level of skin involvement (Steen & Medsger, 2001). Indeed, patients with a high first year mRSS (≥35) showing no improvement clinical improvement had an increased mortality compared to those with a low first year mRSS that showed improvement (Shand et al., 2007). Early lesional skin from SSc patients show inflammatory infiltrates that include T-cells B cells and monocytes, which indicates that both innate and adaptive immune cells could likely play a role in the establishment of fibrosis through cytokine, growth factor and autoantibody production (Gabrielli et al., 2009). Nonetheless, dermal fibroblasts are the key cellular elements responsible for the increased accumulation of the ECM, which can alter in composition over the course of the disease. Fibrillin is a matrix protein that is typically present in the early stages of disease, whereas collagen I, III, V and VII are observed in the reticular dermis of lesional skin in the later stages of disease (Wei et al., 2011). Ultimately, fibrosis of the internal organs can lead to loss of function and if not treated can be life threatening. Aside from mortality, the thickening and rigidity of the skin can be severely debilitating, particularly on the hands and over the joints.

1.2.2 Raynaud’s phenomenon

Raynaud's phenomenon is characterised by an excessive reduction in blood flow to the extremities due to vasospasms (Block & Sequeira, 2001). This is typically brought on by vasoconstriction, which can be triggered by the exposure to cold and stress. Primary Raynaud’s phenomenon presents in the absence of an underlying illness, whereas secondary Raynaud’s

phenomenon occurs in the context of an underlying condition like SSc. Raynaud's phenomenon is thought to occur in more than 90% of patients with SSc and can precede or coincide with other manifestations (Gabrielli et al., 2009). There is also a strong correlation with the presence of anti-centromere antibodies (ACA) that could potentially be used to predict the onset of lcSSc (Gabrielli et al., 2009).

1.2.3 Pulmonary

Pulmonary manifestations of SSc include interstitial lung disease (ILD) and pulmonary arterial hypertension (PAH), which together account for approximately 50% of all SSc-related mortality (Williams et al., 2006); Winstone et al., 2014; Rubio-Rivas et al., 2014). Despite the prognosis of patients affected by PAH, it can presently be improved by mediators of vasodilation such as endothelin-1 antagonists and PDE5 inhibitors (Buckley et al., 2013).

ILD is an umbrella term for several disease subtypes that affect normal lung function, which includes interstitial pneumonitis, interstitial pneumonitis and idiopathic pulmonary fibrosis. No treatment has yet been proven to be effective in modifying the course of ILD. In SSc, the pulmonary function tests can measure both a reduction in the lung capacity or a reduction in the % diffusing capacity for carbon monoxide (%DLCO) that can indicate the presence of ILD and PAH, respectively. ILD and the early inflammatory phase preceding it are commonly detected as a “ground-glass” appearance following high-resolution computed tomography (Williams et al., 2006). ACA can be detected in 70-80% of patients with lcSSc and is associated with a

high risk of PAH, whereas anti-RNA-POL II antibodies and anti-topoisomerase antibodies are associated with increase risk of developing ILD (Gabrielli et al., 2009). Mortality is often associated with right-heart failure as a result of the increased pulmonary vascular resistance and poor DLCO.

1.2.4 Renal

Scleroderma renal crisis (SRC) is characterised by hypertension, hyperreninemia, proteinuria and haematuria that occurs in an estimated 5-10% of SSc patients. Of these, approximately 66% of SSc patients develop SRC within 1 year of diagnosis, rising to ~86% at 4 years and mortality at 5 years is ~30–40% (Denton et al., 2009). In 60% of SCR patients there was a strong correlation with anti-nuclear antibody (ANA) positivity (Denton et al., 2009). Indeed, patients with dcSSc and anti-RNA Pol II antibodies have the highest risk of developing SRC, whereas lcSSc patients may develop SRC later during the course of the disease (Penn et al., 2007). Between 40–66% of SRC patients may never recover normal renal function and some may require chronic dialysis in lieu of renal transplantation (Denton et al., 2009). Both anti-hypertensives and the aggressive use of angiotensin-converting enzyme (ACE) inhibitors to control blood pressure are effective treatments in the majority of cases if diagnosed early (Denton et al., 2009; Eisenberg et al., 2008).

1.2.5 Autoantibodies

The role of ANA in SSc disease pathogenesis is unknown; however, they are key predictors of disease severity, organ involvement and survival in SSc patients, which are currently used as disease biomarkers. There are three major subclasses of specific antinuclear autoantibodies in SSc that have a high specificity compared to HC patients and other connective tissue diseases, which are anti-centromere antibodies, anti–topoisomerase 1 (Scl-70) antibodies and anti–RNA polymerase III antibodies (anti-RNAP) (Nihtyanova & Denton, 2010). Anti-centromere antibodies (ACA) are observed in approximately 70% of lcSSc, while Scl-70 antibodies are observed in approximately 20% of dcSSc patients and anti–RNA polymerase III antibodies are also found in approximately 20% of dcSSc patients (Ho & Reveille, 2003; Katsumoto et al., 2011). The concurrent presence of both ACA and Scl-70 in patients is less than 0.5% and are therefore considered to be exclusive of lcSSc and dcSSc, respectively (Ho & Reveille., 2003). More recent reports have demonstrated that SSc patients with anti-RNAP antibodies were at a higher risk of developing malignancies (Moinzadeh et al., 2014; Joseph et al., 2014). In a subset of anti-RNAP positive patients, somatic mutations of the *POLR3A* locus might be responsible for the initiation of the immune response toward RNAP where the resultant antibodies fail to discriminate between mutant and WT proteins (Joseph et al., 2014).

1.2.6 Genetic factors

SSc is not inherited in a classical Mendelian pattern, although several studies have concluded that genetic risk factors could predispose individuals

to the onset of SSc. A large twin study evaluated 24 monozygotic (MZ) and 18 dizygotic (DZ) twins and found a low concordance rate of 4.7% for SSc. The concordance rates were also found to be the same for both MZ (4.2%) and DZ pairs (5.6%) with a final heritability factor of 0.008 (Feghali-Bostwick et al., 2003). Risk factors include an enrichment of gene single nucleotide polymorphisms (SNPs) in SSc patients, which could confer a predisposition to autoimmunity as many of the identified SNPs are also present in other autoimmune diseases, particularly connective tissue diseases (Gregersen & Behrens., 2006). A large GWAS study in 2010 was used to investigate SSc susceptibility in a Caucasian population with a total of 2296 SSc patients and 5171 controls, which confirmed previous reports identifying SNPs in major histocompatibility complex (MHC) (HLA*DQB1 highest hit rate), STAT4 and IRF5 genes as important predictors of SSc susceptibility (Radstake et al., 2010). Indeed, the association of multiple genetic risk factors may play a role in the breakdown of auto-antigen tolerance and the onset of autoimmunity.

1.2.7 Gene expression profiling

Genome-wide gene expression profiling using DNA microarrays have provided additional insights into the differences between HC and dcSSc skin but might also have a utility in directing the treatment course (Whitfield et al., 2003; Gilbane et al., 2013). Adding to the evidence for the role of TGFβ in SSc, a TGFβ-responsive gene signature can be found in skin biopsies from a subset of dcSSc patients (Sargent et al., 2009). Indeed, microarray analysis can now be used to identify distinct subsets patterns of gene expression and these signatures have been used to describe novel, process driven disease subsets in SSc (Milano et al., 2008). Indeed, on the basis of

proliferative, inflammatory and fibrotic gene expression signatures, three distinct subsets can be identified within dcSSc patients and two within lcSSc patients (Milano et al., 2008). Out of a group of 995 genes consistently expressed across different skin biopsies from SSc patients, 177 genes were found to be associated with the severity of skin disease and correlated with the mRSS in dcSSc patients. Of these genes, *Wif-1* showed low expression while those with high expression included the cell cycle genes *CENPE*, *CDC7* and *CDT1*, *Fibroblast Growth Factor 5* (*FGF5*), *Tumour Necrosis Factor Receptor Superfamily member 12A* (*TNFRSF12A*) and *TRAF interacting protein* (*TRIP*). The use of gene expression profiling has already considerably expanded our understanding of the complexity of SSc and promises to remain a powerful research and diagnostic tool for the disease.

1.2.8 Environmental factors

Environmental challenges (e.g. viruses, drugs, vinyl chloride, epoxy resins, rapeseed oil, gadolinium-based contrast agent and silica) may be a predisposing factor in SSc disease pathogenesis. As an example, silica dust has been well described to be a risk factor for many systemic autoimmune diseases including rheumatoid arthritis, SSc and systemic lupus erythematosus (Gold et al., 2007). As far back as 1967, it was reported that occupational exposure to silica (mainly men) showed a higher than average prevalence of SSc, compared to the general population (Rodnan et al., 1967). Although the exact mechanisms involved are not understood, silica exposure does initiate an inflammatory phenotype and leads to an increased ANA production in humans and in mice (Pfau et al., 2014). Indeed, these

changes increase the risk of autoimmune disease and in mice it was also shown to accelerate the course of systemic autoimmune disease in a lupus-prone strain (Brown et al., 2003). More recently, environmental factors could play a role in the somatic mutation of the *POLR3A* locus, which was associated with the initiation of the immune response to RNAP (Joseph et al., 2014). Both prevalence studies and animal models suggest that the environment may have an underestimated impact on SSc disease pathogenesis.

1.2.9 Scl-GVHD

A widely accepted model of immune-mediated skin fibrosis is chronic sclerodermoid graft versus host disease (Scl-GVHD), a rare form of chronic GVHD that occurs in some patients following the rejection of allogenic bone marrow transplantation (Martires et al., 2011). Indeed, the Scl-GVHD model has been shown to recapitulate the histological and serological features of SSc including skin thickening, lung fibrosis and inflammatory infiltrates (Artlett et al., 1997; Beyer et al., 2010). Therefore it has been used as a model to study the immunopathogenesis of tissue fibrosis and help in the identification of genes common to SSc and scl-GVHD. Initiation of GVHD could be driven by michrochimerism, which is a process were genetically distinct foetal and maternal lymphocytes can cross the placenta during pregnancy (Endo et al., 2002). Interestingly, allogeneic cells in both peripheral-blood and skin-biopsies have been detected in patients with SSc (Artlett et al., 1998). Over time, these foreign cells may become activated by a second event and the hosts may mount a GVHD reaction. At present, the

role of microchimerism in SSc pathogenesis remains undetermined and to some, controversial.

1.2.10 Vasculopathy

Fibroproliferative vasculopathy is a key morbidity factor in SSc with diverse presentation including Raynaud's phenomenon, cutaneous telangiectasia, nail fold capillary alterations, gastric antral vascular ectasia, pulmonary arterial hypertension and SRC. Paradoxically, several pro-angiogenic factors including PDGF, VEGF, ET-1 and TGFβ are upregulated in SSc (Abraham et al., 2009). Predominantly, vasculopathy occurs in the microvasculature; however, it can also manifest in the macrovasculature. Vessel rarefaction commonly affects the capillaries, whereas arterioles and small arteries may be involved in fibroproliferative intimal hyperplasia, which is a proliferation of myofibroblasts and vascular smooth muscle cells (VSMC) within the inner layer of the vessel (intima), usually comprised of one endothelial cell layer (Humbert et al., 2004). The combination of neointimal hyperplasia and capillary rarefaction is responsible for a reduced blood flow to organs, which can cause a chronic state of ischemia and likely contributes to fibrosis and progressive loss of organ function. Since vascular symptoms often precede the fibrotic manifestations, vascular injury is thought to precede the development of fibrosis and subsequently lead to the involvement of both autoimmune and proinflammatory processes (Varga & Abraham, 2007; Ho et al., 2014).

1.3 Fibrosis

Fibrosis is the fundamental characteristic of dcSSc that can occur in multiple organs and manifests as skin fibrosis, loss of esophageal function, collagenous colitis, ILD and impaired cardiac function. The key cellular elements of tissue fibrosis are fibroblasts; mesenchymal cells, which display a spindle-shaped morphology and are instrumental in the development of fibrosis (Gilbane et al., 2013). Fibroblasts are responsible for the continued maintenance of tissue architecture though the secretion of ECM that acts as a global scaffold and thus they have a ubiquitous organ distribution. Fibrosis develops through sustained fibroblasts activation by factors including cytokines as well as growth and angiogenic factors present in the tissue microenvironment (Kim et al., 2011). The uncontrolled activation of fibroblasts can lead to the excessive accumulation of ECM, which can affect normal organ homeostasis through profound changes in the tissue architecture but can also in advanced stages lead to the loss of blood vessels thereby increasing the risk of ischaemic injury. Currently, ILD, which includes idiopathic pulmonary fibrosis, is the leading cause of mortality in SSc patients (Steen & Medsger, 2001; Wells & Denton, 2014).

While therapies that target immunological, vascular and fibrotic processes are required for the effective treatment of SSc, the development of novel anti-fibrotic treatments may be considered a priority given the high risk of mortality associated with fibrosis through internal organ involvement. Although there are currently several clinical trials of targeted therapies underway, there are currently no treatments available that can lead to the remission of fibrosis (Ong & Denton, 2010).

1.3.1 Wound healing

Fibrogenesis is a component of the wound healing response, which is a multi-stage process involving the orchestration of many cells and cellular factors that that can be simplified into the inflammatory, proliferative and re-modelling phases.

Briefly, tissue injury elicits a wound healing response by exposing the underlying collagen, which leads to the activation of the clotting cascade and this results in conversion of the fibrinogen precursor into a fibrin clot (Broughton et al., 2006). In turn, this initiates the recruitment of inflammatory cells, which prime the microenvironment by releasing cytokines and growth factors such as interleukin (IL-1), tumour necrosis factor (TNF) and TGFβ, which are then concentrated by the scaffold of the clot (Eming et al., 2007). Fibroblasts then migrate into the wound site where they are exposed to the primed microenvironment (Broughton et al., 2006). These fibroblasts are further activated to proliferate, secrete and deposit ECM and can also differentiate into highly contractile and secretory myofibroblasts. Further, activated fibroblasts are known to upregulate TGFβ expression, which is fundamental in reproducing the hallmarks of fibrosis. The resolution of the resulting scar tissue usually occurs through myofibroblast apoptosis and revision of proteins in the ECM, such as collagen type III to collagen type I conversion (Klingberg et al., 2013).

In contrast with physiological wound healing, in which myofibroblasts are present only transiently, a key feature in fibrotic diseases is the persistence of myofibroblasts and subsequent fibrogenesis that occurs through ECM contraction, deposition and scarring (Gabbiani et al., 2003).

1.3.2 Extracellular matrix

The ECM is important for the regulation of both cellular function and tissue homeostasis in addition to its structural role (Lu et al., 2011; Cox & Erler, 2011). The ECM controls the distribution of cytokines, growth factors and angiogenic factors as well as providing biochemical and biomechanical cues to the cells it contacts (Kim et al., 2011). These cues have numerous cellular effects known to include cell proliferation, migration, survival and differentiation (Lukashev & Werb, 1998). Therefore, dysregulation of the ECM through mechanical stress, lysyl oxidase and matrix metalloproteinase expression can contribute toward the dysregulation of tissue homeostasis and be a causative factor in disease pathogenesis in fibrotic disorders, including SSc (Schaller, 2010). Indeed, fibrosis is characterised by the excessive deposition of secreted ECM components including collagens, elastins, hyaluronic acid, fibronectin, fibrillins and proteoglycans. Over time, these changes can lead to deleterious effects including matrix rigidity, hypoxia, oxidative stress and the following accumulation of damage associated molecular patterns (DAMPs) (Ho et al., 2014). As a consequence, the dysregulated remodelling of tissue architecture can lead to the loss of normal organ function.

1.3.3 Myofibroblasts

Myofibroblasts (Figure 1.1) are specialised cells that normally increase in number after tissue injury and are an essential component of wound healing owing to their highly contractile nature and increased capacity to secrete ECM (Hinz et al., 2001). The persistence of myofibroblasts in tissues is considered to be a characteristic of fibrotic disease pathology, including SSc

(Zhang & Phan, 1999). Indeed, myofibroblasts are consistently found in higher numbers in skin biopsies from SSc patients, particularly in the reticular dermis, and correlate directly with the mRSS (Farina et al., 2009). While it is known that myofibroblasts can be produced by the activation and the subsequent differentiation of resident fibroblasts, other potential sources include epithelial-to-mesenchymal transition, endothelial-to-mesenchymal transition, pericyte differentiation and the recruitment of circulating fibrocytes (Mori et al., 2005; Humphreys et al., 2010; Piera-Velazquez et al., 2011; LeBleu et al., 2013).

Myofibroblasts highly express ECM proteins including collagen I (composed of two A1(I) and one A2(I) chains); the major component of ECM, collagen III, fibronectin and hyaluronic acid, which are essential for the formation of scar tissue (Frantz et al., 2010). The differentiation of myofibroblasts is dependent on the growth factors present in the microenvironment, which can include platelet-derived growth factor (PDGF), angiotensin II (AII), connective tissue growth factor (CTGF), endothelin-1 (ET-1) and TGFβ (Leask, 2010). For terminal myofibroblast differentiation, fibroblasts first have to pass through the protomyofibroblast stage, requiring mechanical tension from the ECM, increased expression of the extradomain A (ED-A) variant of fibronectin and the formation of stress fibres from β-actin and γ-actin isoforms (Gabbiani, 2003; Hinz, 2010). Under these conditions myofibroblasts become a major source of TGFβ, which is a potent activator for terminal myofibroblast differentiation, in part by SMAD dependent signalling (Desmoulière et al., 1993; Gabbiani, 2003; Ho et al., 2014).

The terminal differentiation of myofibroblasts is characterised by the neo-expression of alpha smooth muscle actin (α-SMA), which is organised into highly contractile stress fibres that are essential for wound closure (Otranto et al., 2012). Hence, high α-SMA expression is routinely used as a marker for activated fibroblasts and the detection of differentiated myofibroblasts by either gene expression or stress fibre detection, respectively (Desmoulière et al., 1993; Hinz et al., 2007; Hinz, 2010).

Myofibroblasts are central in the pathology of tissue fibrosis and a better understanding of the mechanisms of myofibroblast production, inhibition and clearance is an important step for the development of targeted treatment strategies for SSc and other fibrotic diseases.

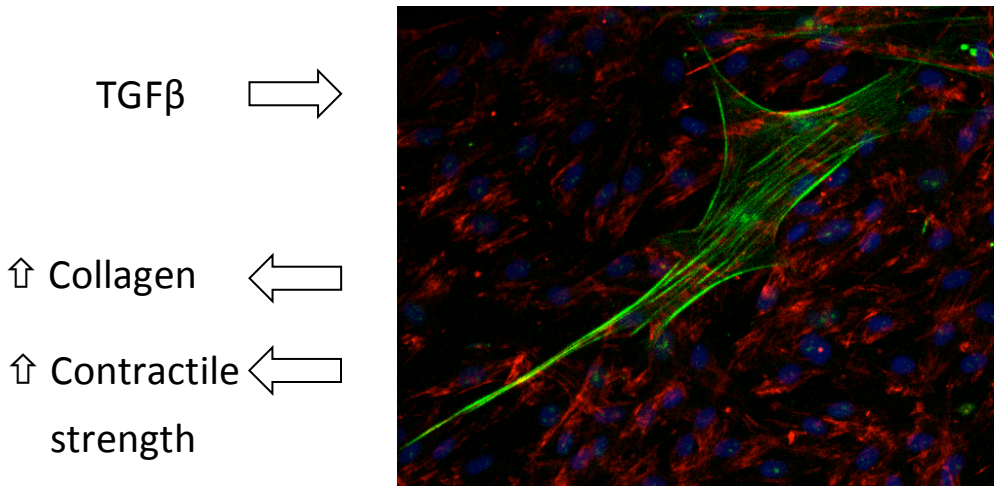

Figure 1.1. The myofibroblast

Activation of fibroblasts by extracellular factors, including TGFβ, can lead to the differentiation of a subset of fibroblasts into myofibroblasts. Myofibroblasts are characterised by the neo-expression of α-smooth muscle actin (α-SMA), which is recruited into contractile stress fibres (green staining) and concomitantly these fibroblasts exhibit an increase in mechanical force generation. Indeed, myofibroblasts are thought to persist in fibrotic diseases, including SSc. Furthermore, Caveolin-1 (CAV-1) (red staining), a key component of the caveolae endocytic pathway described to negatively regulate TGFβ signalling activity, is negative in the myofibroblast population but present in the remaining total fibroblast population and therefore may contribute to the pathogenesis of SSc (see chapter 1.5.4).

1.4 TGFβ superfamily

The transforming growth factor-beta (TGFβ) superfamily includes more than 30 members comprising TGFβ, bone morphogenetic proteins (BMPs), activin, inhibin and growth and differentiation factors (GDFs) (Akhurst & Hata, 2012). These factors are known to play key roles in development, tissue homeostasis, proliferation, differentiation, morphogenesis and wound healing (Beanes et al., 2003; Akhurst & Hata, 2012). Indeed, their roles can be opposed, for example TGFβ inhibits mesenchymal differentiation along the osteoblast, myoblast and adipocyte lineages, while BMPs are known to promote differentiation into adipocytes, osteoblasts and chondrocytes (Derynck & Akhurst, 2007).

There are three known isoforms of TGFβ expressed in mammalian tissues; TGFβ1, TGFβ2 and TGFβ3, which are known to signal through the same receptor pathway but have divergent signalling potential (Roberts & Sporn, 1992). TGFβ1, herein referred to as TGFβ, is the most characterised isoform and has a predominant role in mediating fibrosis (Yu et al., 2003; Ask et al., 2008). Indeed, TGFβ has an almost ubiquitous expression and is the focus of the majority of studies. However, during wound healing there is a spatial and temporal restriction of TGFβ isoforms (1-3), which suggests they may play distinct roles during the repair process (Levine et al., 1993). Unfortunately, TGFβ isoforms in relation to the pathogenesis of SSc is poorly described and therefore unclear whether individual isoforms play a unique role during the disease process.

1.4.1 TGFβ

TGFβ is synthesised as a precursor with an amino-terminal pro-domain termed latency associated peptide (LAP) and is required for both correct protein folding and subsequent homodimerisation. The TGFβ dimer is cleaved in the trans-Golgi apparatus by furin type enzymes, although the pro-peptide remains part of the complex through non-covalent interactions. A further large latent complex (LLC) is formed with latent TGFβ binding proteins (LTBP) that targets it to the ECM whereupon it is stored in this inactive state (Shi et al., 2011). The release of biologically active TGFβ requires dissociation of the LLC from the ECM and the proteolytic cleavage of LAP. This process can be carried out by matrix metaloproteinases (MMPs), pH, reactive oxygen species (ROS), thrombospondin-1 or mechanical stress mediated by the αVβ6 integrin (Massagué et al., 2005; Akhurst & Hata., 2012).

1.4.1.1 TGFβ signalling

The TGFβ signalling pathway is activated when extracellular TGFβ binds to the type II serine-threonine receptor kinase (TβRII), which heterodimerises with the type I receptor kinase (TβRI) and phosphorylates the TTSGSGSG motif within its juxtamembrane domain. Intracellular signalling is propagated via a number of intermediaries including SMADs, MAP Kinase Kinases (MKK), phosphoinositide 3-kinase (PI3K), AKT, c-Jun N-terminal kinase (JNK) and p38 mitogen-activated protein kinases (Huang & Chen, 2012).

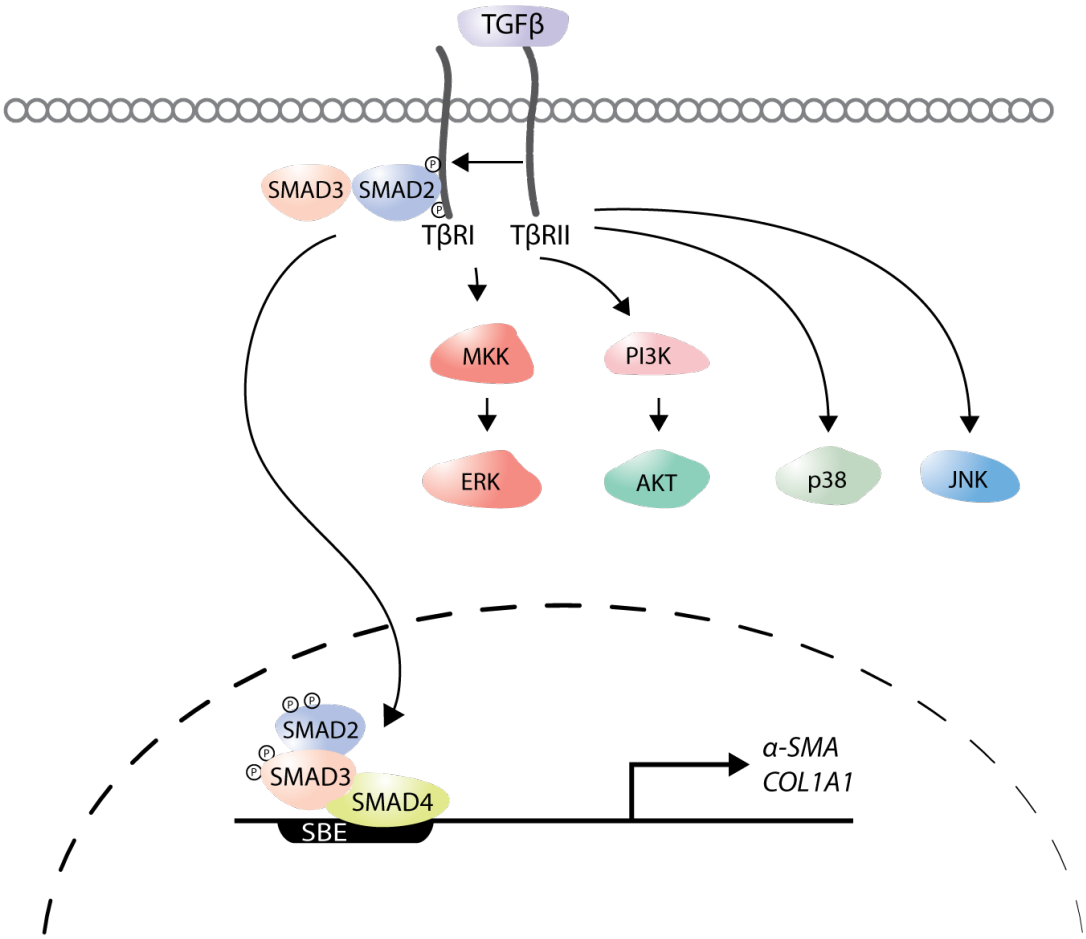

Figure 1.2 The TGFβ signalling pathway

Transforming growth factor-beta (TGFβ) signalling can play a critical role in the regulation of cell growth, differentiation, development and homeostasis. Activation of TGFβ signalling occurs upon engagement of the activated form of the TGFβ ligand with the type II serine-threonine receptor kinases (TβRII). This heterodimerises with the type I receptor kinase (TβRI), initiates TβRI phosphorylation and the subsequent recruitment and phosphorylation of the canonical TGFβ signalling mediators SMAD2 and SMAD3. These mediators can form a complex with SMAD4 and upon translocation to the nucleus transactivatory SMAD3/4 can interact with the SMAD binding elements (SBE) present in gene promoters and upregulate SMAD-responsive TGFβ targets. Alternatively, TGFβ signalling can activate a number of other signalling intermediaries including MAP Kinase Kinases (MKK), phosphoinositide 3-kinase (PI3K), AKT, ERK, JNK and p38 mitogen-activated protein kinases, which direct the expression of SMAD-independent gene targets.

1.4.1.2 SMADS

SMAD proteins can be categorised into three groups 1) Receptor-regulated SMADs (R-SMADs); SMAD1, SMAD2, SMAD3, SMAD5 and SMAD8 that interact with the TGFβ receptors (TβR) 2) inhibitory SMADs (I-SMADs); SMAD6 and SMAD7, which act either as decoys by interfering with either receptor:SMAD or SMAD:SMAD interactions and 3) the common-SMAD (Co-SMAD) SMAD4, which acts as a common binding partner for all R-SMADs (Massagué et al., 2005).

Activation of TβR leads to the recruitment and phosphorylation of the R-SMAD proteins, which are SMAD2/3 for TGFβ and activin signalling or SMAD1, 5, 8 for BMP signalling. The R-SMADs can then bind the Co-SMAD, SMAD4, and translocate to the nucleus. In the TGFβ signalling pathway both SMAD3 and SMAD4 can interact with the conserved SMAD binding element (SBE), a cis-acting DNA sequence (CAGAC), and upregulate TGFβ-inducible genes.

R-SMADs and Co-SMAD contain a conserved MH1 domain (Mad-homology-1) and C-terminal MH2 domain connected by a sequence divergent linker segment. Unlike R-SMADs, the I-SMADs lack an MH1, which is important for DNA-binding activity. The MH2 domain contains hydrophobic regions that facilitate the binding of DNA-binding co-factors and various cytoplasmic proteins, as well as the TGFβ receptors. I-SMADs regulate R-SMAD activation by binding to the TβRI via their MH2 domain, effectively taking part in competitive binding with R-SMADs and preventing the propagation of TGFβ signalling (Massagué et al., 2005a; Huang & Chen, 2012; Kubiczkova et al., 2012). Of the I-SMADs, SMAD6 appears to preferentially inhibit BMP signalling, whereas SMAD7 acts to inhibit the TβRI phosphorylation of

SMAD2/3. SMAD7 acts through direct competition with the receptor and facilitates TβR turnover through the recruitment of the E3 ubiquitin ligases Smurf1 and Smurf2 (Hayashi et al., 1997).

While TGFβ signalling acts primarily thorough the canonical SMAD pathways, it is important to mention that TGFβ can also signal via several non-canonical or non-SMAD-mediated pathways. This includes the activation of tumour necrosis factor (TNF) receptor-associated factor 4 (TRAF4), TRAF6, TGFβ-activated kinase 1 (TAK1), p38 mitogen-activated protein kinase (MAPK), RHO GTPase, phosphoinositide-3-kinase (PI3K), AKT, extracellular signal-regulated kinase (ERK), JUN N-terminal kinase (JNK) and nuclear factor-κB (NF-kB) (Akhurst & Hata, 2012). Indeed, the MAP/MEK/ERK cascade has been shown to modify SMAD activity and thereby modify TGFβ-responsive gene expression; however, this is likely context dependent (Hough et al., 2012). Indeed, in epithelial cells, mesangial cells and fibroblasts non-canonical activation has been shown to be required for the expression of a subset of genes, although in epithelial cells the overexpression of Ras/MEK/ERK can block SMAD nuclear translocation (Hayashida et al., 2003; Leask & Abraham, 2004).

1.5 TGFβ signalling in fibrosis

Dysregulation of the TGFβ pathway highlights its pivotal role in tissue homeostasis. TGFβ signalling has been implicated in the pathogenesis of haemorrhagic telangiectasia, Loeys–Dietz syndrome, pulmonary

hypertension, Marfan's syndrome, cancer and fibrotic disorders. In SSc, TGFβ is though to be fundamental in the pathogenesis of tissue fibrosis and has been extensively used to study the fibrotic processes *in vitro* (Varga & Pasche., 2009). Historic data also suggests that there is an increase in TGFβ isoforms in SSc skin biopsies, although the reliability of many antibodies to discriminate between the different TGFβ isoforms is questionable (Gabrielli et al., 1993; Sfikakis et al., 1993). Also, the measurement of serum levels of TGFβ isoforms has been of limited potential due to the indiscriminate ability of these assays to detect both the latent and active forms of TGFβ. Indeed, the variable reliability of more specific assays and also the *ex vivo* release of TGFβ from platelets represent significant obstacles to precise quantification (Dziadzio et al., 2005). More recent data suggests that circulating levels of TGFβ are not increased and that fibroblasts do not have an increased sensitivity to TGFβ. Rather it is suggested that latent TGFβ is sequestered within the ECM of involved SSc skin and therefore has increased bioavailability (Leask et al., 2002; Dziadzio et al., 2005). In support of this, activators of latent TGFβ such as thrombospondin-1 and integrin αVβ5 (suggested to be similar to αVβ6 integrin activity) have been shown to have an increased expression in SSc tissue and fibroblasts, respectively (Asano et al., 2005; Mimura et al., 2005).

1.5.1 Animal models

TGFβ signalling has been well described in the context of several animal models of SSc that include dermal, renal, hepatic, lung and GVHD variants. For example, bleomycin-induced models of lung and liver fibrosis showed an improvement upon the disruption of the TGFβ pathway by expression of a

chimeric receptor, consisting of the two extracellular domain fragments of the TβRII fused to an immunoglobulin Fc fragment heavy chain (George et al., 1999; Wang et al., 1999). Furthermore, increased TGFβ bioavailability is thought to be the mechanism behind the Tsk-1 mouse model, which develop fibrosis through an increased binding of latent TGFβ caused by an in-frame duplication of fibrillin-1. The TβRIIΔk-fib mouse model employs fibroblast-specific expression of a kinase-deficient TβRII gene that leads to the activation of TGFβ signalling. This activation is thought to be as a result of Wild-type (WT) and mutant receptor complexes being less susceptible to degradation, increasing the cell surface expression of TβRI and thereby increasing TGFβ signalling potential. Indeed, this is a similar pathogenic mechanism to Loeys-Dietz syndrome and the mice do have an increased latent TGFβ presence in the ECM. Over time, these mice develop a dermal fibrosis and also display vasculopathy, similar to SSc. In 25% of TβRIIΔk-fib mice, bleomycin treatment leads to lung fibrosis. Furthermore, injury to their epithelium through treatment with bleomycin or saline solution induced a significant fibrotic response: increased fibroblast proliferation, myofibroblast presence, increased type II collagen and alveolar epithelial cell apoptosis (Derrett-Smith et al., 2013). In support of this, gene profiling between TβRIIΔk-fib mice and WT mice treated with recombinant TGFβ1 were found to be highly similar (Denton et al., 2003; Sonnylal et al., 2007).

The CAV-1$^{-/-}$ model has also been used to study experimental fibrosis. Indeed, TβRs are known to be are endocytosed through two distinct pathways; clathrin-coated pits and CAV-1-associated lipid rafts (Guglielmo et al., 2003). The former pathway facilitates SMAD2 activation leading to the propagation of TGFβ signalling while the latter mediates receptor

degradation (Guglielmo et al., 2003). The first observations showed hyperproliferation of explanted mouse embryonic fibroblasts (MEFs) as well as vascular abnormalities, but no pulmonary fibrosis was evident after 4-5 months (Razani et al., 2001). Subsequent studies in these mice demonstrated a further role for CAV-1 in cardiac hypertrophy, impaired angiogenesis, pulmonary hypertension and also pulmonary fibrosis after 12 weeks (Park et al., 2003; Woodman et al., 2003; Hassan et al., 2006). In addition to pulmonary fibrosis, mice developed skin fibrosis with evidence of increased collagen deposition (Del Galdo et al., 2008). Adenoviral overexpression of CAV-1 in the bleomycin-induced model improved pulmonary fibrosis (Wang et al., 2006). Further, on administration of the caveolin scaffolding domain (CSD) within this model resulted in a distinct improvement in pulmonary fibrosis (Tourkina et al., 2008). Nevertheless, global knockout of CAV-1 lead to a plethora of signalling pathways being affected within several cell types and these mice also displayed several non-SSc related pathologies (Beyer et al., 2010).

1.5.2 Fibroblasts

In dermal fibroblasts, the role of TGFβ/SMAD signalling has also been well established in the production of collagen type I, III and V synthesis as well as several other components of the ECM (Leask et al., 2002; Babak Razani et al., 2001; Wynn, 2008). Indeed, skin fibrosis is generally thought to be driven and or initiated by TGFβ-activated fibroblasts (Smith & LeRoy, 1990; Leask & Abraham, 2004; Wynn, 2008; Varga & Pasche, 2009). Additionally, gene profiling of TGFβ-treated dermal fibroblasts from healthy individuals and from SSc patients identified a TGFβ-responsive gene signature of 674

genes, which was highly represented in dcSSc patient skin (Milano et al., 2008). In contrast, this signature was absent in both lcSSc skin and morphea skin biopsies. This suggests that a TGFβ driven mechanism is uniquely associated with the diffuse form of SSc.

In support of a TGFβ-driven mechanism, SSc fibroblasts taken from involved tissue have been shown to have an increased cell surface expression of both TβRI and TβRII, which suggests these fibroblasts could be more responsive to TGFβ (Ihn et al., 2001; Kubo et al., 2002; Asano et al., 2011). Additionally, myofibroblasts are primed to differentiate in response to growth factors and mechanical stress and can produce TGFβ for autocrine signalling (Desmoulière et al., 1993; Gabbiani, 2003; Ho et al., 2014).

1.5.3 SMAD3

TGFβ signalling is mediated by both SMAD2 and SMAD3; however, there is evidence that SMAD3 may have a differential role. Transgenic mice that have a homozygous deletion of SMAD2 do not survive past the embryonic stage of development, whereas those with a SMAD3 homozygous deletion are viable (Leask & Abraham, 2004). This suggests that SMAD2 is essential for development but also highlights that the potential for differential activities.

Using both DNA microarray and promoter analysis, several early-intermediate genes including *COL1A2*, *COL3A1*, *COL6A1*, *COL6A3*, and *tissue inhibitor of metalloproteinase-1 (TIMP-1)* were identified as SMAD3 dependent targets in human dermal fibroblasts validated using a SMAD3 overexpression and SMAD3$^{-/-}$ mice (Verrecchia et al., 2001). Moreover, the differentiation of myofibroblasts has also been shown to be SMAD3

dependent; overexpression of SMAD3, in contrast to SMAD2, increased TGFβ-induced α-SMA expression in human lung fibroblasts (Gu et al., 2007). Another study found that bleomycin treatment of SMAD3 deficient mice showed attenuated myofibroblast differentiation and activity compared to fibrotic development in WT littermates (Dobaczewski et al., 2010). Notably, the expression of α-SMA was found to be predominantly mediated by the binding of SMAD3 to SMAD binding elements (SBEs) in the α-SMA promoter (Hu et al., 2003; Uemura et al., 2005).

In support of these findings, microarray analysis of fibroblasts from adult *SMAD3*$^{-/-}$ and *SMAD3*$^{+/+}$ mice showed that SMAD3 directly activated immediate-early TGFβ-responsive genes through SMAD3/SMAD4 recruitment to SBEs, which are characteristically found within the promoters of immediate-early target genes (Yang et al., 2003). Further, SMAD3 deficiency showed a significant attenuation of TGFβ-responsive immediate-early target genes that were hyperactivated in SMAD2 deficient murine fibroblasts (Kim et al., 2009; Yang et al., 2003). This suggests that SMAD2 may have an inhibitory activity on TGFβ/SMAD3 signalling.

When taken together these data suggest that SMAD3 is essential for TGFβ-mediated fibrosis and is a potential therapeutic target. Aside from the role of SMAD3 in TGFβ signalling it may also be involved in crosstalk with the Wnt signalling pathway. Indeed, Wnt-3a-induced phosphorylation of SMAD3 has been described, although this activation was inhibited by pre-incubation of fibroblasts with a neutralising anti-TGFβ antibody (Wei et al., 2012).

1.5.4 Caveolin-1

Caveolin-1 (CAV-1) is a 22 KDa integral membrane protein that forms a hairpin loop in the plasma membrane and is indispensible for the structure and function of caveolae. Caveolae are 50- to 100-nm flask-shaped invaginations of the plasma membrane, which represent a morphologically distinct subset of lipid rafts important in receptor-independent endocytosis and act as scaffolding proteins for the regulation of signal transduction (Carver & Schnitzer, 2003). CAV-1 is a member of a family of three membrane proteins; CAV-1, CAV-2 and CAV-3, that all form caveolae. CAV-1 has two isoforms designated α and β, which share an overlapping cellular distribution and differ by a 31 amino acid N-terminus present in the α but not β isoform (Fujimoto et al., 2000). CAV-1 and CAV-3 have high sequence identity, whereas CAV-2 is the most divergent member of the family. Both CAV-1 and CAV-2 are expressed in fibroblasts, endothelial cells, adipocytes, whereas CAV-3 is restricted to muscle cells. Interestingly, smooth muscle cells are the only cell type in which all three proteins are co-expressed. In fibroblasts, studies tend to focus on CAV-1 expression, as CAV-2 is directly dependent on CAV-1 for its expression, membrane targeting and stabilisation (Schubert et al., 2007).

Evidence suggests that CAV-1 plays a key role in the pathogenesis of tissue fibrosis through the regulation of TGFβ signalling. It has been shown that TβRI receptors are present in lipid raft and non–lipid raft domains and can be respectively internalised into CAV-1 and clathrin-dependent early endosome antigen 1 (EEA-1) endocytosis pathways (Guglielmo et al., 2003) (Figure 1.3). Further, it has been shown that non-lipid raft associated

internalisation can promote TGFβ signalling in a SMAD2/SARA dependent mechanism, whereas CAV-1-associated internalisation can downregulate TGFβ signalling through the increased proteasomal degradation of the TGFβ receptor in a SMAD7/Smurf-2 dependent manner (Guglielmo et al., 2003).

In SSc, the expression of CAV-1 has been shown to be significantly decreased in dermal and lung fibroblasts, which exhibit a profibrotic phenotype (Del Galdo et al., 2008; Tourkina et al., 2008). Intracellular signalling can be regulated by a CAV-1 scaffolding domain (CSD) peptide, which is a 20-amino-acid region of CAV-1 (amino acid position 82–101) that interacts with the subdomain IX of many kinases including H-Ras and Src family tyrosine kinases (Li et al., 1996). Indeed, the profibrotic activation of SSc fibroblasts could be abrogated by the use of the CSD peptide both *in vitro* and *in vivo* (Tourkina et al., 2008) suggesting that decreased expression of CAV-1 played a key role in SSc fibroblast activation. Further, CAV-$1^{-/-}$ mice show both skin and lung fibrosis and explanted fibroblasts from these mice showed increased collagen production (Galdo et al., 2008). These data indicate that CAV-1 deficient fibroblasts may share overlapping characteristics with scleroderma fibroblasts and may be important for reproducing a profibrotic phenotype.

Like TGFβ signalling, CAV-1 may also play a role in regulating the canonical Wnt signalling pathway by interacting with the low-density lipoprotein receptor-related protein-6 (LRP-6), which is a single span transmembrane receptor that has been shown to be required for canonical activation (Yamamoto et al., 2006). Indeed, CAV-1 has been shown to positively regulate signal transduction by facilitating the Wnt-3a-induced internalisation

of LRP-6, which correlated with β-catenin accumulation in HEK293 cells (Yamamoto et al., 2006).

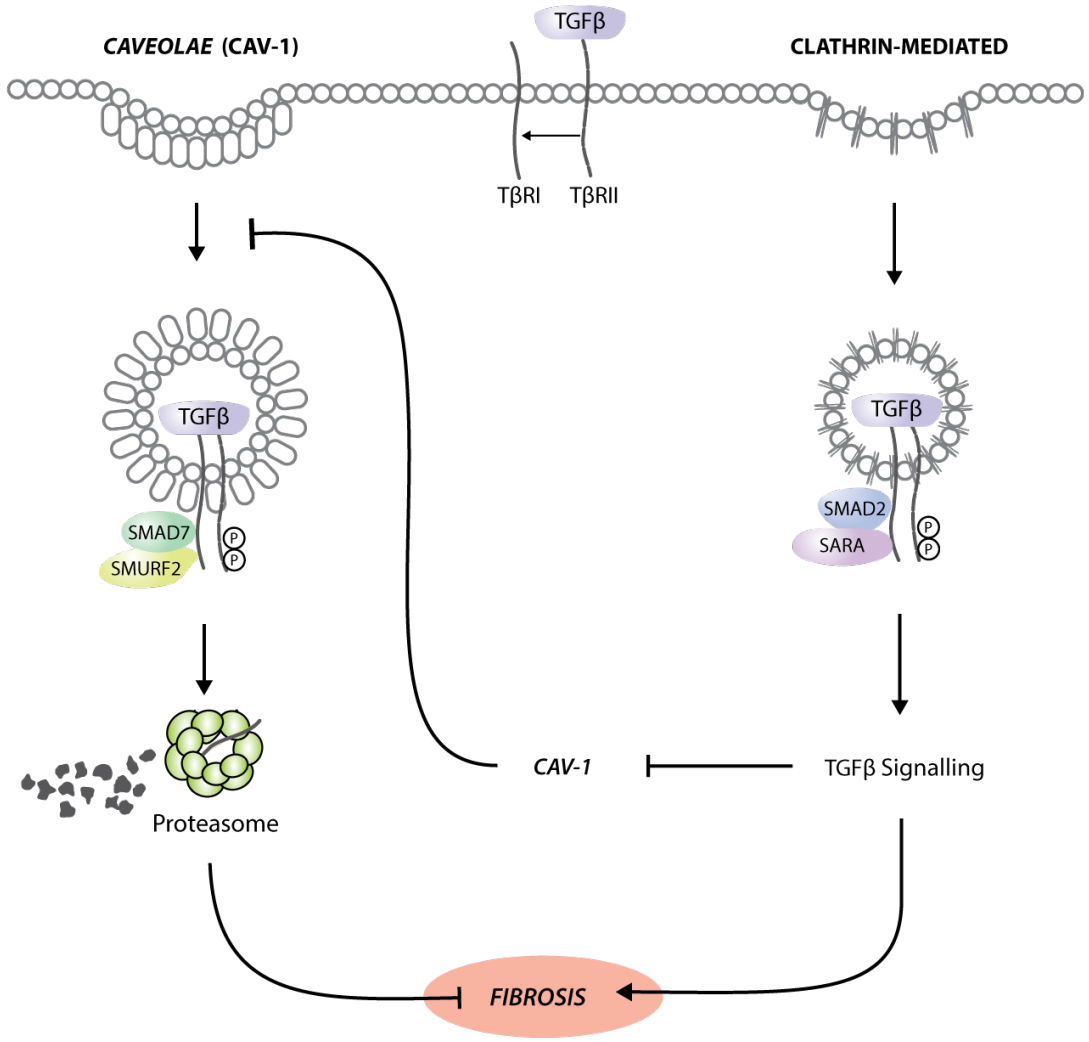

Figure 1.3 Receptor-mediated endocytosis of the TGFβ receptor complex

TGFβ-mediated activation of the TGFβ receptor complex leads to the internalisation of the receptor complex by receptor-mediated endocytosis. This is facilitated by at least two distinct endoyctic pathways, which dictate whether TGFβ signalling is promoted or inhibited. Internalisation via the clathrin-mediated endocytotic pathway is known to propagate TGFβ signalling and is dependent on an association with both SMAD2 and SARA. Alternatively, internalisation complex via caveolae lipid rafts acts to inhibit TGFβ signalling through an association with the inhibitory proteins SMAD7/Smurf2, which facilitates the ubiquitin-mediated proteosomal degradation of the receptor complex. In this model, aberrant TGFβ signalling is though to drive fibrosis by mediating a shift toward clathrin-mediated TβRI/II complex internalisation that results in the upregulation of TGFβ-responsive profibrotic gene targets and the downregulation of CAV-1, the major component of caveolae (Figure adapted from Guglielmo et al, 2003).

1.5.5 TGFβ-mediated post-transcriptional regulation

Eukaryotic mRNAs are stabilised by two key features, the 5′ 7-methylguanosine cap (m7G) and a 3′ poly(A) tail, which are both incorporated upon transcription. eIF4E and the poly(A)-binding protein (PABP) facilitate protection of the transcript from exonuclease activity, associating with the 5’ end at the 3’ end, respectively. Decay of the mRNA transcript can be initiated by the removal of the 5′ cap, known as decapping, which facilitates 5′-3′ exonuclease activity by XRN1. Alternatively, dissociation of the PABPs from the 3′ end can lead to 3′→5′ exonuclease activity or can initiate decapping. The consensus is that the majority of mRNAs are degraded though poly(A)-tail shortening and initiation of a deadenylation-dependent pathway such as the Ccr4/Caf1/Not deadenylation complex and subsequent recruitment of the RNA degrading exosome complex (Figure 1.4). Indeed, the post-transcriptional control of gene expression through mRNA stability and therefore translation allows for dynamic changes in mRNA levels. Dysregulation of this process can contribute to aberrant protein expression and disease (Eberhardt et al., 2007). One well-described method of post-transcriptional regulation is through adenosine and uridine (AU)-rich elements (ARE) that can be harboured within the 3′ untranslated region (3′UTR) of many mRNAs. Generally, AREs are present in the mRNA as repeated AUUUA pentamer sequences, although variations are known to exist (Beisang and Bohjanen, 2012). These sequences facilitate the binding of ARE proteins including human antigen R (HuR), AU-rich element RNA-binding protein 1 (AUF1) and tristetraprolin (TTP-1), which are known to regulate the decay of mRNAs in response to extracellular cues (Houseley & Tollervey, 2009; Schoenberg &

Maquat, 2012). Furthermore, TGFβ has been shown to upregulate the ARE binding protein TTP-1; also known as zinc finger protein 36 homolog (ZFP36), which is part of a family of tandem CCCH zinc-finger proteins that bind to ARE motifs and negatively regulate the stability and/or translational efficiency of target mRNAs (Figure 1.4) (Brooks & Blackshear, 2013). Indeed, the mRNA and protein expression of several ARE containing mRNAs including *TNF*, *COX-2*, *c-MYC* and *CCND1* have previously been shown to be suppressed through TTP-1-meidated mRNA destabilisation (Ogawa et al., 2003; Marderosian et al., 2006; Kang et al., 2014; Blanco et al., 2014).

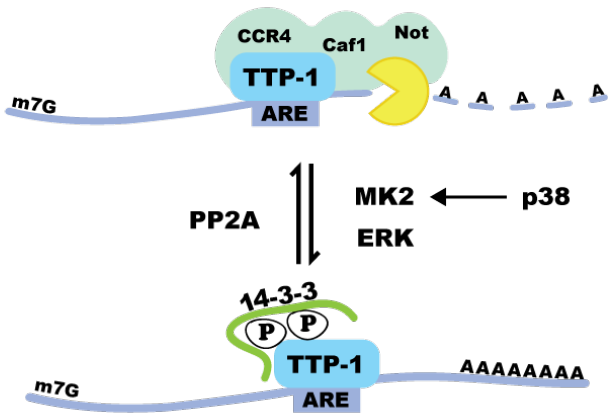

Figure 1.4 mRNA decay: TTP-1 mediated mRNA destabilisation

The majority of eukaryotic mRNAs are degraded though poly(A)-tail shortening. In this illustration, TTP-1 recruits the Ccr4/Caf1/Not deadenylation complex, which reciprocally recruits the RNA degrading exosome complex (yellow) resulting in RNA destabilisation through polyA tail shortening. Post-transcriptional regulation of TTP-1 activity can be achieved though the p38-dependent-MAPK-activated protein kinase 2 (MK2) pathway, which facilitates 14-3-3 adaptor protein binding (Chrestensen et al., 2004; Stoecklin et al., 2004; Sun et al., 2007). The complex of TTP-1 and 14-3-3 proteins has been shown to prevent TTP-1-medaited TNF transcript destabilisation by protecting against serine-threonine phosphatase (PP2A) dephosporylation (Sun et al. 2007). More recently, p38 activation alone was found to be insufficient to inhibit TTP-1-mediated degradation of the TNF transcript, requiring the activation of both the ERK and p38; two downstream targets of the TGFβ signalling pathway (Deleault et al., 2008).

1.6 Wnt signalling

The Wnt family consists of 19 cysteine-rich Wnt ligands that are approximately 350-400 amino acids in size and contain an N-terminal signal peptide important for their secretion. Their eventual secretion and activity requires both glycosylation and palmitoylation events, with the latter catalysed by Porcupine (PORCN) (Gao & Hannoush, 2014). Once secreted, Wnt ligands can then interact with glycosaminoglycans in the ECM, which modulate their distribution, diffusion and therefore their signal transduction potential (Logan & Nusse, 2004).

Wnt ligands signal through the engagement of frizzled receptors (Fz), which are a family of seven-pass transmembrane receptors that contain an N-terminal cysteine rich domain (CRD) that may facilitate Wnt:Fz receptor binding through homodimerisation. This is thought to occur in the presence of single-pass transmembrane protein co-receptors including the LRP-5/-6, receptor tyrosine kinase-like orphan receptor (ROR)-1/-2 and receptor tryrosine kinase (Ryk). Indeed, 10 Fz receptors and at least 5 co-receptors have been described to date. Signal regulation can also be regulated by 4 distinct families of Wnt signalling antagonists; secreted frizzled-related proteins, Dickopff proteins (DKKs), R-spondins and Wnt inhibitory factor-1 (WIF-1) (Kawano & Kypta, 2003).

Wnt signalling has been traditionally categorised into two main pathways i) the canonical Wnt (β-catenin-dependent) pathway (Figure 1.5) and ii) the non-canonical (β-catenin-independent) pathways, which include the planar-cell-polarity (PCP) (also known as the JNK) and the Ca^{2+} pathway (Figure 1.6). Classically, Wnts have been divided into those that activate the

canonical pathways (Wnt-1, Wnt-3a and Wnt-8) and those that activate the non-canonical pathways (Wnt-4, Wnt-5a and Wnt-11). However, more recent evidence suggests that the Wnt signalling co-receptors may play an instrumental role in conferring the signalling pathways elicited. For example, the canonical Wnt-3a and non-canonical Wnt-5a ligands have been shown to be exclusively recruit LRP-5/-6 and Ror-1/-2, respectively (Grumolato et al., 2010).

1.6.1 Canonical Wnt signalling

The term canonical Wnt signalling is used to describe β-catenin dependent signalling (Figure 1.5). In resting cells β-catenin is inhibited by the destruction complex; comprised primarily of the scaffolding proteins AXIN, adenomatous polyposis coli (APC), casein kinase-1 (CK1) and glycogen synthase kinase-3β (GSK-3β) (Stamos & Weis, 2013). AXIN directly interacts with the Armadillo repeats 2–7 of β-catenin, where upon complexed GSK-3β and CK1 can both act to constitutively phosphorylate β-catenin at Ser33/Ser37/Ser45/Thr41 (Stamos & Weis, 2013). Phosphorylated β-catenin is recognised by the E3 ubiquitin ligase β-transducin repeat-containing protein (β-TrCP), which facilitates the subsequent ubiquitination and degradation of β-catenin via the proteosome pathway.

Binding of ‘canonical Wnts' to the extracellular CRD domain of Fz receptors/LRP co-receptors results in the recruitment of dishevelled (Dvl) to the cytoplasmic C-terminal of the Fz receptor and the resultant complex (Wnt/Fz/Dvl) facilitates the recruitment of the destruction complex to the plasma membrane. Here, AXIN binds to the cytoplasmic tail of LRP5/6 and

becomes phosphorylated, lowering its β-catenin binding capacity and is subsequently targeted for proteasomal degradation. As a result of destruction complex inactivation, there is an accumulation of cytosolic stabilised/un-phosphorylated β-catenin, which can then translocate to the nucleus and bind to the TCF/LEF family of transcription factors, in association with the co-activators p300 and CREB-binding protein (CBP). These events lead to transcriptional initiation of canonical Wnt target genes known to be important in the control of processes including differentiation, proliferation, migration and more recently genes those involved in fibrosis.

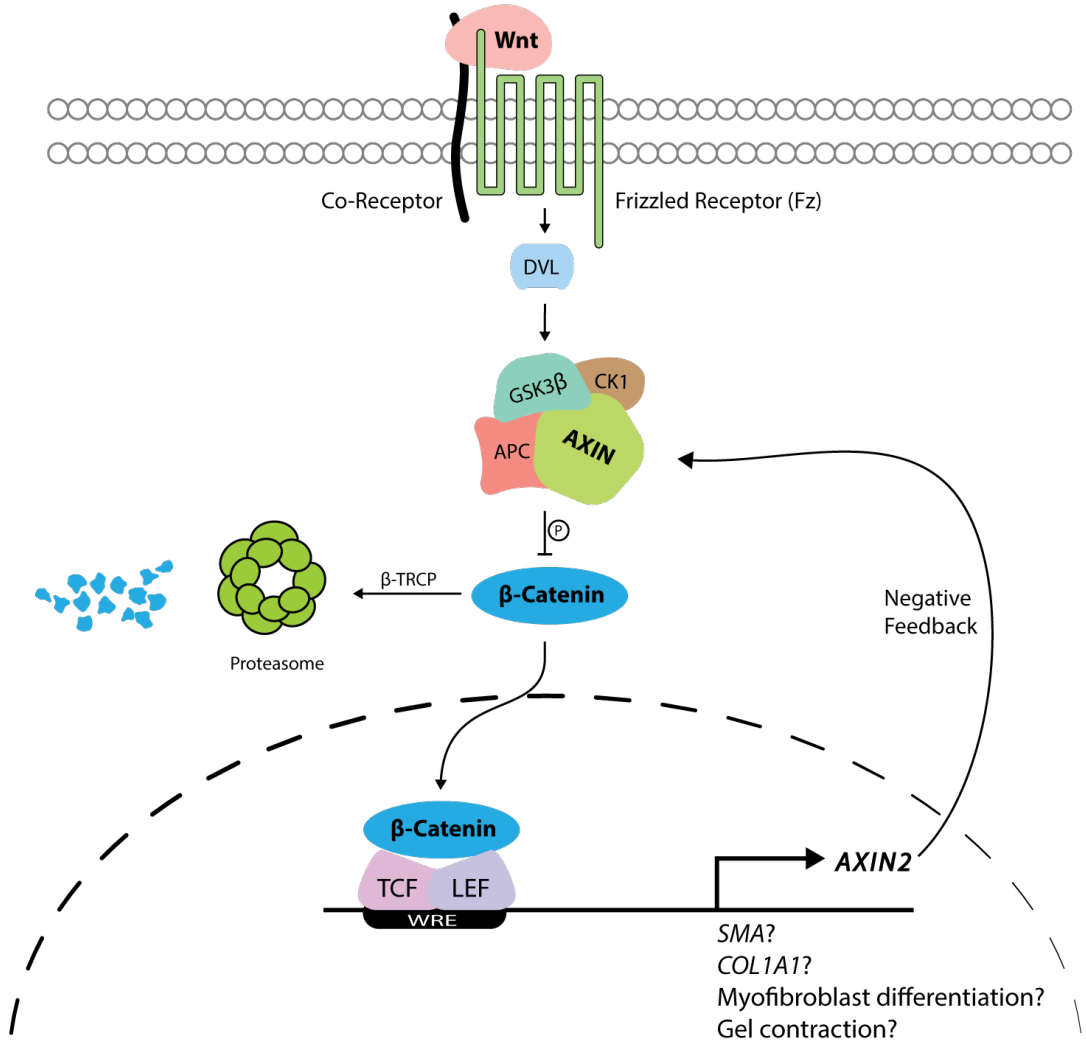

Figure 1.5 Overview of the canonical Wnt signalling pathway

Activation of canonical Wnt signalling occurs upon the binding of a Wnt ligands with a Frizzled receptor (Fz) protein complex containing a co-receptor (LRP5/6). This complex can then recruit the adaptor protein dishevelled (Dvl) to the plasma membrane. Dvl then acts to recruit and inhibit the β-catenin destruction complex whose core components include GSK-3β, APC and AXIN, which are required for the ubiquitin-mediated targeting of β-catenin for proteasomal degradation. This results in the cytoplasmic accumulation of unphosphorylated/stabilised β-catenin, which can then be available for nucleus translocation. β-catenin can then bind to LEF and activate the TCF/LEF transcription factor family and upregulate canonical target genes.

1.6.2 Non-canonical Wnt signalling

Although recent studies have shown that aberrant canonical signalling is potentially involved in fibroproliferative disorders, little is known about the role of non-canonical signalling and its contribution to the fibrotic phenotype. Non-canonical signalling is a collective term for those signalling pathways that are β-catenin independent, used to predominantly describe the JNK pathway (also termed the PCP-like pathway) and the Ca^{2+} pathway, which are associated with tissue polarity and cell migration and proliferation and cell migration, respectively (Figure 1.6) (Kawano & Kypta, 2003); Heisenberg et al., 2000). Wnt-induced stimulation of these pathways requires the Fz receptor family and was long believed to occur independently of co-receptors. However, studies looking at the PCP non-canonical pathway in the alignment of sensory hair cells of the inner ear in mice found that and $Ror2^{-/-}$, like $Wnt\text{-}5a^{-/-}$, exhibit defects in the orientation of these hair cells, which suggest that both Fz and co-receptor binding may be required for non-canonical signalling activation (Qian et al., 2007; Yamamoto et al., 2008).

Induction of the Wnt/Ca^{2+} signalling pathway commences upon Wnt ligand binding with both Fz and co-receptor (Figure 1.6B), which induces intracellular signal transduction through activation of Dvl and membrane bound phospholipase-C (PLC), the later hydrolyses phospholipid phosphatidylinositol 4,5-bisphosphate to the second messengers inositol 1,4,5-triphosphate (IP3) and 1,2-diacylglycerol (DAG). DAG can then activate protein kinase-C (PKC), whereas IP3 binds to the IP3 receptor calcium channel located on the endoplasmic reticulum (ER) to induce calcium flux (Luna-Ulloa et al., 2011). The consequence of elevated $[Ca^{2+}]$ in the cytosol is the activation of calcium-sensitive signalling mediators such as

calmodulin-dependent protein kinase II (CAMKII) and calcineurin (CN). Then, PKC and CN can act together to regulate the activity of nuclear factor of activated T cells (NFAT) transcription factors, whereas CaMKII and PKC can activate both the NF-kB and c-AMP-responsive element binding protein (CREB) transcription factors.

In the Wnt/PCP pathway (Figure 1.6C), Wnt-induced activation of Fz receptors leads to the subsequent activation of Dvl, which in-turn mediates downstream activation of Rac, Rho and Rap small GTPases and JNK. The functions of the PCP pathway are not well understood but are known to be important in convergent extension during development, including the orientation of hair cells in the inner ear and neural tube closure (Yin et al., 2009). The JNK family of stress-activated protein kinases has been shown to be involved in cell motility through cytoskeletal stabilisation of microtubules, and may also regulate gene expression through by phosphorylation of the transcription factor activator protein-1 (AP-1) subunit c-JUN transactivation domain at S63/S73 (Ciani & Salinas, 2007; Lapébie et al., 2011).

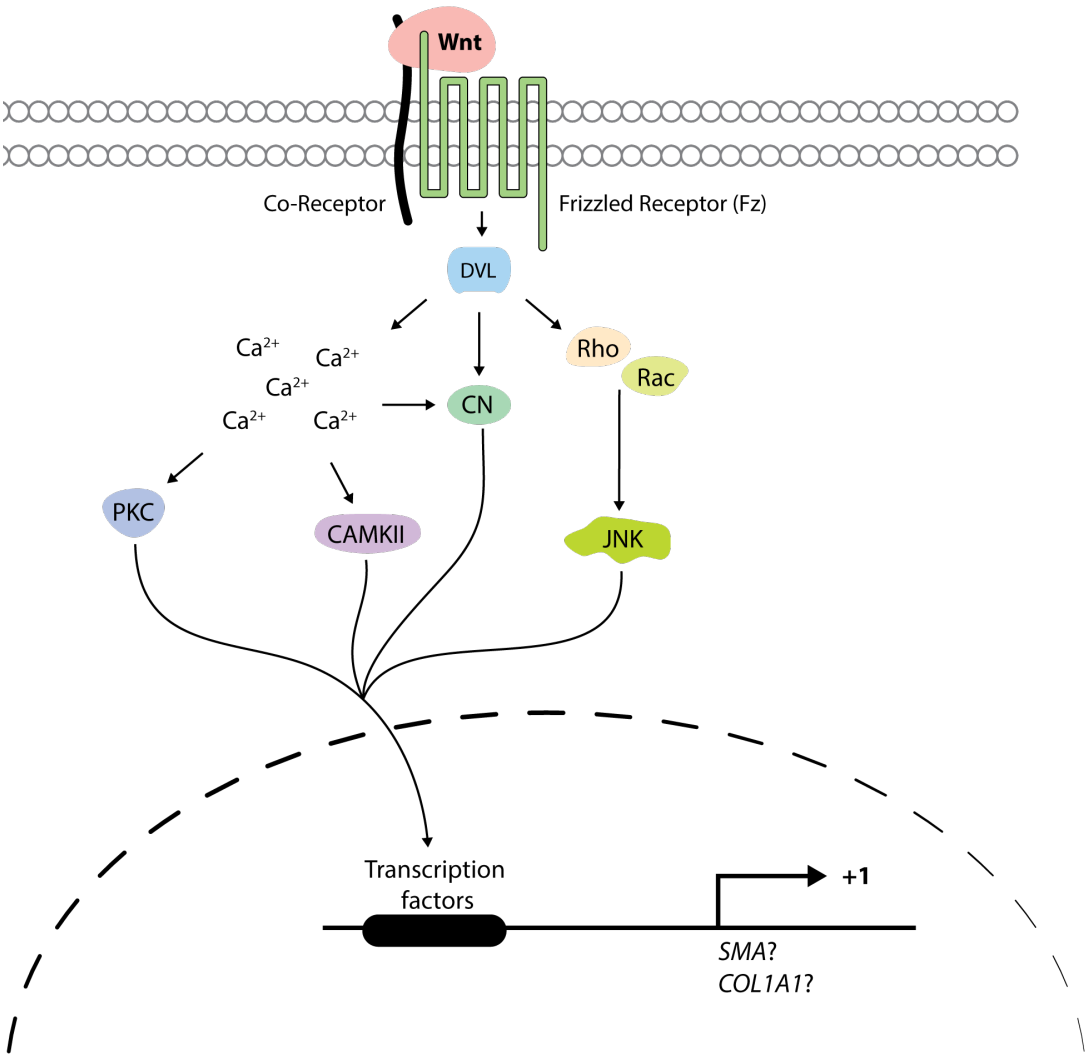

Figure 1.6 Overview of the non-canonical Wnt signalling pathway

Activation of non-canonical Wnt signalling occurs upon the engagement of Wnt ligands with both Frizzled (Fz) and co-receptors (ROR2/RYK), which leads to the recruitment of Dvl to the plasa membrane where it can recruitment and activate small GTPases. This activation leads to the JNK-mediated phosphorylation of c-Jun, an important component of the AP-1 transcription factor leading to the regulation of AP-1-responsive gene targets. Alternatively, activation of Dvl can mediate phospholipase-C (PLC) activity, which hydrolyses phospholipid phosphatidylinositol 4,5-bisphosphate to the second messengers inositol 1,4,5-triphosphate (IP3) and 1,2-diacylglycerol (DAG). DAG can then activate protein kinase-C (PKC), whereas IP3 binds to the IP3 receptor calcium channel located on the endoplasmic reticulum (ER) and both can lead to the induction of calcium flux (Luna-Ulloa et al., 2011). The consequence of elevated [Ca^{2+}] in the cytosol is the activation of calcium-sensitive signalling mediators such as calmodulin-dependent protein kinase II (CAMKII) and calcineurin (CN). PKC and CN can act together to regulate the activity of nuclear factor of activated T cells (NFAT) transcription factors, whereas CaMKII and PKC can act together to activate the nuclear factor kappa-B (NF-κB) and c-AMP-responsive element binding protein (CREB) transcription factors.

1.6.3 Antagonists of Wnt signalling

Wnt antagonists can be divided into two functional classes; the SFRP and the DKK protein families. The SFRP class includes SFRP1-5, WIF-1 and Cerberus, which are generally thought to modulate Wnt signalling by direct binding of Wnts to prevent receptor engagement; however, different context-dependent models of SFRP activity, both inhibitory and activatory, have been proposed (Figure 1.7). On the basis of sequence homology SFRP1, SFRP2 and SFRP5 have high sequence identity, as do SFRP3 and SFRP4, which share 92% sequence identity but are distantly related to SFRP1, 2 and 5. SFRPs contain two conserved domains termed the cysteine-rich domain (CRD) and the netrin-like domains (NTR), which are separated by a linker region and are present at the N- and C-terminus, respectively. Interestingly, CRD that shares 30-50% homology with Fz receptor CRDs including 10 conserved cysteine residues, which might be of functional significance in the homodimerisation with CRDs present in Wnt/Fz receptors (Melkonyan et al., 1997). Whereas the function of the NTR, which contains only six conserved cysteines with several hydrophobic regions is not fully understood; however, these domains are also present in tissue inhibitors of metalloproteinases (TIMPs), type I procollagen C-proteinase enhancer proteins (PCOLCEs) and are thought to be important in the regulation of their activities (Bányai & Patthy, 1999).

SFRPs are conventionally though of as inhibitors of Wnt signalling. The majority of studies have focused on the activities of SFRP1/2, but many have shown activities beyond putative inhibition of Wnt signalling. Indeed, the expression of SFRP1/2 has also been found to be decreased in proliferative keloid tumour tissue, which are benign tumours of the dermis

likely to be Wnt dependant (Russell et al., 2010). Furthermore, in *Sfrp*-1$^{-/-}$ and *Sfrp*-2$^{-/-}$ mice Wnt/β-catenin signalling was inhibited in the optic cup periphery (OCP) as shown by the lack of immunohistochemical staining for unphosphorylated β-catenin; however, these mice also showed an abrogation of Wnt-11 ligand diffusion across the OCP explants that could be restored upon SFRP1 co-treatment, which demonstrated that Wnt signalling activation can be regulated by SFRPs at the level of diffusion (Esteve et al., 2011). Differential effects have also been shown to affect the self-renewal of haematopoietic stem cells, where both SFRP1/2 were able to stimulate the proliferation of haematopoietic progenitor cells; however, only SFRP2 enhanced the differentiation potential of multipotent progenitors (Nakajima et al., 2009).

The role of SFRPs in the regulation of dermal fibroblast biology, either direct or indirect, is currently unknown. Suggestively, SFRP4 was found to be significantly upregulated in the Tsk-1 mouse model of SSc by gene profiling studies and was also highly expressed in the deep dermis of SSc lesional skin in contrast to non-lesional and HC tissues (Bayle et al., 2008). Therefore, SFRP4 might be important in the development of fibrosis independently or in combination with Wnt signalling.

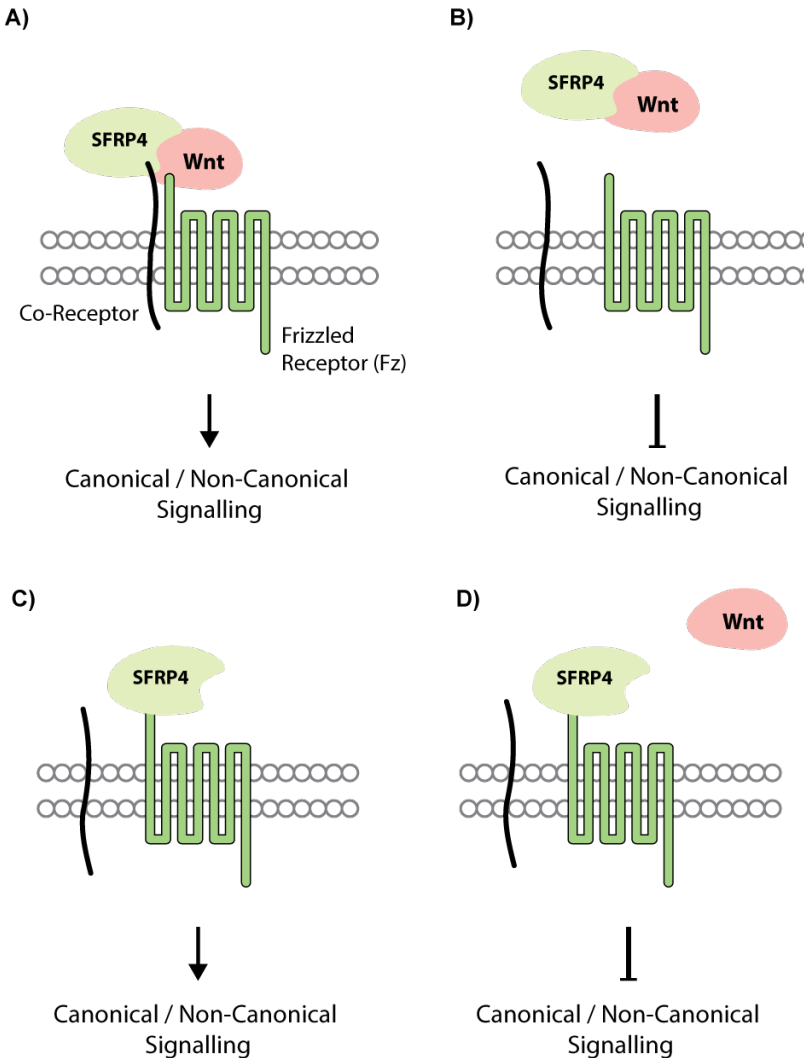

Figure 1.7 Functional models and putative activities for the Secreted Frizzled-Related Protein family

A simplified summary of four independent models of SFRP-mediated Wnt signalling regulation. A) Formation of Wnt-SFRP can act to diffuse or shuttle Wnt to Fz and activate Wnt signalling activity. B) SFRPs may sequester Wnt ligands through direct binding to the netrin-related domain (NTR) and prevent Wnt signalling activity. C) SFRPs may directly bind to Fz, mediated by homodimerisation of their cysteine-rich domains (CRDs), and promote Wnt signalling activity. D) As C, but where SFRP4 binding competes with Wnt ligands to prevent Wnt signalling activity.

1.7 Wnt signalling in fibrosis

Canonical Wnt signalling is known to play a critical role in wound healing primarily through the co-ordination of wound closure. Indeed, β-catenin-dependent transcriptional activity in fibroblasts is increased during the

proliferative phase of wound healing. Several studies have now shown that Wnt signalling may play an important role in the initiation/maintenance of fibrosis. A gene profiling study on NIH-3T3 fibroblasts treated with the canonical Wnt-3a agonist resulted in the upregulation of several key fibrotic mediators including *Ctgf*, *Tgfβ* and *Et-1*, while several genes involved in ECM degradation were supressed (Chen et al., 2007). Additionally, skin from the fibrotic Tsk-1 mouse model showed increased mRNA levels of several genes involved in Wnt signalling including *Wnt-2*, *Wnt-9a*, *Wnt-10b* and *Wnt-11*; *Dapper* (*Dact)-1* and *Dact-2*; Wnt-induced secreted protein 2; and *Sfrp2* and *Sfrp4* (Bayle et al., 2008). Further studies confirmed that *Wnt-10b* mRNA was highly expressed in the bleomycin-induced fibrotic mouse and was differentially expresses in SSc compared to HC skin (Wei et al., 2011b; Beyer et al., 2012). Interestingly, the *in vivo* overexpression of Wnt-10b was sufficient to induce fibrosis: myofibroblast accumulation, progressive loss of subcutaneous adipose tissue, increased collagen deposition and consequent increase in dermal thickness (Wei et al., 2011). Explanted fibroblasts from the Wnt-10b model also showed increased collagen and α-SMA expression (Wei et al., 2011). Consistent with these findings, the inhibition of GSK3-β (a component of the β-catenin destruction complex) was sufficient to induce fibrosis by activation of the canonical pathway and coincided an increase in the presence of dermal fibrosis in both the bleomycin/Tsk-1 mouse models of SSc (Bergmann et al., 2011). Furthermore, the overexpression of β-catenin in the mesenchymal cells of transgenic mice, show increased fibroblast proliferation, motility, invasiveness and also showed aggressive fibromatoses as well as hyperplastic wounding and tumour formation when grafted into nude mice

(Cheon et al., 2002). Two separate studies also showed that the inhibition of Wnt/β-catenin signalling could reduce pulmonary fibrosis in the bleomycin mouse model (Henderson et al., 2010; T. H. Kim et al., 2011).

Interestingly, in β-catenin null fibroblasts TGFβ signalling was unable to induce a common proliferative response or upregulate MMP-3 and MMP-13 (Cheon et al., 2006). This study suggests that β-catenin crosstalk might be involved in the regulation of TGFβ-induced gene expression. Such crosstalk could lead to the synergistic/inhibitory regulation of shared target genes or regulated through the interaction of signalling mediators from both pathways. Also, like TGFβ, the observation that CAV-1 expression can regulate canonical/β-catenin signalling may be a key link between both the Wnt and TGFβ signalling pathways.

1.7.1 Non-canonical signalling in fibrosis

The best characterised example of the Wnt/Ca^{2+} pathway induction is through Wnt-5a engagement of Fz2 in *Xenopus* and zebrafish embryos (Torres et al., 1996; Slusarski et al., 1997). The contribution of this pathway in different diseases may be context dependent given conflicting evidence. For example, the expression of Wnt-5a has been shown to be decreased in the majority of primary tumours from patients with pre-B cell acute lymphoblastic leukaemia (Liang et al., 2003). Consistently, Wnt-5a could function as a tumour suppressor in haematopoietic tissue, as CAMKII-dependent induction of the Ca^{2+} pathway suppressed cyclin-D1 expression and inhibited B cell proliferation. However, in prostate cancer the expression of Wnt-5a correlated with malignancy where cell migration and invasiveness

were likely as a result of the non-canonical JNK pathway activation and upregulation of MMP-1 (Yamamoto et al., 2010). Other studies report similar oncogenic observations in melanoma and lung cancer (Weeraratna et al., 2002; Huang, 2005).

The contribution of the non-canonical pathway in fibroproliferative diseases and in SSc remains largely unstudied. An early study revealed that increased expression of Wnt-5a or Fz2, its receptor, in hepatic stellate cells lead to a significant increase in fibrosis both *in vitro* and *in vivo* (Jiang et al., 2006). Also, in pulmonary tissue of patients with sarcoidosis, Wnt-5a expression was increased and was suggested to be a factor involved in the inflammatory or chronic fibrotic processes (Levänen et al., 2011). Interestingly, Wnt-5a was also shown to increase the proliferation, inhibit apoptosis and to induce fibronectin expression in normal lung-derived fibroblasts (Vuga et al., 2009). Wnt-5a might therefore be a useful agonist to study the effects of non-canonical signalling in fibroblasts.

1.7.2 Canonical signalling in fibrosis

1.7.2.1 β-catenin - a central mediator

β-catenin was first identified as a cytoplasmic protein that linked the cadherin complex to the actin cytoskeleton (McCrea et al., 1991). β-catenin consists of 781 residues in humans and includes 12 Armadillo repeat domains and distinct intrinsically disordered N-terminal and C-terminal domains. Both the N-terminal and C-terminal domain are known be involved in protein:protein interactions; however, the C-terminal domain also houses a transactivatory motif that facilitates Wnt signalling (Valenta et al., 2012). Moreover, β-

catenin can be divided into two spatial populations within a cell. The first is located at the plasma membrane and is bound to the cytoplasmic tails of cadherin and participates in cell adhesion, while the other pool plays a critical role in the TCF/LEF-mediated transcriptional activation (Luo and Lin, 2004).

Canonical Wnt signalling activation results in free cytosolic β-catenin that is then available to undergo nuclear translocation from the cytoplasm; however, β-catenin does not contain a nuclear localisation signal (NLS) and therefore its method of entry is as yet unclear. However, SMAD3 has been suggested to form a complex with β-catenin and play a role in shuttling it to the nucleus in chondrocytes and in the chondrogenic cell line RCJ3.1C5.18 (Li et al., 2006; Zhang et al., 2010).

The presence of nuclear β-catenin leads to the upregulation of Wnt target genes by activating any of the four mammalian TCF/LEF transcription factors (LEF-1, TCF-1, TCF-3 and TCF-4). These TCF/LEF transcription factors require β-catenin to mediate their transactivatory activity and act as repressors in its absence by forming a complex with the Groucho/TLE repressors. Nuclear β-catenin competes with and displaces the Groucho/TLE co-repressors and leads to the initiation of TCF/LEF driven canonical Wnt signalling (Roose et al., 1998; Daniels & Weis, 2005).

1.7.2.1.1 β-catenin crosstalk

β-catenin is also able to interact with other nuclear proteins, which suggests that it may have a more diverse signalling role. A genome-wide loss-of-function screen was evaluated in 85 cancer cell lines, which found that the

survival and transformation of β-catenin-driven cell lines was dependent on β-catenin in complex with the transcriptional regulator YAP1 and the transcription factor TBX5 (Rosenbluh et al., 2012).

Further, the hypoxia-mediated induction of Hypoxia Factor-1 (HIF-1) has been shown to compete with TCF-4 for β-catenin binding resulting in a reduction of TCF/β-catenin-mediated transcription and an increase in HIF-1/β-catenin at the promoters of HIF-1 target genes: supporting cell survival (Kaidi et al., 2007). The function of the HIF-1/β-catenin seems to be context dependent. For example, in cancer cells the HIF-1 protein acts as a repressor of TCF/β-catenin signalling whereas in stem cells HIF-1 leads to activation of this pathway (Mazumdar et al., 2010).

Also, the AP-1 complex has been observed to form a physical and functional co-operation with the TCF/LEF/β-catenin complex (Toualbi et al., 2007). In support of this, chromatin immunoprecipitation sequencing (ChIP-Seq) analysis in colon cancer cell line HCT116 showed that approximately a quarter of all β-catenin enriched regions harbour both TCF and AP-1 binding sites in close proximity in intestinal cancer cell lines (Bottomly et al., 2010). This study also observed that a subset of genes that contained both TCF-4 and AP-1 binding sites were upregulated in response to mitogen and Wnt activation together, in contrast to independent treatments (Bottomly et al., 2010).

These data, when taken together, suggest that there is significant crosstalk at the level of β-catenin. Evidence shows that context is critical and that while this crosstalk can modulate β-catenin/TCF/LEF-mediated transcription, TCF/LEF-independent pathways are also likely to be important in regulating

gene expression. The traditional paradigm of increased β-catenin resulting in hyperactivation of canonical Wnt signalling may therefore in a fact be a misnomer.

1.7.2.1.2 β-catenin in disease

The role of β-catenin in carcinogenesis was first described in colorectal cancer, the majority of tumours had inactivating mutations in APC leading to the inappropriate stabilisation of β-catenin, while activating mutations in β-catenin were present at a much lower frequency (Rubinfeld et al., 1997; Nishita et al., 2000; Wong & Pignatelli, 2002). Mutations in the β-catenin gene were frequently present within the N-terminal Ser/Thr destruction motif, which conferred resistance to APC-mediated regulation (Morin et al., 1997). In a subset of these patients mutations were also localised in the *AXIN2* gene and correlated with an increased nuclear accumulation of β-catenin within tumour cells (Morin et al., 1997).

β-catenin has also been shown to have an important function in fibroproliferative diseases, which is unsurprising given its crucial role in during wound healing through the regulation of dermal fibroblast proliferation, motility and invasiveness (Cheon et al., 2002; Bowley et al., 2007). Indeed, increased β-catenin expression/nuclear localisation was observed in Dupuytren's disease: a superficial fibromatosis of the hand in which hyperproliferation leads to increased collagen deposition in the tissue (Varallo et al., 2003). Similar to the pathogenesis of some cancers, aggressive fibromatosis (desmoid tumours) have also exhibited increased

Wnt/β-catenin signalling associated with both activating mutations of β-catenin or APC (Li et al., 1998; Tejpar et al., 1999).

The induction of stabilised β-catenin in transgenic mice leads to the development of an aggressive fibromatoses and hyperplastic gastrointestinal polyps absent in WT mice and fibroblasts explanted from these β-catenin transgenic mice showed increased proliferation, motility, invasiveness and tumour growth when grafted into nude mice (Cheon et al., 2002). These data suggest that β-catenin is an important regulator of fibroblast phenotype.

Specifically, the role of Wnt/β-catenin signalling is currently under investigation in SSc. Nuclear β-catenin accumulation has repeatedly been observed in the dermis SSc patients, co-localising with a fibroblast-specific marker, but absent in HC tissues (Beyer et al., 2012). In mice, the fibroblast-specific stabilisation of β-catenin lead to fibrosis including dermal thickening, increased collagen expression and myofibroblast count (Beyer et al., 2012). Furthermore, the fibroblast-specific deletion of β-catenin was able to significantly reduce bleomycin-induced dermal fibrosis (Beyer et al., 2012). However, while increased nuclear β-catenin localisation was observed in lung fibroblasts from SSc patients with pulmonary fibrosis, rather than contributing to the fibrotic phenotype the overexpression of Wnt or β-catenin lead instead to increased migratory and proliferative activities (Lam et al., 2011). Therefore the role of β-catenin in regulating the fibrotic activities in SSc fibroblasts remains to be clarified.

1.7.2.2 AXIN - a rate limiting control

AXIN is a 832 or 868 amino acid protein identified through mutations of the mouse fused locus that encoded the *Axin* gene. This gene was shown to regulate embryonic axis formation through the inhibition of the Wnt signalling pathway (Zeng et al., 1997). Using a yeast two-hybrid screening approach, AXIN was shown to directly interact with β-catenin, GSK3-β and APC (Hart et al., 1998). AXIN has two main functional domains, the regulators of G-protein signalling domain (RGS) domain at the N-terminus and the DIX domain at the C-terminus. APC binds to the RGS domain, while the DIX domain may have a role in signal transduction given its ability to interact with the Dvl through its own DIX domains (Cadigan & Nusse, 1997; Fagotto et al., 1999). Other, more central domains facilitate the binding of β-catenin and GSK3-β. In addition, AXIN has also been shown to bind to the C-terminal domain of the low-density LRP-5 and positively regulate signal activation (Luo & Lin, 2004).

AXIN is essential for the formation of the β-catenin destruction complex and plays a critical in the efficient turnover of β-catenin, consistently demonstrated in *Xenopus* to mammalian systems (Hart et al., 1998; Sakanaka et al., 1998; Willert et al., 1999; Salic et al., 2000; Liu et al., 2002). In vertebrates, two AXIN genes are expressed and both act as negative regulators of Wnt signalling (Chia & Costantini, 2005). AXIN2 shares 44% sequence identity to AXIN1 and conserves multiple domains including the RGS and DIX domains as well as the β-catenin, GSK3-β, and SMAD3 binding sites (Chia & Costantini, 2005). While AXIN1 is constitutively expressed, AXIN2 (also called Conductin or Axil) is a direct transcriptional target of the Wnt pathway, facilitated by TCF binding sites present within its

promoter and thereby acts to control Wnt signalling through negative feedback (Jho et al., 2002; Leung et al., 2002; Taniguchi et al., 2002).

Axin1$^{(-/-)}$ transgenic mice are embryonically lethal, whereas Axin2$^{(-/-)}$ mice are viable and fertile but show osteogenic cranial abnormalities (Perry-III et al., 1995; Behrens et al., 1998). Further, the delivery of Axin-2 cDNA can rescue the lethal phenotype in Axin-1$^{(-/-)}$ mice, which indicated that the two proteins share overlapping functional activity (Chia & Costantini, 2005). However, heterozygous *AXIN2* germ line mutations can independently lead to familial tooth agenesis, which would indicate that the two proteins are not redundant and can have distinct roles *in vivo* (Lammi et al., 2004).

Recently, a small molecule inhibitor of the Wnt/β-catenin pathway, XAV939, was discovered to significantly inhibit Wnt3a-induced TOPFlash luciferase reporter activity in HEK293 cells as part of a high-throughput screen (Huang et al., 2009). The decreased level of nuclear β-catenin following Wnt activation was mediated by increased AXIN expression. Mechanistically, the stability of AXIN was enhanced though the XAV939-mediated inhibition of PARsylation (addition of ADP-ribose polymers) by the poly(ADP-ribose) polymerase (PARP) enzymes, specifically though Tankyrases 1/2, which then facilitated the subsequent ubiquitin-mediated degradation of AXIN (Huang et al., 2009). In support of these observations, an AXIN:Tankyrase crystal structure was solved revealing the bivalent complex formation (Morrone et al., 2012).

1.7.2.2.1 AXIN Crosstalk

AXIN, while crucial in Wnt/β-catenin signalling can also interact with proteins that are more representative of other signalling pathways, including those involved in TGFβ signalling. In HEK293 cells, activation of TGFβ signalling was facilitated by AXIN though its ability to bind SMAD7 and in parallel Arkadia; a ubiquitin E3 ligase that acts upon the inhibitory SMAD7 protein (Liu et al., 2006). Further, in resting HepG2 cells, both AXIN and SMAD3 were observed to form a complex that was localised to the cytoplasm (Furuhashi et al., 2001). This interaction was also present in the COS7 fibroblast cell line and was abolished upon the constitutive TβRI activation; additionally, the expression of an AXIN mutant was able to inhibit TGFβ signalling (Furuhashi et al., 2001). A further study showed that SMAD3 stability was controlled by the expression of/interaction with AXIN and GSK3-β in HEK293 cells. The reduction of AXIN/GSK3-β expression lead to stabilisation of SMAD3 and therefore promoted TGFβ signalling (Guo et al., 2008). Taking these data together, AXIN may facilitate the TGFβ–induced activation of SMAD3 or could be important in negatively regulating TGFβ signalling activation.

1.7.2.2.2 AXIN in disease

Unlike β-catenin, little is known about the role AXIN in fibrotic diseases but is considered to be a tumour suppressor given its role in the inhibition of β-catenin signalling. Interestingly, *AXIN* mutations were found in colorectal cancer patients and correlated with nuclear β-catenin accumulation (Morin et al., 1997). Loss of heterozygosity or rearrangements in the genomic locus containing *AXIN2* can contribute to tumour progression through Wnt/β-

catenin signalling (Phelan et al., 1998). The gene itself has also been found to be mutated and can be functionally inactivated in hepatocellular, ovarian and colorectal carcinomas (Liu et al., 2000; Wu et al., 2001; Taniguchi et al., 2002; Liu et al., 2002). Reduced AXIN expression has also been correlated with aggressiveness in both lung and oesophageal squamous cell carcinomas (Xu et al., 2006). Additionally, AXIN2 loss of function studies have shown its involvement in the pathogenesis of certain cancers and tooth agenesis (Lammi et al., 2004; Mazzoni & Fearon, 2014).

Furthermore, in chondrocytes it was observed that TGFβ signalling inhibited the expression of both AXIN1 and AXIN2 in a SMAD3 dependent manner (Dao et al., 2007). Additionally, TGFβ signalling was enhanced by AXIN overexpression (Dao et al., 2007). As Wnt/β-catenin signalling is hyperactivated in SSc patient dermal fibroblasts (Beyer et al., 2010), their phenotype might also depend upon AXIN crosstalk with the TGFβ signalling pathway in parallel with its transitional role in the regulation of Wnt/β-catenin signalling.

1.8 Hypothesis and aims

Activation of the TGFβ and Wnt/β-catenin signalling pathways have been linked to the pathogenesis of tissue fibrosis in SSc. In fibroblasts the mechanism behind Wnt/β-catenin signalling hyperactivation and the consequence of differential SFRP4 expression are largely unknown. Therefore the following questions were asked:

1. Do SSc fibroblasts demonstrate differential Wnt/TGFβ signalling pathway activities compared to HC?
    I. Does this contribute to a fibrotic fibroblast phenotype?
    II. Does this correlate with an increased canonical Wnt signalling activity?

2. Do fibroblasts contribute to the increased SFRP4 expression observed in SSc? And can recombinant SFRP4 treatment of fibroblasts regulate those activities observed in Q1?

3. Is the expression of TGFβ-regulated CAV-1 expression important in reproducing the SSc fibroblast phenotype, independently or as a result of Wnt/TGFβ signalling, observed in Q1 & Q2?

4. Is canonical Wnt signalling hyperactivation in fibroblasts regulated by crosstalk between the Wnt and TGFβ signalling pathways?

2 Methods

2.1 Cell lines and culture

Adult human dermal fibroblasts (Healthy Control, HC) (TCS Cellworks, Buckingham, UK; PromoCell GmbH, Heidelberg, Germany) were immortalised using the stable integration of a human telomerase reverse transcriptase (hTERT) vector that expressed the telomerase catalytic subunit, which maintains cell immortality through the addition of TTAGGG repeats to the telomere ends of the chromosome. These fibroblasts were used as a first screen and subsequent experiments were repeated in HC fibroblasts. Adult dermal fibroblasts were cultured in Dubecco's Modified Eagle's Medium (DMEM) (Sigma-Aldrich, Poole, UK) containing 10% fetal calf serum (Biosera, Ringer, UK). Small molecule inhibitors (Table 4) were introduced prior to stimulation with recombinant human TGFβ (Sigma), Wnt-3a, Wnt-5a, Wnt-10b, Wnt-11a and SFRP4 (R&D systems, Abingdon, UK).

2.2 Study subjects and controls

Informed consent was obtained from all patients, and studies were granted approval by the Leeds Teaching Hospitals NHS Trust Medical Ethics Committee and the Ethical Committee of Verona University. All scleroderma patients fulfilled the American College of Rheumatology (ACR) classification criteria for SSc, classified as dcSSc according to skin involvement evaluated by the modified Rodnan total skin score (mRSS). Patient fibroblasts were taken under the CONVAS study, approved by the LTH REC approval

number 10/H1306/88. Animals used in this study were housed in a clean conventional colony, with access to food and water *ad libitum*. Strict adherence to institutional guidelines was practiced, and full local ethics committee and Home Office approvals were obtained prior to animal procedures.

2.3 Statistical analysis

Statistical analyses were performed using nonparametric Mann-Whitney U tests for unpaired samples, the Wilcoxon signed rank test for paired samples and the Spearman's rank correlation test for correlations. Experimental data are presented as the mean ± standard error of the mean. A P-value <0.05 was considered statistically significant. Statistical analysis was performed using GraphPad Prism software, version 5.0 (San Diego, CA, USA).

2.4 SFRP4 ELISA

The concentration of SFRP4 present in the sera of SSc patients was determined using a commercially available sandwich immunoassay (SFRP4 ELISA, USCNK lLife Science Inc, Wuhan, China) as per the manufacturer's instructions. In summary, a standard curve was prepared by serial dilution with a detection range between 15.6 pg/ml and 1000 pg/ml, using the supplied recombinant protein and standard diluent. Sera samples, diluted 1:200 and protein standards were added to the pre-coated 96 well ELISA plate and incubated for 2 hr at 37^{o}C. Detection reagent A was added for 1 hr at 37^{o}C and the plate washed 3 times using the supplied wash buffer.

Detection reagent B was added for 30 min at 37^{o}C and followed by wash buffer 3 times. Substrate solution was added and catalysis proceeded for a period of up to 5 min at room temperature. The reaction was stopped using stop solution and the absorbance of each well was read at 450 nm using an OpsysMR plate reader (Dynex Technologies).

2.5 TβRIIΔk-fib transgenic mice

The generation of TβRIIΔk-fib transgenic mice has been described previously (Denton et al., 2003). Constitutive activation of TGFβ signalling in transgenic mouse fibroblasts is driven through the fibroblast-specific expression of a kinase deficient TGFβ Receptor II gene, targeted using the specific pro-alpha2(I) collagen (*Col1a2*) gene enhancer and promoter (Denton et al. 2003). Mice were genotyped using PCR with primers specific to *LacZ* as an internal control. Dermal tissue was taken from these mice and each experiment was performed on at least 3 mice for each condition and compared to age-matched littermate controls and then performed at least in duplicate. Mice were aged 6-8 weeks for all experiments.

2.6 Histology studies

Formalin-fixed skin specimens from TβRIIΔk-fib transgenic mice were embedded in paraffin and sections were cut at 5 microns. Skin fibrosis was evaluated by dermal thickness between the dermal-epidermal boundaries to the dermal-subcutaneous fat boundary and further evaluated by Masson's Trichrome blue staining of collagen. Antigen retrieval was carried out using

10 mM citrate buffer and sections were stained with isotype control antibody (Sigma) and anti-AXIN2 antibody (Sigma) followed by for 1 hour incubation at room temperature followed by StreptAB-Complex-HRP (Dako Cytomation, Glostrup, Denmark) for 30 minutes and visualised with 3,3′diamino-benzidine terahydrochloride (DAB; Vector Laboratories). A concentration matched and isotype matched antibody was used for controls. Microscopic analysis was performed using an Olympus BX50 with MicroFire (Optronics, USA) connected to a micro-bright field camera and images were captured using Stereo Investigator software at 10X-20X magnification.

2.7 Short-hairpin RNA mediated gene silencing

shRNAmir GIPZ lentiviral particles were used to transduce HC fibroblasts with either a non-targeting negative control (SCR) or CAV-1 shRNA as listed in Table 1 (Open Biosystems, Surrey, UK). Cells were seeded into a 6 well plate at 50-60% confluence. The medium was changed to 1 ml of serum and antibiotic free DMEM containing a 1:50 dilution of lentiviral particles, with an initial titer of 1 x 10^8 TU/ml, and were incubated at 37^{o}C for 6 hr, after which an additional 1 ml of DMEM/ 10% FCS was added and the fibroblasts were incubated for a further 72 hr. The efficiency of integration was determined for the shRNAmir-containing pGIPZ lentiviral vector microscopically on the basis of vector-driven green fluorescent protein (GFP) co-expression. Stably transduced fibroblasts were then selected in media containing 1.0 µg/ml puromycin (Life Technologies) for 10 days.

Table 1. Lentiviral particle technical data

Catalogue Number	Clone ID	Abbreviated Code	Titre (TU/ml)	Gene Symbol
V3LHS_312897-100991154	V3LHS_312897	shCAV_97	2.38x10^8	CAV1
V2LHS_150248-98912154	V2LHS_150248	shCAV_48	2.95x10^8	CAV1
V3LHS_312899-100989763	V3LHS_312899	shCAV_99	2.96x10^8	CAV1
RHS4348	NA	NA	3.83x10^8	Non-Silencing Sequence

2.8 Small interfering RNA (siRNA) mediated gene silencing

Cells were seeded to reach a confluence of 50-70% on the day of transfection in DMEM/ 10% FCS. N-TER transfection system (Sigma-Aldrich) was used to transfect all siRNA oligos (Table 5) according to the manufacturer's protocol for serum containing media. Transfection efficiency was determined by immunofluorescence using the Alexa Fluor-488 AllStars negative control (Qiagen) in the presence and absence of serum containing media. Briefly, 10 μM siRNA stock was diluted into siRNA dilution buffer, while the N-TER reagent was diluted into dH_2O. Both were vortexed before being mixed together in a ratio of 1:1 and vortexed again. The transfection mix was incubated for 15 min to allow for complex formation, thereafter it was added to DMEM/ 10% FCS at a ratio of 1:10 to yield a final siRNA concentration of 20 nM. Medium was removed form the culture plate and changed in to the medium containing the transfection complexes. Gene

silencing was monitored between 24-96 hr post-transfection and confirmed by qRT-PCR and Western blot. Optimal siRNA delivery into HC fibroblasts cells was performed by first optimising transfection conditions. Serum compatibility was tested post-transfection complex formation, where these complexes were delivered to fibroblasts in serum containing or in serum absent media. This was carried out in parallel with varied molar concentrations of oligonucleotide across a range of 10nM, 20nM and 40nM, while the transfection reagent was kept constant across a 24 hr period. These oligonucleotides contained AlexaFlour-488, which enabled the visualization of transfection efficiency. Using Fluorescent microscopy in tandem with phase-contrast microscopy, two independent images from the same region were used to produce an overlaid image (Sup Figure 10.1).

2.9 RNA extraction and purification

Extraction and purification of total cellular RNA was performed using the RNeasy kit (Qiagen, Crawley, UK) and removal of any contaminating genomic DNA was achieved using on-column DNase I digestion (Qiagen) following the manufacturer's protocol. Briefly, 350 µl RTL buffer was used to directly lyse fibroblasts in culture plate wells and lysates were transferred to microcentrifuge tubes, where an equal volume of 70% ethanol was then added to precipitate RNA and facilitate binding to the RNeasy spin column silica-based membrane. Columns were centrifuged 10,000 x g for 30 seconds at room temperature and supernatant discarded. The columns were then washed with 350 µl RW1 buffer and centrifuged at 10,000 x g for 1 min. On-column DNase I digestion was performed (1:8; DNase I:RDD buffer) for

15 min at room temperature to degrade genomic DNA, then the samples were centrifuged. Columns were washed with RW1 buffer and centrifuged. Next, the columns were washed with RPE buffer and centrifuged at 10,000 x g for 1 min. Columns were centrifuged empty for 2 min in clean collection tubes to remove all traces of carryover RPE. RNA was then eluted from the column using 30 µl of nuclease free water, added directly to the column membrane and centrifuged at 10,000 x g for 1 min into nuclease free microcentrifuge tubes.

2.10 cDNA preparation

cDNA was prepared from RNA samples was prepared using a first-strand cDNA synthesis kit (Life Technologies), following the manufacturers' protocol, to produces a 1:1 conversion of RNA to cDNA. For first stage of synthesis reaction up to 2 µg RNA, 100 ng random primers and 10 mM dNTPs were added to an RNase free thin-walled PCR tube to a total volume of 13 µl and incubated at 65^{o}C for 5 min followed by 1 min incubation on ice to allow primer to anneal to the RNA template. 1x First-strand buffer, 10 mM DTT, 40 units RNaseOUT and 200 units of SuperScript II reverse transcriptase were then added to each reaction to a total volume of 20 µl. The thermal cycler was set to 25^{o}C for 5 min, 50^{o}C 1 hr, 70^{o}C for 15 min. Samples were stored long term at -20^{o}C.

2.11 Measuring RNA and DNA concentrations

DNA and RNA concentrations were determined using the NanoDrop (Thermo-Fischer), which measured the absorbance of the sample at 260 nm and normalised it to the absorbance at 340 nm.

$$c_{DNA} = (A_{260} - A_{340})$$

$$c_{RNA} = (A_{260} - A_{340})$$

Further, the ratio between the 260 nm and 280 nm absorbance measurements was used to evaluate purity. All samples tested reached acceptable levels of DNA ~1.8 and RNA ~2.0.

$$purity \rightarrow \frac{(A_{260} - A_{340})}{(A_{280} - A_{340})}$$

2.12 Primer design

Primers used in qRT-PCR (Table 7) were designed using Primer Express 3.0 software (Applied Biosystems) and were commercially synthesised and quality controlled (MWG Eurofins, Germany). Primers evaluating spliced transcripts of specific genes were designed to lie within exons boundaries. Exclusively, analysis of the *AXIN2* primary transcript utilised primers spanning intron-exon junctions specifically limiting amplification to unprocessed RNA.

Figure 2.1. Schematic representation and location of primers spanning intron-exon junction of exon 3 in the AXIN2 reference sequence.

2.13 Quantitative real-time PCR

SYBR green technology was used to measure the expression of mRNA. 2x Power SybrGreen Master Mix (Applied Biosystems), containing SYBR green and ROX dyes, was mixed with 10-50 ng cDNA and 50 nM forward and reverse primers up to a total volume of 25 µl in MicroAmp Optical 96 reaction plates (Applied Biosystems, UK). All reactions were carried out in triplicate. The plates were sealed using MicroAmp Optical adhesive film (Applied Biosystems) and run on an ABI 7900 Real-time PCR system using the program listed in Table 2. qRT-PCR thermocycler program. The amplification in step 2 was followed by a melting curve analysis in step 3 to ensure the amplification specificity for a given primer set. Only samples that displayed one peak, with high amplitude and a defined melting temperature were included in the analysis. Initial analysis was carried out using SDS v2.3 software (Applied Biosystems). Post-analysis was performed in Excel to determine the normalised gene target amplification using the efficiency-corrected ΔΔCt method.

Table 2. qRT-PCR thermocycler program

Stage	Temp (^{o}C)	Cycles	Time (sec)
1	95	1	10
2	95 60	40	15 60
3	95 60 95	1	15 60 15

2.14 Cell lysate preparation

Cells were incubated on ice and washed twice in ice-cold phosphate buffered saline (PBS) prior to the addition of RIPA cell lysis buffer (Sigma), supplemented with complete protease and phosphatase inhibitor cocktails to the recommended concentration (Roche). Cells were lysed in 6 well plates with 100 µl of lysis buffer, and further disruption was achieved using a cell scraper. Cell lysates were collected into a 1.5 ml microfuge tube and incubated on a rotating mixer for 15 min. Cell debris was pelleted by centrifugation at 16,000 x g at 4^{o}C for 10 min and lysates were collected into new microfuge tubes and the protein concentrations quantified.

2.15 Cytosolic / Nuclear preparation

Cell supernatants were removed and fibroblasts were lysed in 0.5% Triton X-100 lysis buffer (50 mM Tris-HCL (pH 7.5), 0.5% Triton X-100, 137.5 mM NaCl, 10% Glycerol, 5 mM EDTA, protease inhibitor cocktail (Roche)) and further disrupted with a cell scraper. Lysed fibroblasts were centrifuged at 16,000 x g for 10 min at 4^{o}C. The supernatant / cytosolic fraction was transferred to a microcentrifuge tube and the nuclei resuspended 1 ml lysis buffer to wash the pellet and centrifuged at 16,000 x g for 15 min at 4^{o}C. The supernatant was removed and a volume of 1x LDS sample buffer and 1x Reducing agent was added to both the nuclear and cytosolic fractions and reduced at 70^{o}C for 10 min. Samples were run on PAGE gels, Western blotted and developed as previously described. Fractionation was checked using Histone H3 antibody for nuclear purity and hypoxanthine phosphoribosyltransferase 1 (HPRT1) for cytosolic purity.

2.16 Protein quantification

The protein concentration in whole cell lysates was quantified using the bicinchoninic acid (BCA) colorimetric protein assay kit (Thermo-Fisher, UK) as per manufacturer's protocol. Briefly, a standard curve was generated using bovine serum albumin (BSA) sequentially diluted in PBS 1:2 over a range of 0 to 2 mg/ml. Lysates were generally diluted 1:3 and 10 µl of cell lysate and BSA standard were transferred in duplicate into a 96 well plate. BCA reagent A was added 1:50 parts into reagent B, and 200 µl were added to each sample well. The plate was then incubated at 37^{o}C for 30 min to facilitate the colorimetric change. The difference in absorbance was measured at 570 nm using an OpsysMR plate reader (Dynex Technologies, West Sussex, UK) and the protein concentrations in the assay were calculated by generating a standard curve of the known concentration of BSA.

2.17 Western blotting

A volume of cell lysate with a protein concentration of 20-30 µg was added to 1x NuPage lithium dodecyl sulfate (LDS) sample buffer pH 8.0 (Life Technologies) and 1x NuPage reducing agent (Life Technologies) to a total of 45 µl. These protein samples were then incubated at 70^{o}C for 10 min. Reduced samples or 3 µl of a protein ladder 7.5-250 KDa (LI-COR, Cambridge, UK) were then loaded into a NuPAGE® Novex 8-12% Bis-Tris sodium dodecyl sulphate polyacrylamide gel electrophoresis (SDS-PAGE) cassette (Life Technologies) housed in the XCell4 surelock midi cell apparatus, containing 1x SDS MES running buffer (Life Technologies) and

1x antioxidant (Life Technologies) and run at 200 volts for 1 hr. Proteins were transferred from the gel to polyvinylidene difluoride membrane (PVDF) (Amersham, UK) using a midi-transfer apparatus (Bio-Rad, Hertforshire, UK) with 1x NuPage transfer buffer and run at 100 volts for 1 hr at 4^{o}C.

PVDF membrane was blocked in 1x Tris-buffered saline (TBS) pH 7.4 plus milk or BSA for 1 hr at room temperature. Immunodetection was performed using primary antibodies diluted in 1x TBS and incubated with the membrane for 1 hr at room temperature on a roller. Membranes were washed three times in 1x TBS + 0.1% Tween-20 (TBST) for 10 min each. Secondary antibodies that were conjugated to horseradish peroxidase enzyme (HRP) and directed against the primary antibody species, were diluted in 1x TBS and incubated for 1 hr at room temperature. Membranes were then washed for five time 1x TBST for 10 min each. Protein detection was visualised on the membranes by incubation with SuperSignal Pico chemiluminescent substrate (Thermo-Fisher, UK), diluted in a 1:1 ratio of reagent A to reagent B, for 5 min at room temperature. Excess substrate was blotted off the membrane, which was then sealed in plastic wrap and exposed to photographic film. The exposure was then developed in a dark room, using an SRX-101A developer (Konica).

2.18 AXIN2 mRNA and protein stability

The half-life of *AXIN2* mRNA was determined using actinomycin D. Briefly, fibroblasts were serum starved in DMEM/ 0.5% FCS for 24 hours followed by incubation in complete media alone or with 5 ng/ml of TGFβ. 0 to 120 min after the addition of 5 µg/ml of actinomycin D (Sigma-Aldrich), fibroblasts

were harvested and total cellular RNA was isolated. *AXIN2* mRNA was quantified by quantitative real-time PCR (qRT-PCR). Cycloheximide was used to evaluate the protein stability of AXIN2. Fibroblasts were starved in DMEM/ 0.5% FCS for 24 hours prior to treatment with 30µg/ml cycloheximide (Sigma-Aldrich) or media alone and in the presence or absence of TGFβ for 2-6 hr. Cells were lysed, total protein was extracted and normalised for protein concentration as previously described. AXIN2 expression was visualised by Western blot.

2.19 *AXIN2* 3'UTR analysis

Bioinformatics analysis was performed on *AXIN2* mRNA by consulting the online database ARESite (http://rna.tbi.univie.ac.at/cgi-bin/ARESite.cgi) and was found to contain three pentamer motifs in the 3'UTR.

2.20 Plasmid preparation

Competent *E. coli* strain DH5alpha (New England Biolabs) were thawed on ice for 10 minutes. 1 ng of plasmid was triturated and incubated on ice for 30 min. The *E.coli* and plasmid were then heat shocked at 42^{o}C for 0.5 min and cooled on ice for 5 min. Then, 950 µl of room temperature SOC medium was added and was incubated with shaking at 250 rpm, 37^{o}C for 1 hr. 100 µl was then spread on agar plates containing 100 µg/ml ampicillin and incubated at overnight at 37^{o}C. Single colonies from these plates were inoculated into 40 ml LB broth containing 100 µg/ml ampicillin and cultured at 37°C, shaking at 250 rpm for 16 hr. The next day, 3 ml of the suspension was transferred into

a new tube and centrifuged at 10,000 x g for 10 min. The pellet was resuspended in fresh LB broth and mixed 1:1 with 80% glycerol and stored at -80^{o}C as a stock. The plasmid from the remaining 37 ml was harvested using a plasmid plus Midiprep kit (Qiagen), according to the manufacturers instructions. Briefly, the 37 ml were centrifuged at 10,000 x g for 10 min and resuspended in 2 ml Buffer P1, followed by 2 ml P2 and the tube was inverted 6 times and incubated for 3 min at room temperature. Then 2 ml of buffer S3 was added and the tube inverted 6 times. The lysate was transferred to a QIAfilter and incubated for 10 min at room temperature. The lysate was separated from the cell membrane debris by plunger. 2 ml of buffer BB was added to the cleared lysate and inverted 6 times. This was transferred to a Midi spin column with a tube extender and the solution drawn thought as -300 mbar on a vacuum manifold. The midi spin column and captured DNA were washed with 700 µl of buffer ETR followed by 700 µl buffer PE using the vacuum manifold. Residual buffer was removed by placing the midi column in a microcentrifuge tube and centrifuging at 10,000 x g for 1 min. The midi column was then placed in a clean microcentrifuge tube, 200 µl of Buffer EB added and the DNA eluted by centrifugation at 10,000 x g. The DNA concentration was measured and the plasmid used for transfection experiments.

2.21 Plasmid DNA transfection efficiency

Similar to the method employed for siRNA, delivery of plasmid DNA into HC fibroblasts was optimised. Plasmid DNA has a higher barrier of entry into the cell, particularly of primary origin, and therefore a transfection method that captured a significantly cross-section of the cell population would be sought. An IRES-GFP plasmid was used to visualise transfection efficiency by immunofluorescence (Sup Figure 10.2 & Sup Figure 10.3). Given the total length of the reporter constructs that were used in this study (<5Kb), the transfection of the pIRES-GFP (5.2Kb) would be considered equivalent. The pIRES-GFP and Lipofectamine 2000 transfection reagent (TR) were ratios evaluated are noted in Table 3.

.

Table 3. DNA:transfection reagent optimisation

TR (µl)	pIRES-GFP (µg/µl)	Total volume (µl)	Ratio
1	1	1000	1:1
1	2	1000	1:2
2	1	1000	2:1
2	2	1000	2:2
3	1	1000	3:1
3	2	1000	3:2
4	1	1000	4:1
4	2	1000	4:2

2.22 TOPFlash reporter assay

Fibroblasts were transfected with either the TOPFlash TCF/LEF–firefly luciferase reporter vector that contains two sets of 3 copies of the wild-type TCF/LEF consensus sequence (AGATCAAAGGgggta), one of which is in the reverse orientation, or the FOPFlash luciferase reporter vector containing the same sequences but harboring mutations within the consensus sequence that affect DNA:protein binding (gift of R. Moon, University of Washington, Seattle, WA). pCMV-Renilla luciferase vector was co-transfected and this was used as a transfection control. Briefly, in 1 well of a 12 well plate, 1 µg of TOPFlash or FOPFlash vector and 0.1 µg pCMV-Renilla vector were added into 100 µl of Optimem containing 2 µl of Lipofectamine 2000 transfection reagent (Life Technologies) and incubated at room temperature for 15 min. This complex mix was then added drop wise onto fibroblasts cultured in 1 ml DMEM/ 10% FCS in a 12 well plate. The transfection complexes were removed after 2 hr to avoid unnecessary cell death and fibroblasts were washed with PBS and fresh DMEM/ 10% FCS added for 24 hr at 37°C, 5% CO_2. These fibroblasts were then starved for 24 hr prior to stimulation. Stimulations were carried out in DMEM/ 0.5% FCS medium for 2-72 hr with TGFβ the medium removed and stimulated with Wnt-3a in DMEM/ 0.5% FCS for 24 hr. Cells were then harvested and luciferase activity was measured using the dual luciferase reporter assay reagents (Promega), as per the standard protocol, and detected using a luminometer (Berthold Mithras). To account for transfection efficiency, the Firefly luciferase activity was normalised to Renilla luciferase activity and expressed as the percentage change compared to control.

2.23 TGFβ reporter assay

TGFβ activity was measured with both the p3TP-lux construct and the SBE4-Luc luciferase reporter constructs. p3TP-lux contains a 3TP promoter, three consecutive TPA response elements (TGAG/CTCA) and part of the plasminogen activator inhibitor 1 (PAI-1) promoter region cloned into pGL2-Luc. SBE4-Luc contains a Smad3 specific reporter for TGFβ activity, containing four copies of the SBE (GTCTAGAC) cloned into pBV-Luc. 0.75 µg of the p3TP-lux or 1 µg pSBE-luc reporter was transfected along with 0.075 µg or 0.1 µg of pCMV-Renilla luciferase vector, respectively, in 100 µl of Optimem containing 2.5 µl of Lipofectamine 2000 transfection reagent (Life Technologies) according to the manufacturer's instructions. This complex mix was then added drop-wise onto fibroblasts cultured in 1 ml DMEM/ 10% FCS in a 12 well plate. The transfection complexes were removed after 2 hr to avoid unnecessary cell death and fibroblasts were washed with PBS and fresh DMEM/ 10% FCS added for 24 hr at 37°C, 5% CO_2. These fibroblasts were then starved for 24 hr prior to stimulation. Luciferase activity was measured using the dual luciferase reporter assay reagents (Promega) as per the standard protocol and detected using a luminometer (Berthold Mithras). Transfection efficiency was evaluated by normalising Firefly luciferase activity to the Renilla luciferase activity.

2.24 Immunofluorescence

Paraffin embedded tissue biopsies (5µm thick) were deparaffinised by incubation with xylene (Sigma) for 10 min two times and 100% ethanol for 10 min twice. Antigen retrieval was carried out using 10 mM citrate buffer for 20

min. For *in vitro* studies, the fibroblasts were plated in 4-well Falcon culture slides (Becton Dickinson) and initially cultured in 500 µl of DMEM/ 10% FCS per well. Stimulations were performed in DMEM/ 0.5% FCS. The fibroblasts were then washed twice with 1 ml of PBS. Cell monolayers were then fixed in 4% paraformaldehyde (Sigma) for 10 min at room temperature, washed twice with 1 ml of PBS and this was followed by incubation in cell permeablisation buffer (PBS + 0.1% Trition-X100 + 0.2% BSA) for 20 min room temperature.

Sections from both methods were blocked with 2% bovine serum albumin (BSA) for 1 hr at room temperature, prior to incubation with primary antibodies (Table 6) diluted in PBS pH7.4 overnight at 4^{o}C. Sections were then washed three times in PBS before incubation with fluorophore-conjugated secondary antibodies, either sheep anti-rabbit-CY3, anti-mouse-FITC (Table 6) for 1 hr at room temperature. Vector shield mounting medium (Vector, Peterborough, UK) containing 4', 6-diamidino-2-phenylindole (DAPI) was used to stain cell nuclei and to fix the coverslip onto the slide.

2.25 Confocal laser scanning microscopy

Confocal images were acquired using an Olympus BX61 upright fluorescence microscope with 20x dry and 40x oil immersion objectives. Images were captures using EZ-C1 3.80 software (Nikon). DAPI fluorescence was measured using the 405 nm laser with excitation and emissions wavelengths of 345/455 nm, CY3 fluorescence was measured using the TRITC filter with a 543 nm laser (Ex/Em 577/590) and FITC fluorescence was measured using the with a 488 nm laser (Ex/Em 488/507

nm). Widefield fluorescent images were acquired using an Olympus BX61 upright fluorescence microscope with a 20x and 40x objectives.

2.26 Myofibroblast counts

ImageJ software was used to take measurements from two separate fluorescent channels. Under the same conditions, data from the blue channel was captured as a function of the fluorescent DAPI stained nuclei and the red channel captured fluorescent data from the anti-mouse-CY3 used to detect the α-SMA antibody stained stress fibres. The integrated density of florescence (IDF) was taken from both channels and the IDF for each was used to calculate the α-SMA positive fluorescence with respect to nuclei fluorescence in each image. Three separate images were taken per well and all treatments were normalised on either HC fibroblasts or SCR transfected fibroblasts under basal conditions and represented as fold change. This method was validated using individual counts of negative and α-SMA positive nuclei, which exhibited similar results when the data was represented as fold change in positive cells over total cell count.

2.27 Collagen gel contraction assays

Collagen gel contraction assays were prepared from a standard kit (Cell Biolabs). Briefly, one part of fibroblasts were mixed with four parts of collagen gel preparation, added to a 12 well plate and incubated for 1 hr at 37°C for gel polymerisation. Following this incubation, 1 ml of DMEM was added and the plate was incubated for a further day. Next, the gels were

released from the sides of wells, treated or left untreated and 24-72 hr later the images were taken at various time points with a Gel Doc (BioRad). Treatment related mechanical force generation was evaluated as the percentage change in gel area relative to that of untreated controls as determined by ImageJ software.

2.28 Cell viability

The MTT (3-(4,5-Dimethylthiazol-2-yl)-2,5-Diphenyltetrazolium Bromide) assay (Sigma-Aldrich) measures mitochondrial integrity, which can be used as a measure of cell viability and cytotoxicity. Briefly, 1 x 10^4 fibroblasts were plated in 100 µl DMEM/ 10% FCS in a 96 well plate. The medium was removed the next day an the fibroblasts were then starved in DMEM/ 0.5% FCS for 24 hr. Cell treatments were carried out in the presence of the inhibitor or DMSO in a total volume of 200 µl. After which, 20 µl of 5 mg/ml fresh MTT reagent was then added to the plate and incubated for 6 hr at 37^{o}C and 5% CO_2. 180 µl medium was removed, the fibroblasts lysed and the formazan crystals solubilised in 130 µl of DMSO by trituration and left for 10 min. The color change of the yellow MTT to the purple formazan was then measured using a spectrophotometer set to a wavelength of 540 nM. Viability was measured as the percetage change in treated samples compared to DMSO treated controls**.**

Table 4. Small molecule inhibitor inventory

Name	Full designation	Inhibition	Supplier
FH535	N-(2-Methyl-4-nitro)-2,4-dichlorosulfonamide, Wnt Pathway Inhibitor IX	β-Catenin	Calbiochem
SIS3	6,7-Dimethoxy-2-((2E)-3-(1-methyl-2-phenyl-1H-pyrrolo[2,3-b]pyridin-3-yl-prop-2-enoyl))-1,2,3,4-tetrahydroisoquinoline, Specific Inhibitor of Smad3	SMAD3	Calbiochem
XAV939	2-(4-(Trifluoromethyl)phenyl)-7,8-dihydro-5H-thiopyrano[4,3-d]pyrimidin-4-ol, Wnt Pathway Inhibitor V	TNKS1/2	Calbiochem
SD-208	Transforming Growth Factor-β Type I Receptor Kinase Inhibitor V, 2-(5-Chloro-2-fluorophenyl)pteridin-4-yl)pyridin-4-yl amine	TβRI	Calbiochem
JNK Inhibitor	Anthra[1,9-*cd*]pyrazol-6(2*H*)-one, 1,9-pyrazoloanthrone	JNK1/ 2/ 3	Calbiochem
MK-2206	8-[4-(1-aminocyclobutyl)phenyl]-9-phenyl-2H-[1,2,4]triazolo[3,4-f][1,6]naphthyridin-3-one;dihydrochloride	Akt1/ 2/ 3	Calbiochem
Selumetinib	6-(4-bromo-2-chloroanilino)-7-fluoro-N-(2-hydroxyethoxy)-3-methylbenzimidazole-5-carboxamide	MEK1	Calbiochem
Wortmannin	(1S,6bR,9aS,11R,11bR)-1-(methoxymethyl)-9a,11b-dimethyl-3,6,9-trioxo-3,6,6b,7,8,9,9a,10,11,11b-decahydro-1H-furo[4,3,2-de]indeno[4,5-h]isochromen-11-yl acetate	PI3K	Calbiochem
VX-702	6-(N-carbamoyl-2,6-difluoroanilino)-2-(2,4-difluorophenyl)pyridine-3-carboxamide	p38α	Calbiochem
IWP-2	*N*-(6-Methyl-2-benzothiazolyl)-2-[(3,4,6,7-tetrahydro-4-oxo-3-phenylthieno[3,2-*d*]pyrimidin-2-yl)thio]-acetamide	PORCN	Calbiochem

Table 5. siRNA oligonucleotide inventory

Oligo name	Oligo type	Oligo code	Supplier
Caveolin-1	FlexiTube siRNA	Hs_CAV1_7	Qiagen
Caveolin-1	FlexiTube siRNA	Hs_CAV1_10	Qiagen
AllStars Negative Control	FlexiTube siRNA	SI03650318	Qiagen
Negative Control No.1	Silencer Select	4390843	Life Technologies
AXIN1	Silencer Select	s15814	Life Technologies
AXIN2	Silencer Select	s15818	Life Technologies
SMAD3	Silencer Select	s8400	Life Technologies
β-Catenin	Silencer Select	s436	Life Technologies
TTP-1	Silencer Select	s14978	Life Technologies
TTP-1	Silencer Select	s14979	Life Technologies

Table 6. Primary and secondary antibodies inventory

Antibody	MW (KDa)	Host	Catalogue number	Method	Supplier
β-Catenin	92	Rabbit	8480	WB, IF	Cell Signalling Technology
AXIN2	95, 98	Rabbit	2151	WB	Cell Signalling Technology
AXIN1	110	Rabbit	2087	WB	Cell Signalling Technology
α-Smooth Muscle Actin	37	Mouse	ab7817	WB, IF	Abcam
GAPDH	40	Mouse	ab8245	WB	GeneTech
TTP-1	42	Mouse	SAB4200565	WB	Sigma-Aldrich
DKK1	45	Rabbit	SAB4200565	WB	Sigma-Aldrich
Caveolin-1	22	Rabbit	sc-894	WB, IF	Santa Cruz
Phospho-Smad3	52	Rabbit	C25A9	WB	Cell Signalling Technology
Phospho-c-Jun (Ser73)	48	Rabbit	D47G9	WB	Cell Signalling Technology
SFRP4	50	Rabbit	ab32784	WB	Abcam
β-Actin	42	Mouse	AC-74	WB	Sigma-Aldrich
Anti-Rabbit	NA	Sheep	C2306	IF	Sigma-Aldrich

IgG-CY3					
Anti-Mouse IgG-FITC	NA	Sheep	C2306	IF	Sigma-Aldrich
Anti-Mouse IgG-CY3	NA	Sheep	C2181	IF	Sigma-Aldrich
Anti-Mouse IgG–HRP	NA	Sheep	A6782	WB	Sigma-Aldrich
Anti-Rabbit IgG-HRP	NA	Goat	P0448	WB	Dako

Table 7. qRT-PCR primer pair inventory

Primer Name	Sequence 5’ - 3’
COX2_F	GTT CCA CCC GCA GTA CAG AA
COX2_R	AGG GCT TCA GCA TAA AGC GT
V-MYC_F	TGT CAA GAG GCG AAC ACA CA
V-MYC_R	ACC TTG GGG GCC TTT TCA TT
CDKN2A_F	TTC GCT AAG TGC TCG GAG TT
CDKN2A_R	GGA CCG CGG TAT CTT TCC AG
TTP_F	TGC CAA ACC CCA CCC ATA AA
TTP_R	TAC AAG GGA AGC AGA CGA CC
HUR_F	TGG TAG TTA GAC CCC AGG CA
HUR_R	TGC GGC TTG GCA AAT TAC AC
DKK-1_F	GAC TGT GCC TCA GGA TTG TGT
DKK-1_R	CAG ATC TTG GAC CAG AAG TGT CT
SMAD3_F	ATG TCG TCC ATC CTG CCT TT
SMAD3_R	CGT TCT GCT CGC CCT TCT TC
COL1A2_F	GAT GTT GAA CTT GTT GCT GAG G
COL1A2_R	TCT TTC CCC ATT CAT TTG TCT T
CTGF_F	GTG TGC ACT GCC AAA GAT GGT
CTGF_R	TTG GAA GGA CTC ACC GCT G
AXIN2_F	CGG GAG CCA CAC CCT TC
AXIN2_R	TGG ACA CCT GCC AGT TTC TTT
COL1A1_F	CCT CCA GGG CTC CAA CGA G
COL1A1_R	TCA ATC ACT GTC TTG CCC CA

AXIN1_F	GTG GAG AAG GTG GAC TGA TAG G
AXIN1_R	GCT CCT GAG TAC GAG GTC ATC T
CTNNB1_F	AAG GCT ACT GTT GGA TTG ATT CG
CTNNB1 _R	CCC TGC TCA CGC AAA GGT
CAV1_F	TCC CTT CTG GTT CTG TCA
CAV1_R	TCC CTT CTG GTT CTG CA
α-SMA_F	TGT ATG TGG CTA TCC AGG CG
α-SMA_R	AGA GTC CAG CAC GAT GCC AG
Ribo16S_F	GTA ACC CGT TGA ACC CCA TT
Ribo16S_R	CCA TVV AAT CGG TAG TAG CG
SFRP4_F	TGT CTA TGA CCG TGG CGT GT
SFRP4_R	TCC ACT TAA CAT CCT CCG GG
PT9-1_AXIN2_F	TGA TGC GCT GAC GGA TGA TT
PT9-1_AXIN2_R	ATC CAC TCC CAA GCA AGC C

3 Evaluation of SFRP4 expression in SSc patient sera and fibroblasts

Differential gene expression analysis was used to determine highly expressed genes in SSc skin that were similarly expressed in Scl-GVHD skin, the fibrotic variant of GVHD, but not in GVHD or HC skin biopsies (Gillespie et al., 2011). Indeed, any identified genes could be of potential importance in regulating fibrosis or potentially act as biomarkers during fibrosis. The analysis revealed that *SFRP4*, a putative inhibitor of the canonical Wnt signalling pathway, was significantly upregulated in both SSc and Scl-GVHD but not in cGVHD skin biopsies (Gillespie et al., 2011). On this basis, the *ex vivo* expression and *in vitro* expression and function of SFRP4 were investigated to identify a possible association with fibrosis.

3.1 SFRP4 might reflect fibrotic activity in dcSSc patients

As SFRP4 is secreted, the protein concentration was determined in sera from 77 SSc patients and subsequently stratified against SSc disease index criteria. Of the 77 patients' sera tested, 39 were from lcSSc patients, and all were anti-centromere antibody (ACA) positive, while the remaining 38 sera were from dcSSc patients, of which 30 were positive Scl-70 antibody (also known as anti-topoisomerase I). Indeed, these two autoantibodies are typically used as clinical biomarkers in SSc disease classification and typically correlate with lcSSc and dcSSc subsets, respectively.

It was observed that those sera that were ACA negative had a higher mean SFRP4 concentration compared to those that were positive, 36.55 ng/ml ±

2.1 and 27.7 ng/ml ± 1.45, respectively ($P<0.001$) (Figure 3.1A). Conversely, patients negative for Scl-70 had a lower mean concentration of SFRP4 than those that were positive for the autoantibody, 28.71 ng/ml ± 1.67 compared to 36.19 ng/ml ± 2.51, respectively ($P<0.05$) (Figure 3.1A). Univariate analysis showed that the SFRP4 concentration did not correlate with the mRSS in the overall population (Figure 3.1B). However, SFRP4 concentrations inversely correlated with a reduced pulmonary function, as indicated by a reduction in the percentage diffusing lung capacity for carbon monoxide (%DLCO) (Figure 3.1C).

However, this might be as a result of the presence of idiopathic lung disease (IDL), pulmonary arterial hypertension (PAH) or, indirectly due to lung fibrosis. Therefore, the mRSS in patients with a normal-like lung function, DLCO ≥ 70.0%, was stratified against SFRP4 concentration and a direct relationship was observed in this subpopulation ($r=0.40$; $P<0.05$) (Figure 3.1D).

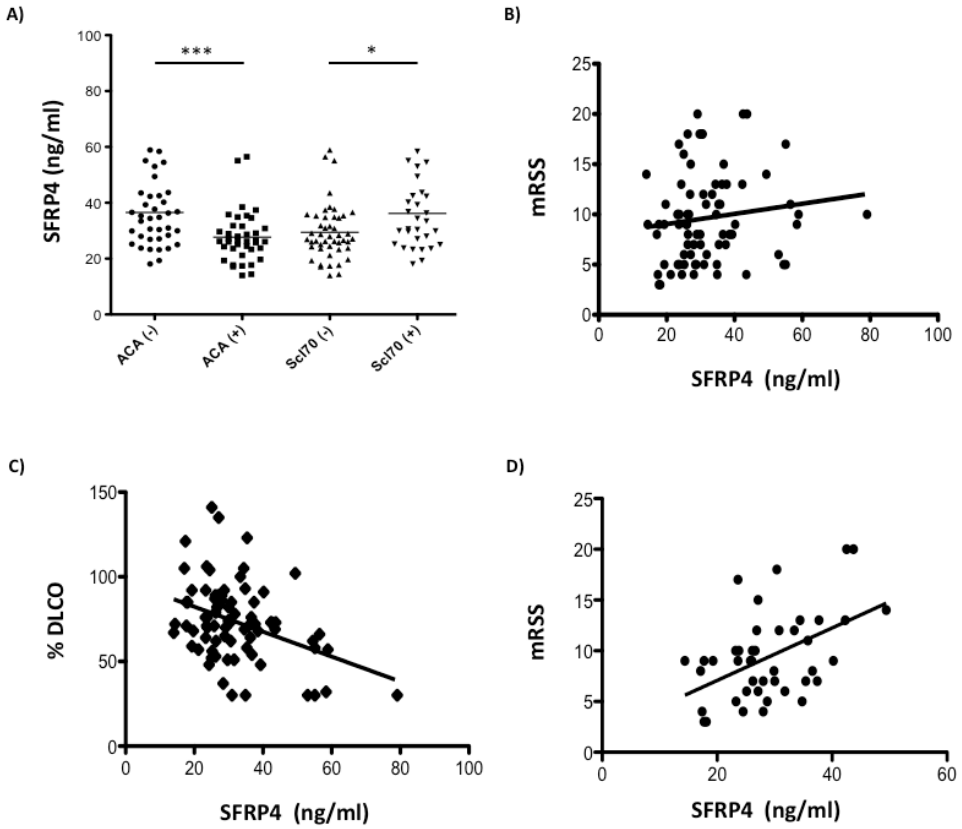

Figure 3.1 Increased SFRP4 concentration could reflect fibrotic activity in dcSSc patients.

Stratification of SFRP4 concentration against disease index criteria included A) ACA and Scl-70 autoantibody presence B) % diffusion lung capacity of carbon monoxide (%DLCO) C) mRSS and D) mRSS in patients with %DLCO of >70% (normal-like). Data shown as mean, n=77; Mann-Whitney test for unpaired, Wilcoxon test for paired samples and correlations were calculated using Spearman's rank correlation test, *P=0.05, ***P = 0.001.

3.2 SFRP4 expression is increased in SSc fibroblasts and regulated by canonical Wnt and TGFβ signalling

The mean concentration of SFRP4 in patient sera was higher in those positive for Scl-70, a biomarker typically associated with the fibrotic dcSSc subset. Taking this, together with the observation by Bayle *et al.,* who showed that expression was increased in fibroblast-like cells resident in the deep dermis of lesional dcSSc skin (Bayle et al., 2008), fibroblasts were

likely to contribute to the increased expression of SFRP4 in dcSSc tissues. Therefore, SFRP4 expression was quantified in fibroblasts from HC and SSc patients and also the factors involved in eliciting this expression were also investigated.

Indeed, the expression of *SFRP4* was increased by 364% ($P<0.0001$) in SSc compared to HC fibroblasts at basal level, and this observation was further confirmed at protein level (Figure 3.2A). Next, the factors involved in the regulation of SFRP4 expression were explored. As unconfirmed reports have described SFRP4 as a putative Wnt antagonist, both canonical (β-catenin-dependent) and non-canonical Wnt signalling pathway activation were investigated, using Wnt-3a (canonical ligand) and Wnt-5a (non-canonical ligand) agonist treatments, respectively. In addition, TGFβ signalling was also evaluated due to its fundamental role in reproduction of the fibrotic SSc phenotype.

Following treatment with Wnt-3a, *SFRP4* expression was induced by 144.0% ($P<0.0001$) in HC fibroblasts, while Wnt-5a treatment showed no significant effect on *SFRP4* expression. Interestingly, TGFβ treatment induced a 362.0% ($P<0.05$) increase in SFRP4 expression in HC fibroblasts (Figure 3.2B). Next, SSc fibroblasts were treated under the same conditions; like HC fibroblasts, Wnt-3a induced *SFRP4* expression by 206.1% ($P<0.0001$), and Wnt-5a treatment again showed no effect, while TGFβ treatment induced expression by 365.6% (Figure 3.2B). Indeed, for each treatment condition the induction of *SFRP4* expression was similar between HC and SSc fibroblasts (Figure 3.2B). At protein level however, SFRP4 expression was unchanged following both Wnt-3a and Wnt-5a treatment

although TGFβ treatment could still be observed to induce SFRP4 expression in both HC and SSc fibroblasts (Figure 3.2B).

As TGFβ induced the greatest change in expression of SFRP4, irrespective of fibroblast type, the mechanism of TGFβ-induced SFRP4 expression was evaluated in HC fibroblasts. TGFβ treatment mediated a dose-dependent increase in *SFRP4* expression following treatment at a concentration of 1.0 and 5.0 ng/ml (maximal effect) expressed by 138.4 and 198.0%, respectively (Figure 3.2C). Interestingly, at a concentration of 10 ng/ml *SFRP4* expression was significantly downregulated to 64.5% (Figure 3.2C). Treatment of HC with 5 ng/ml TGFβ showed a time-dependent increase in *SFRP4* expression by 170.9%, to 348.2% at 48 and 72 hr, respectively ($P<0.05$) (Figure 3.2D). This time-dependent increase in expression was also evident at protein level and coincided with increased expression of α-SMA, a fibroblast activation marker, and also showed an expected inverse relationship with CAV-1 expression at both 48 and 72 hr.

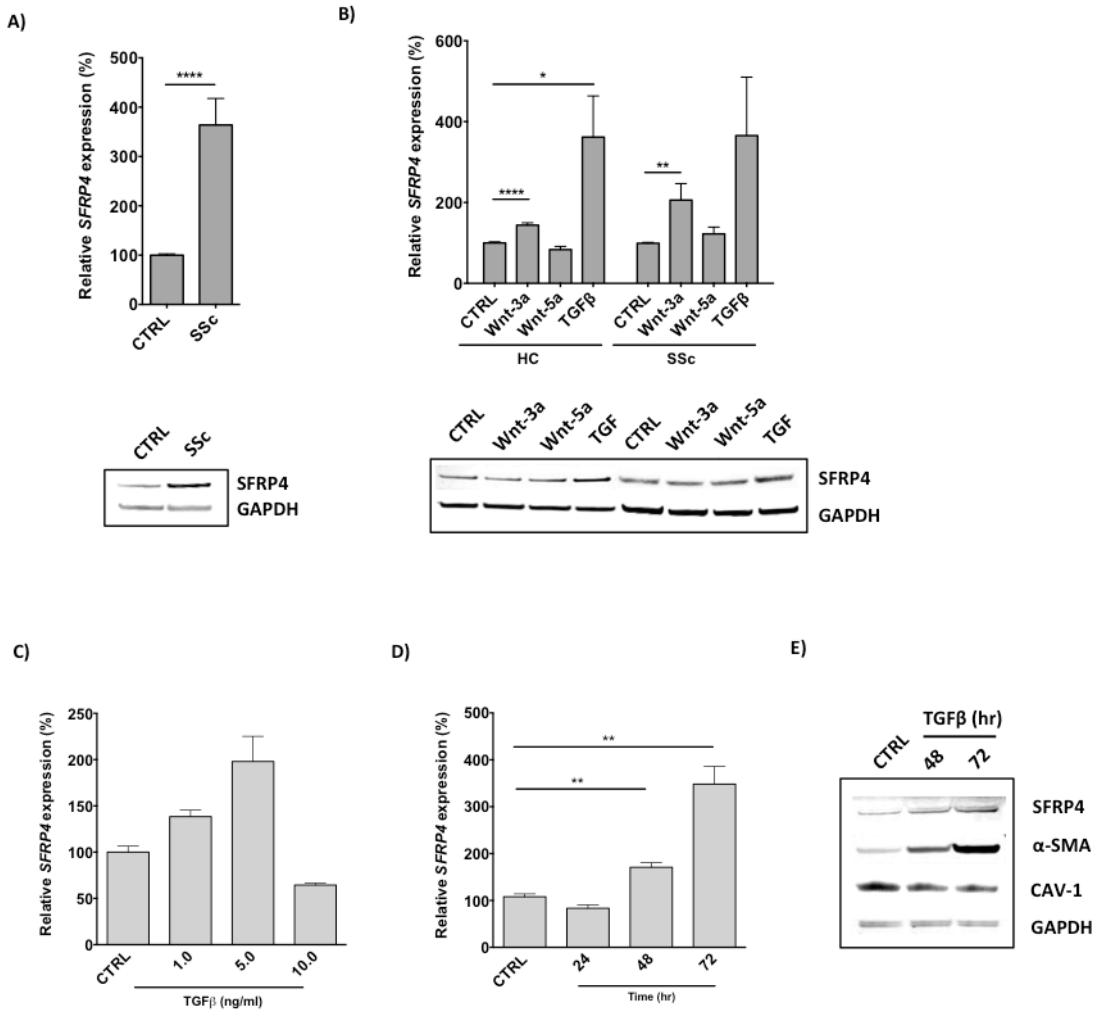

Figure 3.2 SFRP4 expression is increased in SSc fibroblasts and regulated by canonical Wnt and TGFβ signalling

SFRP4 expression was determined in HC and SSc fibroblasts at A) basal level or B) following 24 hr treatment with Wnt-3a (100 ng/ml), Wnt5a (100 ng/ml) or TGFβ (5 ng/ml) and quantified by qRT-PCR. Protein expression of SFRP4 and GAPDH (loading control) were determined by Western blot at C) basal level or D) following 72 hr treatments described in B. Following TGFβ treatment both C) dose (1.0, 5.0, 10.0 ng/ml) and D) time (24, 48, 72 hr) dependent effects upon SFRP4 expression were quantified by qRT-PCR. E) Protein expression of SFRP4, α-SMA, CAV-1 and GAPDH (loading control) were determined following 72 hr TGFβ treatment (5 ng/ml) by Western blot. Data shown as mean ± SEM, n=4; Mann-Whitney test for unpaired samples, *P=0.05, **P=0.05, ****P = 0.0001.

3.3 SFRP4 does not regulate canonical Wnt signalling activity or augment fibroblast activation

As SFRP4 is described as a putative inhibitor of the canonical Wnt signalling pathway its role in the regulation of canonical Wnt signalling was investigated in HC fibroblasts. Canonical/β-catenin-mediated signalling was determined by TOPFlash reporter activity, driven by the TCF/LEF transcription factor activation. Following treatment of HC fibroblasts with the canonical Wnt-3a agonist, TOPFlash activity was induced by 5.3-fold and Wnt-3a co-treatment with SFRP4 at either 100 or 1000 ng/ml showed a weak tend toward the inhibition of TOPFlash activity, reduced to 4.5-fold and 4.4-fold, respectively. Despite this reduction, no dose-dependent effect on the amplitude of TOPFlash activity was observed (Figure 3.3A).

Next, as SFRP4 was significantly induced by TGFβ it was therefore considered to have a potential role in the regulation of TGFβ-induced profibrotic activity. To investigate this further, rhSFRP4 was used to treat HC and SSc fibroblasts over a dose series of 100-1000 ng/ml and the effect on fibroblast activation determined through the expression of α-SMA, a known fibroblast activation marker. While TGFβ induced a significant upregulation, a trend toward a reduction in α-SMA expression was observed following independent SFRP4 treatment in both HC and SSc fibroblasts (Figure 3.3B). However, this was not found to be a dose-dependent effect and fibroblasts were affected similarly over the SFRP4 concentration series (Figure 3.3B). Further, SFRP4 at 100 and 1000 ng/ml showed no effect on myofibroblast presence in contrast to the significant increase induced by TGFβ treatment in both HC and SSc fibroblasts (Figure 3.3C).

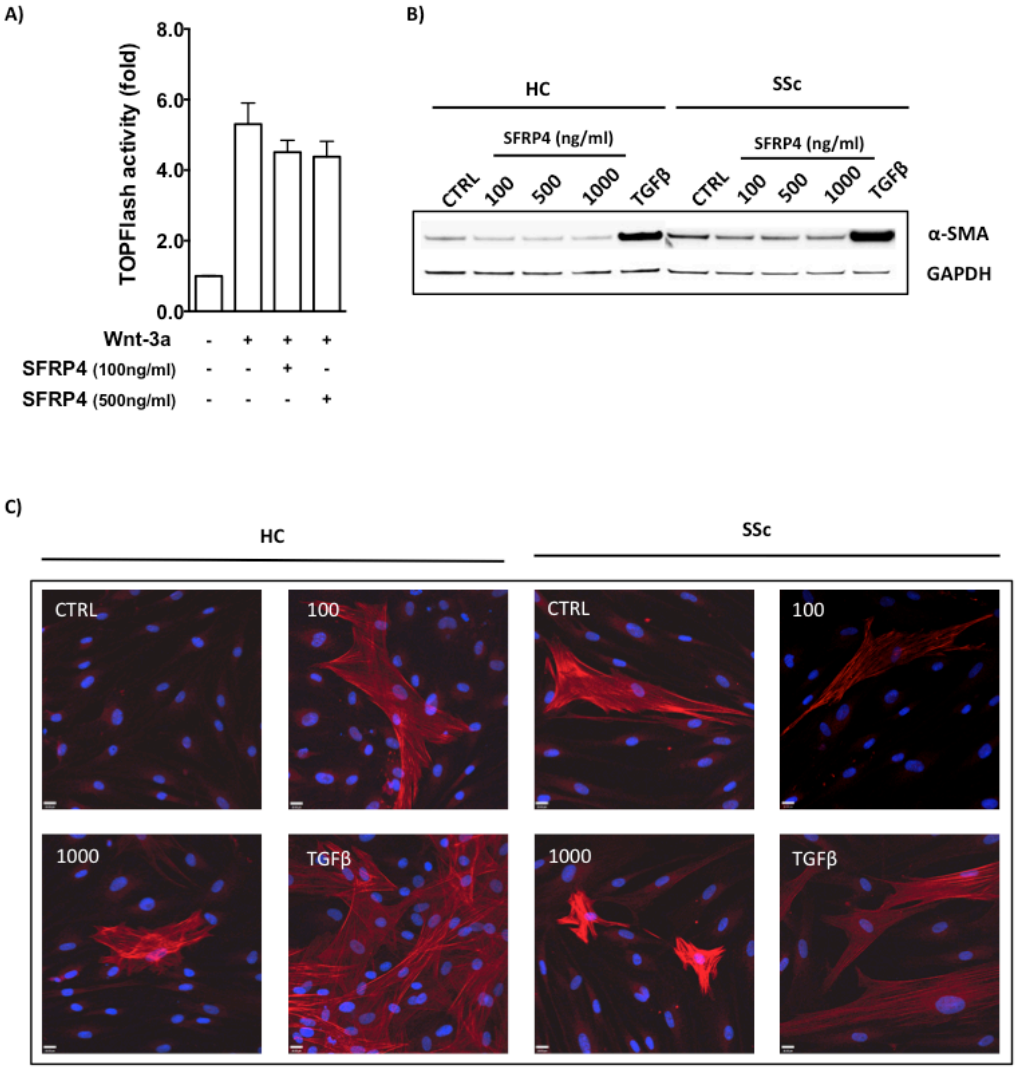

Figure 3.3 SFRP4 does not regulate canonical Wnt signalling activity or augment fibroblast activation

A) HC fibroblasts were treated with Wnt-3a (100ng/ml) in the presence and absence of SFRP4 for 24 hr and canonical signalling activity was determined by TOPFlash luciferase activity. Next, HC and SSc fibroblasts were treated with rhSFRP4 (100, 500, 1000 ng/ml) or TGFβ for 72 hr to evaluate any profibrotic activation through α-SMA and GAPDH (loading control) protein expression, determined by Western blot or D) myofibroblast differentiation was determined by α-SMA stress fibril formation by confocal microscopy using a CY3-conjugated secondary (red) directed against anti-α-SMA antibody, nuceli were stained with DAPI (blue) (magnification 20x). Data shown as mean ± SEM, n=2-3; Mann-Whitney test for unpaired samples.

3.4 DISCUSSION: Evaluation of SFRP4 expression in SSc patient Sera and fibroblasts

Differential gene expression analysis revealed that SFRP4, a putative inhibitor of the canonical Wnt signalling pathway, was highly upregulated in SSc skin comparable to Scl-GVHD, the fibrotic variant of GVHD, but not in GVHD or HC skin biopsies (Gillespie et al., 2011). It is notable that other reports have suggested that components of the Wnt signalling pathway are highly represented in models of experimental fibrosis by tissue and microarray studies and therefore SFRP4 could be of potential importance in regulating fibrosis (Bayle et al., 2007; Beyer et al., 2012; Wei et al., 2012). Since SFRP4 is a soluble protein, the concentrations present in SSc patient sera were determined to evaluate whether these might reflect the degree of fibrotic activity in SSc patients either directly or indirectly, and might also indicate its utility as a potential biomarker. Indeed, the mean SFRP4 concentration was higher in Scl-70 positive and lower in ACA positive patients; two SSc specific autoantibodies linked to the diffuse (dcSSc) and limited (lcSSc) subsets, respectively (Figure 3.1A). These data suggested that the increased concentrations of SFRP4 might be associated with the dcSSc subset, which was further supported by reciprocal tests for negative and positive autoantibody presence for either Scl-70 or ACA, respectively (Figure 3.1A). Despite an association with the dcSSc subset, no correlation was observed with the mRSS, a measure of fibrotic skin involvement. In addition, while there was no correlation with the forced vital capacity (FVC) an inverse correlation was identified with the %DLCO, where lower %DLCO can indicate a worsening lung function (Figure 3.1C). Indeed, a reduced %DLCO may be more representative of patients presenting with PAH and

ILD (Hudson et al., 2013; Sivova et al., 2013). Therefore, patients that had a normal %DLCO (>70%) were selected and, on analysis, those showed a direct relationship between SFRP4 concentration and mRSS (Figure 3.1D). These data supported the hypothesis that SFRP4 might reflect the degree of fibrotic activity in dcSSc patients; however, the plotted data presented do not show clearly defined relationships by linear regression. In order to be conclusive, these correlations should not be dependent on outliers and therefore by increasing the number of patients tested these correlations could be confirmed or disproved. Despite this limitation, the expression and potential function of SFRP4 were investigated further, *in vitro*, to identify any possible association with fibrotic activity.

Indeed, fibrobalsts are the key cellular mediators of fibrosis, and Bayle *et al.,* have previously shown that SFRP4 expression is increased *in vivo* in cells resident in the deep dermis of lesional dcSSc skin that were thought to be morphologically similar to fibroblasts (Bayle et al., 2008). This was supported by the mean concentration of SFRP4, which was higher in Scl-70 positive patients, a marker typically associated with the fibrotic dcSSc. Together, these data suggested that fibroblasts likely contributed to the increased expression of SFRP4 observed in patient sera. In support of this hypothesis, a comparative analysis of HC and SSc fibroblasts showed that SFRP4 expression, at both mRNA and protein level, was distinctly upregulated in dcSSc fibroblasts (Figure 3.2A). These data suggested that the increased SFRP4 observed could in fact be attributable to the fibroblast lineage.

As a putative Wnt antagonist, SFRP4 was likely to be regulated by canonical (β-catenin-dependent) and/or non-canonical (β-catenin-independent) Wnt

signalling pathway activation. In addition, TGFβ signalling was also evaluated due to its fundamental role in reproduction of the fibrotic phenotype *in vitro* (Varga & Pasche, 2009). Accordingly, a comparative analysis between HC and SSc fibroblasts revealed that both canonical Wnt signalling and TGFβ signalling could upregulate the expression of *SFRP4*; however, only TGFβ treatment upregulated SFRP4 expression at protein level (Figure 3.2B). On this basis, further experiments determined the dose- and time-dependent nature of TGFβ signalling in HC fibroblasts (Figure 3.2C-E). As SFRP4 expression was not evident following Wnt agonist treatment, this could be an effect of recombinant protein activity or its expression might be deficient as a result of indirect regulation by the canonical Wnt signalling pathway. Whether TGFβ induced SFRP4 expression was direct or indirect was not determined.

These data suggest that both canonical Wnt signalling and TGFβ crosstalk might act in parallel might act to negatively regulate canonical Wnt signalling through the upregulation of the putative inhibitor of Wnt signalling, SFRP4, Indeed, the Tsk-1 model of experimental fibrosis revealed that several components of the Wnt signalling pathways are upregulated, including *Wnt-2*, *Wnt-9a*, *Wnt-10b* and *Wnt-11*; *Dapper* (*Dact)-1* and *Dact-2*; *Wnt-induced secreted protein 2*; *Sfrp2*, *Sfrp4*, which suggest that the control of Wnt signalling might be important in resolving fibrosis (Bayle et al., 2008).

While SFRP4 is putatively involved in the regulation of the Wnt signalling pathway, the possibility remained that SFRP4 might be also be involved in the regulation of the TGFβ signalling pathway and therefore preliminary

experiments to test these hypotheses were the subsequent considerations of this study.

Canonical Wnt-3a agonist treatment of HC fibroblasts showed a clear activation of canonical Wnt signalling determined by TOPFlash reporter activity, a reporter driven by β-catenin-mediated activation of the TCF/LEF transcription factors (Figure 3A).

rhSFRP4 co-treatments were used to evaluate the putative inhibitory function of SFRP4 upon Wnt-3a-induced canonical Wnt signalling activation. Higher SFRP4 concentrations were used than those found in SSc patient sera. This was deemed necessary, as the local concentration of SFRP4 in tissues might be higher and, irrespective of cell-type, previous studies used SFRP4 at concentration that ranged between 125 pg/ml-400 ng/ml (Carmon & Loose, 2008; Muley et al., 2010). Therefore 100 ng/ml was decided to be an adequate starting concentration and 500 ng/ml was also included incase the activity of the recombinant protein was modest.

However, SFRP4 proved to be ineffective as a canonical Wnt signalling inhibitor, despite moderate to high doses SFRP4 co-treatment, which failed to reduce Wnt-3a-induced canonical signalling activity by any significant margin (Figure 3.3A). This data corroborates a previous study that found that while SFRP4 formed a complex with Wnt-3a (0-140nM), detected by surface plasmon resonance, in contrast to SFRP1/ SFRP2 (0-16nM) the Wnt-3a-induced expression of total β-catenin was unaffected (Wawrzak et al., 2007). These data suggest that SFRP4 might act to titrate the inhibitory activities of other SFRPs and preserve Wnt agonist activatory activity. Supporting this

hypothesis, SFRP1/2 were both found to be expressed simultaneously in haematopoietic stem cells and while both contributed to proliferation they had opposing effects upon self-renewal, which in essence provides evidence that the concentration balance between SFRPs can have a profound consequence on cellular function (Nakajima et al., 2009).

Of note was the ability of SFRPs to form complexes with Fz receptors facilitated via CRD:CRD interaction and that this interaction alone may be sufficient to activate Fz receptors signal transduction (Uren et al., 2000). In addition to Fz receptors, SFRP2 was able to participate in a complex with α5β1 integrin, in association with fibronectin, which mediated the protection of human mammary cancer cells from apoptosis (Lee et al., 2004). Therefore, SFRPs might independently activate receptor-mediated signal transduction independently of Wnt and might directly regulate fibroblast biology. Consequently, independent SFRP4 treatment was investigated for any agonistic effects on fibroblast activation and preliminary results indicated that, across a dose range of 100-1000 ng/ml, there was no increase in α-SMA expression or myofibroblast presence in both HC and SSc fibroblasts (Figure 3.3B, C). Far from activating fibroblasts, SFRP4 appeared to reduce the baseline expression of α-SMA. In light of these data and despite the absence of a dose effect, the possibility remained that SFRP4 might act to limit fibroblast activation though the regulation of Wnt/TGFβ signalling, which were subsequently explored in combinational co-treatment experiments, discussed in the next chapter.

Overall, these data suggested that the increased SFRP4 observed could in fact be attributable to the fibroblast lineage and also might be indicative of an

increased canonical Wnt or TGFβ signalling activity. Despite indications that the mean concentration of SFRP4 might be associated with dcSSc patients, an increased sample size is required. Further, rhSFRP4 did not appear to lead to profibrotic fibroblast activation nor did it limit canonical Wnt-induced activation of the canonical Wnt signalling pathway, despite its putative function as a Wnt antagonist.

4 Comparative analysis of Wnt/TGFβ signalling pathway activation and profibrotic gene expression in SSc and HC fibroblasts

Comparable to TGFβ signalling, activation of the Wnt/β-catenin signalling pathway has more recently been linked to the fibroblast-mediated pathogenesis of tissue fibrosis though tissue expression studies and models of experimental fibrosis (Beyer et al., 2012; Wei et al., 2012). Interestingly, both pathways contribute to the upregulation of SFRP4 expression, which is increased in the Tsk-1 mouse model of fibrosis, correlated with mRSS in a subset of patients sera and was also increased in SSc fibroblasts (Figure 3.1D; Figure 3.2A) (Bayle et al., 2008). Therefore, it was determined, irrespective of the microenvironment, whether SSc fibroblasts in comparison to HC fibroblasts could demonstrate a differential response to Wnt/TGFβ signalling, whether this contributed to downstream fibrotic activities and whether SFRP4 expression might regulate these activities.

4.1 Canonical and non-canonical ligands have respective similarity based on sequence homology and phylogeny

In SSc both Wnt-10b (canonical agonist) and Wnt-11a (non-canonical agonist) have been shown to be highly differentially expressed in the Tsk-1 mouse model of experimental fibrosis and more recently Wnt-10b in SSc skin biopsies (Bayle et al., 2007; Beyer et al., 2012). Furthermore, Wei *et al*., have shown that fibroblasts explanted from Wnt-10b transgenic mice have increased canonical Wnt signalling and that this correlated this with an

increase in both Type-1 collagen and *α-SMA* gene expression. Since they were more relevant in SSc, canonical Wnt-10b and non-canonical Wnt-11a agonists were to be included as part the *in-vitro* studies with SFRP4.

However, in HC fibroblasts treatment with either Wnt-10b or Wnt-11a did not induce *AXIN2* expression, a direct target of canonical Wnt signalling pathway, in contrast to the 342.2% ($P<0.01$) increase following Wnt-3a treatment in HC fibroblasts (Figure 4.1A). This was subsequently confirmed by TOPFlash reporter activity, which was unchanged following Wnt-10b or Wnt-11a treatment but induced by 3.8-fold ($P<0.05$) following Wnt-3a treatment (Figure 4.1B). In a panel of genes, comprised of *COL1A1*, *α-SMA* and *CTGF*, only Wnt-3a treatment marginally induced *COL1A1* expression by 133.8% otherwise genes expression was unchanged (Figure 4.1C, E). Recombinant human Wnt-10b and Wnt-11a were not commonly cited in publications at this time and therefore the activities quoted by the supplier were unsupported. However, both Wnt-3a and Wnt-5a were more described in the literature to elicit canonical and non-canonical activities, respectively. Therefore a phylogenetic analysis was performed, using full-length protein reference sequences from Wnt-3a, Wnt-5a, Wnt-11a and Wnt-10b as a validation for the inclusion of both Wnt-3a and Wnt-5a recombinant human proteins in place of Wnt-10 and Wnt-11a for this study. Phylogenetic alignment was based on protein structure similarity using Wnt-2 as a putative backbone due to its activity being associated with both canonical and non-canonical signalling activation. Indeed, on analysis of branching from an unrooted tree, similarities between Wnt-3a / Wnt-10b and Wnt-5a / Wnt-11a were observed following divergence from Wnt-2 protein sequence, which may also confer similar functional activities (Figure 4.1F, G).

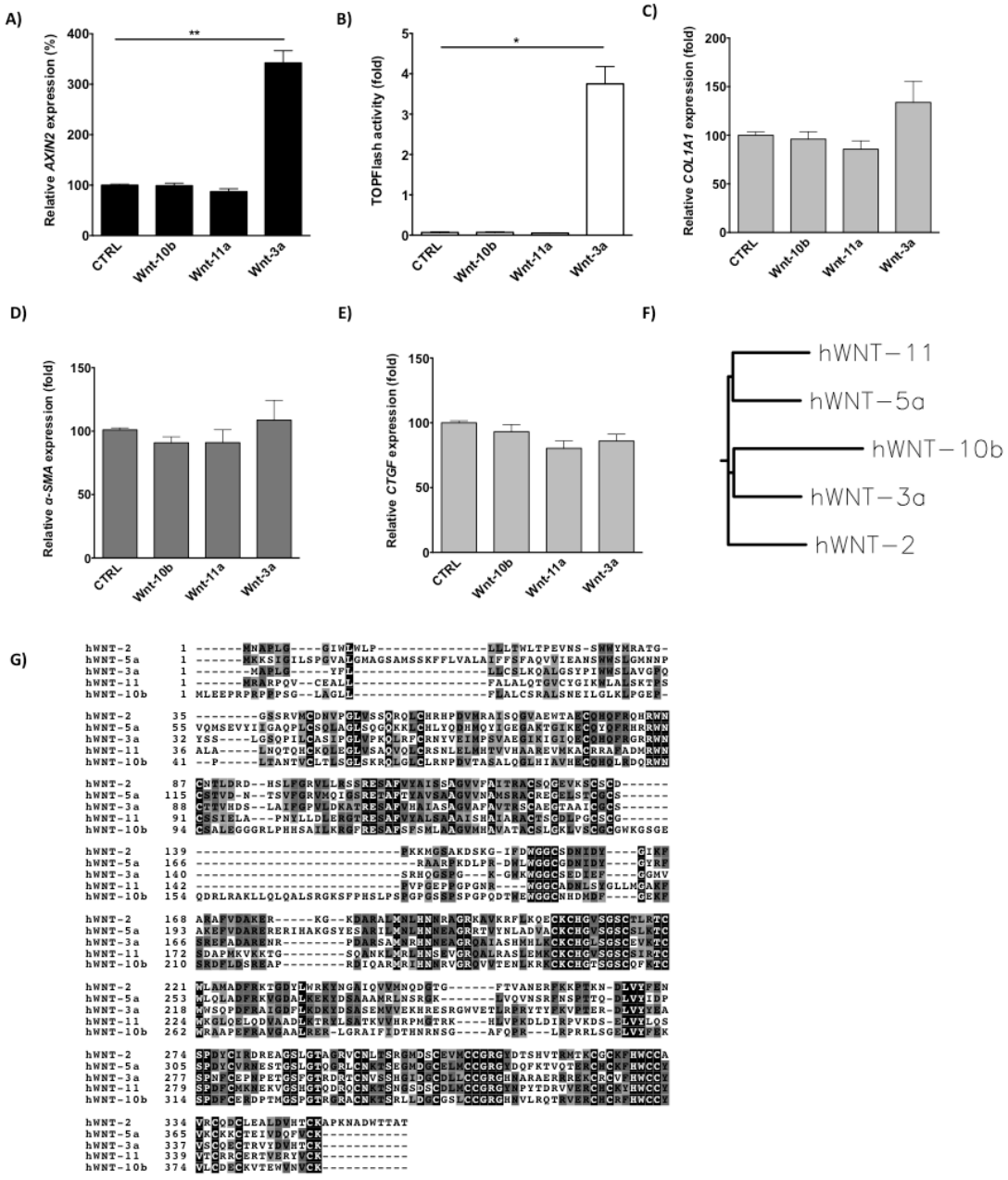

Figure 4.1 Canonical and non-canonical ligands have respective similarities based on sequence homology and phylogeny

HC fibroblasts were treated with Wnt-10b (200 ng/ml), Wnt-11a (200 ng/ml) or Wnt-3a (100 ng/ml) for 24 hr. Canonical Wnt signalling pathway activation of was evaluated through A) *AXIN2* gene expression, quantified by qRT-PCR or B) TOPFlash reporter activity, determined by luciferase activity. The effect upon profibrotic gene expression was also determined for C) *COL1A1* D) *α-SMA* and E) *CTGF*, quantified by qRT-PCR. Finally, protein similarity between canonical Wnt-3a, Wnt10b and non-canonical Wnt-11a and Wnt-5a were compared, using a bidirectional Wnt-2 as a backbone, through F) phylogenic analysis and G) multiple sequence alignment as determined by the ClustalX bioinformatics. Data shown as mean ± SEM, n=4; Mann-Whitney test for unpaired samples, **P*=0.05, ****P*=0.01.

4.2 SSc fibroblasts have an increased response to canonical Wnt signalling that is unaffected by rhSFRP4 treatment

In an experimental model of SSc, activation of the canonical Wnt signalling pathway has been shown to promote a Wnt-induced fibrosis that characteristically involves fibroblast activation, myofibroblast accumulation and increased collagen deposition (Wei et al. 2011). Consequently, the increased expression of SFRP4 in SSc may be as a result of persistent activation of the Wnt signalling pathway. Therefore, following Wnt-3a treatment a comparative analysis between HC and SSc fibroblasts was used to evaluate i) any differential regulation of profibrotic gene expression (*COL1A1* and *α-SMA*) and ii) any differential canonical Wnt signalling activity. The effect of independent or Wnt-3a co-treatment with SFRP4 was also investigated for modulatory effects on both profibrotic gene expression and canonical signalling activity.

First, profibrotic gene expression was determined. At basal level, *COL1A1* showed no significant difference in expression between HC and SSc fibroblasts (Figure 4.2A). Following Wnt-3a treatment, *COL1A1* gene expression was increased by 118.2% ($P<0.05$) in HC and 155.1% ($P<0.001$) in SSc fibroblasts, which was a significant increase in SSc compared to HC fibroblasts ($P<0.01$) (Figure 4.2A). Independent SFRP4 treatment showed no significant change in *COL1A1* expression in HC fibroblasts, in contrast to the 137.3% increase ($P<0.01$) in SSc fibroblasts (Figure 4.2A). When Wnt-3a was co-treated with SFRP4 no further effects were observed in both HC and SSc fibroblasts (Figure 4.2A).

Similarly, at basal level *α-SMA* showed no significant difference in expression between HC and SSc fibroblasts (Figure 4.2B). Following Wnt-3a treatment *α-SMA* expression was increased by 173.0% ($P<0.0001$) in HC and 352.2% ($P<0.0001$) in SSc fibroblasts, which was a significant increase in response by SSc fibroblasts ($P<0.001$) (Figure 4.2B). Independent SFRP4 treatment showed no significant change in *α-SMA* expression in HC fibroblasts although expression was increased to 167.1% in SSc fibroblasts and this was found to be significantly different from HC levels ($P<0.05$) (Figure 4.2B). When Wnt-3a was co-treated with SFRP4 there was no significant effect on Wnt-3a-induced *α-SMA* upregulation in either HC or SSc fibroblasts (Figure 4.2B). Despite being increased at mRNA level, α-SMA protein expression was not induced by Wnt-3a treatment, and independent or Wnt-3a co-treatment with SFRP4 showed no significant effect on expression in both HC and SSc fibroblasts (Figure 4.2C).

Next, these conditions were evaluated for an effect on the activation of the canonical Wnt signalling pathway determined by quantification of a direct Wnt-induced target of canonical Wnt signalling pathway, *AXIN2*. Interestingly, SSc fibroblasts showed a significant reduction in the expression of *AXIN2* expressed at basal level, which was reduced to 51% of HC levels (Figure 4.2D). Following Wnt-3a treatment *AXIN2* expression was induced by 190.0% ($P<0.0001$) in HC and 253.8% ($P<0.0001$) in SSc fibroblasts, which was a significant increase in response in SSc compared to HC fibroblasts ($P<0.01$) (Figure 4.2D). Independent or Wnt-3a co-treatment

with SFRP4 both showed no significant effect on *AXIN2* expression in both HC and SSc fibroblasts (Figure 4.2D).

Validation of the *AXIN2* expression data was performed using TOPFlash activity under the same conditions. Consistently, basal TOPFlash activity showed no significant difference in activation between HC and SSc fibroblasts (Figure 4.2E). Wnt-3a Treatment induced TOPFlash activity by 3.7-fold ($P<0.05$) in HC and 12.0-fold ($P<0.05$) in SSc fibroblasts, which was a significant increase in response in SSc compared to HC fibroblasts ($P<0.05$) (Figure 4.2E). Independent or Wnt-3a co-treatment with SFRP4 showed no significant effect on the expression of *AXIN2* in either HC or SSc fibroblasts (Figure 4.2E).

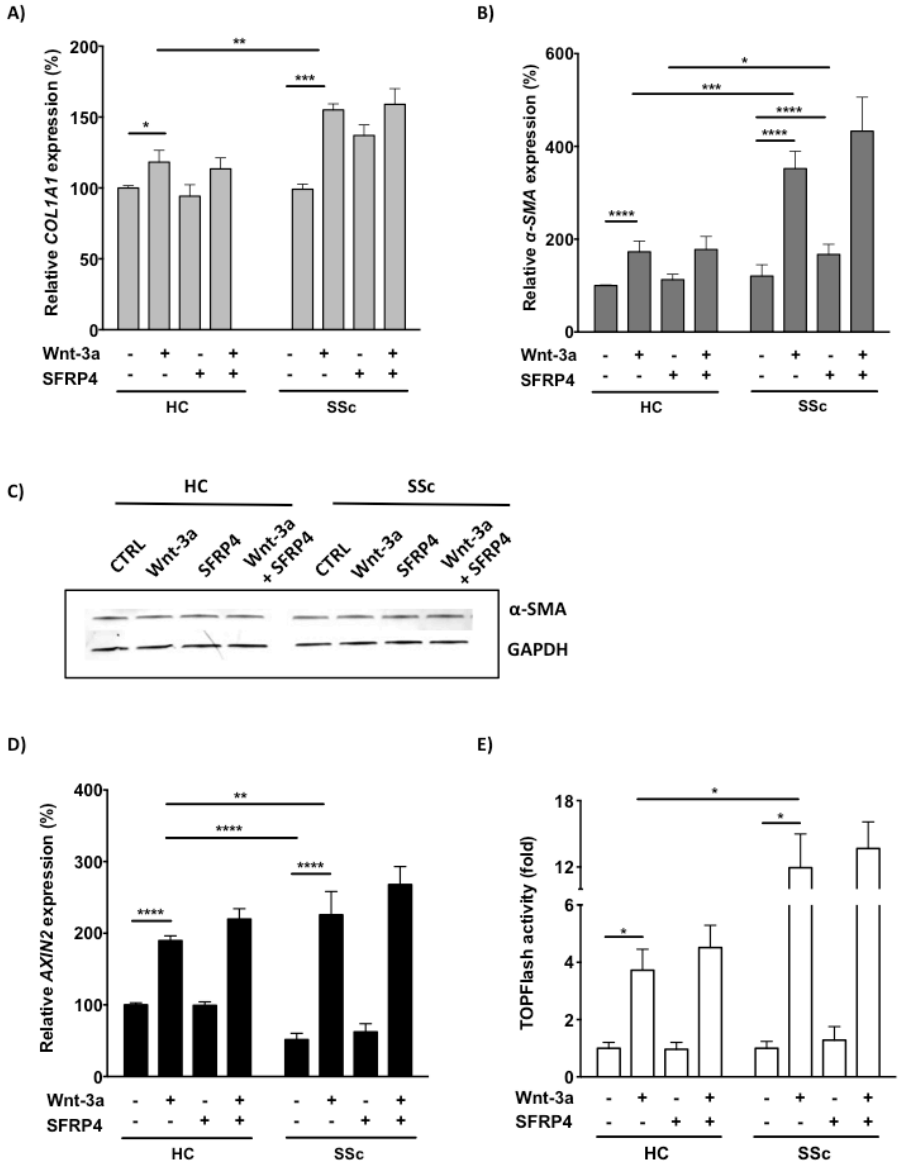

Figure 4.2 SSc fibroblasts have an increased response to canonical Wnt signalling that is unaffected by rhSFRP4 treatment

Differential profibrotic gene expression and canonical Wnt singalling activation were compared between HC and SSc fibroblasts treated with canonical agonist Wnt-3a (100 ng/ml) in the presence and absence of putative Wnt inhibitor SFRP4 (70 ng/ml). The effect on profibrotic genes A) *COL1A1* and B) *α-SMA* were determined following 24 hr treatment and quantified by qRT-PCR. C) Following 72 hr treatment, protein expression of α-SMA and GAPDH (loading control) were used as a confirmation of profibrotic activity, determined by Western blot. Canonical Wnt signalling activation was evaluated following 24 hr treatment by D) *AXIN2* expression, a canonical Wnt target gene, quantified by qRT-PCR and by E) TOPFlash reporter activity, quantified by luciferase activity. All quantitative data were normalised on basal HC levels. Data shown as mean ± SEM, n=4; Mann-Whitney test for unpaired samples, *P=0.05, **P = 0.01, ***P=0.001, ****P = 0.0001.

4.3 Non-canonical treatment showed no profibrotic or canonical Wnt signalling activity and SFRP4 had no modulatory activity

In contrast to canonical Wnt signalling, the role of the non-canonical Wnt signalling pathway in fibrosis is not well described, particularly with regard to SSc. Like canonical Wnt signalling, the non-canonical pathway may be involved in the activation of fibroblasts (Jiang et al., 2006; Levänen et al., 2011; Vuga et al., 2009). Therefore following treatment with a classical non-canonical agonist, Wnt-5a, a comparative analysis between HC and SSc fibroblasts was used to evaluate i) any differential regulation of profibrotic gene expression and ii) any crosstalk and in-turn differential canonical Wnt signalling activation. The effect of independent or Wnt-5a co-treatment with SFRP4 was also investigated for any modulation of non-canonical signalling effects on both profibrotic gene expression and canonical signalling activity.

First, Wnt-5a-induced profibrotic gene expression was determined alongside Wnt-5a co-treatment with SFRP4. Wnt-5a treatment showed no effect on *COL1A1* expression in HC fibroblasts in contrast to the 135.3% ($P<0.0001$) induction in SSc fibroblasts (Figure 4.3A). Wnt-5a co-treatment with SFRP4 did not show any further effect upon the Wnt-5a-induced effects on of *COL1A1* expression in HC or SSc fibroblasts (Figure 4.3A).

Next, Wnt-5a increased *α-SMA* expression by 122.0% and 133.3% in HC and SSc fibroblasts, respectively (Figure 4.2B). However, Wnt-5a co-treatment with SFRP4 showed no further in both HC and SSc fibroblasts (Figure 4.3B). At protein level however, α-SMA expression was not induced by Wnt-5a or affected by Wnt-5a co-treatment with SFRP4 in both HC and SSc fibroblasts (Figure 4.3C).

Despite Wnt-5a being classified as a non-canonical agonist, the effect on canonical Wnt signalling was evaluated to exclude the possibility that any observed effects could be mediated via activation of this pathway. Indeed, *AXIN2* expression was not induced by Wnt-5a or by Wnt-5a co-treatment with SFRP4 in both HC and SSc fibroblasts (Figure 4.3D). Similarly, TOPFlash activity was not induced by Wnt-5a treatment Figure 4.3E).

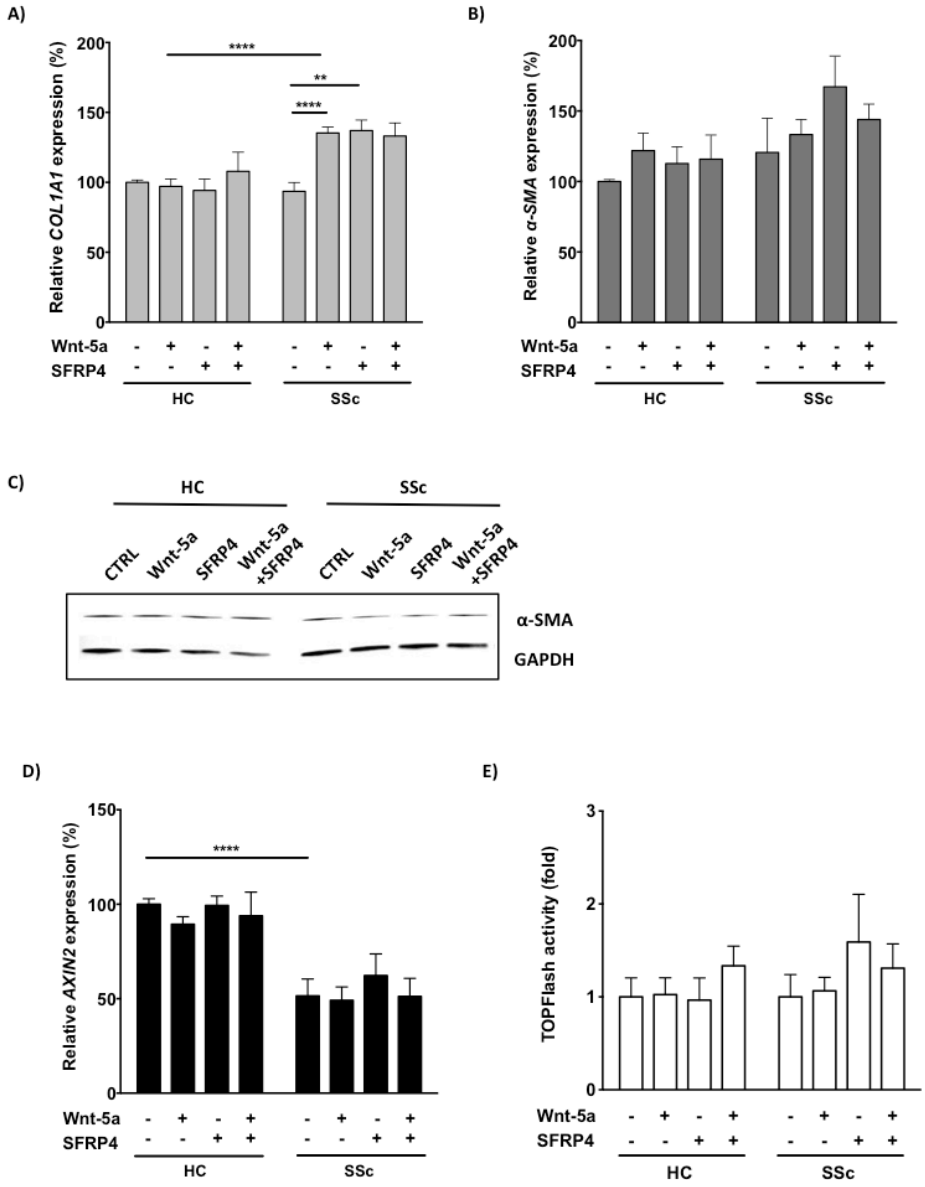

Figure 4.3 Non-canonical treatment showed no profibrotic or canonical Wnt signalling activity and SFRP4 had no modulatory activity

Differential profibrotic gene expression and canonical Wnt singalling activation were compared between HC and SSc fibroblasts treated with non-canonical agonist Wnt-5a (100 ng/ml) in the presence and absence of putative Wnt inhibitor SFRP4 (70 ng/ml). The effect on profibrotic genes A) *COL1A1* and B) *α-SMA* were determined following 24 hr treatment and quantified by qRT-PCR. C) Following 72 hr treatment, protein expression of α-SMA and GAPDH (loading control) were used as a confirmation of profibrotic activity, determined by Western blot. Canonical Wnt signalling activation was evaluated following 24 hr treatment by D) *AXIN2* expression, a canonical Wnt target gene, quantified by qRT-PCR and by E) TOPFlash reporter activity, quantified by luciferase activity. All quantitative data were normalised on basal HC levels. Data shown as mean ± SEM, n=4; Mann-Whitney test for unpaired samples, ***P* = 0.01, *****P* = 0.0001.

4.4 TGFβ-mediated profibrotic and canonical Wnt signalling activities are not regulated by SFRP4

While SFPR4 showed no significant regulatory effects independently or in tandem with Wnt agonist treatments (Figure 4.2 & Figure 4.3), the fact remained that TGFβ signalling was able to significantly upregulate SFRP4 expression in fibroblasts (Figure 3.2B). Accordingly, SFPR4 could play a potential role in the regulation of TGFβ signalling. Therefore a comparative analysis between HC and SSc fibroblasts was used following TGFβ treatment to evaluate i) the known effect on profibrotic gene expression and ii) whether TGFβ regulated canonical Wnt signalling activity. The effects of independent or TGFβ co-treatment with SFRP4 were also investigated for any modulation of effects elicited by TGFβ signalling on both profibrotic gene expression and canonical signalling activity.

First, TGFβ-induced profibrotic gene expression was determined alongside independent and co-treatment with SFRP4. TGFβ induced *COL1A1* expression by 229.0% ($p<0.0001$) and 206.0% ($p<0.0001$) in HC and SSc fibroblasts, respectively (Figure 4.4A). TGFβ co-treatment with SFRP4 did not affect *COL1A1* expression in HC fibroblasts and in SSc fibroblasts co-treatment showed a trend toward inhibition of *COL1A1* expression, which was decreased to 163.3% but this was not found to be statistically significant (Figure 4.4A).

Next, TGFβ induced *α-SMA* expression by 116.3% ($P<0.01$) and 142.5% ($P<0.01$) in HC and SSc fibroblasts, respectively. Interestingly, TGFβ co-treatment with SFRP4 increased *α-SMA* expression by 205.0% ($P<0.05$) in HC fibroblasts but had no significant effect on expression in SSc fibroblasts

when compared to TGFβ treatment alone (Figure 4.4B). At protein level, TGFβ treatment also showed a significant induction of α-SMA expression, however, TGFβ co-treatment with SFRP4 showed no further effects (Figure 4.4C).

Next, these treatments were evaluated in 3D collagen gels seeded with HC or SSc fibroblasts. Fibroblast-induced contraction 3D collagen gel has been utilised as a comparable measure of fibroblast-induced contraction of tissues characteristic during fibrosis. The consequence of increased α-SMA expression is the increased potential for fibroblast to myofibroblast differentiation, where α-SMA stress fibrils polymerisation is characteristic, and the functional consequence is the generation of increased contractile force on the ECM. At basal level, there was no spontaneous contraction of SSc compared to HC fibroblasts (Figure 4.4D). Also there was no significant difference in TGFβ-induced 3D collagen gel contraction between HC and SSc fibroblasts, which were contracted to 51.5% and 56.8% of controls, respectively (Figure 4.4D). Interestingly, SFRP4 treatment increased the collagen gel area in both HC and SSc fibroblasts by 13.4% (Figure 4.4C). However, TGFβ co-treatment with SFRP4 did not greatly affect the TGFβ-induced gel contraction, which contracted to 57.2% and 67.9% in HC and SSc fibroblasts, respectively (Figure 4.4D).

Finally, canonical Wnt signalling activation was evaluated. TGFβ reduced the expression of *AXIN2* to 50.0% ($P<0.0001$) and 16.0% ($P<0.0001$) in HC and SSc fibroblasts, respectively (Figure 4.4E). TGFβ co-treatment with SFRP4 had no effect on the TGFβ-induced downregulation of *AXIN2* in either HC or SSc fibroblasts (Figure 4.4E).

These data were then validated by TOPFlash activity. TGFβ to inhibited TOPFlash activity to 59.6% ($P<0.05$) in HC fibroblasts but showed no significant effect on SSc fibroblasts (Figure 4.4F). SFRP4 treatment showed no significant effect on TOPFlash activity in HC fibroblasts but showed a trend a trend toward increased activity in SSc fibroblasts, induced by 1.3-fold (Figure 4.4F). TGFβ co-treatment with SFRP4 did not affect TOPFlash activity in HC fibroblasts but showed a trend a trend toward increased activity in SSc fibroblasts by 1.6-fold (Figure 4.4F).

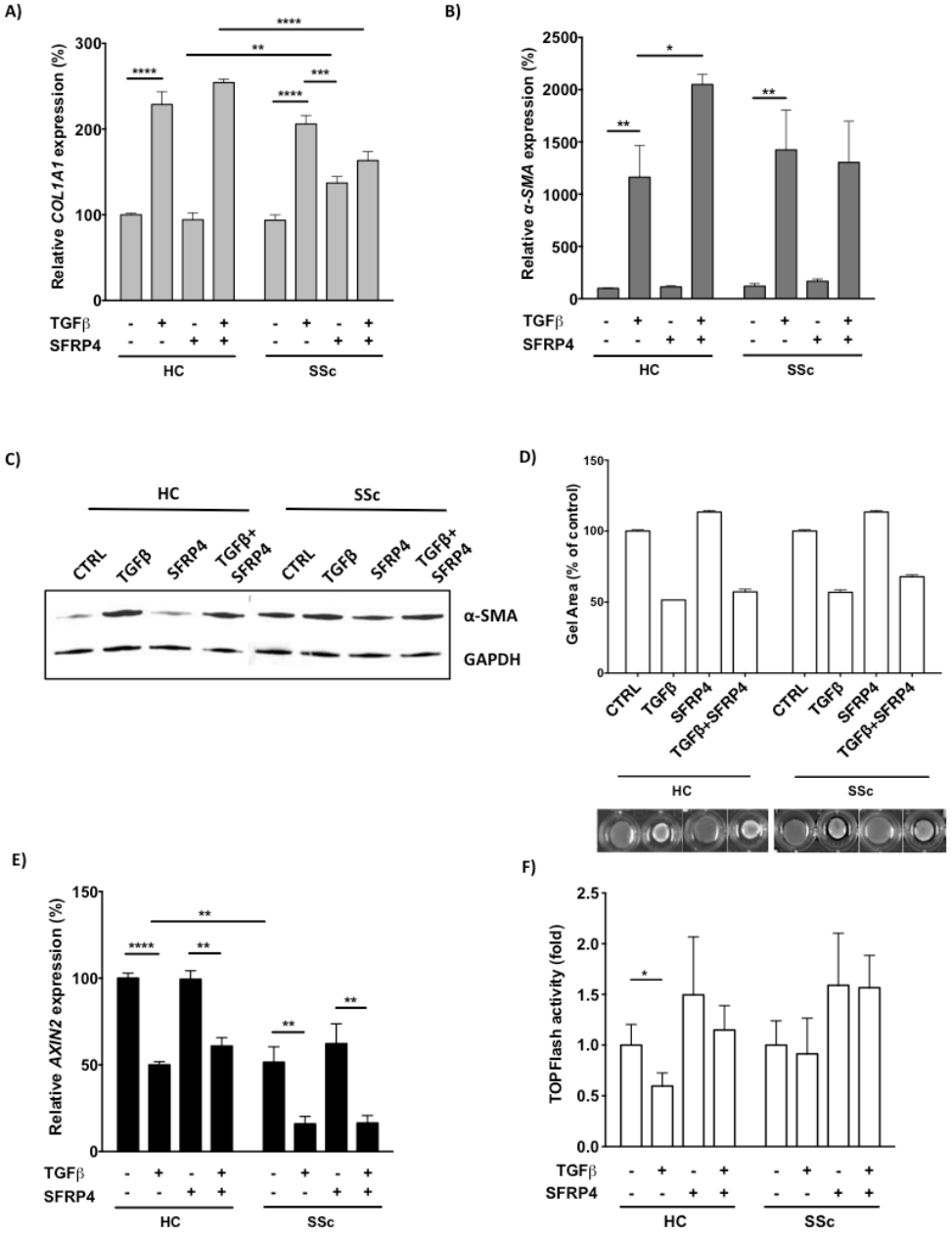

Figure 4.4 TGFβ-mediated profibrotic and canonical Wnt signalling activities are not regulated by SFRP4

Differential profibrotic gene expression and canonical Wnt singalling activation were compared between HC and SSc fibroblasts treated with TGFβ (5 ng/ml) in the presence and absence of putative Wnt inhibitor SFRP4 (70 ng/ml). The effect on profibrotic genes A) *COL1A1* and B) *α-SMA* were determined following 24 hr treatment and quantified by qRT-PCR. C) Following 72 hr treatment, protein expression of α-SMA and GAPDH (loading control) were used as a confirmation of profibrotic activity, determined by Western blot. Canonical Wnt signalling activation was evaluated following 24 hr treatment by E) *AXIN2* expression, a canonical Wnt target gene, quantified by qRT-PCR and by F) TOPFlash reporter activity, quantified by luciferase activity. All quantitative data were normalised on basal HC levels. Data shown as mean ± SEM, n=4; Mann-Whitney test for unpaired samples, **P*=0.05, ***P* = 0.01, *****P* = 0.0001.

4.5 DISCUSSION: Comparative analysis of Wnt/TGFβ signalling pathway activation and profibrotic gene expression in SSc and HC fibroblasts

The Wnt-10b (canonical) and Wnt-11a (non-canonical) agonists display high differential expression in the dermis of the Tsk-1 mouse model of experimental fibrosis, and Wnt-10b more recently in SSc skin biopsies (Bayle et al., 2007; Beyer et al., 2012). Furthermore, Wei *et al*., have shown that fibroblasts explanted from Wnt-10b transgenic mice have increased canonical Wnt signalling, which correlated this with an increase in both Type-1 collagen and *α-SMA* gene expression (Wei et al., 2012). Although Wnt-11a activity has not been directly studied in relation to fibrosis, upregulation of Wnt-11a by TGFβ in renal epithelial cells has been shown to promote non-canonical signalling-mediated mesenchymal gene expression, including *α-SMA* (Zhang et al., 2012). Therefore Wnt-10b and Wnt-11a agonists were to be investigated as part of this study due to their biological relevance in the disease state. A limitation of this study was the absence of a reliable assay to evaluate non-canonical signalling. In contrast to Wnt-10b, Wnt-11a is described as a non-canonical agonist and therefore its activity would generally be thought to be β-catenin-independent. However, non-canonical agonists have been observed to activate canonical signalling in various bilological contexts (Kikuchi et al., 2009). *In vitro* analysis of Wnt-10b and Wnt-11a, in contrast to Wnt-3a, demonstrated a failure to activate two determinants of canonical Wnt signalling, *AXIN2* mRNA expression, a direct Wnt-induced target, and TOPFlash activity (Figure 4.1A, B). This was despite Wnt-3a concentration (100 ng/ml) being half that of the other agonists. All Wnt agonists initially showed no effect on genes associated

with profibrotic activity; however, Wnt-3a treatment did show a trend toward increased *COL1A1* expression (Figure 4.1C-E). Accordingly, due to inactivity, Wnt-10b and Wnt-11a were excluded from the study. While the activity of Wnt-11a might demonstrate non-canonical activities, like Wnt-10b, the recombinant protein was not commonly cited in publications at this time and therefore the activities quoted by the supplier were unsupported by independent studies. Widely cited in the literature, Wnt-3a (canonical) and Wnt-5a (non-canonical) agonists had consistently been shown to activate canonical and non-canonical signalling, respectively. Indeed, Wnt-3a canonical signalling activity was already validated by gene expression and reporter activation (Figure 4.1A, B). Therefore these widely cited agonists were putative surrogates for Wnt-10b and Wnt-11a activity.

As a secondary confirmation for the inclusion of Wnt-3a/Wnt-5a as surrogates of Wnt-10b/Wnt-11a, a phylogenetic analysis was performed based of protein structure similarity. This used the full-length protein reference sequences for Wnt-3a, Wnt-5a, Wnt-11a Wnt-10b and Wnt-2, where Wnt-2a, which was associated with both canonical and non-canonical signalling activation, acted as a backbone. On branch analysis of a derived unrooted tree, Wnt-3a and Wnt-10b were found to be closely related as were Wnt-5a and Wnt-11a based on divergence from Wnt-2 protein sequence (Figure 4.1F, G). These similarities may confer similar functional activities already demonstrated in the literature. Therefore these agonists were used as surrogates in place of Wnt-10b and Wnt-11a.

To determine whether canonical Wnt signalling was increased in SSc fibroblasts, comparative analyses were performed between explanted SSc patient and HC fibroblasts following canonical Wnt-3a treatment. SSc fibroblasts demonstrated an increased response to canonical Wnt signalling activation that was consistent between two gold standard measures of canonical Wnt signalling activity: *AXIN2* mRNA expression and TOPFlash reporter activation. These *in vitro* analyses expand upon previous studies that have shown canonical Wnt signalling to be hyperactivated within SSc skin biopsies but related this to differential Wnt agonist expression (Beyer et al., 2012; Wei et al., 2011; Akhmetshina et al., 2012). Furthermore, no spontaneous activation of canonical Wnt signalling was observed in SSc fibroblasts, which would suggest that fibroblasts do not display an autocrine activation of canonical Wnt signalling and that this activity is likely caused by the production of Wnt agonists by other cell types present in the local microenvironment (Figure 4.2D, E).

Prominently, *AXIN2* expression was significantly downregulated in SSc compared to HC fibroblasts (Figure 4.2D). Downregulation of AXIN2, a key scaffold component of the β-catenin destruction complex, could explain the increased amplitude of canonical Wnt signalling, a subsequent evaluation discussed later in this report.

This analysis also examined the ability of Wnt-3a-induced canonical signalling to upregulate the expression of two profibrotic genes, *COL1A1* and *α-SMA.* In SSc fibroblasts, Wnt-3a-induced profibrotic gene expression was more pronounced, which coincided with an increased canonical Wnt signalling activity (Figure 4.2A, B). However, despite changes at mRNA

level, α-SMA protein expression, a key marker of fibroblast activation, was unaffected by canonical Wnt signalling activation (Figure 4.2C). Unfortunately, collagen protein expression could not be included as part of this study due to the unreliability of several antibodies, which represents a study limitation. Overall, canonical Wnt signalling, while increased in SSc fibroblasts, had minimal effects on fibrotic activation.

This adds to conflicting literature describing a role for Wnt-3a-induced canonical Wnt signalling in the regulation profibrotic gene expression. Studies in mouse fibroblasts have shown that mouse recombinant Wnt-3a treatment can induce myofibroblasts differentiation, visualised by α-SMA stress fibre formation (Carthy et al., 2011). Wei *et al* demonstrated that adenoviral overexpression of Wnt-3a in foreskin fibroblasts increased *COL1A2* and *α-SMA* expression by 2.0-fold and 2.7-fold, respectively, following 6 days of culture (Wei et al., 2011). Despite the use of Wnt-3a overexpression only a 2.7-fold increase in *α-SMA* expression was achieved. In contrast, *α-SMA* expression in HC fibroblasts was induced by >100-fold following 1 day of TGFβ treatment, which would suggest that the relative role of Wnt in activating the profibrotic phenotype is insubstantial by comparison (Figure 4.4B). However, there are notable exceptions in the literature where no significant change in *α-SMA* expression is observed in response to Wnt-3a treatment. Microarray analysis of NIH-3T3 mouse fibroblasts treated with Wnt-3a for 6 hr showed no substantial direct induction of profibrotic/matrix remodeling genes, including *α-SMA* (Chen et al., 2007). In a subsequent study, *COL1A2* and *α-SMA* expression were not inducible by Wnt-3a overexpression in rat cardiac fibroblasts and could only be induced by overexpression of the Fz1 receptor (Laeremans et al., 2010). Several key

differences between these studies could explain the conflicting results. One possible explanation lies in species variation, where the biological relevance of a human condition is more suggestive from fibroblasts derived from human subjects, where the disease presents, than from our mammalian counterparts. Indeed, not all biological pathways are conserved between species and the regulation of those that are might diverge (Mestas & Hughes, 2004). Once species is considered, then the topographic location of the fibroblasts becomes important. For example, neonatal fibroblasts have differential gene expression compared to adult fibroblasts, which can explain functional differences between the two including migration, contracture and differentiation (Schor et al., 1985; Moulin et al., 2001). Furthermore, gene profiling studies have shown that there are distinct patterns of gene expression from fibroblasts derived from different anatomical regions (Castor et al., 1962; Chang et al., 2002). One consequence may extend to the ability of cells to respond to extracellular cues through the differential regulation of pathway components, which could include those associated with Wnt signalling. Comparatively, biopsies should be taken from patients at sites that have involved skin and analysed against matched regions from HC donors. In this study, it was difficult to source adult fibroblasts from the forearm and instead were sourced from the temple, abdomen and breast.

The contribution of the non-canonical pathway in fibroproliferative diseases, including in SSc, remains largely unstudied. Despite this, limited reports indicate that non-canonical signalling may have fibrotic consequences. Therefore a comparative analysis between HC and SSc fibroblasts was used

to determine the effect on non-canonical agonist treatment on profibrotic gene expression and canonical Wnt signalling. SSc fibroblasts, in contrast to HC fibroblasts, showed an induction of *COL1A1* expression in response to Wnt-5a, which could indicate that non-canonical signalling might be selectively utilised in SSc fibroblasts (Figure 4.3A). Similar expression levels were induced for *α-SMA* in both SSc and HC fibroblasts; however, protein expression of α-SMA confirmed that this level of expression at mRNA level was not translated to protein (Figure 4.3B, C). Therefore, the minimal induction of *COL1A1* expression suggests that the aforementioned hypothesis is an unlikely outcome, although protein expression data are unavailable and cannot be used as a secondary confirmation. Like canonical signalling, these data suggest that non-canonical signalling is not a significant factor in profibrotic gene expression. This is in contrast to a report that showed that expression of Wnt-5a in hepatic stellate cells, or its receptor, Fz2, increased fibrosis both *in vitro* and *in vivo* (Jiang et al., 2006). However, in SSc fibroblasts no clear differential effect from HC fibroblasts was evident and therefore the expression of Fz receptor expression is likely not to be significantly different. A later report showed that Wnt-5a expression correlated with inflammatory or chronic fibrotic processes in pulmonary tissues from patients with sarcoidosis (Levänen et al., 2011). In contrast to fibrotic activity, Wnt-5a has also been shown to affect proliferation and apoptosis in lung-derived fibroblasts (Vuga et al., 2009). Therefore, Wnt-5a, rather that augmenting profibrotic gene expression might have more important functions in alternative biological processes.

In addition, Wnt-5a showed no crosstalk with the canonical Wnt signalling pathway (Figure 4.3D, E). Unfortunately, no reliable non-canonical readouts

were available and therefore the ability of Wnt-5a to induce non-canonical Wnt signalling activity is unconfirmed, although might be indicated by Wnt-5a-induced *COL1A1* mRNA in SSc fibroblasts.

As a putative Wnt signalling inhibitor, rhSFRP4 might be expected to function in the dampening of the agonist-induced canonical Wnt signalling response; however, several models of SFRP activity have been reported that support both additive or inhibitory functions. SFRP1 and SFRP3 can bind Wnt1 and XWnt8, through the NTR domain and antagonise canonical Wnt signalling activity in both *Xenopus* and medaka-fish embryos (Lopez-Rios et al., 2008; Leyns et al., 1997; Wang et al., 1997). Furthermore, SFRP1/2 were found to bind to and antagonise Wnt-3a-induced β-catenin accumulation in L-cells (mouse fibroblasts) (Wawrzak et al., 2007). In contrast, another study described the promotion of Wnt:Fz complexes on addition of SFRP1 at concentrations between 20-200 ng/ml and therefore an additive effect could also be predicted (Uren et al., 2000). Respectively, these studies support a model where SFRPs sequester Wnt agonists and thereby prevent receptor activation or act to shuttle Wnt ligands to the frizzled receptor to elicit Wnt signalling activation. In this study, the co-treatment of Wnt-3a or Wnt-5a with SFRP4 showed no effect on canonical Wnt signalling activity or profibrotic gene expression beyond those induced by independent Wnt-treatments and, in addition, no differential effects were observed between HC and SSc fibroblasts (Figure 4.2 Vs. Figure 4.3). Therefore, these results were not in agreement with either of the aforementioned standard models. Dicussed previously, Wawrzak et al.

demonstrated that SFRP4 could bind Wnt-3a but that this complex could not moderate Wnt-3a-induced β-catenin accumulation (Wawrzak et al., 2007). The authors suggested that these SFRPs might act as carrier proteins and facilitate the transport and diffusion of Wnt agonists in the tissue, which could explain the inactivity displayed by SFRP4 in co-treatment experiments; however, a complex set of experiments would need to be performed in order to confirm this diffusion hypothesis.

In the literature, the contribution of TGFβ signalling towards profibrotic gene expression has already been well described. Therefore the TGFβ-induced upregulation of both *COL1A1* and *α-SMA* in fibroblasts indicated the potential for the induction of these profibrotic genes, which demonstrated the low efficacy of canonical Wnt-3a-induced expression, discussed previously.

SSc fibroblasts displayed increased basal α-SMA protein expression; however, protein expression was consistently unchanged compared to HC fibroblasts (Figure 4.4A-C). Following on from this, no spontaneous contraction was observed in 3D collagen gels in contrast to the contraction observed following TGFβ (Figure 4.4D), which suggested that increased α-SMA expression in fibroblast does not necessarily correlate with contractile potential and therefore, indirectly, myofibroblast presence. More interesting was the observation that TGFβ treatment significantly downregulated *AXIN2* expression in both SSc and HC fibroblasts (Figure 4.4E). Contrary to previous reports, TGFβ did not induce canonical Wnt signalling as measured by TOPFlash activity (Figure 4.4F). These data indicated that TGFβ might crosstalk with the Wnt signalling pathway through the regulation of *AXIN2*

expression. On analysis of a gene profiling study evaluating of TGFβ responsive genes, as defined by the intrinsic dcSSc gene signature from Milano et al., a distinct Wnt signalling profile was not observed in dermal fibroblasts from dcSSc patients. However, on further inspection of the supplementary data, two important negative regulators of Wnt signalling were significantly downregulated, *AXIN2* and *DKK-1* (Milano et al., 2008; Sargent et al., 2009). This suggests that the TGFβ-mediated effects on canonical Wnt signalling might be as a result of crosstalk with these two proteins and AXIN2 expression was the subject of further investigation in this report.

Previously observed, TGFβ signalling upregulated SFRP4 protein expression in preference to Wnt signalling and therefore SFRP4 could potentially be involved in the regulation of the TGFβ signalling pathway, independent of any effects on Wnt signalling (Figure 3.2B). In conflict with this hypothesis, TGFβ co-treatment with SFRP4 showed only a trend toward inhibition of *COL1A1* expression in SSc fibroblasts and had no effect in HC fibroblasts; however, no protein data were available to support this observation (Figure 4.4A). The opposite effect was observed for *α-SMA* where TGFβ co-treatment with SFRP4 increased its expression in HC but not in SSc fibroblasts; however, protein expression data did not support this differential observation and showed no effect past that of independent TGFβ treatment (Figure 4.4B, C). In support of the α-SMA protein expression data, TGFβ co-treatment with SFRP4 showed no further contraction past that induced by independent TGFβ treatment in either HC or SSc fibroblasts (Figure 4.4D).

Similarly, TGFβ co-treatment with SFRP4 showed no effect upon canonical Wnt signalling activation beyond those observed following independent TGFβ treatment (Figure 4.4E, F). Therefore these data suggest that SFRP4 does not regulate the TGFβ signalling pathway. As a further confirmation TGFβ signalling amplitude would need to be investigated.

Finally, the independent effects of SFRP4 treatment on profibrotic gene expression and canonical Wnt signalling activity were evaluated in a comparative analysis between HC and SSc fibroblasts. Consistently, SFRP4 treatment showed no ability to regulate canonical Wnt signalling activity, as measured by *AXIN2* expression and TOPFlash activity (Figure 4.1D, E). However, the expression of *COL1A1* and *α-SMA* profibrotic genes were increased by SFRP4 treatment but only in SSc fibroblasts, by 137.3% and 167.1%, respectively (Figure 4.1A, B). This could suggest an agonistic role for SFRP4 in SSc fibroblasts, as has been observed for SFRP2, which was able to participate in a complex with fibronectin and α5β1 integrin to inhibit apoptotic events (Lee et al., 2004). Contrary to this prediction, the expression of α-SMA protein following independent SFRP4 treatment remained unchanged (Figure 4.1C). Taking this observation into account, those changes observed for *COL1A1* at mRNA level, which were similar to those induced for *α-SMA,* were unlikely to be significant at protein level. Therefore these data do not support an agonistic role for SFRP4 in profibrotic gene expression.

Overall, SSc fibroblasts displayed an increased response to canonical Wnt signalling activation and, at basal level, had a reduction in the expression of

AXIN2 compared to HC fibroblasts. In contrast to TGFβ, the canonical and non-canonical agonists, despite increased profibrotic gene expression, showed no profound increase in profibrotic fibroblast activation as determined by the expression of fibroblast activation marker α-SMA. In addition, rhSFRP4 co-treatment had no modulatory affect upon any agonist-mediated activities and independent treatment was unable to demonstrate any agonistic activities. The absence of any profound effects by rhSFRP4 could indirectly supported a model of activity whereby SFRPs might act as carrier proteins and facilitate the transport and diffusion of Wnt agonists in the tissue; however, a complex set of experiments would need to be performed in order to confirm this hypothesis.

5 CAV-1 expression in the reproduction of SSc fibroblast phenotype

Myofibroblasts are known to be key mediators of fibrosis and are though to persist in fibrotic tissues, including in SSc, and cause both increased ECM protein deposition as well as increased contracture in tissues (Hinz et al., 2001; Farina et al. 2009). Myofibroblasts and SSc fibroblasts have been described to have a reduced CAV-1 expression, a key component of the caveolae endocytic pathway described to negatively regulate TGFβ signalling activity (Guglielmo et al. 2003). As CAV-1 has been linked to the expression of profibrotic genes, this led to the hypothesis that CAV-1 negative fibroblasts might reproduce the profibrotic or canonical Wnt signalling amplitude observed in SSc fibroblasts (Del Galdo et al., 2008; Tourkina et al., 2008). Determination of whether the increased canonical Wnt signalling in SSc fibroblasts was a consequence of CAV-1 depletion was primarily evaluated.

5.1 Stable expression of shCAV-1 in HC fibroblasts

In a resting population of HC fibroblasts, myofibroblasts were identified by immunofluorescence through the arrangement of α-SMA into stress fibers (green striations) (Figure 5.1A). Further, these myofibroblasts were observed to be CAV-1 negative in contrast to the majority of CAV-1 positive (stained red) undifferentiated fibroblasts (Figure 5.1A). However at basal level, SSc fibroblasts showed a wide variation in the level of *CAV-1* expression with a mean reduction to 84.3% compared to HC fibroblasts (Figure 5.1B). Next,

the effect of Wnt-3a or Wnt-5a treatment on the expression of *CAV-1* was evaluated and both ligands induced a marginal trend toward decreased *CAV-1* expression, whereas TGFβ treatment significantly downregulated *CAV-1* expression to 43.2% ($P<0.05$) or 50.4% in HC and SSc fibroblasts, respectively (Figure 5.1B). Consistent with this observation the protein expression of CAV-1 was not significantly reduced in SSc fibroblasts nor was there an increased expression of α-SMA when compared to HC fibroblasts (Figure 5.1C).

In spite of the marginal reduction in CAV-1 expression in SSc fibroblasts, the hypothesis that CAV-1 negative fibroblasts may reproduce the profibrotic or canonical Wnt signalling amplitude observed in SSc fibroblasts was further investigated. HC fibroblasts were used to create stable cell lines with reduced CAV-1 expression. When transduced with the pGIPZ lentiviral vector, HC fibroblasts stably expressed either a non-targeting sequence (SCR) or an shRNA sequence targeted against CAV-1 (shCAV) (Figure 5.1D). Following antibiotic selection the retention of the construct, expressing either the SCR or shCAV-1 sequence, within fibroblasts was evaluated by immunofluorescence, which showed that the construct was present and was integrated into all SCR / shCAV lines and all fibroblasts within these lines (Figure 5.1E). One SCR construct and three CAV-1 shRNA constructs (shCAV_48, shCAV_97 and shCAV_99) were comparatively evaluated for an effect on CAV-1 expression. Indeed, at basal level *CAV-1* expression was increased by 197.8% in shCAV_48 and reduced to 57.2% ($P<0.01$) and 28.7% ($P<0.01$) in shCAV_97 and shCAV_99, respectively (Figure 5.1F).

Similarly, the expression of CAV-1 protein was found to be significantly reduced in shCAV_97 and shCAV_99 constructs, but not shCAV_48, compared to SCR controls (Figure 5.1G). Also, the basal expression of α-SMA and SFRP4 were assayed and were not found to be spontaneously affected by reduced CAV-1 expression (Figure 5.1G). Accordingly, both shCAV_97 and shCAV_99 constructs were utilised for further studies and were termed shCAV.

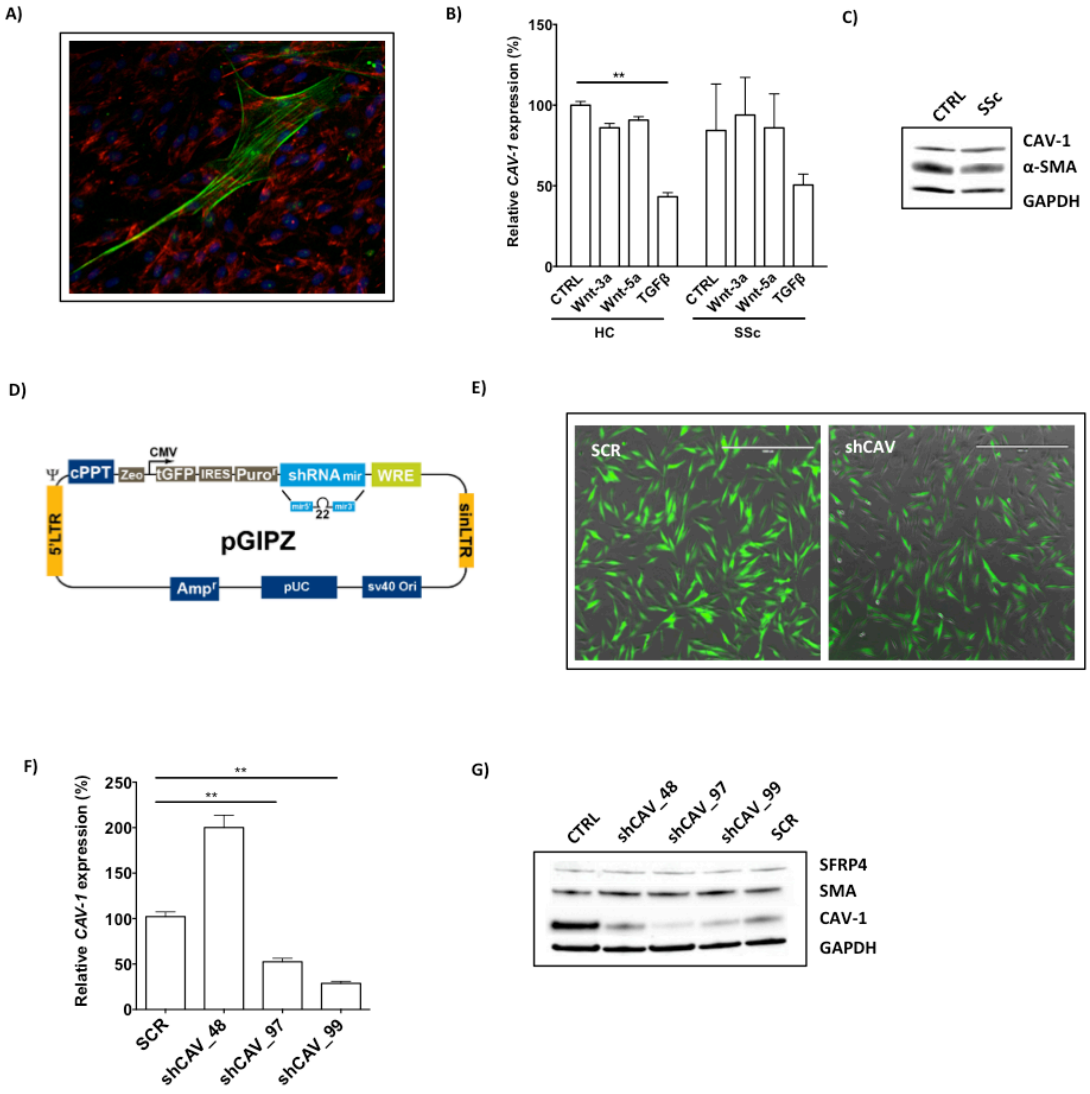

Figure 5.1 Stable expression of shCAV-1 in HC fibroblasts

A) In resting HC fibroblasts, myofibroblasts were visualised by α-SMA stress fibril formation using confocal microscopy to detect fluorescence from a FITC-conjugated secondary antibody directed against the anti-α-SMA antibody (green stain), CAV-1 expression was also assessed by a CY3-conjugated secondary targeted against the anti-CAV-1 antibody (red stain) and nuclei were stained with DAPI (blue stain). In both HC and SSc fibroblasts CAV-1 expression was determined by B) mRNA expression, quantified by qRT-PCR or C) protein expression determined by Western blot following 24 and 72 hr treatments, respectively. To determine whether depletion of CAV-1 could reproduce an SSc fibroblast-like phenotype, HC fibroblasts were transduced with D) pGIPZ lentiviral vector containing either a SCR or shCAV sequence. E) Stable transduction was determined following antibiotic selection by immunofluorescence using vector-driven GFP expression (green). Subsequently, CAV-1 expression was evaluated in fibroblasts expressing the distinct shCAV sequences (shCAV_48, shCAV_97 or shCAV_99) through F) mRNA expression, quantified by qRT-PCR and by G) protein expression alongside SFRP4, α-SMA (fibroblast activation marker) and GAPDH (loading control), determined by Western blot. Data shown as mean ± SEM, n=3-4; Mann-Whitney test for unpaired samples, ***P*=0.01.

5.2 CAV-1 has no regulatory role in the increased SFRP4 expression observed in SSc fibroblasts

To determine whether depletion of CAV-1 could reproduce the increased SFRP4 expression observed in SSc fibroblasts either in the presence or absence of stimuli, stable shCAV expressing fibroblast lines were created.

In shCAV compared to SCR fibroblasts, *CAV-1* mRNA expression was silenced by 75.5% ($P<0.0001$), which was consistent with the substantial reduction in CAV-1 protein (Figure 5.2A, B). At basal levels, SFRP4 gene expression in shCAV fibroblasts was unchanged compared to SCR fibroblasts (Figure 5.2C). Following Wnt-3a treatment, *SFRP4* expression was induced by 173.6% ($P<0.001$) and 180.3% ($P<0.01$) in SCR and shCAV fibroblasts, respectively (Figure 5.2C). Wnt-5a treatment showed no significant increase in *SFRP4* expression, while TGFβ induced SFRP4 expression by 207.9% ($P<0.01$) and 200.2% ($P<0.05$) in SCR and shCAV fibroblasts, respectively (Figure 5.2C).

SFRP4 protein expression was unaffected by both Wnt-3a and Wnt-5a treatments, whereas TGFβ treatment increased SFRP4 expression in both SCR and shCAV fibroblasts (Figure 5.2D). No significant differences in SFRP4 expression could be observed at mRNA or protein level between SCR and shCAV fibroblasts following any treatment conditions (Figure 5.2D).

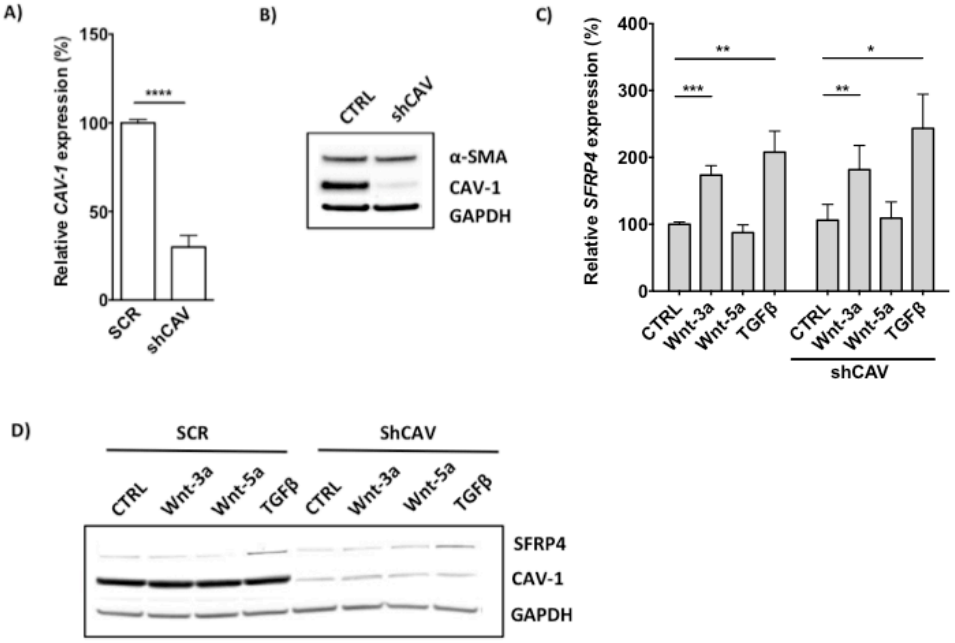

Figure 5.2 CAV-1 has no regulatory role in the increased SFRP4 expression observed in SSc fibroblasts

SFRP4 expression was determined at basal level in SCR and shCAV fibroblasts by A) mRNA expression, quantified by qRT-PCR and B) protein expression, determined by Western blot. Fibroblasts were also treated with Wnt-3a (100 ng/ml), Wnt5a (100 ng/ml) or TGFβ (5 ng/ml) for 24 hr prior to determine any differential effects on C) *SFRP4* mRNA expression following 24 hr treatment, quantified by qRT-PCR. D) Protein expression of SFRP4 and GAPDH (loading control) were also evaluated following 72 hr treatment, determined by Western blot. Data shown as mean ± SEM, n=4; Mann-Whitney test for unpaired samples, **P*=0.05, ***P* = 0.01, ****P*=0.001, *****P* = 0.0001.

5.3 CAV-1 does not augment canonical Wnt-induced profibrotic or canonical Wnt signalling activities observed in SSc fibroblasts irrespective of SFRP4 treatment

As CAV-1 expression in fibroblasts had been shown to negatively regulate profibrotic gene expression, it was determined whether in the absence of CAV-1 and following treatment with Wnt-3a there was i) any differential regulation of profibrotic gene expression and ii) any differential canonical

Wnt signalling activation. Also the effect of independent, or Wnt-3a co-treatment, with SFRP4 was also investigated for modulatory effects on both profibrotic gene expression and canonical signalling activity.

When profibrotic gene expression was examined, basal *COL1A1* expression was not affected between SCR and shCAV fibroblasts. Following Wnt-3a treatment, *COL1A1* gene expression was marginally increased by 126.9% ($P<0.001$) and 113.2% ($P<0.001$) in SCR and shCAV fibroblasts, respectively (Figure 5.3A). Wnt-3a co-treatment with SFRP4 showed no significant effect upon the Wnt-3a-induced increase in *COL1A1* expression and independent SFRP4 treatment also showed no significant effect on expression (Figure 5.3A).

Like *COL1A1*, *α-SMA* expression was unchanged at basal level between SCR and shCAV fibroblasts (Figure 5.3B). Wnt-3a treatment induced *α-SMA* expression in SCR and shCAV fibroblasts to similar levels, induced by 187.2% ($P<0.001$) and 194.6% ($P<0.01$), respectively (Figure 5.3B). Wnt-3a co-treatment with SFRP4 showed no significant effect on the Wnt-3a-induced increase in *α-SMA* expression in SCR fibroblasts but showed a trend toward increased expression in shCAV fibroblasts, 194.6%, although this was not found to be significant (Figure 5.3B). Independent SFRP4 treatment also showed no effect on *α-SMA* expression in SCR or shCAV fibroblasts (Figure 5.3B).

At protein level, CAV-1 was confirmed to be significantly downregulated in shCAV compared to SCR fibroblasts (Figure 5.3C). However, α-SMA expression, despite being increased at mRNA level, was unchanged

following Wnt-3a treatment, Wnt-3a co-treatment with SFRP4 and also following independent SFRP4 treatment (Figure 5.3C).

Finally, the effect of CAV-1 expression on canonical Wnt signalling activity was determined and at basal level there was no change in *AXIN2* expression between SCR and shCAV fibroblasts (Figure 5.3D). Following Wnt-3a treatment, *AXIN*2 expression levels were similarly expressed by 195.9% ($P<0.0001$) and 193.9% ($P<0.0001$) in SCR and shCAV fibroblasts, respectively (Figure 5.3D). Wnt-3a co-treatment with SFRP4 did not affect Wnt-3a-induced *AXIN2* expression in either SCR or shCAV fibroblasts and independent SFRP4 treatment also showed no effect (Figure 5.3D).

These data were then confirmed by TOPFlash activity. Indeed, at basal level there was no change in TOPFlash activity between SCR and shCAV fibroblasts (Figure 5.3E). Wnt-3a treatment induced TOPFlash activity by 5.4-fold ($P<0.001$) in SCR and 4.5-fold ($P<0.001$) in shCAV fibroblasts, although the reduction in shCAV fibroblasts was not found to be significant (Figure 5.3E). Wnt-3a co-treatment with SFRP4 showed no effect on Wnt-3a-induced TOPFlash activity and independent SFRP4 treatment also showed no effect in SCR or shCAV fibroblasts (Figure 5.3E).

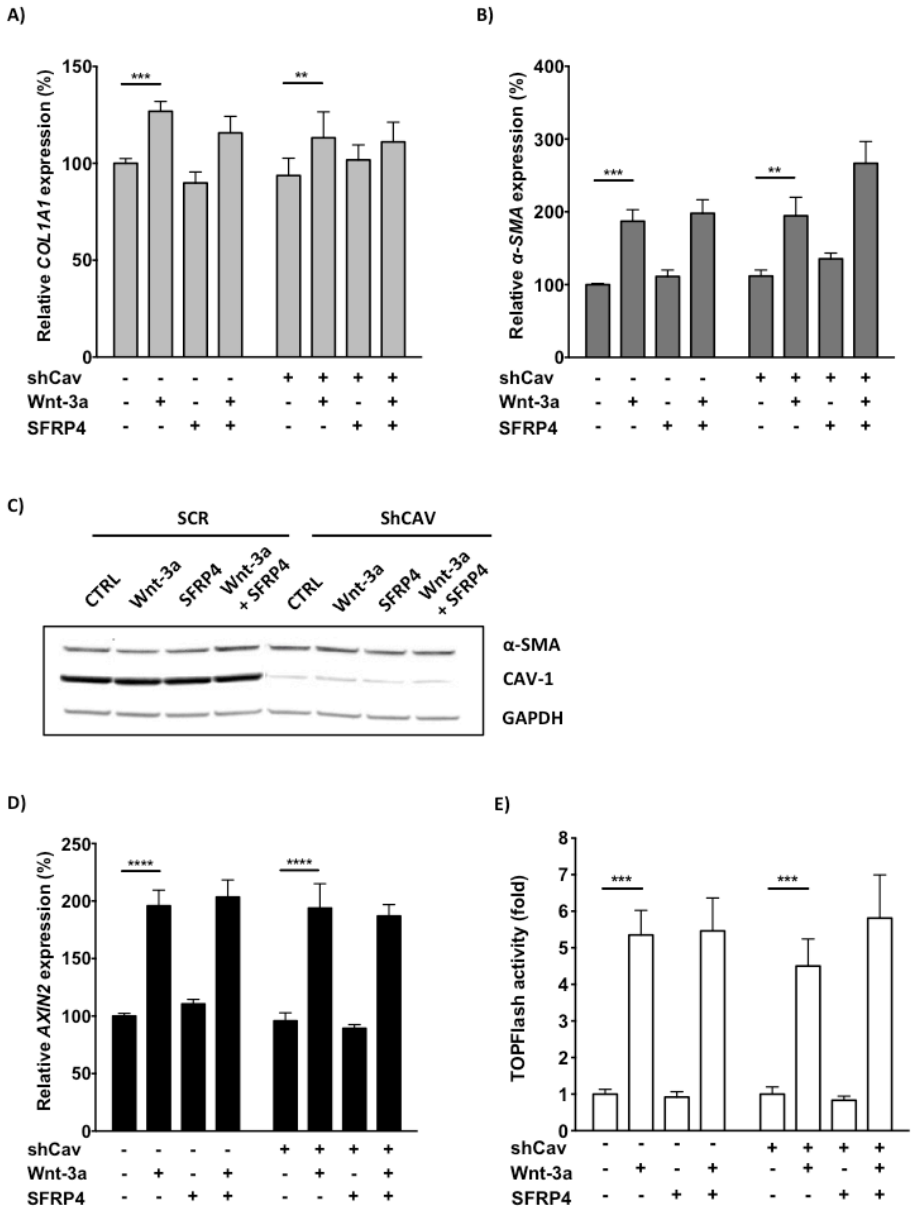

Figure 5.3 CAV-1 does not augment canonical Wnt-induced profibrotic or canonical Wnt signalling activities observed in SSc fibroblasts irrespective of SFRP4 treatment

Differential profibrotic gene expression and canonical Wnt singalling activation were compared between SCR and CAV-1 depleted shCAV fibroblasts treated with canonical agonist Wnt-3a (100 ng/ml) in the presence and absence of SFRP4 (70 ng/ml). The effect on profibrotic genes A) *COL1A1* and B) *α-SMA* were determined following 24 hr treatment and quantified by qRT-PCR. C) Following 72 hr treatment, protein expression of α-SMA and GAPDH (loading control) were used as a confirmation of profibrotic activity, determined by Western blot. Canonical Wnt signalling activation was evaluated following 24 hr treatment by D) *AXIN2* expression, a canonical Wnt target gene, quantified by qRT-PCR and by E) TOPFlash reporter activity, quantified by luciferase activity. All quantitative data were normalised on basal HC levels. Data shown as mean ± SEM, n=4; Mann-Whitney test for unpaired samples, ***P* = 0.01, ****P*=0.001, *****P* = 0.0001.

5.4 CAV-1 does not augment non-canonical or SFRP4 activities

Next it was determined whether in the absence of *CAV-1* i) there was an increased profibrotic response to non-canonical Wnt-5a treatment and ii) whether this could be due to crosstalk with the canonical signalling pathway. The effect of independent or Wnt-5a co-treatment with SFRP4 was also investigated for modulatory effects on both profibrotic gene expression and canonical signalling activity.

When profibrotic gene expression was examined, Wnt-5a treatment and Wnt-5a co-treatment with SFRP4 showed no effect on *COL1A1* expression in either SCR or shCAV fibroblasts (Figure 5.4A). In contrast, Wnt-5a induced *α-SMA* expression by 122.6% ($P<0.001$) in SCR and 141.0% ($P<0.05$) in shCAV fibroblasts, which was found to be significantly different between SCR and shCAV fibroblasts ($P<0.05$) (Figure 5.4A).

Wnt-5a co-treatment with SFRP4 showed a trend toward increased *α-SMA* expression in SCR fibroblasts, increased to 139.0%, and in shCAV fibroblasts, increased to 168.3% (Figure 5.4B). The difference in *α-SMA* expression following Wnt-5a co-treatment with SFRP4 was found to be significantly increased in shCAV fibroblasts compared to SCR fibroblasts (Figure 5.4B).

At protein level and consistent with mRNA data, α-SMA expression was unchanged at basal level (Figure 5.4C). However, Wnt-5a treatment or Wnt-5a co-treatment with SFRP4, despite being increased at mRNA level, showed no effect on the expression of α-SMA in both SCR and shCAV fibroblasts (Figure 5.4C).

Next the effect of CAV-1 expression on canonical Wnt signalling activity was determined under the same conditions. *AXIN2* expression was unaffected by Wnt-5a treatment in SCR fibroblasts, whereas expression was decreased to 75.6% ($P<0.01$) in shCAV fibroblasts (Figure 5.4D). Wnt-5a co-treatment with SFRP4 reduced *AXIN2* expression to 84.1% in HC fibroblasts but had no effect in shCAV fibroblasts compared to Wnt-5a treatment alone (Figure 5.4D). However, no significant increase in TOPFlash activity was observed following Wnt-5a treatment in both SCR and shCAV fibroblasts (Figure 5.4E). Furthermore, Wnt-5a co-treatment with SFRP4 also showed no effect on Wnt-5a-induced TOPFlash activity in HC fibroblasts but was increased by 1.6-fold in shCAV fibroblasts, although this was not found to be significant (Figure 5.4E).

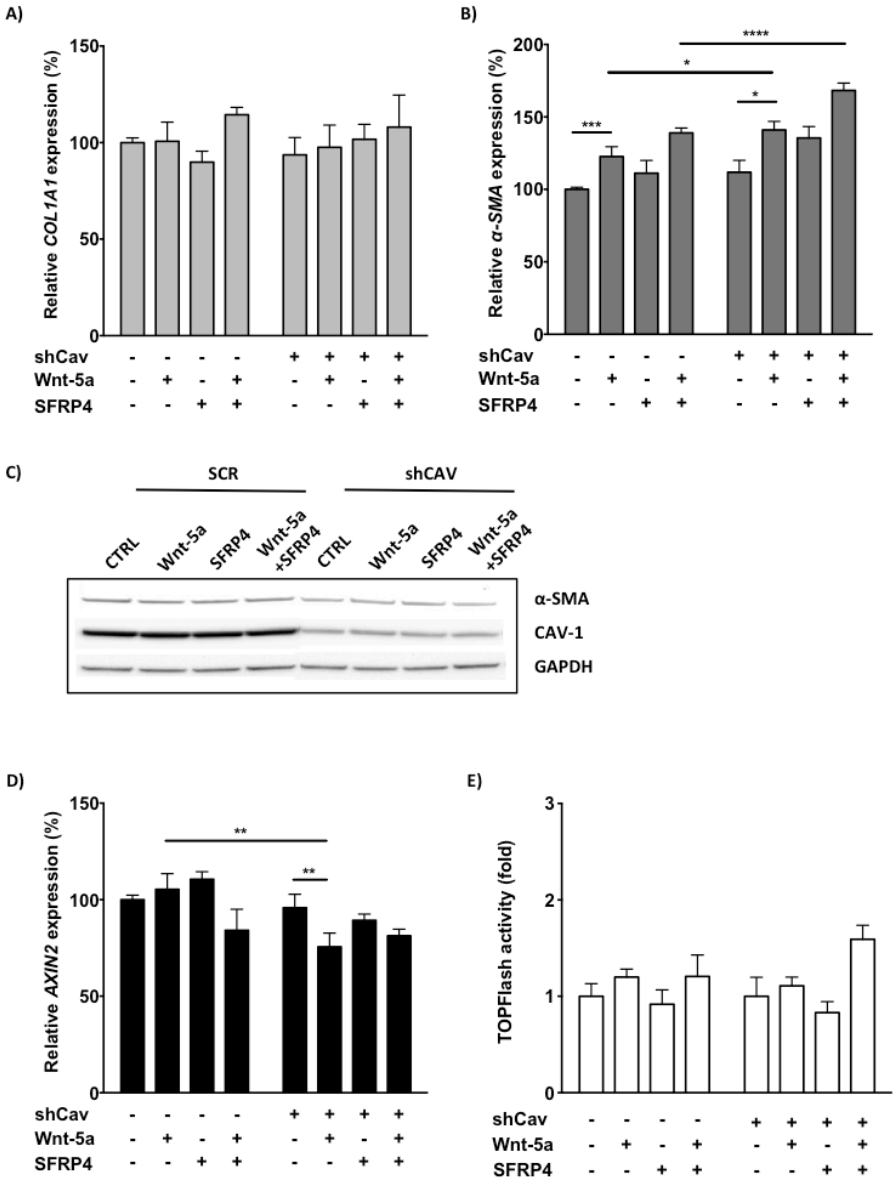

Figure 5.4 CAV-1 does not augment non-canonical or SFRP4 activities

Differential profibrotic gene expression and canonical Wnt singalling activation were compared between SCR and CAV-1 depleted shCAV fibroblasts treated with non-canonical agonist Wnt-5a (100 ng/ml) in the presence and absence of SFRP4 (70 ng/ml). The effect on profibrotic genes A) *COL1A1* and B) *α-SMA* were determined following 24 hr treatment and quantified by qRT-PCR. C) Following 72 hr treatment, protein expression of α-SMA and GAPDH (loading control) were used as a confirmation of profibrotic activity, determined by Western blot. Canonical Wnt signalling activation was evaluated following 24 hr treatment by D) *AXIN2* expression, a canonical Wnt target gene, quantified by qRT-PCR and by E) TOPFlash reporter activity, quantified by luciferase activity. All quantitative data were normalised on basal HC levels. Data shown as mean ± SEM, n=4; Mann-Whitney test for unpaired samples, **P*=0.05, ***P* = 0.01, ****P*=0.001, *****P* = 0.0001.

5.5 CAV-1 does not regulate TGFβ-mediated profibrotic gene expression or canonical Wnt signalling activity irrespective of SFRP4 treatment

Next, it was determined whether TGFβ treatment in the absence of *CAV-1* i) increased profibrotic gene expression and ii) modulated TGFβ-induced effects on canonical Wnt signalling activity. The effect of independent or TGFβ co-treatment with SFRP4 was also investigated for modulatory effects on both profibrotic gene expression and canonical signalling activity.

TGFβ induced a similar increase in *COL1A1* expression in SCR and shCAV fibroblasts by 230.3% ($p<0.001$) and 282.0% ($p<0.01$), respectively (Figure 5.5A). TGFβ co-treatment with SFRP4 showed a trend toward a reduction in *COL1A1* expression by 186.7% in SCR and 210.9% in shCAV fibroblasts (Figure 5.5A). *α-SMA* expression was also induced following TGFβ treatment by 1067.0% ($P<0.0001$) and 1646.6% ($P<0.01$) in SCR and shCAV fibroblasts, respectively (Figure 5.5B). TGFβ co-treatment with SFRP4 showed an increase in the expression of *α-SMA* by 2030.2% in SCR fibroblasts, which was not found to be statistically significant, and no additional induction was observed in shCAV fibroblasts (Figure 5.5B).

Next, canonical Wnt signalling activity was determined in relation to CAV-1 expression. At basal level, *AXIN2* expression was unchanged between SCR and shCAV fibroblasts and following TGFβ treatment *AXIN2* expression was reduced to 47.6% ($P<0.0001$) and 38.8% ($P<0.0001$) in SCR and shCAV fibroblasts, respectively (Figure 5.5C). TGFβ co-treatment with SFRP4 did not affect the TGFβ-induced downregulation of *AXIN2* (Figure 5.5C). In support of these data, TOPFlash activity was not significantly induced by TGFβ or affected by TGFβ co-treatment with SFRP4 in both SCR and

shCAV fibroblasts (Figure 5.5D).

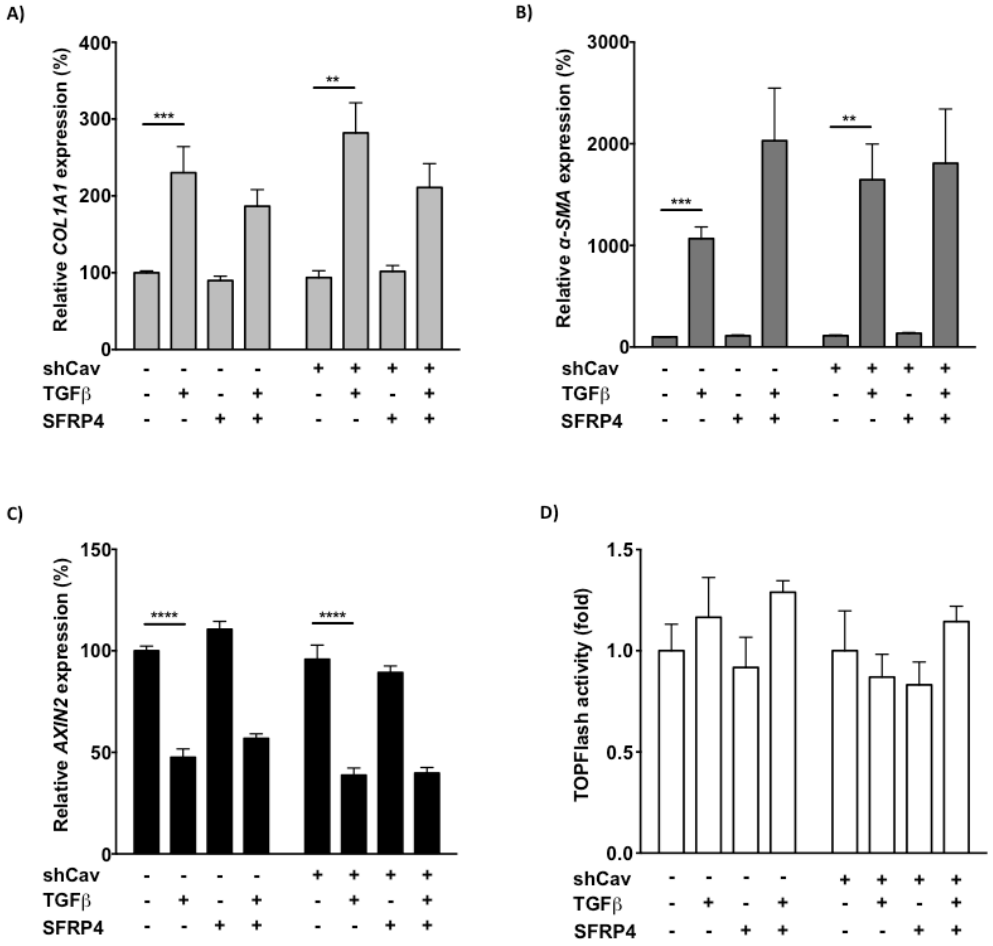

Figure 5.5 CAV-1 does not regulate TGFβ-mediated profibrotic gene expression or canonical Wnt signalling activity irrespective of SFRP4 treatment

Differential profibrotic gene expression and canonical Wnt singalling activation were compared between SCR and CAV-1 depleted shCAV fibroblasts treated with TGFβ (5 ng/ml) in the presence and absence of SFRP4 (70 ng/ml). The effect on profibrotic genes A) *COL1A1* and B) *α-SMA* were determined following 24 hr treatment and quantified by qRT-PCR. C) Following 72 hr treatment, protein expression of α-SMA and GAPDH (loading control) were used as a confirmation of profibrotic activity, determined by Western blot. Canonical Wnt signalling activation was evaluated following 24 hr treatment by D) *AXIN2* expression, a canonical Wnt target gene, quantified by qRT-PCR and by E) TOPFlash reporter activity, quantified by luciferase activity. All quantitative data were normalised on basal HC levels. Data shown as mean ± SEM, n=4; Mann-Whitney test for unpaired samples, ***P* = 0.01, ****P*=0.001, *****P* = 0.0001.

5.6 DISCUSSION: CAV-1 expression in the reproduction of SSc fibroblast phenotype

CAV-1 is downregulated in SSc patient fibroblasts and its expression has been shown to be important in regulating profibrotic gene expression, including collagen and α-SMA, through the inhibition of caveolae-mediated negative regulation of TGFβ signalling (Guglielmo et al., 2003; Del Galdo et al., 2008; Tourkina et al., 2008). In this study, myofibroblasts were identified, by immunofluorescence, through their arrangement of α-SMA into stress fibers and were confirmed to have a low expression of CAV-1 in contrast to the majority of fibroblasts that were CAV-1 positive (Figure 5.1A). Myofibroblasts are known to be key mediators of fibrosis and are though to persist in fibrotic tissues, including in SSc, and cause both increased ECM protein deposition as well as increased contracture in tissues (Hinz et al., 2001; Farina et al. 2009). Therefore, this led to the hypothesis that CAV-1 negative fibroblasts might reproduce elements of the SSc fibroblast phenotype, which might overlap with the profibrotic myofibroblast phenotype.

In this study, CAV-1 expression in SSc fibroblasts varied greatly, which could be due to dilution of myofibroblasts relative to the total SSc fibroblast population (Figure 5.1C).

TGFβ-mediated a substantial decrease in the expression of CAV-1 in contrast to Wnt-3a treatment, which indicated that any differential effects mediated by CAV-1 expression would likely be as a result of TGFβ rather than canonical Wnt signalling (Figure 5.1B).

To examine whether the increased SFRP4 expression, profibrotic gene expression and/or canonical Wnt signalling amplitude observed in SSc

fibroblasts could be regulated by CAV-1 expression, stable primary fibroblast lines were expressing either shRNA targeted against CAV-1 or a SCR sequence were created. Of the shCAV-1 expressing primary fibroblast lines, shCAV_97 and shCAV_99 showed a markedly reduced expression of CAV-1 compared to SCR fibroblasts (Figure 5.1F, G). This observation was found to be greater several passages after successful transduction and can be observed at protein level in the successive data sets.

First, the stable shCAV-1 expressing fibroblast lines were utilised to determine whether CAV-1 depleted fibroblasts could reproduce the increased expression of SFRP4 observed in SSc fibroblasts. Despite a profound reduction in CAV-1 protein expression, no spontaneous increase SFRP4 expression was observed nor was there any differential expression in response to Wnt-3a, Wnt-5a or TGFβ treatments compared to SCR fibroblasts. Therefore the increased expression of SFRP4 in both SSc and HC fibroblasts following TGFβ and canonical Wnt signalling was independent of CAV-1 regulation.

Next, in the absence of CAV-1 the effects of Wnt-3a, Wnt-5a and TGFβ were readdressed to determine any similarity with the differential responses observed in SSc compared to HC fibroblasts.

The first hypothesis investigated was whether CAV-1 negative fibroblasts might reproduce the Wnt-3a-induced increase in profibrotic gene expression and canonical Wnt signalling activation observed in SSc fibroblasts. In the absence of CAV-1, the Wnt-3a-induced effects on profibrotic gene

expression and canonical signalling activation were highly similar to those of SCR fibroblasts, which indicated that CAV-1 expression was not responsible for either the increased profibrotic gene expression or canonical signalling activation observed in SSc fibroblasts (Figure 4.1A-E Vs. Figure 5.3A-E). Furthermore, the reduced expression of *AXIN2* in SSc fibroblasts was also found to be independent of CAV-1 expression (Figure 4.1D Vs. Figure 5.3D).

These data were in contrast to a previous studies that showed that β-catenin was recruited to the cell membrane through the overexpression of CAV-1 thereby preventing canonical signalling induced by either Wnt-1 or β-catenin overexpression in NIH-3T3 fibroblasts (Galbiati et al., 2000). Similarly, β-catenin accumulation and Wnt signalling amplitude were positively regulated by the CAV-1-dependent internalisation of LRP6 in HEK293, HeLaS3 or CHO cells (Yamamoto et al., 2006).

Similarly, non-canonical Wnt-5a-induced activities were evaluated for differential responses following CAV-1 depletion. In contrast to SSc fibroblasts, *COL1A1* in was not induced by Wnt-5a or SFRP4, which initially suggested that CAV-1 was required for the elicited activity in SSc fibroblasts, although protein confirmation would be required (Figure 4.3A Vs. Figure 5.4A). Also, the expression of *α-SMA* was marginally increased; however, no effect on protein expression was observed (Figure 5.4B, C). Therefore the lack of any effect on α-SMA protein expression likely reflects the magnitude of effect upon collagen protein expression. This would therefore support the inference that CAV-1 did not regulate a differential Wnt-5a-induced

profibrotic effect in agreement with the lack of a differential effect between SSc and HC fibroblasts (Figure 4.3A-C).

Arguably, canonical Wnt signalling was also unaffected by Wnt-5a treatment in the absence of CAV-1 (Figure 5.4D, E). While *AXIN2* expression was decreased by Wnt-5a treatment, the relatively small 24.4% reduction was unlikely to be observable at protein level (Figure 5.4D). Although unlikely, these data could suggest that in the absence of CAV-1, Wnt-5a-induced non-canonical signalling could partially reproduce the decreased *AXIN2* expression observed in SSc fibroblasts (Figure 4.2D Vs. Figure 5.4D). To test this hypothesis further, non-canonical pathway activation would first need to be confirmed.

In addition to Wnt signalling, the effects of CAV-1 depletion upon TGFβ-induced signalling activities were also evaluated. In the absence of CAV-1, TGFβ treatment showed no differential expression of both *COL1A1* and *α-SMA* profibrotic genes compared to SCR fibroblasts (Figure 5.5A, B). This was not in agreement with several reports using siRNA mediated down-regulation of CAV-1, which have shown that the TGFβ-induced expression of α-SMA, collagen type I and fibronectin was enhanced in silenced cells (Wang et al., 2006; Del Galdo., 2008). Although siRNA technology has been considerably improved in recent years, the expression of these genes could be as a result of siRNA-mediated off-target effects. Further, these could lead to activation of as Toll-like receptors (TLR) 7/8, which recognise pathogen associated molecular proteins like single stranded RNA and lead to the upregulation of pro-inflammatory and interferon gene expression. By using

the endogenous cellular processing machinery, optimised shRNAmir constructs allow for sustainable gene silencing using low concentrations that have less chance of mediating off-target effects (Rao et al., 2009). One contrasting study, utilising an shRNA approach, showed that xenografts in nude mice, that were established by injection of either WT or shCAV1 neonatal dermal fibroblasts along with B16F10 melanoma cells, showed that while there was an increased tumor growth in shCAV xenografts, the intratumoral collagen deposition was unchanged in B16F10/shCAV1 compared to B16F10/WT tumors (Capozza et al., 2012). Although Del Galdo et al., showed that CAV-1 null fibroblasts explanted from mice showed increased *COL1A1* and *α-SMA* production, this could be attributed to the global deletion of CAV-1 in all cell types and the resultant environment the fibroblasts are exposed to prior to *in vitro* culture (Del Galdo et al., 2008).

Canonical signalling activity was subsequently evaluated following CAV-1 depletion, which showed no effect on basal *AXIN2* expression, in contrast to the reduction in SSc fibroblasts, or TOPFlash activity (Figure 5.5C, D). Therefore the TGFβ-induced downregulation of *AXIN2* expression, observed in both HC and SSc fibroblasts, was independent of CAV-1 regulation, which is potently downregulated by TGFβ. Indeed, this reduced expression of *AXIN2*, a regulatory component of Wnt signalling, could be an important factor contributing toward the increased canonical Wnt signalling amplitude observed in SSc fibroblasts.

Next, CAV-1 regulatory effects upon Wnt/TGFβ co-treatment with SFRP4 were evaluated for completeness to determine any differential activities.

In the absence of CAV-1, co-treatment of Wnt-3a or Wnt-5a with SFRP4 showed no further effect beyond that of HC fibroblasts for both profibrotic gene expression and canonical Wnt signalling activity under the same experimental conditions (Figure 4.2 Vs. Figure 5.3 & Figure 4.3 Vs. Figure 5.4, respectively). Comparative analysis showed that TGFβ co-treatment with SFRP4 had no differential effect on *COL1A1* expression in the absence of CAV-1, although protein data were unavailable to support this observation (Figure 5.5A). In the absence of CAV-1, the expression pattern for *α-SMA* was highly similar to that of SSc fibroblasts, which showed no increase in expression compared to HC fibroblasts; however, those data were also concluded to be inconsequential on analysis of protein expression (Figure 4.4B Vs. Figure 5.5B). Finally, both measures of canonical Wnt signalling activation showed no further effect following co-treatment with SFRP4 beyond that of independent TGFβ treatment (Figure 4.4E, F). These results suggest that CAV-1 does not differentially regulate rhSFRP4 activty to facilitate the increased profibrotic gene expression or increased canonical Wnt signalling activity observed in SSc fibroblasts following Wnt/TGFβ treatments.

Finally, the independent effects of rhSFRP4 treatment on profibrotic gene expression and canonical Wnt signalling activity were evaluated in the presence and absence of CAV-1. In SSc fibroblasts, the increased expression of *COL1A1* and *α-SMA* observed following SFRP4 treatment was

not observed in the absence of CAV-1, which could suggest that this is regulated independently of CAV-1 (Figure 4.2A, B Vs. Figure 5.3A, B); however, these increases at mRNA level were unlikely to influence protein expression as has been observed on several occasions with relation to α-SMA expression. Finally, the absence of any SFRP4-induced effect on canonical Wnt signalling activity was maintained following the depletion of CAV-1 (Figure 4.2D, E Vs. Figure 5.3D, E).

Overall, the prediction that CAV-1 expression might reproduce the increased canonical Wnt signalling response was not supported. Additionally, CAV-1 showed no regulatory activity on profibrotic fibroblast activation, as determined by the expression of fibroblast activation marker α-SMA, or canonical signalling activity at both basal levels and in response to TGFβ/Wnt agonists. Similarly, rhSFRP4 co-treatments and independent rhSFRP4 treatments also showed no differential activities. The subsequent focus of this study was to determine the mechanism behind the increased canonical Wnt signalling response observed in SSc fibroblasts and to determine the consequence, if any, on profibrotic fibroblast activation.

6 Crosstalk between the TGFβ and Canonical Wnt signalling pathways

As previously discussed, characteristically, fibrosis develops through the sustained activation of fibroblasts by factors including cytokines, growth factors and angiogenic factors present in the microenvironment (Varga & Pasche 2009; Kim et al., 2011). Activation of the TGFβ and Wnt/β-catenin signalling pathways have both been linked to the pathogenesis of tissue fibrosis in SSc (Beyer et al., 2012; Wei et al., 2011). While the level of crosstalk between the pathways is considered to be significant it is relatively under described. Principally, the increased canonical Wnt signalling response displayed by SSc fibroblasts might in fact be regulated by crosstalk between the TGFβ and Wnt and signalling pathways.

6.1 SSc fibroblasts display increased canonical Wnt/β-catenin signalling and a reduction in *AXIN2* expression

Characteristically, fibrosis develops through the sustained activation of fibroblasts and several studies have shown that β-catenin might be a central mediator shown in both SSc patients and experimental models of fibrosis (Beyer et al., 2012; Wei et al., 2012). One possibility was the potential for explanted SSc fibroblasts, from dcSSc patients, to self-activate through autocrine signalling and induce the canonical Wnt signalling pathway independent of the tissue microenvironment. In order to determine this, TOPFlash reporter activity was used to evaluate canonical β-catenin-activated TCF/LEF transcription. When compared to HC fibroblasts, SSc

fibroblasts showed no significant difference in the basal level of TOPFlash activity (Figure 6.1A). Next, TOPFlash assays were performed to see whether SSc fibroblasts displayed an increased response to canonical Wnt activation compared to HC fibroblasts. SSc fibroblasts displayed an increased response to canonical Wnt activation compared to HC fibroblasts, displaying 9.8-fold increase in TOPFlash activity following stimulation with Wnt-3a, which was significantly higher than the 4.8-fold increase observed in HC fibroblasts ($P<0.01$) (Figure 6.1A). Consistent with this, Wnt-3a-induced a 5.0-fold increase in *AXIN2* mRNA expression in SSc fibroblasts compared to the 1.8-fold increase in HC fibroblasts ($P<0.001$) (Figure 6.1B). Interestingly, the basal expression of *AXIN2* expression in SSc fibroblasts was reduced to 52% of HC fibroblasts ($P<0.01$) (Figure 6.1B). Although SSc fibroblasts were unavailable for comparative analysis, HC fibroblasts showed a time-dependent increase in Wnt-3a-induced β-catenin nuclear localisation, most abundant at 240 and 360 min (Figure 6.1D).

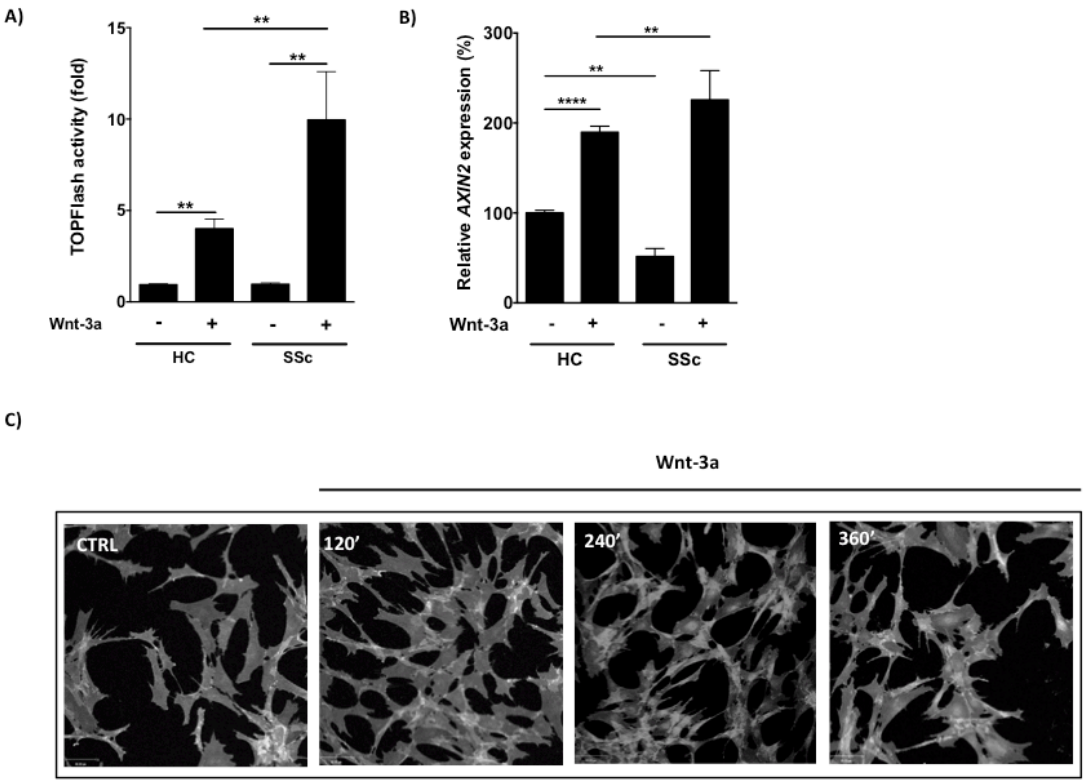

Figure 6.1 SSc fibroblasts display increased canonical Wnt/β-catenin signalling and a reduction in *AXIN2* expression

Differential canonical Wnt signalling activity was determined in additional HC and SSc fibroblasts. A) Fibroblasts were transfected with the TOPFlash reporter and following 24 hr treatment with Wnt-3a (100ng/ml) canonical Wnt signalling activity was determined by luciferase activity. B) HC fibroblasts were treated with Wnt-3a (100ng/ml) for 24 hr or for 0-360 min and *AXIN2* expression determined, quantified by qRT-PCR or C) Wnt-induced β-catenin localisation was determined by immunofluorescence using a CY3-conjugated secondary (grey) directed against anti-β-catenin antibody (magnification 200X). Data shown as mean ± SEM, n=3-5; Mann-Whitney test for unpaired samples, ***P*=0.01, *****P*=0.0001.

6.2 TGFβ signalling reproduces the reduced expression of AXIN2 observed in SSc fibroblasts

TGFβ plays a pivotal role in tissue homeostasis and numerous studies have demonstrated the TGFβ-induced profibrotic effects of TGFβ both *in vitro* and *in vivo*, which reproduce many of the hallmarks of fibrosis observed in SSc (Leask & Abraham, 2004; Wynn, 2008; Varga & Pasche, 2009). Increased TGFβ signalling has been proposed in SSc fibroblasts and at the very least a

subset of SSc patients display a TGFβ-regulated gene expression signature (Asano et al., 2005; Mimura et al., 2005; Milano et al., 2008; Sargent et al., 2009). Therefore to determine whether the observed reduction of AXIN2 in SSc fibroblasts was TGFβ-responsive, HC fibroblasts were treated with recombinant TGFβ and the effect upon AXIN2 expression and Wnt signalling activity were evaluated.

TGFβ-stimulated HC fibroblasts showed a 51% reduction in the expression of *AXIN2* expression at 24 hr ($P<0.0001$), which was equivalent to the basal level of *AXIN2* expression in SSc fibroblasts, 52% of HC levels (Figure 6.2A). Nevertheless these SSc fibroblasts showed a further reduction of AXIN2 expression to 20% of HC levels in the presence of TGFβ ($P<0.01$) (Figure 6.2A). Concordantly, AXIN2 protein expression in HC fibroblasts was significantly reduced following TGFβ treatment, which was again equivalent to the expression of AXIN2 in untreated SSc fibroblasts (Figure 6.2B).

To check whether TGFβ could induce canonical activation the level of TOPFlash activity was determined. Interestingly, TGFβ reduced the basal level of TOPFlash activity in HC fibroblasts by 0.6-fold and this was similar to the 0.3-fold reduction in SSc fibroblasts (Figure 6.2C).

As TGFβ was unable to induce TOPFlash activity, the nuclear localisation of β-catenin was evaluated following TGFβ or Wnt-3a treatment. Despite no meaningful depletion of β-catenin in the cytosolic fraction and in contrast to TOPFlash reporter data, TGFβ induced a notable increase in the nuclear fraction at 240 min and 360 min post-treatment, similar to the levels induced by Wnt-3a at 360 min, used as positive control (Figure 6.2D). The TGFβ-induced nuclear localisation of β-catenin was validated by

immunofluorescence of HC fibroblasts. Similar to the nuclear/cytosolic fractionation data, β-catenin was clearly distributed around the nucleus at 240 and 360 min following TGFβ treatment, although the majority of β-catenin was still observed to be membrane associated (Figure 6.2E).

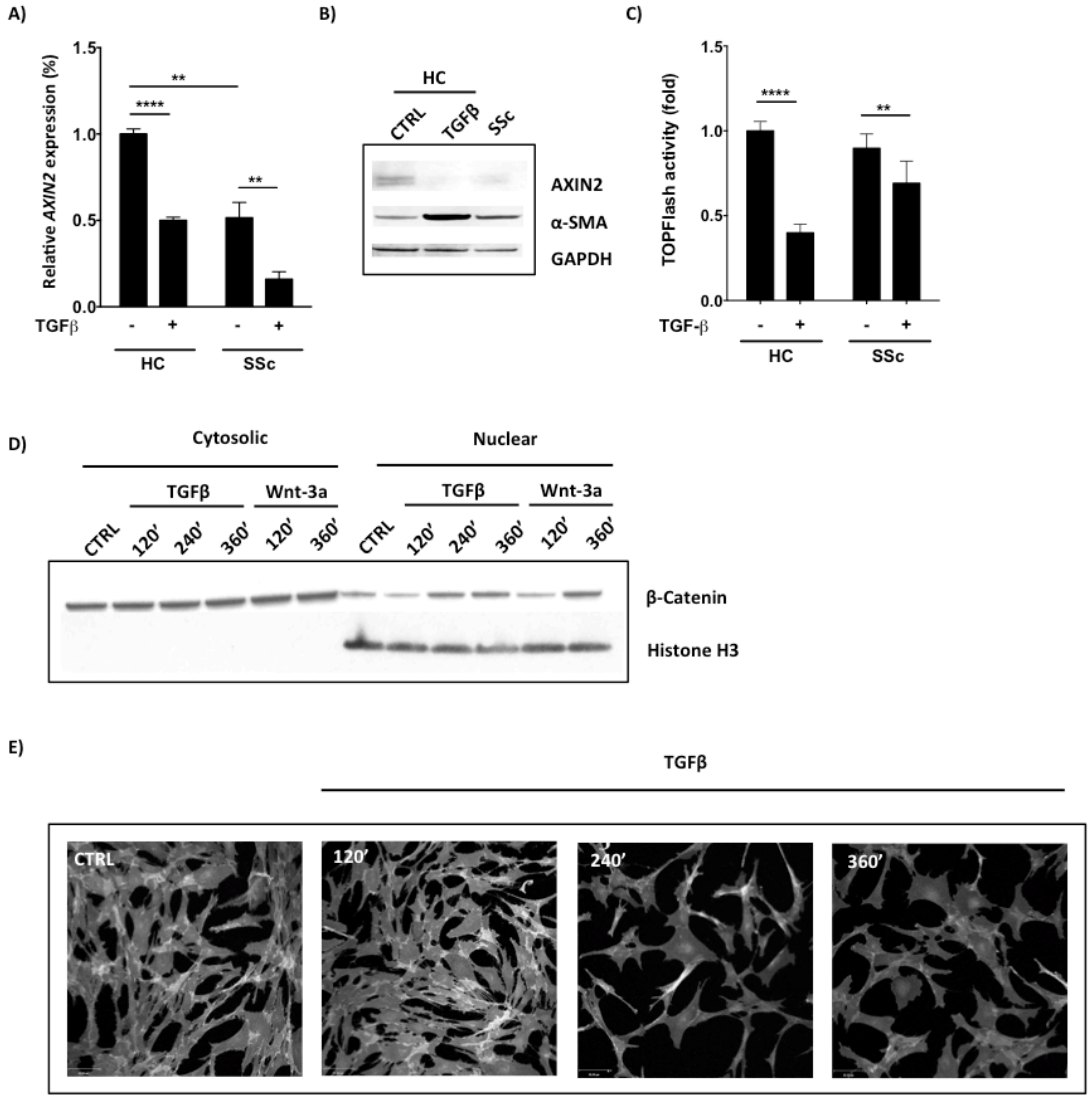

Figure 6.2 TGFβ signalling reproduces the reduced expression of AXIN2 observed in SSc fibroblasts

Comparative analysis between HC and SSc fibroblasts was used to determine whether AXIN2 expression was TGFβ-responsive. A) *AXIN2* expression was evaluated after stimulation with TGFβ (5ng/ml) for 24 hr, quantified by qRT-PCR or B) AXIN2, α-SMA (+ve) and GAPDH (loading control) protein expression were determined in treated HC and in resting HC and SSc fibroblasts. C) HC and SSc fibroblasts were transfected with the TOPFlash reporter and canonical signalling activity quantified by luciferase activity under the same treatment conditions. D) In HC fibroblasts, cytosolic/nuclear β-catenin localisation was determined following TGFβ (5ng/ml) treatment for 0-360 min by Western blot or E) β-catenin localisation as determined by immunofluorescence using a CY3-conjugated secondary (grey) against anti-β-catenin (200X magnification). Data shown as mean ± SEM, n=3-5; Mann-Whitney test for unpaired samples, ***P*=0.01, *****P*=0.0001.

6.3 TβRIIΔk-fib transgenic mice exhibit fibrosis and a reduction in Axin-2 positive nuclei

To evaluate *in vivo*, whether the downregulation of AXIN2 expression was a consequence of TGFβ signalling the TβRIIΔk-fib mouse mode was utilised, which demonstrate a ligand-independent and fibroblast-specific constitutive activation of the TGFβ signalling pathway that can ultimately lead to the development of fibrotic tissue involvement in a proportion of these mice.

In fact, DNA microarray analysis between WT mice treated with TGFβ and the TβRIIΔk-fib mouse model were found to be highly similar (Denton et al. 2003; Sonnylal et al. 2007). Consistent with previously published data, 6-8 weeks old TβRIIΔk-fib mice showed a significant increase in dermal thickness and loss of subcutaneous fat compared to WT (Figure 6.3B). Also, Massons Trichrome staining of the tissues showed a significant increase in the amount of collagen deposited in the dermis in TβRIIΔk-fib mouse tissue (Figure 6.3C). Immunohistochemistry staining of the same biopsies showed a decreased number of Axin-2 positive nuclei present in the dermis of TβRIIΔk-fib tissue compared to WT (white arrows depicting negative nuclei), but this was not absolute (Figure 6.3D). Counts of Axin-2 positive nuclei revealed that TβRIIΔk-fib tissue showed a 28% reduction compared to WT tissues (Figure 6.3E).

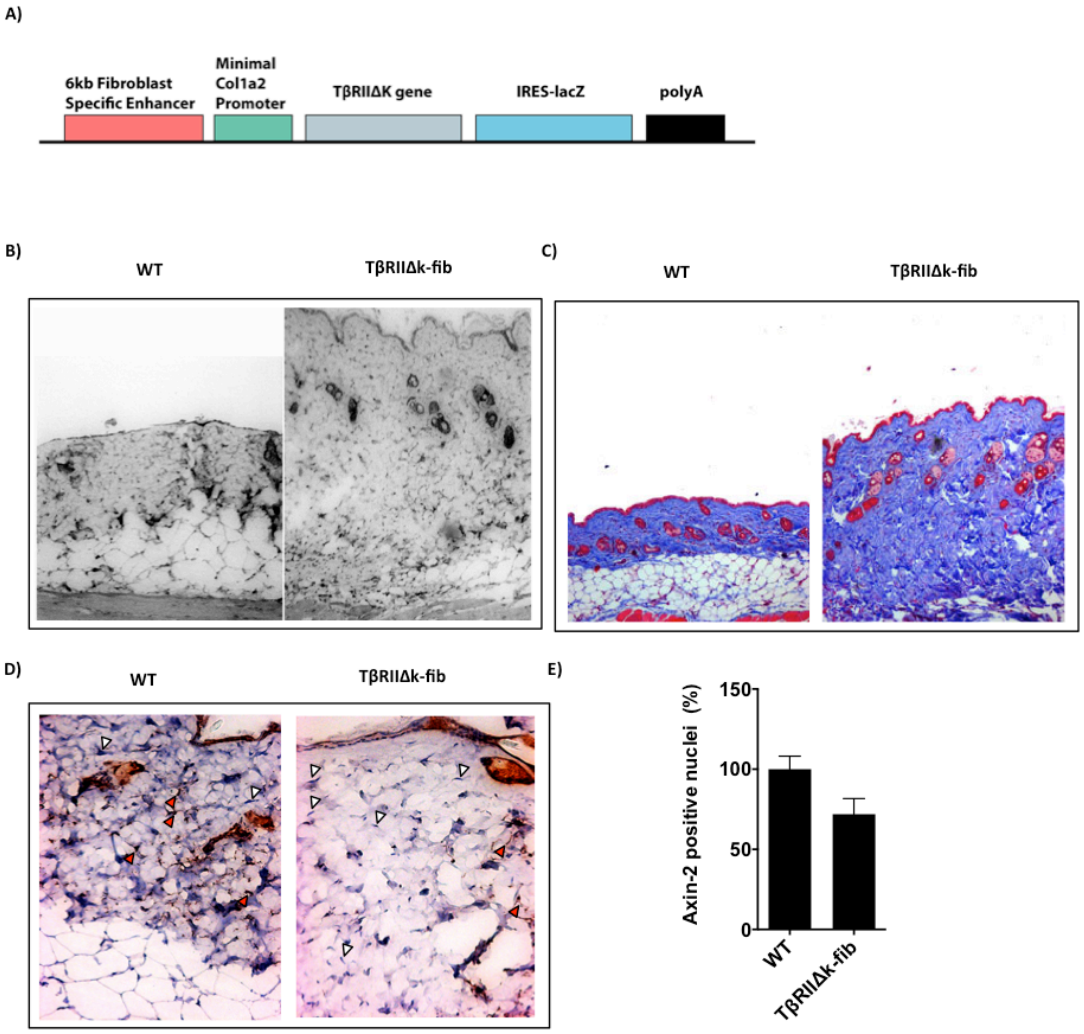

Figure 6.3 TβRIIΔk-fib transgenic mice exhibit fibrosis and a reduction in Axin-2 positive nuclei

Fibrosis and Axin-2 expression were compared between TβRIIΔk-fib transgenic mice, with fibroblast-specific constitutive activation of TGFβ signalling, and age-matched WT littermates. A) Schematic representation of the TβRII kinase-deficient transgene construct (TβRIIΔk-fib), regulated by a fragment of the *Col1a2* enhancer (–19.5 to –13.5 kb) fused with a minimal *Col1a2* promoter that also directs expression to the fibroblast lineage. B) Dermal fibrosis was evaluated by the distance between the muscle and epidermal boundary and by C) collagen deposition as determined by Masson's trichrome staining. D) In the same skin biopsies from B and C, Axin-2 expression was evaluated by immunohistochemistry (stained brown), where positive and negative nuclei are highlighted with red and white arrows, respectively. E) Counts of Axin-2 positive nuclei were taken from the same biopsies as D. Original magnification 400X. Data shown as mean ± SEM, n=3.

6.4 TGFβ priming of fibroblasts reproduces the increased canonical Wnt signalling response observed in SSc fibroblasts independent of Wnt secretion

One possible consequence of the decreased AXIN2 expression observed in SSc fibroblasts, which was also observed following TGFβ stimulation of HC fibroblasts, would be a reduced ability to negatively regulate β-catenin-mediated activity. Therefore, to determine whether the TGFβ-mediated downregulation of AXIN2 expression was responsible for the increased sensitivity of fibroblasts to canonical Wnt ligands, sequential stimulation experiments were performed in which HC fibroblasts were incubated first with TGFβ (TGFβ priming) and then subsequently treated with Wnt-3a.

TGFβ-primed fibroblasts showed a 3.1-fold increase in TOPFlash activity compared to fibroblasts treated with Wnt-3a alone ($P<0.01$) (Figure 6.4A). Interestingly, this was equivalent to the enhanced response to canonical Wnt signalling observed in SSc fibroblasts, which showed a 3.8-fold increase in TOPFlash activity compared to HC fibroblasts ($P<0.05$) (Figure 6.4B). Subsequently, the maximum increase in TOPFlash activity following TGFβ priming was investigated. While the effect of TGFβ priming on TOPFlash activity was observable within 2 hr by 1.6-fold, this was increased over time to 2.0-fold and 2.5-fold at 4 and 6 hr, respectively (Figure 6.4C). However, maximal effects were observed following 24 hr treatment and were sustained at 48 and 72 hr increased by 4.0-fold, 4.3-fold and 4.1-fold, respectively (Figure 6.4D).

Therefore, the effect of 24 hr TGFβ priming upon AXIN2 expression was subsequently evaluated. As expected, Wnt-3a treatment increased *AXIN2* expression by 287.2% in contrast to the reduction to 48.0% following TGFβ

treatment (Figure 6.4E). In TGFβ-primed fibroblasts, Wnt-3a induced a 247.1% increase in *AXIN2* expression, which was comparable to that observed following treatment with Wnt-3a alone. (Figure 6.4E). This effect was confirmed at protein level where TGFβ-primed fibroblasts showed increased expression of AXIN2 comparable to that induced by Wnt-3a treatment alone (Figure 6.4F). Consistent with previous observations TGFβ treatment alone induced a reduction of AXIN2 both at RNA and protein levels (Figure 6.4E-F).

In order to determine whether the increased canonical Wnt signalling observed in TGFβ-primed fibroblasts was a direct effect of an increase in nuclear β-catenin, nuclear localisation experiments were performed.

Nuclear β-catenin was increased in TGFβ-primed fibroblasts treated with Wnt-3a; however, the levels were equivalent to TGFβ treatment alone (Figure 6.4G). These levels were much higher than those observed following Wnt-3a treatment alone (Figure 6.4G). Consistently, no depletion of β-catenin in the cytosolic cellular fraction was observed (Figure 6.4G). In contrast, a concomitant reduction of SMAD3, a positive control for TGFβ-induced activity, was evident in cytosolic fraction and was increased in the nuclear fraction for both (Figure 6.4G).

To determine whether TGFβ-induced β-catenin nuclear localisation was dependent on the expression/secretion of canonical Wnt ligands and ultimately a consequence of increased Wnt-induced signalling, blockade of Wnt secretion was utilised. This was achieved using the inhibitor of Wnt Production-2 (IWP-2) to block the palmitoylation of intracellular Wnt proteins, thereby reducing their solubility and preventing their subsequent secretion.

Concurrent with previous data, TGFβ treatment did not significantly deplete the cytosolic fraction; however, a significant increase in nuclear β-catenin was observed and was unchanged in the presence of IWP-2 at concentrations of 200nM, 1.0 μM (5.0-fold excess) and also at 2 μM (10.0-fold excess) (Figure 6.4H).

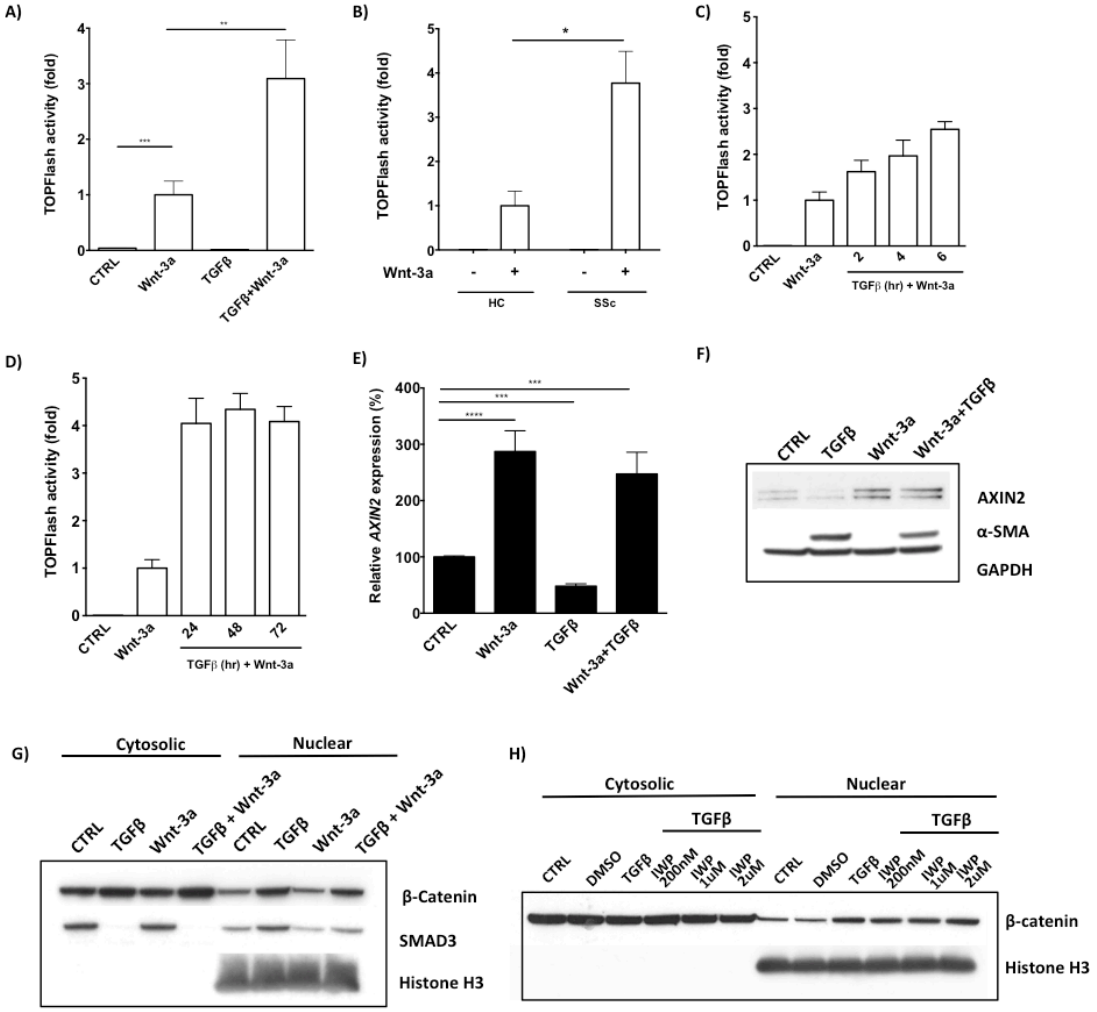

Figure 6.4 TGFβ priming of fibroblasts reproduces the increased canonical Wnt signalling response observed in SSc fibroblasts independent of Wnt secretion

TGFβ-primed fibroblasts were compared against HC counterparts to determine whether TGFβ could reproduce the increased sensitivity observed in SSc fibroblasts. A) HC fibroblasts were transfected with the TOPFlash reporter and treated with (primed) or without TGFβ (5 ng/ml) for 24 hr, followed by Wnt-3a treatment (100 ng/ml) for 24 hr before TOPFlash activity was quantified by luciferase activity. B) The relative amplitude in canonical Wnt signalling activity between SSc and HC fibroblasts was determined by TOPFlash activity following Wnt-3a treatment for 24 hr. TOPFlash activity was measured relative to Wnt-3a-treated HC fibroblasts, set to 1-fold (100% activation). C-D) As in A, but TGFβ treatment was carried out for 2-72 hr prior to Wnt-3a treatment. E) Under the same experimental condition in A, the effects on *AXIN2* expression, quantified by qRT-PCR. F) As in A, where Wnt-3a treatment was carried out for 72 hr prior to determination of AXIN2, α-SMA (+ve) and GAPDH (loading control) protein expression by Western blot. G) Cytosolic/nuclear localisation of β-catenin and SMAD3 (+ve) were determined by Western blot following 240 min TGFβ treatment. H) TGFβ-mediated β-catenin nuclear localisation was determined following IWP-2-mediated inhibition of Wnt secretion, incubated 1 hr prior to 240 min TGFβ treatment. Data shown as mean ± SEM, n=3-5; Mann-Whitney test for unpaired samples, **P*=0.05, ***P*=0.01, ****P*=0.001, *****P*=0.0001.

6.5 AXIN2 silencing reproduces the increased canonical Wnt signalling response observed in TGFβ-primed fibroblasts

Since TGFβ has a multitude of intracellular targets, to determine whether the observed downregulation of AXIN2 was sufficient to explain the increased responsiveness of fibroblasts to canonical Wnt-induced signalling AXIN2 expression was downregulated by siRNA.

First, control siRNA conjugated to AlexaFluor-488 was transfected into HC fibroblasts and used to determine the transfection efficiency by immunofluorescent visualisation across a 10-40 nM concentrations (Sup Figure 10.1). At an oligonucleotide concentration of 20nM, transfection efficiency was deemed to be optimal and was therefore utilised in all further transfection experiments (Figure 6.5A).

Next, HC fibroblasts were transfected with either *AXIN2*-specific siRNA (siAXIN2) or scramble control oligonucleotide (SCR). A 48% reduction in *AXIN2* expression was achieved in siAXIN2 compared to SCR fibroblasts ($P<0.05$) (Figure 6.5B). Similar results were also observed at protein level, where AXIN2 expression was significantly downregulated at 48 and 72 hr post-transfection, while the expression of AXIN1 remained unaffected (Figure 6.5C).

Next, canonical Wnt signalling amplitude was evaluated in siAXIN2 fibroblasts treated with Wnt-3a, and normalised relative to treated SCR fibroblasts. Wnt-3a treatment increased TOPFlash activity in siAXIN2 fibroblasts 5.9-fold more than in SCR-treated fibroblasts ($P<0.05$) (Figure 6.5D).

Of note, Wnt-3a treatment of untransfected HC fibroblasts induced an increase in TOPFlash activity equivalent to the level induced in SCR fibroblasts (Figure 6.5D).

Parallel experiments determined whether a reduction in AXIN2 expression could modulate TOPFlash activity in response to TGFβ. In siAXIN2 fibroblasts a 0.7-fold decrease in TOPFlash activity was observed compared to SCR controls; however, the response to TGFβ in siAXIN2 fibroblasts was similar to that observed in SCR fibroblasts decreased to 0.4-fold and 0.6-fold, respectively (Figure 6.5E).

Finally, to determine whether AXIN2 expression was involved in the regulation of TGFβ signalling activity, total TGFβ reporter activity was evaluated in siAXIN2 fibroblasts. While no spontaneous increase in TGFβ activity was observed in siAXIN2 fibroblasts, a 2.0-fold increase in TGFβ reporter activity was observed following Wnt-3a treatment, which was greater than the 1.4-fold increase observed in SCR fibroblasts (Figure 6.5F).

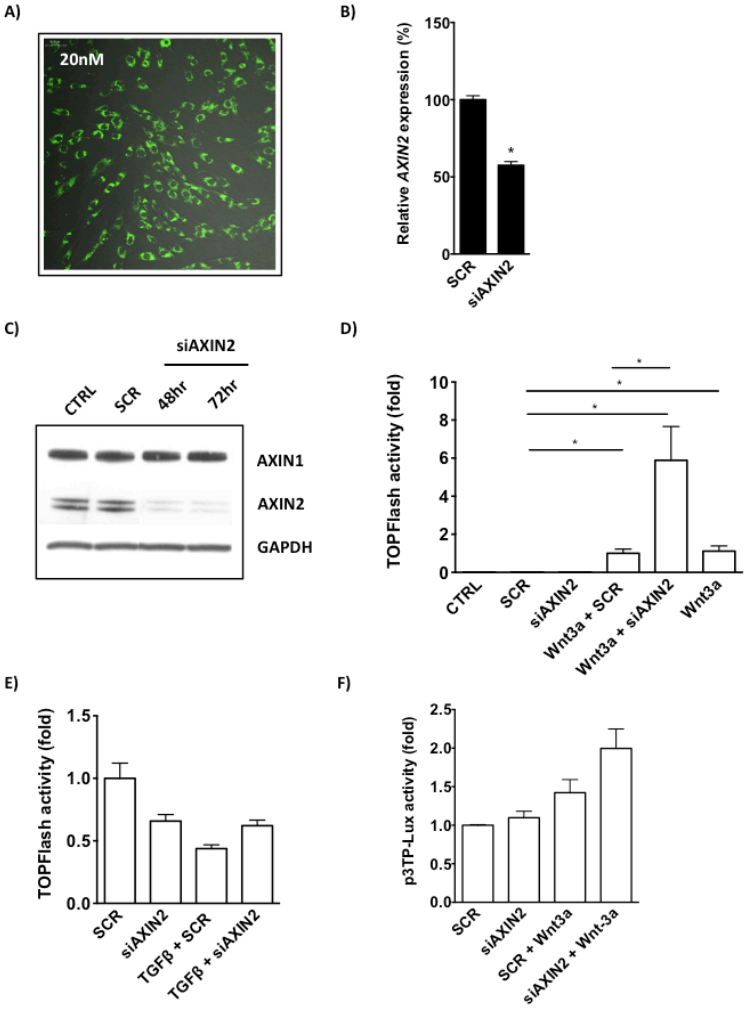

Figure 6.5 AXIN2 silencing reproduces the increased canonical Wnt signalling response observed in TGFβ-primed fibroblasts

AXIN2 depletion was used to determine wether TGFβ-mediated AXIN2 downregulation was sufficient for the increased canonical Wnt signalling amplitude observed in TGFβ-primed fibroblasts. A) HC fibroblasts were transfected with negative control siRNA coupled to AlexaFluor488 (green) and transfection efficiency was determined visually by immunofluorescence. B) HC fibroblasts were either transfected with scrambled (SCR) or *AXIN2*-specific siRNA (siAXIN2) for 72 hr and *AXIN2* mRNA expression was quantified by qRT-PCR or C) protein expression of AXIN1, AXIN2 and GAPDH (loading control) were determined following 48-72 hr transfection by Western blot. D) HC fibroblasts were transfected with TOPFlash reporter 24 hr prior to transfection with AXIN2 or SCR siRNA for 72 hr. Subsequently, cells were treated with or without Wnt-3a for a further 24 hr and canonical signalling activation determined by luciferase activity relative to Wnt-3a-treated SCR fibroblasts; set to 1-fold (100% activation). E) As in D, where Wnt-3a was substituted for TGFβ. TGFβ signalling activity was subsequently evaluated in HC fibroblasts by F) transfection with p3TP-Lux reporter (Total TGFβ activity) 24 hr prior to transfection with siAXIN2 or SCR siRNA for 72 hr. Subsequently, cells were treated with or without Wnt-3a for a 24 hr and TGFβ signalling activity was evaluated by luciferase activity relative to SCR fibroblasts. Data shown as mean ± SEM, n=3-5; Mann-Whitney test for unpaired samples *P=0.05.

6.6 AXIN2 has a greater effect than AXIN1 upon canonical Wnt signalling amplitude

AXIN1 shares 45% amino acid sequence homology to AXIN2 and is also important in the formation and function of the β-catenin destruction complex (Chia & Costantini 2005). However, functional studies have also demonstrated their activities may not be entirely redundant (Lammi et al. 2004). Therefore the relative contribution of AXIN1, compared to AXIN2, towards the regulation of canonical Wnt signalling amplitude was investigated.

First, the expression of *AXIN1* in HC fibroblasts was examined following TGFβ treatment and was downregulated to 80.2% and 66.9% at 48 and 72 hr, respectively (Figure 6.6A). This was significantly less than the TGFβ-mediated downregulation of *AXIN2*, reduced to 60.7% as soon as 10 min (Figure 7.1B). Importantly, despite a slight downregulation at mRNA level, TGFβ treatment did not alter the protein expression of AXIN1 up to 72 hr later (Figure 6.6B).

Despite this, parallel experiments were conducted to determine the relative role of AXIN1 expression in the regulation of canonical Wnt signalling amplitude. Here, HC fibroblasts were transfected with siRNA targeted against *AXIN1* (siAXIN1) or SCR oligonucleotide. A significant downregulation of AXIN1 expression was observed in siAXIN1 fibroblasts compared to SCR (Figure 6.6C). Next, canonical signalling was then evaluated in siAXIN1 fibroblasts by TOPFlash activity. Following Wnt-3a treatement TOPFlash activity was increased by 1.9-fold in siAXIN1 compared to Wnt-3a treated SCR fibroblasts ($P<0.05$) (Figure 6.6D). Overall, AXIN1 depletion displayed an increase in canonical Wnt activity that was

4.0-fold less than that observed in siAXIN2 fibroblasts (Figure 6.6D vs. Figure 6.5D).

Similar experiments investigated whether a reduction in AXIN1 expression could modulate TOPFlash activity in response to TGFβ. Indeed, siAXIN1 fibroblasts showed a 0.7-fold decrease in TOPFlash activity compared to SCR controls (Figure 6.6E). In the presence of TGFβ, both siAXIN1 and SCR fibroblasts showed no significant change in TOPFlash activity, 0.7-fold and 1.0-fold, respectively (Figure 6.6E).

Next, to determine the effect of AXIN1 expression on the amplitude of the TGFβ signalling pathway, this was evaluated using the p3TP-lux reporter, which measured total TGFβ signalling activity. While in siAXIN1 fibroblasts basal TGFβ signalling activity was reduced by 0.3-fold, a 1.3-fold and 1.4-fold increase was observed following TGFβ treatment in siAXIN1 and SCR fibroblasts, respectively (Figure 6.6F).

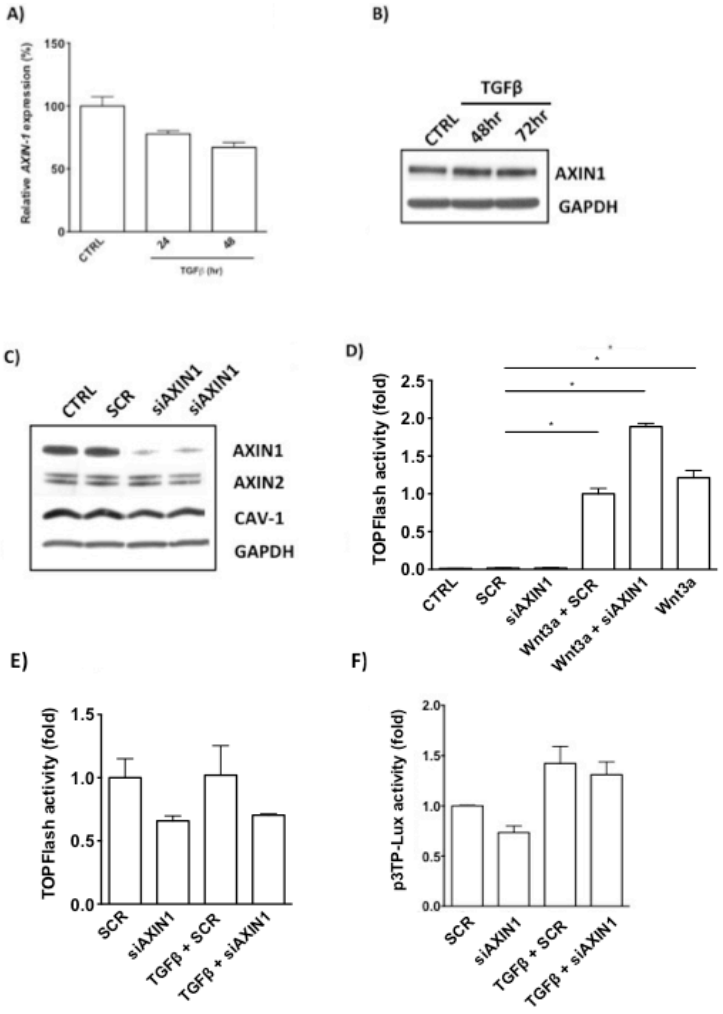

Figure 6.6 AXIN2 has a greater effect than AXIN1 upon canonical Wnt signalling amplitude

The contribution of AXIN1 relative to AXIN2 in the regulation of canonical Wnt signalling was evaluated. A) HC fibroblasts were treated with TGFβ for 24-48 hr and *AXIN1* expression quantified by qRT-PCR or B) TGFβ treated for 48-72 hr prior to determination of AXIN1 and GAPDH (+ve) protein expression by Western blot. C) HC fibroblasts were transfected with scrambled (SCR) or *AXIN1*-specific siRNA (siAXIN1) for 72 hr and AXIN1, AXIN2 (-ve) and GAPDH (loading control) protein expression determined by Western blot. D) HC fibroblasts were transfected with TOPFlash reporter 24 hr prior to transfection with siAXIN1 or SCR for 72 hr. Subsequently, cells were treated with or without Wnt-3a for 24 hr and canonical Wnt signalling activation was evaluated by TOPFlash activity, determined by luciferase activity relative to Wnt3-a-treated SCR fibroblasts; set to 1-fold (100% activation). Next, TGFβ activity was evaluated. E) As in D, where Wnt-3a was substituted for TGFβ. TGFβ signalling activity was subsequently evaluated in HC fibroblasts by F) transfection with p3TP-Lux reporter (Total TGFβ activity) 24 hr prior to transfection with siAXIN2 or SCR siRNA for 72 hr. Subsequently, cells were treated with or without Wnt-3a for a 24 hr and TGFβ signalling activity was evaluated by luciferase activity relative to SCR fibroblasts. Data shown as mean ± SEM, n=3-5; Mann-Whitney test for unpaired samples *P=0.05.

6.7 Stabilisation of AXIN can inhibit the increased canonical signalling observed in TGFβ-primed fibroblasts

As AXIN2 negatively regulated the amplitude of canonical Wnt signalling it was important to validate whether the increased canonical Wnt signalling response induced in TGFβ-primed fibroblasts was a specific effect of AXIN2 downregulation. Therefore, the bioavailability of AXIN2 protein was increased in fibroblasts through the stabilisation of AXIN protein expression using a small molecule inhibitor, XAV-939, which has been shown to protect AXIN from proteasomal degradation (Huang et al. 2009).

The ability of XAV-939 to protect AXIN2 protein from proteolytic degradation was evaluated. HC fibroblasts were treated with XAV-939 and a step-wise increase in the level of AXIN2 protein expressed was observed across a dose range of 0.3-10.0 μM (Figure 6.7A). Next, the concentration at which XAV-939 conferred protective activity in the presence of TGFβ was determined. The expression of AXIN2 remained stable in the presence of TGFβ when treated with XAV-939 across a dose range of 1.0-10.0 μM (Figure 6.7B). Consistent with the known role of AXIN2, in the presence of XAV-939, the Wnt-3a-induced increase in TOPFlash activity was by 0.6-fold, 0.5-fold or 0.5-fold at 10.0, 3.0 and 1.0 μM of XAV-939, respectively (Figure 6.7C). This validated the ability of XAV-939 to regulate the amplitude of canonical Wnt signalling through AXIN stabilisation.

Subsequently, XAV-939 was used to determine the relative role of AXIN2 downregulation towards the increased amplitude of canonical Wnt signalling observed in TGFβ primed fibroblasts or whether other TGFβ targets

mediated this activity. Consistent with previous data, Wnt-3a treatment of TGFβ-primed fibroblasts showed a 2.1-fold increase in TOPFlash activity compared to HC fibroblasts (P<0.05) (Figure 6.7C). This increase in TGFβ-primed fibroblasts was reduced in the presence of XAV-939 and equivalent to the total Wnt-3a-induced activation observed in HC fibroblasts, reduced to to 0.9-fold, 0.9-fold or 1.0-fold at 10.0 μM, 3.0 μM and 1.0 μM, respectively (P<0.05) (Figure 6.7C).

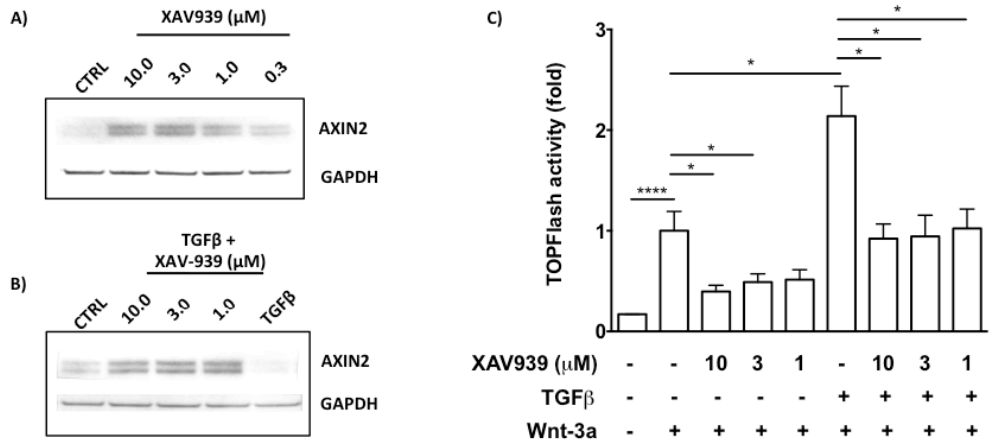

Figure 6.7 Stabilisation of AXIN can inhibit the increased amplitude of canonical signalling observed in TGFβ-primed fibroblasts

A) In HC fibroblasts, AXIN stabilisation was determined following XAV-939 treatment (1.0-10.0 μM for 24 hr and AXIN2 and GAPDH (loading control) protein expression were determined by Western blot. B) AXIN stability was evaluated in the presence of TGFβ treatment (5 ng/ml) and protein expression of AXIN2 and GAPDH (loading control) were determined by Western blot. C) To determine if AXIN stabilisation was sufficient to ablate the TGFβ-mediated increase in canonical Wnt signalling, HC fibroblasts were transfected with the TOPFlash reporter for 24 hr then treated with TGFβ (primed) or left untreated for 24 hr. Subsequently, fibroblasts were treated with or without XAV-939 (1.0-10.0 μM) 1 hr prior to Wnt-3a treatment (100ng/ml) for a further 24 hr prior to the determination of TOPFlash activity, quantified by luciferase activity. Data shown as mean ± SEM, n=3-5; Mann-Whitney test for unpaired samples *P=0.05, ****P=0.0001.

6.8 DISCUSSION: Crosstalk between the TGFβ and Canonical Wnt signalling pathways

Having previously demonstrated that SSc fibroblasts had an exaggerated canonical Wnt signalling response to canonical Wnt-3a treatment (Figure 4.2D, E), a further series of experiments in different SSc and HC patients reconfirmed these observations (Figure 6.1A). Consistently, SSc fibroblasts had a reduced basal expression of *AXIN2* and, following Wnt-3a treatment, a concomitant increase in canonical Wnt signalling (Figure 6.1B). These data indicated that explanted SSc fibroblasts, under basal conditions, do not display an autonomous increase in canonical Wnt signalling and instead imply that these fibroblasts are primed to respond to canonical Wnt agonist. This extends upon previous studies that support the role of differential Wnt ligand expression in the increased activation of the canonical Wnt signalling pathway (Akhmetshina et al., 2012; Beyer et al., 2012; Wei et al., 2012). Indeed, the increased canonical Wnt signalling activation consistently observed in SSc skin biopsies (nuclear β-catenin staining) may be as a consequence of both of these factors working in parallel.

Due to the limited availability of samples from SSc patients, a direct comparison, between β-catenin translocation in SSc and HC fibroblasts, to determine the differential effects upon the kinetics and integrated density of fluorescence could not be performed. However, immunofluorescence data from HC fibroblasts showed a distinct nuclear β-catenin localisation following Wnt-3a treatment, which supported the methodology and analysis of TOPFlash reporter data (Figure 6.1C). This data also showed that while Wnt-induced β-catenin translocation localised around the nucleus, an en masse translocation was not observed, similar to other studies that also

showed an unremarkable translocation pattern in fibroblasts (Carthy et al. 2011; Wei et al. 2012; Akhmetshina et al. 2012). Indeed it has long been know that β-catenin can interact with the cytoplasmic tails of cadherins and participate in cell adhesion processes, therefore, aside from a critical role in TCF/LEF-mediated transcriptional activation, β-catenin might also play a wider role in regulating other biological mechanisms (Ko et al., 2001; Luo & Lin 2004).

In SSc, the link between TGFβ signalling in the activation and differentiation of fibroblasts is well described and its involvement in the pathogenesis of tissue fibrosis compelling (Varga & Pasche 2009). Of note was the fact that a key gene profiling study evaluating TGFβ responsive genes intrinsic to the dcSSc subset, did not display a distinct Wnt signalling profile in dcSSc patients dermal fibroblasts (Milano et al., 2008; Sargent et al., 2009). However, on further inspection of the supplementary data, two important negative regulators of Wnt signalling were significantly downregulated, namely *AXIN2* and *DKK-1*, which could explain the reduced expression of *AXIN2* in SSc fibroblasts observed previously (Figure 6.1B). Therefore, the effect of TGFβ signalling upon the expression of AXIN2 was evaluated by comparative analysis of SSc and HC fibroblasts. In support of the gene profiling study, TGFβ induced a significant downregulation of AXIN2 expression in HC fibroblasts, which was equivalent to the basal levels expressed in SSc fibroblasts (Figure 6.2A, B). These data could support an autocrine or constitutive TGFβ signalling activity within explanted SSc fibroblasts. Additionally, TGFβ signalling has recently been described to

influence canonical Wnt signalling activation in fibroblasts, through downregulation of the Wnt antagonist DKK-1 (Akhmetshina et al., 2012). One important contrast with the previous study was a consistent absence of TOPFlash reporter induction in fibroblasts following TGFβ treatment (Figure 6.2C). In support of our results, two seminal papers identified the mechanism by which the TGFβ pathway can influence canonical Wnt signalling amplitude. The homeobox *twin* (*Xtwn*) gene, similar to *AXIN2*, was identified as a direct Wnt-responsive target that was under the control of the LEF1 transcription factor in *Xenopus* (Laurent et al., 1997). Differential analysis of Xtwn and the TOPFlash reporter constructs found that the former was TGFβ responsive while the later was not (Labbe et al., 2000; Nishita et al., 2000). This was found to be dependent on the presence of SBEs, located in the Xtwn promoter that were absent in the TOPFlash reporter, but which could be made TGFβ-inducible by the inclusion of SBE upstream of the TCF/LEF consensus sequences (Labbe et al., 2000; Nishita et al., 2000). Labbe et al., also concluded that TGFβ-dependent activation of LEF1 target could be independent of β-catenin; however, reinterpreting these data, β-catenin was essential as its loss significantly affected the induction of the promoter system by approximately 362% (Labbe et al., 2000). Together, these data indicate the critical nature of β-catenin in canonical (β-catenin-mediated) Wnt signalling and the further augmentation that can result from the presence of SBEs within the promoter sequences of a subset of canonical target genes.

Paradoxically, TGFβ, like Wnt-3a, induced β-catenin nuclear translocation in HC fibroblasts in contrast to the absence of TOPFlash activity (Figure 6.2C

Vs. D). Furthermore, this translocation was subsequently confirmed by β-catenin immunofluorescence data (Figure 6.2E). Again, due to the lack of patient samples experiments could not be carried out to confirm whether the effects observed in HC fibroblasts were similar to SSc fibroblasts and this represents a limitation of the analysis. These conflicting data would need to be resolved and promoter analysis of genes known to be upregulated by canonical Wnt signalling would be a logical first step. Although *AXIN2* is a direct Wnt-induced target other targets would need to be included due to the effect of TGFβ upon *AXIN2* expression. Overall, whether TGFβ-induced nuclear β-catenin translocation takes part in TCF/LEF mediated canonical Wnt signalling is debatable.

Like HC fibroblasts, TGFβ treatment also reduced *AXIN2* expression levels in SSc fibroblasts (Figure 6.2A). Explanted fibroblasts from the TβIIΔk-fib transgenic model, which have a constitutive and fibroblast-specific activation of TGFβ signalling, do display increased activation of TGFβ signalling pathways; however, these fibroblasts were also refractory to further TGFβ treatment (Denton et al. 2003). Together, these data would indicate that explanted SSc patient fibroblasts are not refractory to TGFβ treatment and therefore constitutive TGFβ signalling might not be a characteristic. This adds to a body of evidence that is already conflicting on the role of autocrine TGFβ signalling within SSc fibroblasts (Desmoulière et al. 1993; Kubo et al. 2002; Ihn et al. 2001; Gabbiani 2003; Asano et al. 2011; Ho et al. 2014).

Since TGFβ was discovered to mediate the downregulation of AXIN2 expression in HC fibroblasts *in vitro*, this was subsequently validated *in vivo*

using the TβRIIΔk-fib mouse model, described previously. This model displayed evidence of fibrosis through increased dermal thickness, loss of subcutaneous fat and increased collagen deposition, which were consistent with the literature (Figure 6.3A-C) (Denton et al. 2003). Specifically, Axin-2 positive nuclei for were reduced in the dermal tissues of this model but the reduction was not absolute, which might be a consequence of the ECM (Figure 6.3D, E). The ECM regulated the distribution of cytokines, growth factors and angiogenic factors, as well as providing biochemical and biomechanical cues to the cells it contacts, including fibroblasts (Kim et al. 2011). Consequently, the absence of complete Axin-2 repression could be as a result of spatiotemporal Wnt release from the ECM, which would either restore or increase Axin-2 expression at those sites. In fact, in the human TGFβ-primed fibroblast model, discussed later as a surrogate of the SSc fibroblast canonical Wnt signalling phenotype, AXIN2 expression could be restored following canonical Wnt treatment (Figure 6.4E, F). Nonetheless, the fact that more Axin-2 negative nuclei were present in this model ultimately supports the hypothesis that TGFβ signalling mediates the downregulation of AXIN2 expression in fibroblasts, which might also be important in the profibrotic activation of fibroblasts and hence the pathogenesis of tissue fibrosis.

AXIN2 plays an essential role in regulating the activity of the canonical Wnt pathway; acting as a critical scaffold protein required for the formation of the β-catenin destruction complex, which is responsible for facilitating ubiquitin-mediated β-catenin proteosomal degradation (Sakanaka et al., 1998; Salic et

al., 2000; Liu et al., 2002). Thus, the reduction of AXIN2 expression observed in SSc fibroblasts could facilitate their increased canonical Wnt signalling response through suboptimal destruction complex assembly and this might also be perpetuated by aberrant TGFβ signalling activity.

Indeed, HC fibroblasts primed with TGFβ and subsequently treated with a canonical Wnt agonist could reproduce both the reduced expression of AXIN2 and the increased amplitude of canonical Wnt signalling observed of SSc fibroblasts (Figure 6.4A). The canonical Wnt signalling amplitude displayed by TGFβ-primed fibroblasts, following canonical Wnt agonist treatment, was equivalent to that of SSc fibroblasts in the absence of TGFβ-priming (Figure 6.4A, B). Further analysis revealed that the TGFβ-mediated downregulation of AXIN2 might be a transient event as canonical Wnt signalling activity significantly upregulated its expression (Figure 6.4E, F). Therefore a mechanism must be in place to sustain the reduced AXIN2 expression in SSc fibroblasts, which could involve autocrine/constitutive TGFβ signalling, a long-described if controversial characteristic of SSc fibroblasts (Desmoulière et al. 1993; Gabbiani 2003; Ho et al. 2014).

Consistent with previous data, TGFβ induced nuclear translocation of β-catenin and this was equivalent in TGFβ-primed fibroblasts (Figure 6.4G). Canonical Wnt treatment induced nuclear translocation that was on average less than that induced by TGFβ, which could indicate a reduced recombinant protein activity. In addition, the ability of TGFβ to induce β-catenin nuclear translocation could be attributed to an elevation in Wnt secretion; however, there are sparse protein data available to confirm this postulated activity (Chong et al., 2009). Opposing this hypothesis was the absence of

TOPFlash activation following TGFβ treatment, which would be predicted to be induced by the release of canonical Wnt ligands. To further examine this, Wnt secretion was blocked using a small molecule inhibitor, IWP-2, to inactivate porcupine (PORCN), which mediates the required parmitolylation of Wnts to facilitate their secretion (Gao & Hannoush 2014). Interestingly, TGFβ could still mediate β-catenin nuclear translocation independent of Wnt secretion (Figure 6.4H).

These data indicate that the increased canonical Wnt signalling response in TGFβ-primed fibroblasts was not as a result of an increased nuclear translocation of β-catenin or caused by an increase in Wnt secretion. Indeed, canonical Wnt-3a treatment had a clear and consistent affect on TOPFlash reporter activity while TGFβ showed no activation, which would suggest that TGFβ- and Wnt-3a-induced signalling could utilise β-catenin in a divergent manner (discussed further on Page 232). Overall, these data further supported the hypothesis that TGFβ-primed fibroblasts, like SSc fibroblasts, have an increased responsiveness to canonical Wnt ligands. This increased responsiveness could be as a result of a downregulated AXIN2 expression and was therefore the subject of further evaluation in this study.

As TGFβ signalling downregulated AXIN2 expression but also regulates a multitude of intracellular targets, siRNA-mediated AXIN2 downregulation was employed to determine whether this was sufficient to explain the increased responsiveness of TGFβ-primed fibroblasts to canonical Wnt-induced signalling (Figure 6.1A). Following the depletion of AXIN2 expression, the canonical Wnt signalling response was significantly

increased to levels that were equivalent to those observed in both the TGFβ-primed fibroblast model and ultimately in SSc fibroblasts (Figure 6.5A-D; Figure 6.4A; Figure 6.1A). This was in further support of the hypothesis that the downregulation of AXIN2 was sufficient to reproduce the increased canonical Wnt signalling amplitude observe in SSc fibroblasts, independent of other TGFβ-mediated activities.

In parallel, the absence of TOPFlash activity following TGFβ treatment was not affected by AXIN2 depletion activity (Figure 6.5E).

Furthermore, AXIN2 depletion was also used to evaluate whether Wnt-induced canonical Wnt signalling could affect total TGFβ signalling activity. This was performed due to the conflicting literature on role of AXIN in the regulation of TGFβ signalling activity. For example, AXIN expression can positively regulate TGFβ signalling, negatively regulate TGFβ signalling by destabilising SMAD3, but has also been observed to positively regulate TGFβ signalling by facilitating the ubiquitin-mediated degradation of SMAD7; an endogenous inhibitor of the TGFβ signalling pathway (Koinuma., 2003; Wei et al. 2006; Dao et al., 2007). Interestingly, AXIN2 depleted fibroblasts showed a 30% increase in total TGFβ activity, which suggested that the TGFβ-mediated downregulation of AXIN2 might also act to augment the Wnt-induced TGFβ signalling response (Figure 6.5F). In support of this, a previous study found that Wnt-3a could induce phosphorylation of SMAD3 in fibroblasts, which could be prevented by the pre-incubation with a neutralising anti-TGFβ1 antibody (Wei et al. 2012). However, as the TGFβ reporter assay was not as robust as the TOPFlash assay, more replicates would be required for this preliminary data to achieve significance.

Nevertheless, this represents another element of crosstalk between the Wnt and TGFβ pathways, where AXIN2 expression can act in a reciprocal manner.

The increased canonical Wnt signalling amplitude in TGFβ-primed fibroblasts mediated by AXIN2 downregulation, could have also be as a result of an effect on AXIN1, which shares 45% amino acid sequence identity to AXIN2, and is also important in the formation and function of the β-catenin destruction complex (Chia & Costantini 2005). However, functional studies have demonstrated that their activities may not be entirely redundant. Therefore the relative contribution of AXIN1 to the increased canonical signalling amplitude inducible in TGFβ-primed fibroblasts was investigated.

Notably, while TGFβ treatment affected the expression of AXIN1 at transcriptional level it was not observed at translational level (Figure 6.6A, B). This would support the supposition that *AXIN2* is the more important dynamically regulated TGFβ-responsive target, which is supported by its downregulation in a previously discussed gene profiling study in dcSSc fibroblasts (Milano et al., 2008; Sargent et al., 2009).

Despite this, the evaluation of the relative contribution AXIN1 in the regulation of canonical Wnt signalling amplitude was continued. The specific depletion of AXIN1 expression could regulate canonical Wnt signalling amplitude (Figure 6.6C, D); however, this increased amplitude was 4.0-fold lower compared with AXIN2 depletion experiments (Figure 6.6D Vs. Figure 6.5D). These results suggest that in the TGFβ-primed fibroblast model, AXIN2 is dynamically regulated by TGFβ signalling and therefore plays an

critical role in regulating canonical Wnt signalling amplitude in preference to AXIN1.

In addition, like AXIN2, the absence of TGFβ-inducible TOPFlash activity was not affected by AXIN1 depletion activity (Figure 6.6E).

Finally, the requirement of AXIN1 expression in the regulation of TGFβ signalling activity was determined by total TGFβ reporter activity within siAXIN1 fibroblasts. Consistent with AXIN2 depletion, AXIN1 depletion had no additional effect on TGFβ signalling amplitude (Figure 6.6F Vs. 8.3A). These data supported the independent role of AXIN2 as the critical regulator of canonical Wnt signalling amplitude in response to TGFβ priming.

As a reciprocal method to determine the necessity of TGFβ-mediated AXIN2 downregulation for the increased canonical Wnt signalling amplification in fibroblasts, XAV939-mediated inhibition of AXIN proteosomal degradation was employed (Huang et al., 2009). Accordingly, at basal levels, XAV-939 protected the expression of AXIN2, leading to an increase in expression (Figure 6.7A, B). As expected, XAV-939 inhibited the canonical Wnt signalling response in HC fibroblasts (Figure 6.7C). Moreover, the hyperactivation of canonical Wnt signalling observed in TGFβ-primed fibroblasts was inhibited by AXIN stabilisation and was restored to levels that were equivalent to activated HC fibroblasts (Figure 6.7C). This evidence suggested that AXIN2 is a critical mediator of canonical Wnt signalling hyperactivation, although other factors likely contribute to the complete inhibition of β-catenin-mediated activity.

Overall, this supports the hypothesis that TGFβ-induced downregulation of AXIN2 expression is a critical mechanism that regulates the increased canonical Wnt signalling amplitude observed in both the TGFβ-primed and AXIN2 depletion models, but this could not be subsequently confirmed in SSc fibroblasts due to limited availability (Figure 6.4A & Figure 6.5D, respectively). Furthermore, these data extend upon the previously discussed hypothesis, that the increased canonical Wnt signalling observed in fibroblasts resident in SSc patient skin goes beyond the differential expression of Wnt ligands (Akhmetshina et al., 2012; Beyer et al., 2012; Wei et al., 2012). Instead, these data strongly implied that increased Wnt/β-catenin activation observed in SSc fibroblasts could also be a consequence of TGFβ-priming. Indeed, the increased canonical Wnt signalling activation that is consistently observed in SSc skin biopsies (by nuclear β-catenin staining) may be as a consequence of both of these factors working in parallel.

7 TGFβ-mediated regulation of AXIN2 expression: Determining a mechanism

The TGFβ-mediated downregulation of AXIN2 in HC fibroblasts was sufficient to reproduce an equivalent increase in canonical Wnt signalling response characteristic of SSc fibroblasts. However, the initial mechanism by which TGFβ induced this downregulation was subsequently investigated in a continuation of these experiments. Hence, the kinetics of AXIN2 downregulation were determined alongside reciprocal TβRI blockade. Subsequent analysis of key TβR protein kinase signalling intermediates, in addition to ARE binding proteins, were evaluated for potential transcriptional and post-transcriptional effects upon *AXIN2* expression, respectively.

7.1 TGFβ-mediated downregulation of AXIN2 is initially mediated by mRNA degradation

First the dose effect and subsequently the kinetics of TGFβ-mediated AXIN2 downregulation were initially determined. TGFβ mediated a dose-dependent reduction in the *AXIN2* expression by 87.8%, 46.8% and 51.3% at 1.0, 5.0 (maximal effect) and 10 ng/ml, respectively (Figure 7.1A). This was subsequently found to be time-dependent as TGFβ mediated a reduction in *AXIN2* expression to 60.7%, 54.5%, 45.7%, 41.1% and 38.0% at 10, 30, 60, 120 and 240 min, respectively ($P<0.05$) (Figure 7.1B). Further, TGFβ-mediated a longitudinal downregulation with transcriptional expression reduced to 33.3%, 39.6% and 38.7% at 24, 48 and 72 hr, respectively ($P<0.05$) (Figure 7.1C).

At protein level, TGFβ was able to reduce AXIN2 expression as soon as 2 hr following stimulation, which was reduced further by 4 and 6 hr (Figure 7.1D). Also, TGFβ showed a longitudinal repression of AXIN2 at a period of 48 and 72 hr (Figure 7.1E). Interestingly, blockade of *de novo* protein synthesis achieved by cycloheximide treatment showed depletion of AXIN2 expression within 2 hr (Figure 7.1F). These data indicated that the expression of AXIN2 protein was dynamically regulated and this could be achieved by either a transcriptional or post-transcriptional mechanism.

While the intrinsic and TGFβ-mediated turnover of AXIN2 protein was a potential regulatory mechanism, the rapid downregulation of *AXIN2* expression with a 10 min period of TGFβ treatment suggested either an affect on transcription or an early post-transcriptional mechanism. Therefore, blockade of *de novo* transcription was used to determine the half-life of *AXIN2* mRNA. These experiments showed that the half-life of *AXIN2* mRNA was 109 min, whereas in the presence of TGFβ this decreased to 26 min, which equated to a 4.2-fold increase in the rate of mRNA decay (Figure 7.1G) ($P<0.01$). This indicated that TGFβ could play a role in the regulation of mRNA stability.

To determine whether TGFβ could regulate the transcription of *AXIN2* in parallel to its effects on mRNA stability, the effect on the *AXIN2* primary transcript was evaluated. Initially, TGFβ induced an increase in the expression of the *AXIN2* primary transcript by 126.9% and 199.6% at 10 ($P<0.001$) and 30 min ($P<0.05$), respectively (Figure 7.1H). At periods greater than this, TGFβ reduced *AXIN2* primary transcript expression to 82.9%, 55.8% or 49.4% at 60, 120 and 240 min, respectively ($P<0.05$)

(Figure 7.1H). This was in contrast to the mature transcript that was downregulated across the same time periods (Figure 7.1B). These data indicated that regulation of *AXIN2* by TGFβ involved both mRNA decay and, at later time points, transcription.

Additionally, the increase in the expression of a second messenger of TGFβ signalling, *CTGF,* was used as a positive control for TGFβ activity. In general, TGFβ showed a time-dependent increase in the expression of the *CTGF* mature transcript, an initial decrease in expression was observed at 10 and 30 min of 43.2% and 71.4% that was significantly increased at 60, 120 and 240 min by 151.1%, 434.8% and 456.1%, respectively ($P<0.05$) (Figure 7.1I).

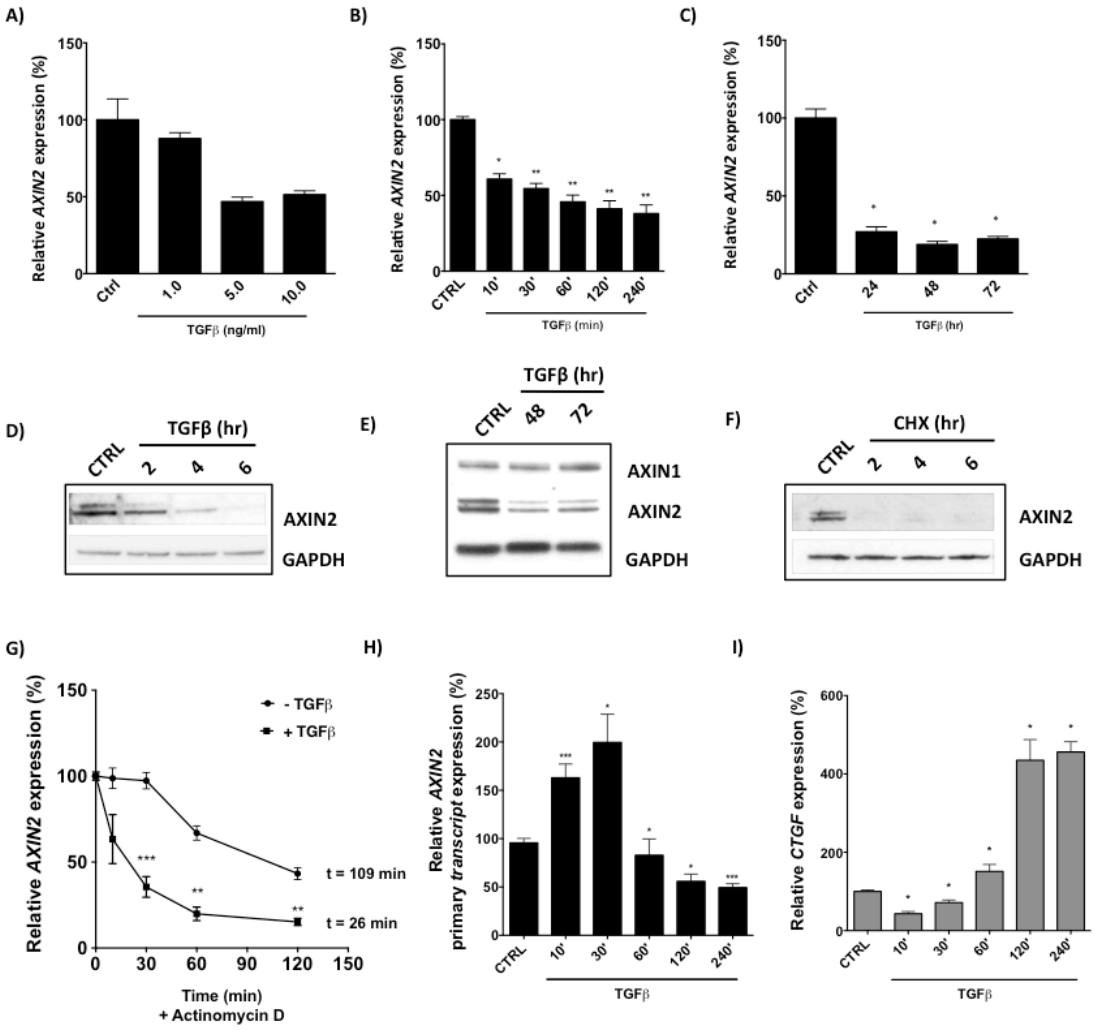

Figure 7.1 TGFβ-mediated downregulation of AXIN2 is initially mediated by mRNA degradation

The kinetics of TGFβ-mediated AXIN2 downregulation were initially determined in HC fibroblasts A) Fibroblasts were treated with TGFβ (1.0-10.0 ng/ml) for 24 hr and *AXIN2* mRNA was quantified by qRT-PCR. B) HC fibroblasts were treated with 5 ng/ml TGFβ (maximal effect) for 10-240 min or C) 24-72 hr and *AXIN2* mRNA quantified by qRT-PCR. D) Protein expression of AXIN2, AXIN1 and GAPDH (loading control) following 2-6 hr TGFβ treatment or E) 24-72 hr treatment were determined by Western blot. F) AXIN2 protein turnover was determined by cycloheximide treatment (100 ug/ml) for 2-6 hr and subsequent determination of AXIN2 and GAPDH (loading control) expression by Western blot. G) AXIN2 half-life was also evaluated by treatment with or without TGFβ for 10-120 minutes in the presence of actinomycin D (1 µg/ml) and *AXIN2* expression was quantified by qRT-PCR. The transcriptional effects of TGFβ were determined by TGFβ treatment for 0-120 min and the effect on H) *AXIN2* primary transcript, using primers spanning the intron-exon 3 boundary (see chapter 2.12), and I) *CTGF* mRNA expression (+ve) were quantified by qRT-PCR. Data shown as mean ± SEM, n=3-8; Mann-Whitney test for unpaired samples **P*=0.05, ***P*=0.01, ****P*=0.001.

7.2 TβRI kinase blockade prevents the TGFβ-mediated downregulation of AXIN2

To determine whether the TGFβ-induced downregulation of *AXIN2* was a direct effect of TβRI activation, experiments were performed in HC fibroblasts in the presence of the TβRI-kinase inhibitor, SD-208, which has been shown to selectively antagonise TβRI-induced signalling (Uhl 2004).

Consistent with our previous data, TGFβ signalling reduced the expression of *AXIN2* to 36.0% ($P<0.05$) at 24 hr. On the contrary, in the presence of SD-208 *AXIN2* expression remained at 94.0% of control levels following TGFβ treatment (Figure 7.2A). Similarly, the expression of *DKK-1* was downregulated by TGFβ to 43.8% and partially prevented in the presence of SD-208, reduced to only 77.3% ($P<0.05$) (Figure 7.2B). As a positive control for the activity of SD-208, the TGFβ-induced expression of *α-SMA* and *ET-1* expression were evaluated as a known target of TβRI-induced signalling. As expected, inhibition of TβRI-induced signalling by SD-208 signalling prevented the 510% induction of *α-SMA* expression, reducing it to 97.7% compared to controls ($P<0.05$) (Figure 7.2C). Similarly, TβRI-induced *ET-1* expression was significantly inhibited reduced from 525.7% to 117.4% in the presence of SD-208 (Figure 7.2D).

At protein level, HC fibroblasts treated with TGFβ showed a significant downregulation in the expression of AXIN2 and a concomitant increase in the expression of *α-SMA* at both 48 and 72 hr (Figure 7.2E). In line with mRNA data, the blockade of TβRI signalling prevented the TGFβ-induced downregulation of AXIN2 and also prevented the upregulation of *α-SMA* expression at both 48 and 72 hr (Figure 7.2E).

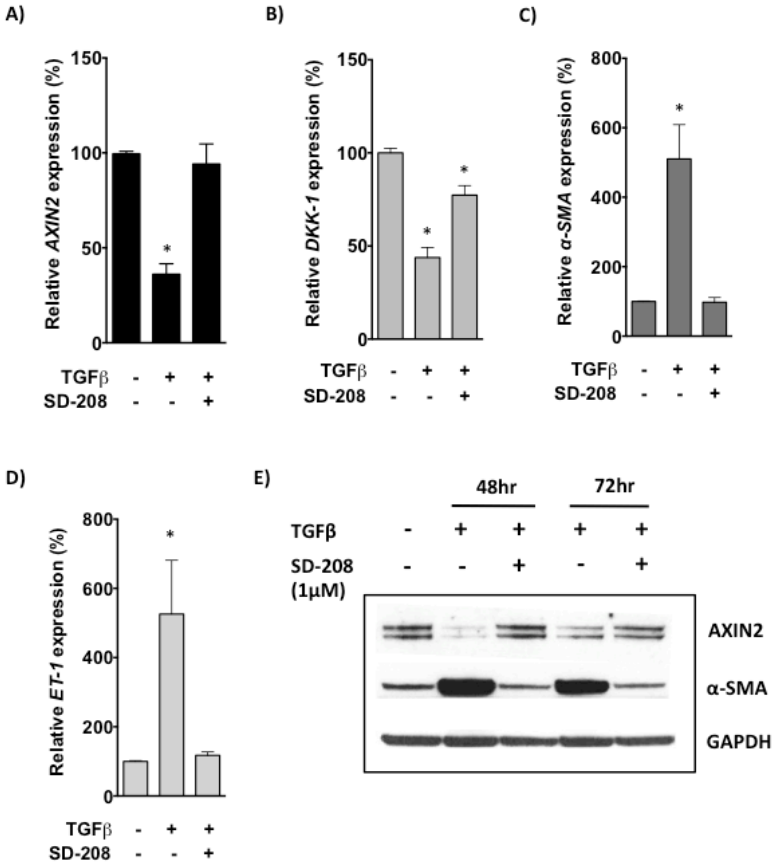

Figure 7.2 TβRI kinase blockade prevents the TGFβ-mediated downregulation of AXIN2

HC fibroblasts were treated with the TβRI kinase inhibitor SD-208 (1 μM) for 1 hr prior to 24 hr TGFβ treatment. The effect on A) *AXIN2* mRNA expression as well as positive control genes B) *DKK-1* C) *α-SMA* and D) *ET-1* were quantified by qRT-PCR. E) Following TGFβ treatment for 48 and 72 hr, AXIN2 protein expression together with α-SMA (+ve) and GAPDH (loading control) were determined by Western blot. Data shown as mean ± SEM, n=3-4; Mann-Whitney test for unpaired samples *P=0.05.

7.3 TβRI kinase blockade can increase AXIN2 expression in SSc fibroblasts

Next, preliminary data were obtained to investigate whether the decreased expression of AXIN2 in SSc fibroblasts could be a consequence of self-activation of the TGFβ signalling pathway.

Therefore, TβRI signalling was inhibited in SSc fibroblasts using the validated SD-208 inhibitor. The blockade of TβRI signalling by SD-208 increased the expression of *AXIN2* by 16.7% and 22.6% at 1.0 and 3.0 μM, respectively ($P<0.05$) (Figure 7.3A). Also, the expression of *DKK-1* was increased by 37.0% and 72.7% at 1.0 and 3.0 μM, respectively (Figure 7.3B). As positive controls, the expression of two known TGFβ-mediated profibrotic genes were evaluated. As anticipated, SD-208 inhibited *α-SMA* expression to 73.0% and 78.5% at 1.0 and 3.0 μM, respectively (Figure 7.3C). Inhibition was also observed for *COL1A1* expression, which was reduced to 53.5% and 58.2% at 1.0 and 3.0 μM, respectively ($P<0.05$) (Figure 7.3D).

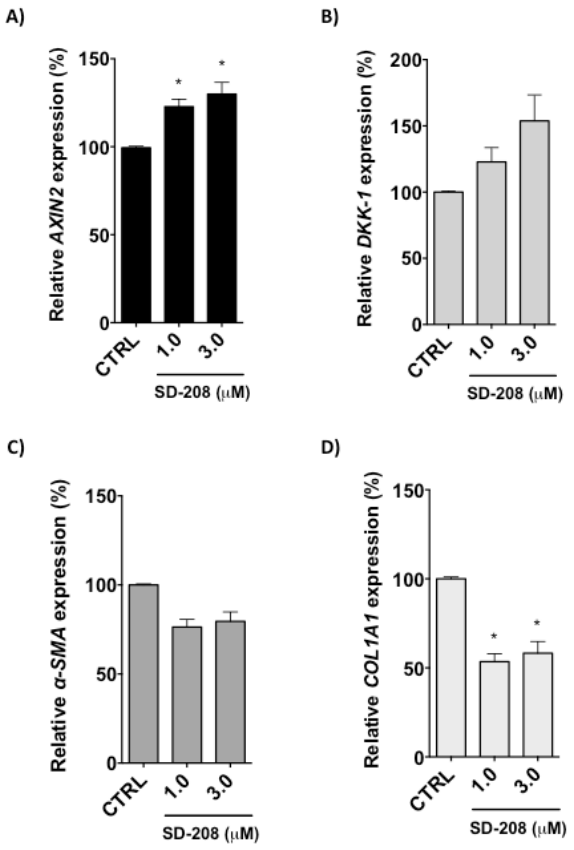

Figure 7.3 TβRI kinase inhibition can increase AXIN2 expression in SSc fibroblasts

Basal SSc patient fibroblasts were treated with the TβRI kinase inhibitor SD-208 (1 or 3 μM) for 48 hr and the effect on A) AXIN2 mRNA expression as well as other TGFβ-responsive genes B) *DKK-1* C) *α-SMA* and D) *COL1A1* were quantified by qRT-PCR. Data shown as mean ± SEM, n=4; Wilcoxon test for paired samples **P*=0.05.

7.4 SMAD3 does not mediate the TGFβ-induced downregulation of AXIN2

In the TGFβ signalling pathway, the activation of TβRI recruits and phosphorylates two important signalling mediators SMAD2 and SMAD3, which are known to be critical to fibrotic gene activation in fibroblasts. However, as SMAD3 is a known transcriptional component, able to interact with those genes that contain SBE within their promoters and therefore might be have a functional role in the TGFβ-mediated downregulation of

AXIN2 expression. To test this hypothesis, SIS3, a selective inhibitor of SMAD3 phosphorylation, was used to prevent the activation of SMAD3 and any associated activities.

First, the independent treatment of HC fibroblasts with SIS3 showed a dose-dependent inhibition of *AXIN2* expression, reduced to 62.1%, 80.0% and 95.5% at 10.0, 3.0 and 1.0 μM, respectively (Figure 7.4A). However, light microscopy showed that at 10.0 μM SIS3 there was a significant alteration in cell morphology, which consistently lead to cell detachment and was therefore excluded from the dose series (data not shown). Next, the effects of SMAD3 inhibition on TGFβ-mediated gene expression was evaluated, specifically with respect to *AXIN2* expression.

Consistent with all other experiments, TGFβ-mediated a 41.8% downregulation of *AXIN2* expression (Figure 7.4B). In the presence of SIS3 there was no significant effect on the TGFβ-induced downregulation of *AXIN2* expression, which remained downregulated by 46.7%, 41.7% and 36.1% at 7.0, 6.0 and 5.0 μM, respectively (Figure 7.4B). As a positive control for the activity of the inhibitor, the expression of α-SMA, a SMAD3 transcriptional target, was evaluated. Indeed, the TGFβ-induced 686.2% increase in *α-SMA* expression was inhibited in the presence of SIS3 to 65.0% and 579.2% at 6.0 and 3.0 μM, respectively (Figure 7.4C). Similarly, α-SMA protein expression was significantly inhibited at doses of 7.0, 6.0 and 5.0 μM SIS3 (Figure 7.4D).

To validate the effects of SMAD3 inhibition, HC fibroblasts were transfected with siRNA targeted against *SMAD3* (siSMAD3) or SCR oligonucleotide. In siSMAD3 fibroblasts, *SMAD3* mRNA expression was reduced to 39.0% of

SCR controls (Figure 7.4E). Following TGFβ treatment, *SMAD3* expression was reduced further to 17.1% in SCR fibroblasts, which was similar to the 11.2% reduction observed in siSMAD3 fibroblasts (Figure 7.4E).

Under the same experimental conditions, siSMAD3 fibroblasts showed a basal reduction of *AXIN2* to 70.2% of the levels present in SCR controls (Figure 7.4F). Then in the presence of TGFβ, *AXIN2* expression was reduced further to 46.4% in siSMAD3 fibroblasts, which was equivalent to the 49.0% expression observed in SCR controls (Figure 7.4F). Again, *α-SMA* expression was used as a positive control for the inhibition of SMAD3 activity. Indeed, *α-SMA* expression was relatively unchanged in siSMAD3 fibroblasts at 92.9% of SCR controls (Figure 7.4G). Following TGFβ treatment, *α-SMA* expression was increased by 624.1% in siSMAD3 fibroblasts; however, this was significantly reduced compared to the 1007.2% increase observed in SCR controls (Figure 7.4G).

The effect of SMAD3 reduction and the concomitant effect on the level of SMAD3 bioavailability were evaluated in relation to AXIN2 expression. At basal level, AXIN2 expression was reduced in siSMAD3 fibroblasts (Figure 7.4H). TGFβ treatment induced a reduction in AXIN2 expression in SCR fibroblasts and was further reduced in siSMAD3 fibroblasts (Figure 7.4H).

Like AXIN2, the expression of α-SMA was reduced at basal level in siSMAD3 fibroblasts compared to SCR controls (Figure 7.4H). In the presence of TGFβ, SCR fibroblasts showed a significant induction of α-SMA expression that was significantly reduced in siSMAD3 fibroblasts (Figure 7.4H).

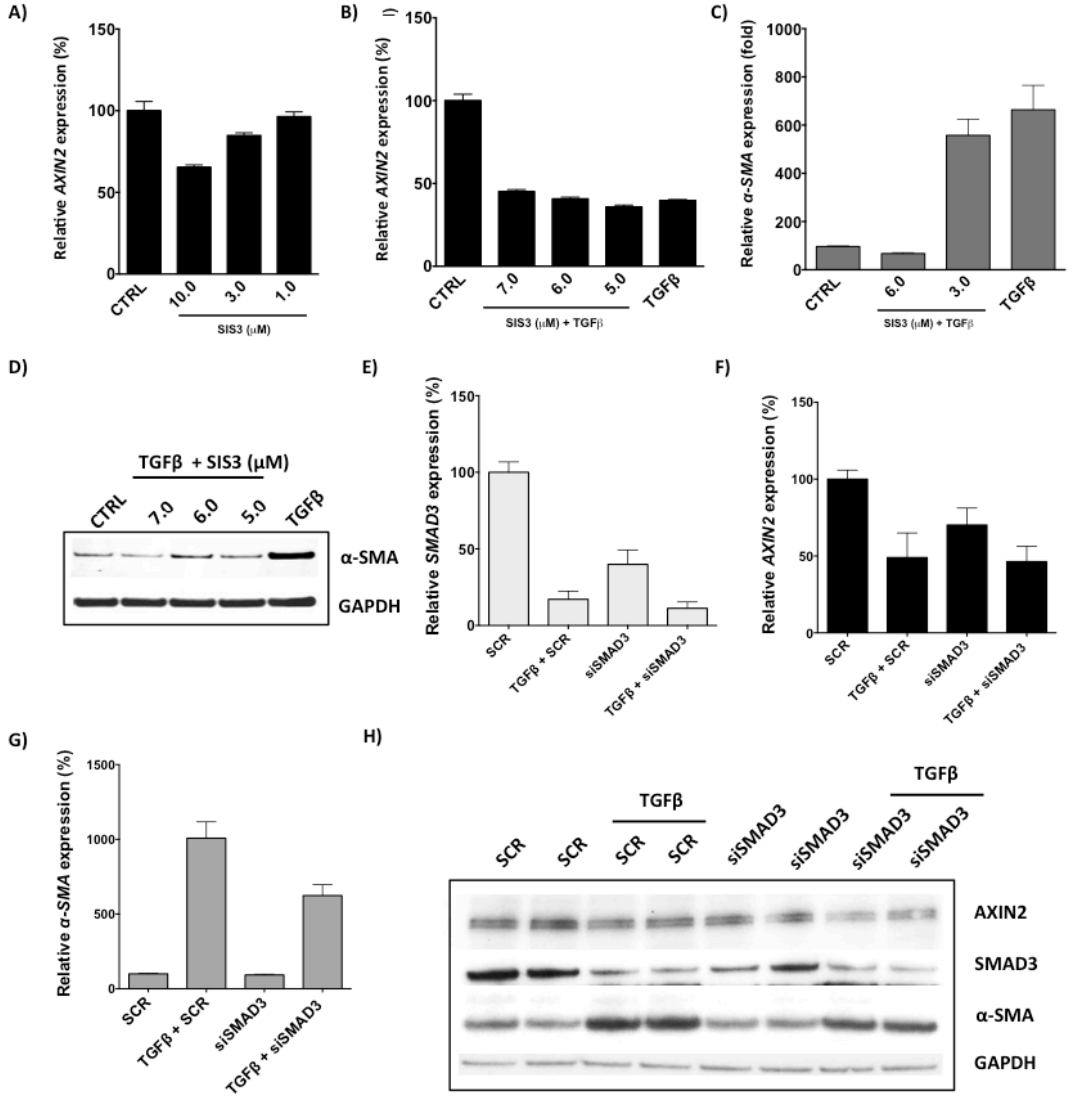

Figure 7.4 SMAD3 does not mediate the TGFβ-induced downregulation of AXIN2

SMAD3 was evaluated for its potential to involvement in the TGFβ-meditated downregulation of AXIN2 expression in HC fibroblasts. A) The effect on basal *AXIN2* expression and B) TGFβ-meditated *AXIN2* downregulation were determined by SIS3 SMAD3 inhibitor treatment for 24 hr and 1 hr prior to 24 hr TGFβ treatment (5 ng/ml), respectively, where C) *α-SMA* expression served as a positive control, and all were quantified by qRT-PCR. D) Following 72 hr treatment with SIS3, α-SMA protein expression was determined by Western blot and served as a further control for SIS3 inhibitor activity. These effects were subsequently confirmed by SMAD3 siRNA (siSMAD3) gene silencing. HC fibroblasts were transfected with SMAD3 siRNA (siSMAD3) or SCR oligonucleotide for 72 hr prior to TGFβ treatment for 24 hr and the effect on E) *SMAD3*, F) *AXIN2* and G) *α-SMA* (+ve) expression were quantified by qRT-PCR. H) Under the same conditions, TGFβ treatment was extended to 72 hr and the protein expression of AXIN2, SMAD3, α-SMA (+ve) and GAPDH (loading control) were determined by Western blot. Data shown as mean ± SEM, n=3.

7.5 SMAD3 is required for the efficient activation of the canonical Wnt signalling response

Although SMAD3 was not required for the TGFβ-mediated downregulation of AXIN2 expression (Figure 7.4A-H), inhibition experiments would suggest that SMAD3, like β-catenin, was required for Wnt-3a-induced canonical Wnt signalling activity, described later in this study (Figure 8.4A, B and E, F, respectively). Therefore it was determined whether Wnt-3a, like TGFβ, could lead to the phosphorylation (activation) of SMAD3, induce SMAD3 nuclear translocation and, subsequently, the consequence of SMAD3 depletion in relation to canonical Wnt signalling activity was determined.

Included as a positive control, TGFβ caused a significant increase in SMAD3 phosphorylation in HC fibroblasts by 30 min that returned to basal level by 60 min (Figure 7.5A). Interestingly, Wnt-3a treatment also induced SMAD3 phosphorylation, albeit to a lesser extent, at 30 min that again returned to basal level by 60 min (Figure 7.5A).

Subsequently, Wnt-3a or TGFβ co-treatment with 5.0 μM of the SMAD3 inhibitor SIS3 ablated the agonist-induced increases in SMAD3 phosphorylation observed at 30 min (Figure 7.5B).

Furthermore, Wnt-3a treatment also induced SMAD3 nuclear translocation by 360 min despite no change in the cytosolic fraction (Figure 7.5C). Similarly, TGFβ treatment increased SMAD3 nuclear localisation and this was greatest at 120 min and decreased over time up to 360 min (Figure 7.5C). However, only TGFβ treatment showed a significant depletion of SMAD3 in the cytosolic cell fraction at 120, 240 and 360 min (Figure 7.5C).

Finally, the effect of SMAD3 depletion on canonical Wnt signalling activation

was investigated. Expectedly, SMAD3 protein levels were reduced in siSMAD3 fibroblasts compared to SCR or untreated fibroblasts (Figure 7.5D). Following Wnt-3a treatment, TOPFlash activity was increased by 57.2-fold in SCR fibroblasts, which was equivalent to the treatment of untransfected controls (Figure 7.5E). Interestingly, Wnt-3a-induced TOPFlash activity in siSMAD3 fibroblasts was 27.2-fold less that SCR fibroblasts further, which further supported the potential role of SMAD3 crosstalk with the canonical Wnt pathway (Figure 7.5E).

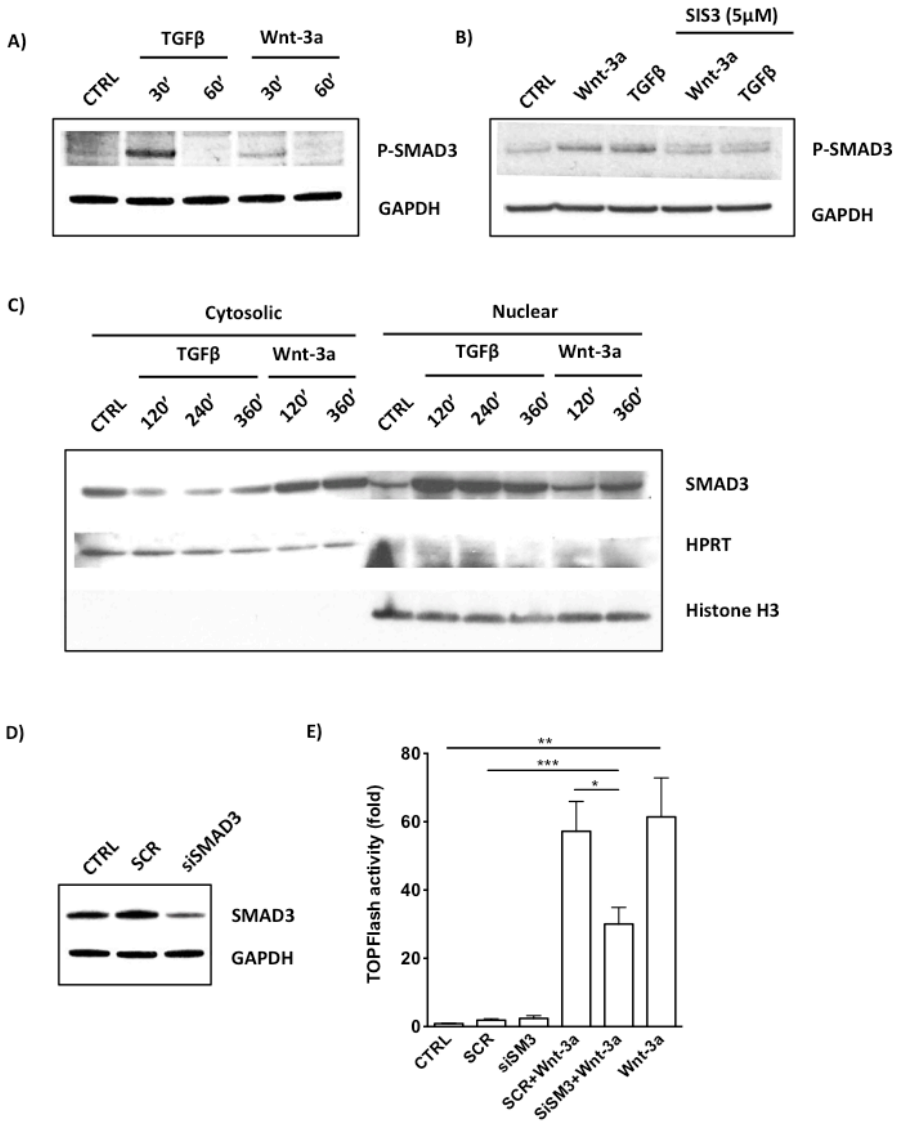

Figure 7.5 SMAD3 is required for the efficient activation of the canonical Wnt signalling response

SMAD3 regulation of canonical Wnt signalling amplitude was evaluated in HC fibroblasts. A) Fibroblasts were treated with TGFβ or Wnt-3a for 30-60 min and SMAD3 phosphorylation (activation) was determined by Western blot. B) Fibroblasts were treated with SMAD3 inhibitor SIS3 1 hr prior to TGFβ or Wnt-3a for 30 min and SMAD3 phosphorylation and GAPDH expression (loading control) were determined by Western blot. C) Cytosolic/nuclear localisation of SMAD3, HPRT (cytosolic marker) and Histone H3 (nuclear marker) were evaluated following TGFβ or Wnt-3a treatment for periods between 0-360 min and visualised by Western blot. D) Fibroblasts were transfected with SMAD3 siRNA (siSMAD3) or scrambled oligonucleotide (SCR) and SMAD3 and GAPDH (loading control) expression were determined by Western blot. E) Canonical signalling was determined by transfection of fibroblasts with the TOPFlash reporter for 24 hr and subsequently fibroblasts were transfected with siSMAD3 or SCR for 72 hr prior to treatment with Wnt-3a (100ng/ml) for 24 hr before TOPFlash activity was determined by luciferase activity. Data shown as mean ± SEM, n=3-4; Mann-Whitney test for unpaired samples **P*=0.05, ***P*=0.01, ****P*=0.001.

7.6 Additional downstream kinases of the TGFβ pathway are not involved the regulation of *AXIN2* mRNA decay

As SMAD3 was not involved in the TGFβ-mediated downregulation of AXIN2 expression, alternative downstream mediators of the TGFβ signalling pathway were evaluated. MK-2206-mediated AKT1/2/3 inhibition had no effect on TGFβ-mediated *AXIN2* downregulation despite a dose-dependent (0.3-10.0 μM) reduction in *α-SMA* expression (Figure 7.6A, B). Inhibitors targeted against PI3K (Wortmannin) and MEK1/2 (Selumetinib) also had no effect on TGFβ-mediated *AXIN2* downregulation and showed no significant decrease in *α-SMA* expression (Figure 7.6C-F)

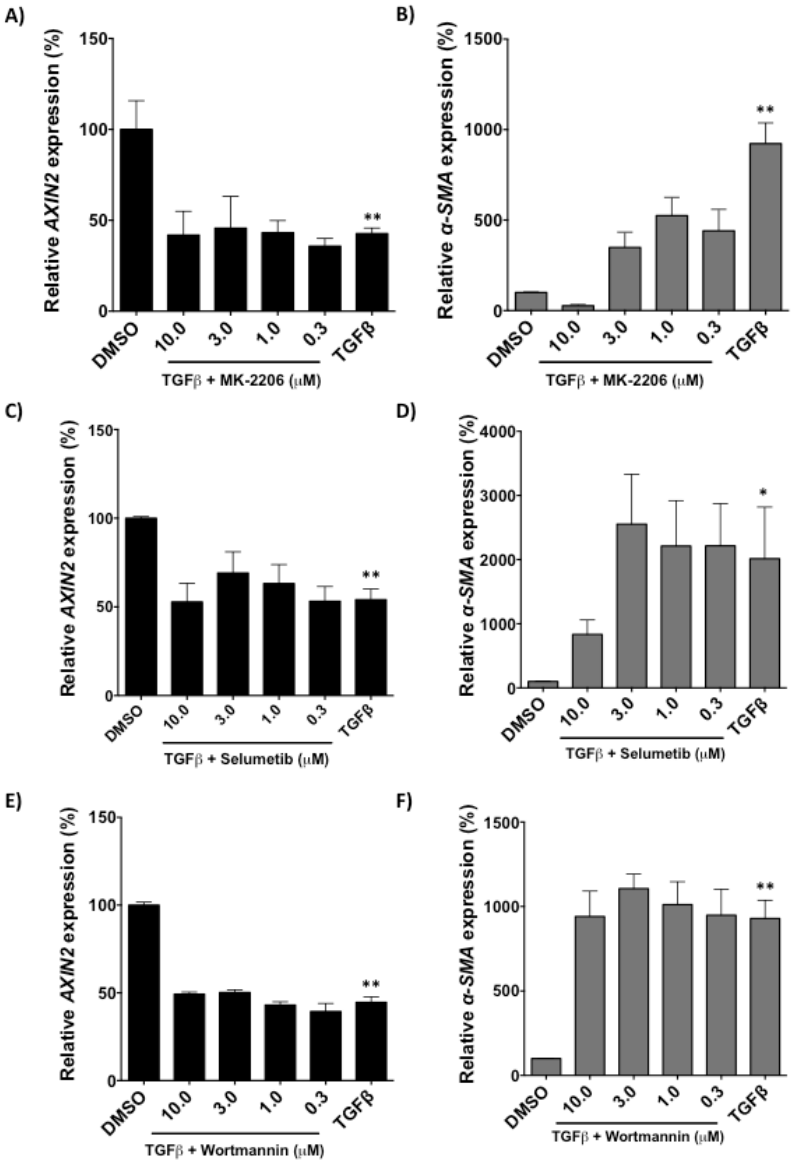

Figure 7.6 Additional downstream kinases of the TGFβ pathway are not involved in *AXIN2* mRNA decay

The activity of the inhibitors A-B) MK-2206 (AKT1/2/3), C-D) Selumetinib (MEK1/2) and E-F) Wortmannin (PI3K) were compared for their effect on *AXIN2* and fibroblast activation marker *α-SMA* expression following HC fibroblasts inhibitor treatment (10-0.3 μM) 1 hr prior to 24 hr TGFβ treatment and quantified by qRT-PCR. Data shown as mean ± SEM, n=3-4; Mann-Whitney test for unpaired samples *P=0.05, **P=0.01.

7.7 p38 could potentially regulate TGFβ-induced *AXIN2* downregulation

Finally, the involvement of p38 MAP kinase in TGFβ-mediated downregulation of *AXIN2* was investigated. HC fibroblasts were treated with the p38α/β inhibitor VX-702 in the presence and absence of TGFβ. While TGFβ induced the downregulation of *AXIN2* expression to 45.9%, a partial restoration was observed in the presence of VX-702 where expression was increased to 69.0%, 67.7%, 58.8% and 50.0% at 10.0, 3.0, 1.0 and 0.3 μM, respectively (Figure 7.7A).

Next, the activity of VX-702 was evaluated using a control gene panel. In this panel *α-SMA* expression was used as a control for TGFβ activity, *DKK-1* expression was used to evaluated the effect of inhibition on a second inhibitor of the canonical Wnt signalling pathway and *c-MYC / CDKN2A* were included as known p38-regulated gene targets. Indeed, the 578.4% induction in *α-SMA* expression by TGFβ was partially inhibited in the presence of VX-702 to 406.0%, 544.3%, 568.0% at concentrations of 10.0, 3.0 and 1.0 μM, respectively (Figure 7.7B). The TGFβ-induced downregulation of *DKK-1* to 28.8% was relatively unchanged in the presence of VX-702 and was expressed by 18.6%, 35.8%, 46.5%, or 46.2% at 10.0, 3.0, 1.0 and 0.3 μM, respectively (Figure 7.7C). *c-MYC* expression was increased *to* 271.6% following TGFβ treatment and in the presence of VX-702 showed inhibition to 192.2%, 158.2%, 201.6% and 200.3% at 10.0, 3.0, 1.0 and 0.3 μM, respectively (Figure 7.7D). Finally, a potent inhibition of *CDK2A* expression was observed in the presence of VX-702, which was induced by 170.1% following TGFβ and inhibited to 63.4%, 75.6% or 81.3% and 74.6% at 10.0, 3.0, 1.0 and 0.3 μM, respectively (Figure 7.7E).

However, as the maximum effect of VX-702 inhibition was only 31%, a second p38 inhibitor, SB202190, was used to validate the role p38 in *AXIN2* expression. In contrast to the results presented in Figure 1.13A, the TGFβ-induced downregulation of *AXIN2* to 60.0% was not significantly affected in the presence of SB202190 and was expressed by 66.4%, 66.0%, 68.6% or 63.8% at 10.0, 3.0, 1.0 and 0.3 μM, respectively (Figure 7.7F). Indeed, partial inhibition of the TGFβ-induced downregulation of *AXIN2* expression was observed using VX-702 but was absent when using SB202190.

Next, the activity of SB202190 was evaluated using the same gene panel used previously. Here, TGFβ induced a 1086.1% increase in *α-SMA* expression that was significantly inhibited in the presence of SB202190 by 197.7%, 278.6%, 428.9% and 667.6% at 10.0, 3.0, 1.0 and 0.3 μM, respectively (Figure 7.7G). *DKK-1* expression was reduced to 42.1% following TGFβ treatment and there was no significant change observed in the presence of SB202190, repressed by 37.4%, 39.6%, 50.6% or 47.4% expression at 10.0, 3.0, 1.0 and 0.3 μM, respectively (Figure 7.7H). However, the TGFβ-induced 415.4% increase in *c-MYC* expression was reduced to 186.5%, 199.5% and 271.2% at 10.0, 3.0, 1.0 and 0.3 μM SB202190, respectively (Figure 7.7I). Similarly, the TGFβ-induced 370.1% increase in *CDK2A* expression was reduced to 126.8%, 140.5%, 173.6% at 10.0, 3.0, 1.0 and 0.3 μM SB202190, respectively (Figure 7.7J).

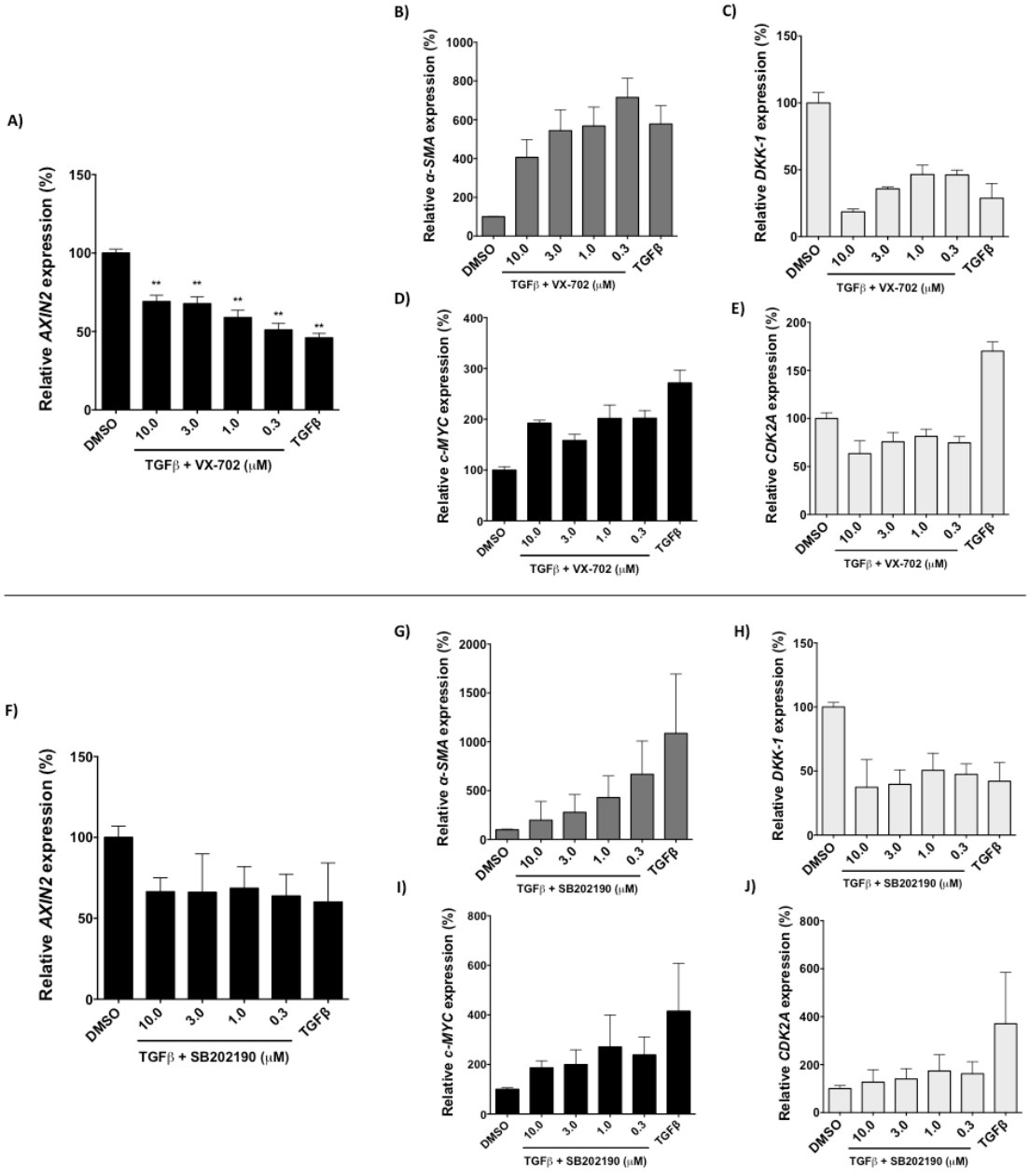

Figure 7.7 p38 could potentially regulate TGFβ-induced *AXIN2* downregulation

The effect of p38 inhibition on TGFβ-mediated *AXIN2* downregulation was determined in HC fibroblasts. p38 inhibitors (10-0.3 μM) were preincubated 1 hr prior to TGFβ treatment for 24 hr. A-E) The activities of p38 inhibitor VX-702 and F-J) SB202190 were compared for their effects upon *AXIN2* expression as well as positive control genes *α-SMA*, *DKK-1*, *c-MYC* and *CDK2A,* quantified by qRT-PCR. Data shown as mean ± SEM, n=3-5; Mann-Whitney test for unpaired samples ***P*=0.01.

7.8 The *AXIN2* transcript contains a TTP-1 ARE-binding protein sequence and TGFβ negatively regulates *TTP-1* expression

As the investigation into the signalling intermediates responsible for the TGFβ-induced downregulation of AXIN2 were not conclusive, the post-transcriptional mechanism by which TGFβ induced the 4.2-fold increase in *AXIN2* mRNA degradation was explored further. While post-transcriptional regulation is complex, it is thought that the majority of eukaryotic mRNAs are degraded though the shortening of their poly(A)-tails, which in-turn initiates a deadenylation-dependent pathway that leads to the recruitment of the RNA-degrading exosome complex (Houseley & Tollervey 2009). Therefore a bioinformatics approach was used to detect any 3'UTR AU-rich elements (ARE) binding sequences present within the *AXIN2* transcript. Hence, *AXIN2* was found to harbour several ARE binding motifs that could potentially recruit the ARE-binding proteins TTP-1, HUR and AUF-1 (Figure 7.8A). Indeed, these predicted protein interactions could potentially regulate the stability of *AXIN2* mRNA.

In preliminary experiments, TGFβ-treated HC fibroblasts showed a downregulation of *TTP-1* expression to 14.7%, 52.2% and 44.1% at 2, 4, and 6 hr, respectively ($P<0.05$) (Figure 7.8B). Further, TGFβ reduced *TTP-1* expression longitudinally to 65.3%, 58.6%, and 59.6% at 24, 48 and 72 hr, respectively ($P<0.05$) (Figure 7.8C). Next, the expression of *HUR* was unchanged in response to TGFβ at early time points of 2, 4 and 6 hr expressed by 111.3%, 113.3% and 126.4%, respectively (Figure 7.8D). Longitudinally, a trend toward decreased expression was observed expressed by 74.7% 74.5% and 87.2% at 24, 48 and 72 hr, respectively

(Figure 7.8E).

AXIN2 expression served as a positive control and was downregulated by 27.9%, 48.2% and 39.2% at 2, 4 and 6 hr, respectively ($P<0.05$) (Figure 7.8F). Longitudinally, TGFβ downregulated the expression of *AXIN2* by 53.1%, 45.2% and 50.2% at 24, 48 and 72 hr, respectively ($P<0.05$) (Figure 7.8G). The expression of *AUF-1* was not included due to unreliable primer pairs (data not shown).

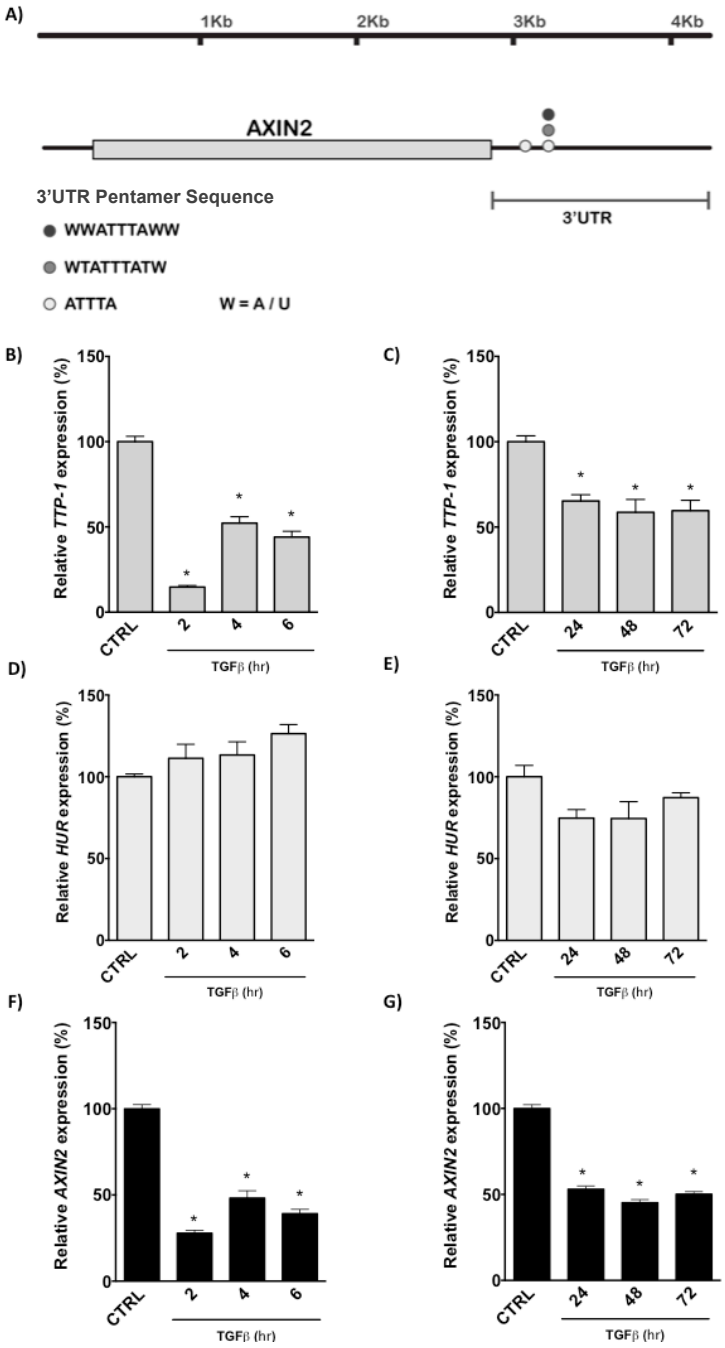

Figure 7.8 *AXIN2* transcripts contain ARE-binding protein sequences and TGFβ negatively regulates *TTP-1* expression

A) Bioinformatics analysis of *AXIN2* mRNA identified AU-rich element (ARE) binding motifs within the 3'UTR, predicted to bind RNA regulating proteins TTP-1 and HUR. TGFβ regulation of C) *TTP-1* D-E) *HUR* and F-G) *AXIN2* (+ve) expression were determined in HC fibroblasts following TGFβ treatment for 2-72 hr and quantified by qRT-PCR. Data shown as mean ± SEM, n=4; Mann-Whitney test for unpaired samples **P*=0.05.

7.9 Inhibition of TTP-1 potentially upregulates AXIN2 expression

As TGFβ negatively regulated TTP-1, the effect of basal TTP-1 depletion upon the expression of AXIN2 was evaluated. HC fibroblasts were therefore transfected with siRNA targeted against *TTP-1* (siTPP-1) or SCR oligonucleotide. In siTTP-1 fibroblasts at 48 and 72 hr, *TTP-1* expression was reduced to 41.9% and 35.7% ($P<0.001$), respectively (Figure 7.9A). Concomitantly, *AXIN2* expression was increased by 162.1% ($P<0.01$) at 48 hr, which was then reduced to 109.5% by 72 hr (Figure 7.9B).

DKK-1 expression was used to evaluate the effect of TTP-1 expression on a second endogenous inhibitor of the canonical Wnt signalling pathway. Similarly, *DKK-1* showed a 161.5% ($P<0.01$) increase in expression at 48 hr decreasing to 124.3% at 72 hr (Figure 7.9C). Finally, α-SMA expression served as a control for TGFβ activity and showed a minor increase in expression of 116.1% at 48hr and a reduced expression of 78.3% ($P<0.05$) at 72 hr (Figure 7.9D).

At protein level, TTP-1 expression remained relatively unchanged compared to GAPDH loading controls (Figure 7.9E). Despite this, AXIN2 expression showed a significant upregulation in siTTP-1 fibroblasts compared to SCR controls at both 48 and 72 hr (Figure 7.9E). Similarly, DKK-1 expression was also increased in siTTP-1 fibroblasts compared to SCR controls at 48 hr and 72 hr (Figure 7.9E). Finally, the expression of α-SMA and AXIN1 were used as negative controls. Both proteins showed no significant change expression in siTTP-1 fibroblasts compared to SCR fibroblasts at either time point (Figure 7.9E).

Following validation, a time-course was performed in order to evaluate whether reduced TTP-1 expression could significantly affect the TGFβ-induced downregulation of *AXIN2*. As TGFβ regulated the stability of *AXIN2* within a period of 60 min (Figure 7.1G), expression was determined at 0-120 min. In siTTP-1 fibroblasts, *TTP-1* expression was reduced to 94.5% compared to SCR controls (Figure 7.9F). In the presence of TGFβ, *TTP-1* expression was increased in SCR fibroblasts by 210.5% at 30 min, and decreased over time to 173.2% at 60 min and 83.3% at 120 min (Figure 7.9F). In contrast, siTTP-1 fibroblasts showed no increase in *TTP-1* expression, expressed by 72.1% at 30 min, 87.4% at 60 min and was significantly reduced to 26.7% at 120 min (Figure 7.9F).

Despite the variable silencing of TTP-1 expression, the basal level of *AXIN2* was increased by 216.3% ($P<0.05$) in siTPP-1 compared to SCR fibroblasts (Figure 7.9G). This expression was reduced over time decrease to 140.7% ($P<0.05$), 156.4% ($P<0.05$) and 87.4% was observed at 30, 60 and 120 min, respectively (Figure 7.9G). TGFβ treatment of SCR fibroblasts reduced *AXIN2* expression to 96.4% at 30 min, 95.5% at 60 min and more noticeably to 64.0% at 120 min in SCR fibroblasts (Figure 7.9G).

The expression of *COX2*, a known TTP-1 regulated target, served as a positive control for TTP-1-mediated activity. As expected, siTPP-1 fibroblasts showed a significant increase in basal *COX2* expression by 393.0%($P<0.05$) compared to SCR controls and following TGFβ treatment this expression was reduced over time to 198.2%, 95.1% and 34.0% at 30, 60 and 120 min, respectively (Figure 7.9H). Similarly, TGFβ treatment downregulated *COX2* expression over time in SCR fibroblasts to 134.0%, 83.5% and 43.5% at 30,

60 and 120 min, respectively (Figure 7.9H).

As a positive control for TGFβ signalling activity, the TGFβ-mediated expression of the early-intermediate gene *CTGF* was evaluated. At basal level, *CTGF* expression in siTTP-1 fibroblasts was similar to that of SCR fibroblasts at 90.4% (Figure 7.9I). In siTTP-1 fibroblasts, *CTGF* expression was increased to 78.7% at 30 min, 213.5% at 60 min and 539.7% at 120 min ($P<0.05$) (Figure 7.9I). This was similar to the TGFβ-induced expression observed in SCR fibroblasts, which increased by 232.5%, 280.0% and 507.1% at 30, 60 and 120 min, respectively ($P<0.05$) (Figure 7.9I).

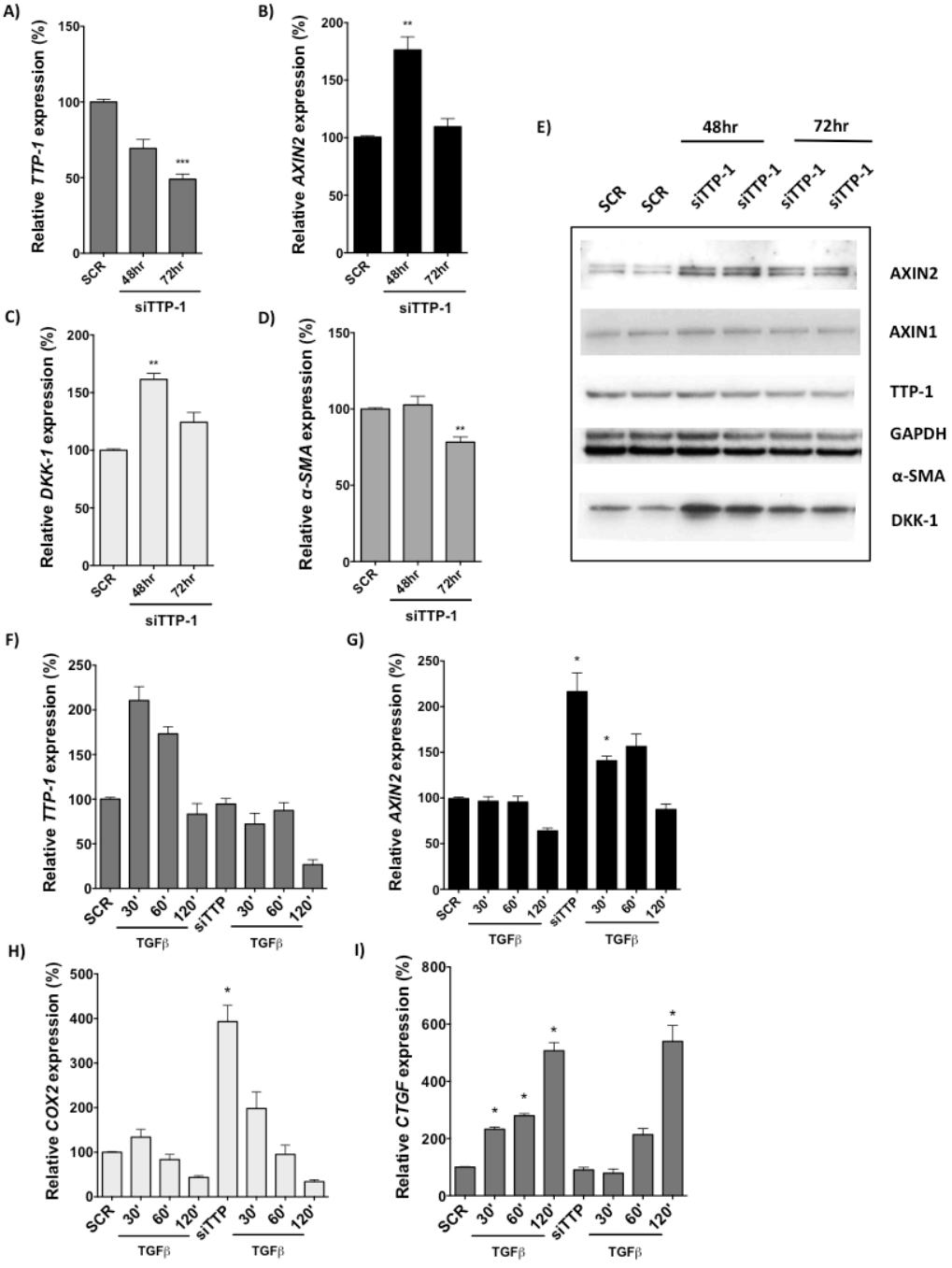

Figure 7.9 Inhibition of TTP-1 potentially upregulates AXIN2 expression

The effect of TTP-1 downregulation on the expression of putative target AXIN2 was determined by treatment of HC fibroblasts with *TTP-1* siRNA (siTTP-1) or SCR oligonucleotide for up to 72 hr. Basal expression of A) *TTP-1* B) *AXIN2* C) *DKK-1* and D) *α-SMA* were quantified by qRT-PCR. E) Protein expressions of these genes were also determined by Western blot in addition to AXIN1 (-ve) and GAPDH (loading control). Subsequently, the effect of TTP-1 downregulation on TGFβ-responsive gene expression was determined by following the addition of TGFβ for 0-120 min and the expression of F) *TTP-1* (+ve), putative target G) *AXIN2* H) *COX2* (+ve) and I) *CTGF* (+ve) were quantified by qRT-PCR. Data shown as mean ± SEM, n=3-5; Mann-Whitney test for unpaired samples **P*=0.05, ***P*=0.01.

7.10 DISCUSSION: TGFβ-mediated regulation of AXIN2 expression: Determining a mechanism

Consistently in this study, it has been shown that TGFβ mediates the downregulation of AXIN2 expression and that this is sufficient to reproduce the increased canonical Wnt signalling response observed in SSc fibroblasts. However, the mechanism by which this downregulation was achieved was still unknown and was therefore investigated further.

At a moderate dose of TGFβ, a rapid reduction in the expression of *AXIN2* was observable within 10 min and persisted for up to 72 hr (Figure 7.1A-C), which suggested that the expression of *AXIN2* might be regulated at post-transcriptional level and facilitate the dynamic regulation of AXIN2 protein expression (Figure 7.1F). This dynamic regulation was also reflected at translational level by a reduction as soon as 2 hr and up to 72 hr (Figure 7.1D, E). In demonstration of the context dependent nature of this model, AXIN2 expression was not similarly effected by TGFβ treatment until 24 hr post-treatment in chondrocytes (Dao et al., 2007).

Further supporting a post-transcriptional mechanism, transcriptional inhibition experiments revealed that TGFβ signalling influenced the half-life of *AXIN2* mRNA by increasing the rate of mRNA decay by 4.2-fold (Figure 7.1G). In contrast with the expression of the mature *AXIN2* transcript, within 0-60 min *AXIN2* RNA destabilisation is one of the first events initiated following TGFβ treatment, while transcriptional regulation might play a more prominent role at later time points (Figure 7.1B Vs. H). Overall, these data provide a mechanistic insight into the processes involved the TGFβ-mediated downregulation of AXIN2 expression, specifically attributable to dermal fibroblasts.

To supplement the mechanistic data, the effect of TGFβ receptor blockade was determined using the TβRI-kinase inhibitor SD-208, which has been shown to selectively antagonise TβRI-induced signalling and thereby inhibit profibrotic activity in lung fibroblasts (Kapoun et al., 2006). In the absence of TβRI activation, TGFβ treatment was unable to suppress AXIN2 mRNA and protein expression in addition to other TGFβ-regulated genes targets (Figure 7.2A-E). This analysis also showed that inhibition of TGFβ-mediated *DKK-1* downregulation, a regulator of canonical Wnt singalling, was consistent with recent literature (Akhmetshina et al., 2012). This provides further evidence for the crosstalk between the TGFβ and Wnt signalling pathways, where TGFβ acts to downregulate at least two negative regulators critical for the control of canonical Wnt signalling.

Utilising available SSc fibroblasts, similar TβRI-kinase inhibition experiments were performed, in the absence of TGFβ to evaluate whether SSc fibroblasts displayed phenotyptic changes consistent with the hypothesis of autocrine/constitutive TGFβ signalling activation within these fibroblasts. In support of this, blockade of TβRI signalling upregulated the expression of *AXIN2*/*DKK1*, which are both reproducibly downregulated following TGFβ treatment (Figure 7.3A, B). Again, consistent with the hypothesis a concomitant downregulation of *α-SMA*/*COL1A1* expression was observed, which are known to be upregulated by TGFβ signalling (Figure 7.3C, D). Although confirmation at extended time points and protein expression would be required as a prior confirmations, these data would suggest that autocrine/constitutive activation of TGFβ signalling cannot be ruled out as a

characteristic of explanted dcSSc fibroblasts (Desmoulière et al. 1993; Gabbiani 2003; Ho et al. 2014).

Overall, these data augment previous observations by demonstrating the potential regulation of the canonical Wnt signalling pathway through the aberrant activation of the TGFβ signalling pathway in SSc fibroblast, both of which could have important functions in SSc disease pathogenesis, including fibrosis.

Following TβRI activation, SMAD3 is recruited and concomitantly phosphorylates SMAD2, two principal mediators of canonical TGFβ signalling. SMAD3 can act as a critical transcriptional component to directly activate immediate-early TGFβ-responsive genes, containing SBEs within their promoters, including α-SMA (Hu et al. 2003; Yang et al. 2003; Uemura et al. 2005). Therefore, SMAD3 activity/availability might have a role in the regulation of *AXIN2* transcription, which follows on from the post-transcriptional effect of TGFβ described previously.

This hypothesis was evaluated using a selective SMAD3 phosphorylation inhibitor; SIS3, which was used to prevent SMAD3 phosphorylation/activation and thereby prevent its mediation of downstream activities (Jinnin et al., 2006). In the absence of TGFβ treatment, SMAD3 inhibition reduced the basal expression of *AXIN2* (Figure 7.4A); however, showed no effect on the TGFβ-induced downregulation of *AXIN2* expression in contrast to repression observed for α-SMA (Figure 7.4B-D). This is contrary to an observation in chondrocytes, which showed that eventual downregulation of *AXIN* by TGFβ signalling was SMAD3 dependent (Dao et

al., 2007). Subsequent evaluation using siRNA-mediated depletion of SMAD3 was consistent with effects described for the SIS3 inhibitor (Figure 7.4H). These data indicate that while SMAD3 might be important for the steady-state expression of AXIN2; TGFβ-induced AXIN2 downregulation was independent of SMAD3 expression/activity and therefore mediated by an alternative mechanism in fibroblasts.

Further evidence suggested that SMAD3, an essential component of the TGFβ signalling pathway, is also an important component of the canonical Wnt signalling pathway. Indeed, canonical Wnt-3a agonist treatment lead to the phosphorylation (activation) of SMAD3, which could be abolished by SMAD3 inhibitor co-treatment (Figure 7.5A, B). This was in agreement with a previous study that also showed Wnt-3a-induced phosphorylation of SMAD3 (Wei et al. 2012). This was further supported by the canonical Wnt-induced nuclear translocation of SMAD3 (Figure 7.5C). Extending upon this observation, a more direct role for the participation of SMAD3 in canonical Wnt signalling pathway was indicated by the significant inhibition of the canonical Wnt signalling pathway in SMAD3 depleted fibroblasts (Figure 7.5E).

Suggestively, SMAD3 has been shown to directly interact with both AXIN and β-catenin in independent studies (Chia & Costantini 2005; Jian 2006; Liu et al. 2006; Tian et al. 2013). As discussed previously, due to the absence of SBEs within the promoter region of the TOPFlash reporter construct the reduction in canonical Wnt signalling in SMAD3 depleted fibroblasts was is suggestive of a direct effect on TCF/LEF transcriptional activity and not by SBE-mediated transactivation.

Therefore these observations could represent novel elements of crosstalk between the canonical Wnt the TGFβ signalling pathways within fibroblasts. In light of these data, it is possible that the previously observed increase in total TGFβ signalling activity following canonical Wnt treatment, that was increased further by canonical Wnt signalling hyperactivation, was as a result of a Wnt-induced increase in SMAD3 activity (Figure 6.5F), although further experiments would be required.

As SMAD3 was not directly involved in the TGFβ-mediated downregulation of AXIN2 expression, additional downstream mediators of the TGFβ signalling pathway were henceforth evaluated. Preliminary analysis of several kinases including PI3K, MEK1 and AKT1/2/3 indicated that, having no effect on TGFβ-induced repression, they were unlikely to play a key role in the TGFβ-mediated transcriptional or post-transcriptional downregulation of *AXIN2* (Figure 7.6A-F).

Only the inhibition of p38 MAPK was found to have a partial inhibitory effect on TGFβ-mediated downregulation of *AXIN2*. This partial inhibition was achieved using the VX-702 p38 inhibitor (maximum of 31%), which showed a trend toward a dose effect and also showed an active inhibitory profile for both TGFβ- and p38-regulated genes (Figure 7.7A-E). In contrast, the use of a second p38 inhibitor, SB202190, showed no inhibition of TGFβ-mediated *AXIN2* downregulation in contrast to its inhibitory activity upon other TGFβ- and p38-regulated genes (Figure 7.7F-J).

As VX-702 only showed a partial of inhibition across a standard dose range,

this suggested the possibility that an off-target effect might be responsible for this activity. The second possibility was that the standard error present in the *AXIN2* expression data for the SB202190 experimental series masks the VX-702-mediated partial inhibitory effect; however, analysis of each data individually revealed no such concealment (data not shown). A more intriguing hypothesis can be derived from the fact that VX-702 is known to have a 14-fold higher potency for the p38α isoform compared to p38β isoform. In contrast, the inhibition of p38 by SB202190 has not been described as being selective for a particular isoform. Therefore, one possibility might be that the p38 isoforms have opposing regulatory effects. The disparate roles of the p38 isoforms have been shown in the regulation of apoptosis in Jurkat cells (T-cells), where SB202190 induced apoptosis by inhibition of p38α/β; however, expression of the p38β isoform effectively rescued the phenotype while p38α expression showed a modest increase toward apoptotic activity (Nemoto et al., 1998). Therefore the balance between these two isoforms might have important consequences. Specifically, the p38α isoform may mediate the TGFβ-mediated downregulation of *AXIN2* expression while the p38β isoform opposes p38α activity. Further support for utilisation of p38 in this specific pathway can be implied from its known role in the regulation of TTP-mediated RNA decay, discussed next (Brooks & Blackshear 2013).

In parallel, the post-transcriptional mechanism by which TGFβ mediated the downregulation of AXIN2 was also investigated. Notably, the majority of eukaryotic mRNAs are degraded though the shortening of their poly(A)-tails,

which can initiate the recruitment of the RNA-degrading exosome complex through a deadenylation-dependent pathway (Houseley & Tollervey 2009). As this is known to be regulated by ARE harboured within the 3′UTR of many mRNAs, a bioinformatics analysis was performed on the *AXIN2* transcript and several ARE binding motifs were detected (Figure 7.8A). These motifs are known to recruit ARE-binding proteins including TTP-1, HUR and AUF-1, which could potentially regulate the stability of *AXIN2* mRNA (Figure 7.8A). Indeed, the mRNA and protein expression of several ARE containing mRNAs including *COX2*, *TNF*, *c-MYC* and *CCND1* are known to be regulated by TTP-1-mediated destabilisation, in addition TTP-1 expression has also been shown to be TGFβ responsive (Ogawa et al., 2003; Marderosian et al., 2006; Kang et al., 2014; Blanco et al., 2014).

Pertaining to the later observation, TGFβ treatment inhibited TTP-1 expression in HC fibroblasts in contrast to these studies (Figure 7.8B, C) (Ogawa et al., 2003; Blanco et al., 2014). Despite this, the possibility remained that TGFβ might increase TTP-1 activity, which could then lead to the destabilisation of the *AXIN2* transcript and the resulting TGFβ-mediated decrease in TTP-1 expression might act as a restorative negative regulatory mechanism.

TTP-1 protein expression studies were impeded by the lack of a specific antibody, which apart from being highly non-specific also showed no change in expression following TGFβ treatment (data not shown), despite the previously observed downregulation at mRNA level. Interestingly, the TGFβ-induced expression pattern for *TTP-1* showed a similar profile to that of *AXIN2* (Figure 7.8B, C Vs. F, G). Taking these data together with the

absence of reliable primers to detect *AUF1* expression and the minimal effect of TGFβ upon *HUR* expression, only TTP-1 was subsequently carried forward for further investigation into the mechanism of TGFβ-mediated downregulation of *AXIN2*.

Additionally, p38 is a known negative regulator of TTP-1 activity and, in tandem with ERK, has been shown to prevent TTP-1-mediated destabilisation of ARE containing mRNAs, which could potentially include *AXIN2* (Figure 1.4) (Deleault, Skinner & Brooks 2008). This would be in contrast to the previous observation where p38 inhibition partially prevented TGFβ-mediated downregulation of *AXIN2* (Figure 7.7A). However, as previously discussed, the potential for differential activities of p38 isoforms could account for this disparity.

Initially, the effect of siRNA-mediated TTP-1 depletion upon the basal expression of AXIN2 was determined in HC fibroblasts. Indeed, in contrast to α-SMA, a temporal increase in the expression of both AXIN2 and DKK1, endogenous inhibitors of Wnt signalling, were observed at both transcriptional and translational level (Figure 7.9A-D). This supported the hypothesis that TTP-1 might regulate *AXIN2* mRNA stability.

As TGFβ-mediated destabilisation of the *AXIN2* transcript most likely occurred within a 60 min window (Figure 7.1B Vs. H), a short TGFβ time-course was performed in order to determine any differential effects on the kinetics of TGFβ-induced *AXIN2* downregulation within TTP-1 depleted fibroblasts. On analysis of this data, one important shortcoming resided in

was the reproducibility of *TTP-1* silencing, which was not achieved prior to TGFβ treatment in this experimental series (Figure 7.9F Vs. A). As a result, the possibility remained that the effects observed in TTP-1 silenced fibroblasts may be due to off-target effects.

However, several effects that would have been predicted to occur in TTP-1 depleted fibroblasts were observed. For example, *COX2*, a known TTP-1 regulated gene, and *AXIN2* expression were significantly increased in TTP-1 depleted fibroblasts and showed a similar decrease in expression over time following TGFβ treatment (Figure 7.9G, H) (Kang et al., 2015). As *CTGF* expression was not affected in the same manner, this would have supported the specificity of the effect found for *AXIN2* expression (Figure 7.9I).

A further limitation was observed in subsequent evaluations of TTP-1 expression. As discussed previously, the TGFβ-induced downregulation of *TTP-1* expression is in contrast to the literature (Figure 7.8A, B) (Ogawa et al., 2003; Blanco et al., 2014). This result was difficult to confirm due to the lack of TTP-1 antibody specificity (data not shown); however, when a second TTP-1 antibody was utilised, no significant change in TTP-1 protein expression was found following TGFβ treatment (data not shown) and this was further confounded by the minute effect observed in TTP-1 silenced fibroblasts (Figure 7.9E). Therefore the reliability of the antibodies is in question. The potential involvement of TTP-1 activity in the regulation of *AXIN2* expression still remains to be conclusively determined. To further evaluate the effect of TGFβ signalling upon TTP-1 activity, irrespective of expression, would require a complex series of biochemical experiments to validate the hypothesis given the unreliability of the antibodies.

Overall, these data indicate that TGFβ initially mediates AXIN2 downregulation by increasing its rate of mRNA degradation. That this is required for the increased response of fibroblasts to canonical Wnt signalling, and equivalent to that observed in SSc fibroblasts. Preliminary evidence suggests that the basal repression of AXIN2 in SSc fibroblasts might be mediated by activation of the p38 signalling pathway, although this is not conclusive. In addition, the *AXIN2* transcript contains an ARE at its 3'UTR, which potentially regulates mRNA degradation through ARE binding protein-mediated destabilisation.

8 The consequence of canonical Wnt signalling hyperactivation upon profibrotic activation of fibroblasts

Fibrosis is a fundamental hallmark of SSc. Patients with dcSSc have a higher extent of fibrotic involvement in both the skin and internal organs, which increases the risk of developing severe complications (Penn et al. 2007). Further, the severity of the diffuse cutaneous disease is associated with the level of fibrotic skin involvement (Steen & Medsger, 2001). TGFβ signalling is fundamental in the pathogenesis of tissue fibrosis but more recently studies have shown overactivation of canonical Wnt signalling during fibrosis in SSc and in other fibrotic models (Bayle et al. 2007; Wei, et al. 2011; Yu et al. 2003; Ask et al. 2008; Varga & Pasche 2009). However, the nature of this activation is yet to be identified and the relative crosstalk with the TGFβ pathway is unclear. In this study it has been identified that TGFβ can increase the amplitude of the canonical Wnt signalling pathway through the downregulation of AXIN2 expression. Therefore the fibrotic consequences of increased canonical Wnt signalling pathway were evaluated in the both TGFβ-primed and AXIN2 depletion models of canonical Wnt signalling hyperactivation. Correspondingly, β-catenin was also evaluated due to its fundamental function as a downstream regulator of canonical Wnt signalling.

8.1 TGFβ priming does not significantly effect profibrotic fibroblast activation

The TGFβ-primed model of canonical Wnt signalling hyperactivation was evaluated for its potential effects on profibrotic gene expression, myofibroblast generation and ECM contractile capacity.

This was first evaluated in TGFβ-primed fibroblasts using two known markers of fibroblast activation *α-SMA* and *COL1A1* expression. Indeed, HC fibroblasts treated with Wnt-3a showed a 136.3% ($P<0.05$) increase in *α-SMA* expression in contrast to the 905.9% ($P<0.01$) increase in expression following TGFβ treatment (Figure 8.1A). When fibroblasts were primed with TGFβ and sequentially treated with Wnt-3a, *α-SMA* expression was increased to 1090.1% ($P<0.05$); however, this was not found to be statistically significant when compared to independent TGFβ treatment (Figure 8.1A). Similarly, *COL1A1* expression was inhibited following Wnt-3a treatment, which was reduced to 87.8%, and this was in contrast to the 308.4% ($P<0.05$) increase in expression by TGFβ (Figure 8.1B). In TGFβ-primed fibroblasts, Wnt-3a treatment lead to a 294.4% ($P<0.001$) increase in *COL1A1* expression that was equivalent to the expression in TGFβ treated fibroblasts (Figure 8.1B).

In agreement with mRNA data, the expression of α-SMA protein was unchanged following treatment with Wnt-3a and this was in contrast to the significant upregulation following TGFβ treatment (Figure 8.1C). Further, TGFβ-primed fibroblasts that were subsequently treated with Wnt-3a were not significantly different from TGFβ-treated fibroblasts (Figure 8.1C).

As a validation, fibroblast-mediated contraction of 3D collagen gels were

also used to evaluate profibrotic activity. 3D Collagen gels were seeded with HC fibroblasts, polymerised and floated in low-serum medium. In the presence of Wnt-3a medium, collagen gel contraction was not significantly different to control gels, 90.3% (Figure 8.1D). However, TGFβ treatment induced collagen gel contraction and reduced the gel area to 65.1%, which was equivalent to the contraction to 65.3% exhibited by Wnt-3a-treated TGFβ-primed fibroblasts, (Figure 8.1D).

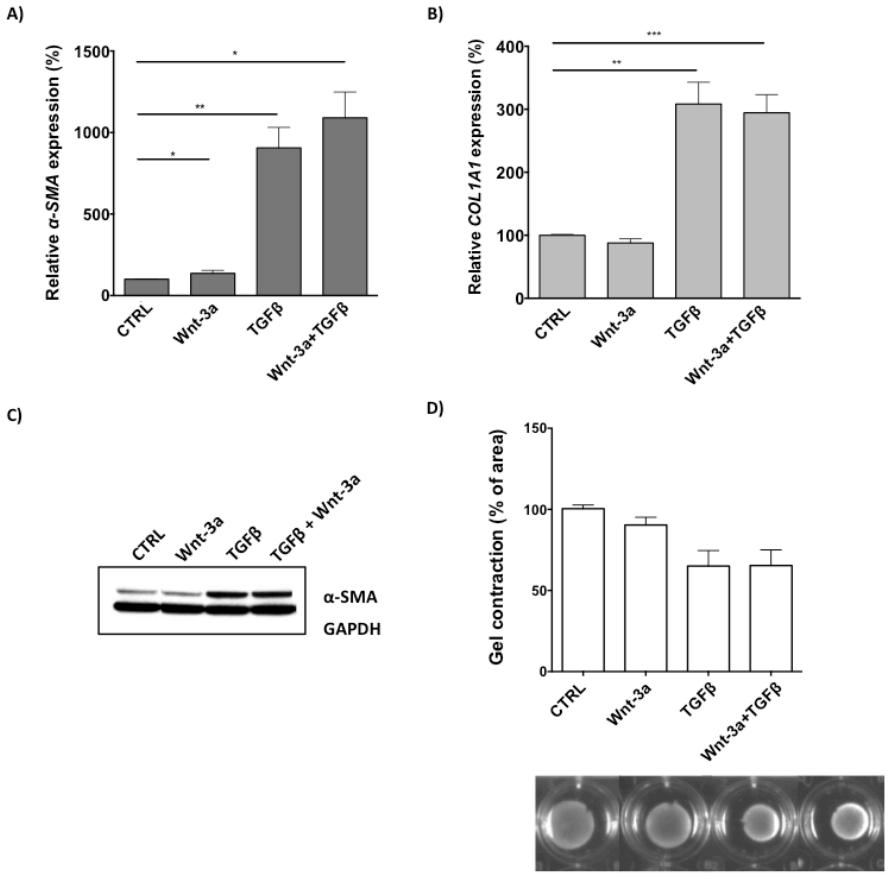

Figure 8.1 TGFβ priming does not significantly effect profibrotic fibroblast activation

TGFβ-primed canonical Wnt signalling hyperactivation was evaluated for significant profibrotic effects. A-B) HC fibroblasts were primed with TGFβ (5 ng/ml) or left untreated for 24 hr, subsequently treated with Wnt-3a for 24 hr and the expression of *α-SMA* and *COL1A1* were quantified by qRT-PCR. C) As in A, where Wnt-3a treatment was carried out for 72 hr and subsequenty fibroblast activation marker α-SMA and GAPDH (loading control) protein expression were determined by Western blot. D) Under the same condition as C, relative fibroblast-mediated 3D collagen gel contraction was quantified according to gel surface area. Data shown as mean ± SEM, n=3-5; Mann-Whitney test for unpaired samples **P*=0.05, ***P*=0.01.

8.2 Increased canonical Wnt signalling in AXIN2 silenced fibroblasts has no effect on profibrotic activation

Complementary to TGFβ-primed model, the AXIN2 depletion model of canonical Wnt signalling hyperactivation was subsequently evaluated for its potential effects on profibrotic gene expression, myofibroblast generation

and ECM contractile capacity.

Here, *AXIN2* expression severed as a positive control and was silenced to 57.5% in siAXIN2 compared to SCR fibroblasts (Figure 8.2A). When treated with Wnt-3a, *AXIN2* expression was increased by 167.7% in SCR fibroblasts and to 115.1% in siAXIN2 fibroblasts (Figure 8.2A).

Next the effect on *α-SMA* and *COL1A1* profibrotic gene expression was evaluated. Indeed, *α-SMA* expression showed no change in expression in siAXIN2 fibroblasts, 100.2% compared to SCR controls (Figure 8.2B). Wnt-3a treatment also showed no significant change *α-SMA* expression in either SCR or siAXIN2 fibroblasts, expressed by 105.4% and 110.4%, respectively (Figure 8.2B).

Interestingly, a 172.2% increase in *COL1A1* expression was observed in siAXIN2 fibroblasts at basal level, compared to SCR controls (Figure 8.2C). Indeed, this was greater than the 137.8% induced by Wnt-3a in SCR fibroblasts; however, less than the 217.7% increase in Wnt-3a-treated siAXIN2 fibroblasts (Figure 8.2C).

At protein level, the expression of AXIN2 was significantly downregulated in siAXIN2 compared to SCR fibroblasts (Figure 8.2D). Following Wnt-3a treatment, AXIN2 expression was upregulated in both siAXIN2 and SCR fibroblasts compared to controls, while α-SMA expression was unaffected throughout (Figure 8.2D).

Like SCR fibroblasts, AXIN2 expression was upregulated following Wnt-3a treatment, but the increase was greater in SCR fibroblasts, in contrast to the unaffected expression of α-SMA (Figure 8.2D).

Next, the differentiation state of siAXIN2 fibroblasts was evaluated based on α-SMA stress fibril formation and quantified by the concomitant increase in the integrated density of fluorescence (IDF). At basal level, the IDF of siAXIN2 fibroblasts was reduced to 0.9-fold compared to SCR fibroblasts. In the presence of Wnt-3a, SCR fibroblasts the IDF was increased by 1.1-fold, but this was reduced to 0.8-fold in siAXIN2 fibroblasts (Figure 8.2E). As a positive control, normal myofibroblast differentiation was evaluated in an untransfected population of HC fibroblasts in response to treatment. HC fibroblasts treated with Wnt-3a or TGFβ increased the IDF by 1.7-fold and 3.4-fold, respectively (Figure 8.2E).

Finally, the effect of increased canonical Wnt signalling on collagen gel contraction was evaluated in the siAXIN2 model. Collagen gels were seeded with either siAXIN2 or SCR fibroblasts and under basal conditions there was no significant change in gel surface area, 99.1% of SCR gel area (Figure 8.2F). In the presence of Wnt-3a, there was a trend toward increased collagen gel contraction with the gel area reduced to 88.7% and 88.3% in SCR and siAXIN2 fibroblasts, respectively (Figure 8.2F).

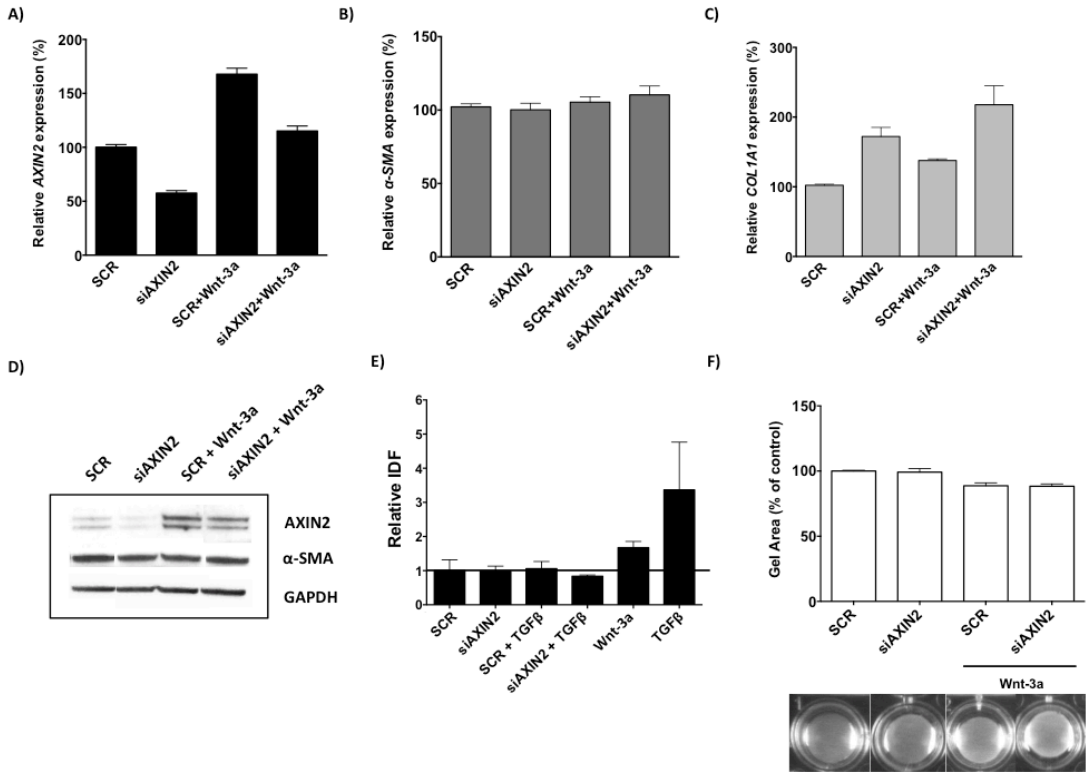

Figure 8.2 Increased canonical Wnt signalling in AXIN2 silenced fibroblasts has no effect on profibrotic activation

The profibrotic effects of AXIN2 depletion-mediated canonical Wnt signalling hyperactivation were evaluated. HC fibroblasts were transfected with AXIN2 (siAXIN2) or SCR siRNA for 72 hr. A) Following Wnt-3a treatment for 24 hr the expression of A) *AXIN2* (+ve) and profibrotic genes B) *α-SMA* and C) *COL1A1* were quantified by qRT-PCR. D) After 72 hr Wnt-3a treatment, the protein expression of AXIN2 (+ve), fibroblast activation marker α-SMA and GAPDH (loading control) were determined by Western blot. E) Myofibroblast counts were determined by the relative integrated density of fluorescence (IDF) from α-SMA positive staining of fibroblasts, under the same conditions as D, quantified using ImageJ. F) Relative fibroblast-mediated 3D collagen gel contraction was quantified according to gel surface area under the same condition as D. Data shown as mean ± SEM, n=2-4.

8.3 AXIN2 does not regulate TGFβ-induced profibrotic fibroblast activation

While TGFβ clearly regulates the amplitude of canonical signalling through the downregulation of AXIN2, it was possible that this downregulation facilitated the profibrotic activity of TGFβ. Therefore preliminary experiments

were performed to determine any differential profibrotic activities following AXIN2 depletion.

First, the effect of AXIN2 expression on the amplitude of the TGFβ signalling pathway was evaluated using TGFβ-induced luciferase reporters. The p3TP-lux reporter measured total TGFβ activity and SMAD-mediated activity was measured by pSBE-Luc activation. In siAXIN2 fibroblasts, total TGFβ activity showed no basal increase compared to SCR fibroblasts and in the presence of TGFβ, there was a 4.3-fold induction in siAXIN2 fibroblasts, which was equivalent to the 3.7-fold increase observed in SCR fibroblasts (Figure 8.3A). Similarly, TGFβ-induced a 2.5-fold induction of SMAD-mediated TGFβ activity in siAXIN2 fibroblasts, which was also equivalent to the 2.7-fold increase in TGFβ-treated SCR fibroblasts (Figure 8.3B).

Despite this data, the profibrotic effects of TGFβ in siAXIN2 fibroblasts were evaluated. Consistently, α-SMA expression was unchanged at basal level in siAXIN2 fibroblasts compared to SCR fibroblasts (Figure 8.3C). Following TGFβ treatment, a significant increase in α-SMA expression was observed in siAXIN2 fibroblasts, although this was not significantly different to the level induced in SCR fibroblasts (Figure 8.3C).

Next, myofibroblast differentiation was evaluated based on α-SMA stress fibril formation as quantified by the concomitant increase in the IDF. Indeed, no change in the IDF between siAXIN2 and SCR fibroblasts were observed (Figure 8.3D). Following treatment with TGFβ, a 1.8-fold increase in the IDF was observed in SCR fibroblasts, which was similar to the 1.7-fold increase in siAXIN2 fibroblasts (Figure 8.3D). As a positive control, untreated HC fibroblasts increased the IDF by 3.4-fold in response to TGFβ (Figure 8.3D).

Finally, 3D collagen gels were seeded with either siAXIN2 or SCR fibroblasts. Consistently, there was no significant change in collagen gel contraction in siAXIN2 fibroblasts, 97% of SCR fibroblasts gel area (Figure 8.3E). TGFβ treatment induced a significant decrease in collagen gel area to 59.0% ($P<0.01$) in SCR fibroblasts and a trend toward an increased contraction was observed in siAXIN2 fibroblasts, 51.6% ($P<0.01$) of SCR control gel area (Figure 8.3E).

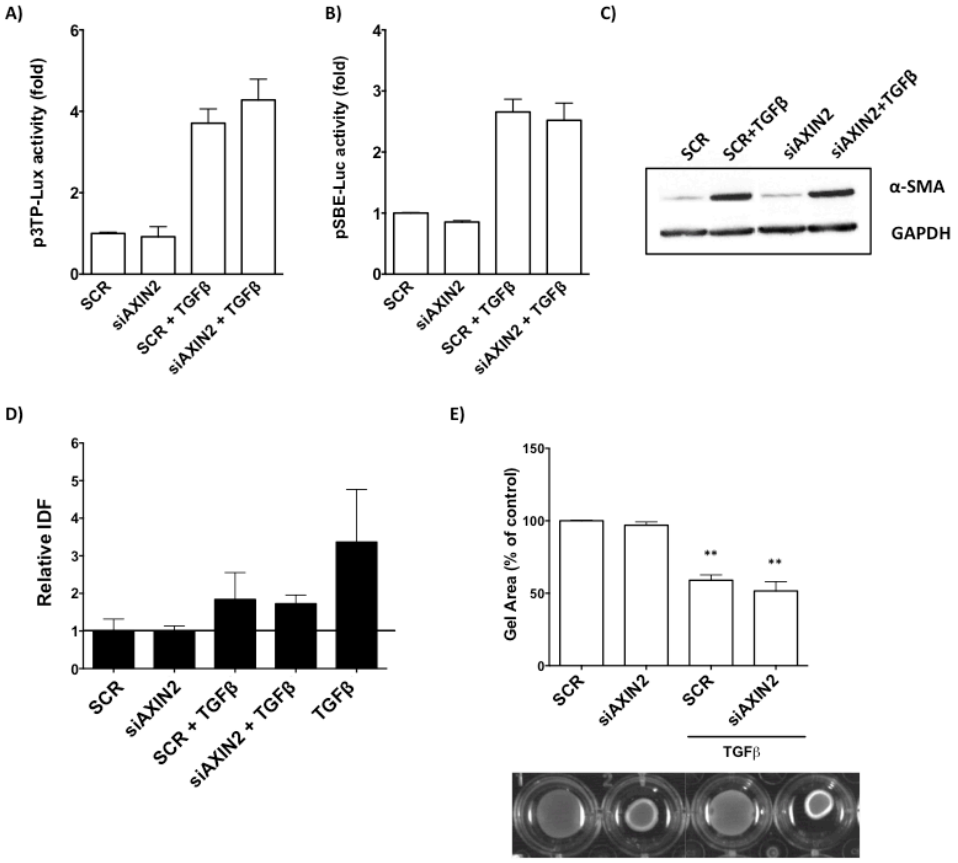

Figure 8.3 AXIN2 does not regulate TGFβ-induced profibrotic fibroblast activation

The contribution of reduced AXIN2 expression towards TGFβ signalling amplitude and TGFβ-mediated profibrotic activities were determined. HC fibroblasts were transfected with TGFβ reporters A) p3TP-Lux (Total activity) or B) pSBE-Luc (SMAD-mediated activity) 24 hr prior to transfection with AXIN2 or SCR siRNA for 72 hr. Fibroblasts were subsequently treated with TGFβ for a further 24 hr and TGFβ signalling activity was determined luciferase activity. C) As in A, where TGFβ treatment was for 72 hr and the protein expression of AXIN2 (+ve), fibroblast activation marker α-SMA and GAPDH (loading control) were determined by Western blot. D) Myofibroblast counts were determined by the relative integrated density of fluorescence (IDF) from α-SMA positive staining of fibroblasts, under the same conditions as in C, quantified using ImageJ. E) Relative fibroblast-mediated 3D collagen gel contraction was quantified according to gel surface area under the same condition as C. Data shown as mean ± SEM, n=3-4; Mann-Whitney test for unpaired samples ***P*=0.01.

8.4 β-catenin and SMAD3 are required for canonical Wnt signalling and basal *α-SMA* and *COL1A1* expression

Recently, *in vivo* fibroblast-specific β-catenin stabilisation has been shown to lead to fibrosis through characteristic hallmarks including dermal thickening, increased collagen expression and myofibroblast presence (Beyer et al. 2012). However, *in vitro* canonical Wnt signalling hyperactivation in fibroblasts achieved using two independent models, TGFβ-priming and AXIN2 depletion (Figure 6.7 & Figure 7.1), have not supported these observations. Therefore the direct effect of modifying β-catenin activity was evaluated with respect to profibrotic gene expression using inhibitor studies.

As a first measure to explore the putative activity of the β-catenin inhibitor FH535, canonical Wnt signalling activity was measured by *AXIN2* expression and TOPFlash activity, in the presence and absence of a β-catenin inhibitor, FH535. Wnt-3a induced a 512.5% ($P<0.05$) increase in *AXIN2* expression that was inhibited in the presence of FH535 to 146.2%, 346.1% or 498.3% at 10.0, 3.0 and 1.0 μM, respectively (Figure 8.4A). Similarly, the Wnt-3a-induced 19.4-fold ($P<0.01$) increase in TOPFlash activity was inhibited to 7.0-fold, 7.5-fold or 10.6-fold at 10.0, 3.0 and 1.0 μM FH535, respectively (Figure 8.4B).

Concomitantly, the FH535-mediated effects on the expression of both *α-SMA* and *COL1A1* were evaluated. Wnt-3a treatment induced *α-SMA* expression by 136.0% ($P<0.05$) and showed a dose-dependent inhibition to 46.4%, 81.1%, and 107.9% at 10.0, 3.0 and 1.0 μM FH535, respectively (Figure 8.4C). Although Wnt-3a treatment did not induce *COL1A1* expression in the presence of FH535 a dose-dependent decrease in

expression was observed to 26.8%, 66.1%, and 89.7% at 10.0, 3.0 and 1.0 μM, respectively (Figure 8.4D).

In parallel, the effects exhibited by β-catenin inhibition were contrasted with those of SMAD3 inhibitor SIS3, which as a known regulator of fibrotic gene expression acted as a positive control. On evaluation of canonical Wnt signalling activity, Wnt-3a induced a 380.3% ($P<0.05$) increase in *AXIN2* expression that was inhibited to 130.0%, 306.3% or 343.3% at 5.0, 3.0 and 1.0 μM SIS3, respectively (Figure 8.4E). Further, SIS3 also inhibited the 17.4-fold ($P<0.01$) increase in Wnt-3a-induced TOPFlash activity to 1.1-fold, 4.4-fold or 9.8-fold at 5.0, 3.0 and 1.0 μM, respectively (Figure 8.4F).

The expression of both *α-SMA* and *COL1A1* were concomitantly evaluated. Wnt-3a induced *α-SMA* expression by 194.3% and this was dose-dependently inhibited in the presence of SIS3 to 28.7%, 155.3% and 192.5% at 5.0, 3.0 and 1.0 μM SIS3, respectively (Figure 8.4G). Wnt-3a treatment did not induce *COL1A1* expression and while SIS3 treatment had no effect significant effect at 3.0 or 1.0 μM, expressed by 92.4% and 90.6%, respectively (Figure 8.4H), 5.0 μM SIS3 treatment lead to a 55.0% reduction in basal expression.

Subsequently, the basal effects of β-catenin and SMAD3 inhibition were preliminarily evaluated independent of Wnt treatment. The expression of *α-SMA* was significantly inhibited by 20.5% and 56.8% in the presence of 10.0 μM FH535 and 3.0 μM of SIS3, respectively ($P<0.01$) (Figure 8.4I). This was also observed for *COL1A1* expression which was inhibited by 54.5% ($P<0.05$) and 28.6% ($P<0.01$) at 10.0 μM FH535 and 3.0 μM of SIS3, respectively (Figure 8.4J). Protein expression of α-SMA also confirmed a

significant reduction following FH535 and SIS3 treatments (Figure 8.4K).

Notably, the cell viability of fibroblasts co-treated with SIS3 and FH535 were evaluated by MTT assay under the same conditions. SIS3 showed no notable differences in cell viability in contrast to FH535, which showed a dose dependent increase across the 0.3-10.0 μM dose range (maximum of 163.2% at 3.0 μM after 72 hr) at both 24-72 hr time points (Sup Figure 10.5).

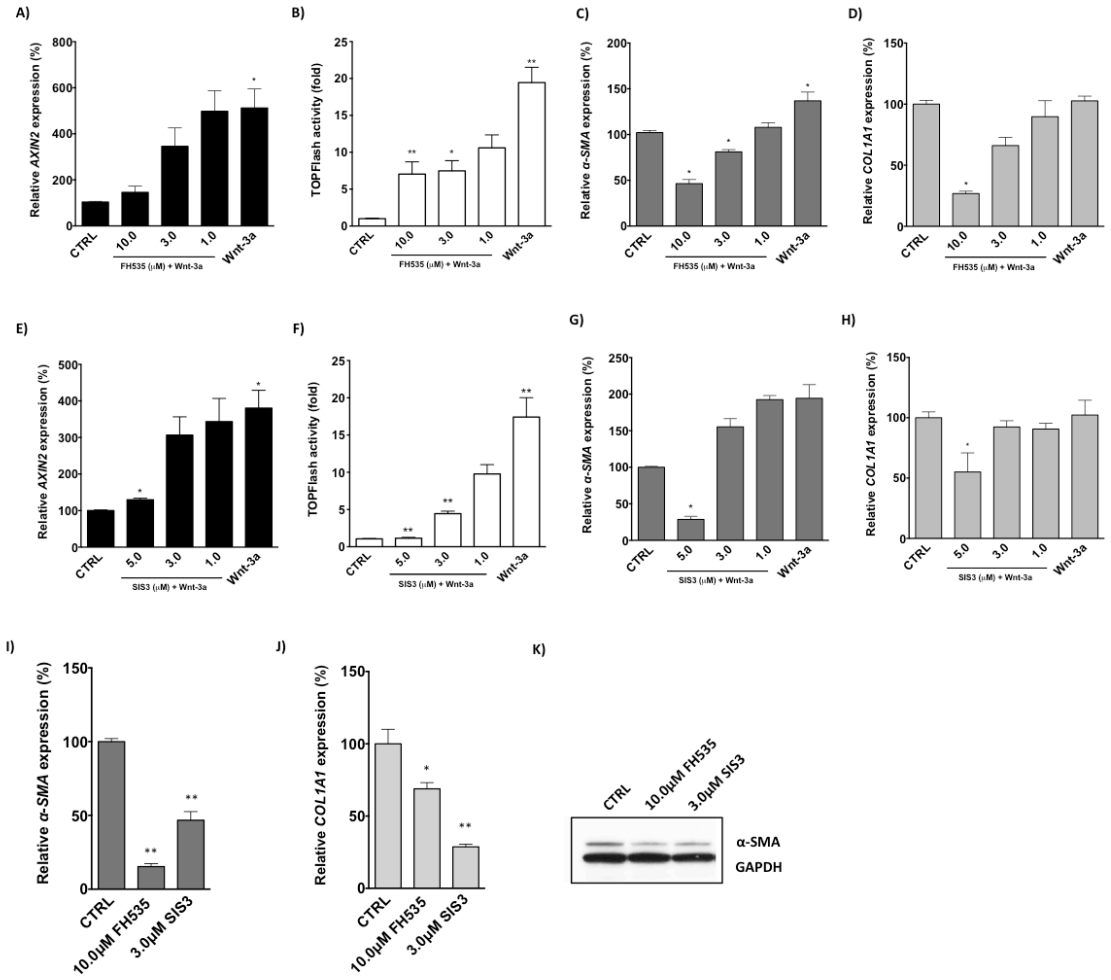

Figure 8.4 β-catenin and SMAD3 are required for canonical Wnt signalling and basal *α-SMA* and *COL1A1* expression

The direct effect of inhibiting β-catenin (FH535) activity was evaluated against SMAD3 inhibition (SIS3) with respect to profibrotic gene expression and canonical Wnt signalling. HC fibroblasts were treated with FH535 (A-D) or SIS3 (E-H) inhibitors (0.3-10.0 μM) 1 hr prior to Wnt-3a (100 ng/ml) treatment for 24 hr. Canonical Wnt signalling was determined by A, E) *AXIN2* expression, quantified by qRT-PCR or by B, F) TOPFlash reporter luciferase activity, transfected 24 hr prior to experimental start. Expression of profibrotic genes C, G) *α-SMA* and D, H) *COL1A1*, under the same conditions as A, were quantified by qRT-PCR. Additionally, HC fibroblasts were treated with FH535 (10.0 μM) and SIS3 (3.0 μM) for 24 hr and the basal expression of I) *α-SMA* and J) *COL1A1* profibrotic genes were quantified by qRT-PCR. K) Basal protein expression of fibroblast activation marker α-SMA was determined following 72 hr inhibitor treatment by Western blot. Data shown as mean ± SEM, n=5; Mann-Whitney test for unpaired samples **P*=0.05, ***P*=0.01.

8.5 β-catenin is required for the TGFβ-induced profibrotic activation of fibroblasts

Like canonical Wnt signalling, TGFβ clearly induced the nuclear translocation of β-catenin and this was independent of Wnt secretion (Figure 6.4H), it was possible that TGFβ-induced profibrotic activities might in part be regulated by β-catenin. Hence the consequence of β-catenin inhibition was evaluated upon profibrotic gene expression and ECM contractility were evaluated.

HC fibroblasts were treated with TGFβ in the presence and absence of FH535 (0.3-10.0 μM). TGFβ-mediated the downregulation of *AXIN2*, included as a positive control, to 63.2% and in the presence of FH535, a dose dependent reduction was observed to 26.3%, 49.6% and 63.7% by 10.0, 3.0 and 1.0 μM FH535, respectively ($P<0.05$) (Figure 8.5A).

The expression of fibroblast activation marker *α-SMA* was similarly effected, increased by 1014.5% following TGFβ and reduced to 36.8%, 586.4% and 926.6% in the presence of 10.0, 3.0 and 1.0 μM FH535, respectively ($P<0.05$) (Figure 8.5B). This was also observed for *COL1A1* expression, which was induced by 371.9% following TGFβ and inhibited in the presence of FH535 to 85.7%, 256.7% and 291.0% at 10.0, 3.0 and 1.0 μM, respectively ($P<0.05$) (Figure 8.5C).

In turn, this was confirmed by α-SMA protein expression, where the TGFβ-mediated increase in expression was dose dependently decreased by FH535 across the dose series (Figure 8.5D).

Finally, the effect on fibroblast-mediated 3D collagen gel contraction was evaluated using 10.0 μM FH535, which showed the greatest effect on α-SMA expression (Figure 8.5D).

In the presence of FH535, contractile force was reduced and gel area was increased to 112.1% compared to basal controls (Figure 8.5E). TGFβ treatment induced gel contraction and reduced the gel area to 67.4% of controls. In contrast, this was partially prevented by co-treatment with FH535, where the gel area was reduced to only 88.5% (Figure 8.5E).

Additionally, under the same conditions, FH535 mediated a dose-dependent increase in fibroblasts cell viability across the dose range of 0.3-10.0 μM (maximum of 215.4% at 3.0 μM following 72 hr) at both 24 hr and 72 hr time points (Sup Figure 10.4).

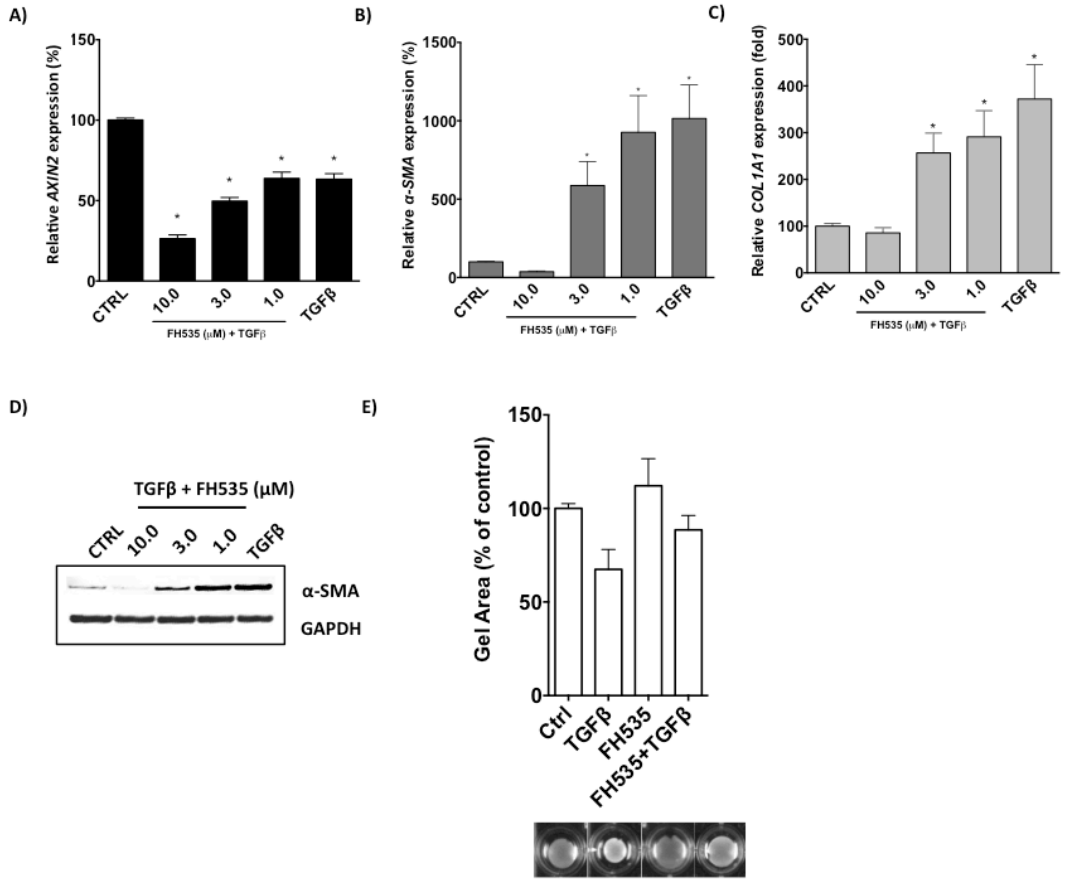

Figure 8.5 β-catenin is required for the TGFβ-induced profibrotic activation of fibroblasts

To determine the function of of β-catenin in TGFβ-induced profibrotic activities, FH535-mediated of β-catenin inhibiton (FH535) was employed. HC fibroblasts were treated with the FH535 inhibitor (1.0, 3.0 and 10.0 μM) for 1 hr prior to 24 hr TGFβ treatment and A) *AXIN2* (+ve) expression, a canonical Wnt target, and B) *α-SMA* and C) *COL1A1* profibrotic gene expression were determined by qRT-PCR. D) As in A, but following 72hr TGFβ treatment, the expression of fibroblast activation marker α-SMA and GAPDH (loading control) were determined by Western blot. E) Relative fibroblast-mediated 3D collagen gel contraction was quantified according to gel surface area under the same condition as in D. Data shown as mean ± SEM, n=3-4; Mann-Whitney test for unpaired samples *P=0.05.

8.6 β-catenin negatively regulates the profibrotic activation of fibroblasts

Complementary to inhibitor studies, the function of β-catenin in regulating TGFβ-mediated profibrotic activity was subsequently evaluated by siRNA-mediated β-catenin depletion in HC fibroblasts.

β-catenin silenced fibroblasts (siβcat) showed a profound reduction in expression of β-catenin at 48 hr and this was decreased further by 72 hr compared to SCR fibroblasts (Figure 8.6A). This repression was reproducible and persisted for a minimum of 144 hr (Figure 8.6B).

TGFβ treatment significantly increased the depleted levels of β-catenin present in siβcat fibroblasts equivalent to the basal levels present in SCR fibroblasts, while not affecting SCR fibroblasts levels (Figure 8.6B). TGFβ treatment also induced a profound increase in the expression of fibroblast activation marker α-SMA in siβcat fibroblasts, which was greater than that observed in SCR fibroblasts (Figure 8.6B).

To confirm these data, 3D collagen gels were seeded with either siβcat or SCR fibroblasts. In resting siβcat fibroblasts, collagen gels showed evidence of gel contraction, reduced by 14.6% ($P<0.05$) compared to SCR fibroblast seeded gels (Figure 8.6C). Following TGFβ treatment, a significant increase in collagen gel contraction was observed in siβcat fibroblasts, which reduced gel area by 72.5% ($P<0.05$) in contrast to the 46.8% ($P<0.01$) reduction in SCR fibroblasts, compared untreated SCR controls (Figure 8.6C).

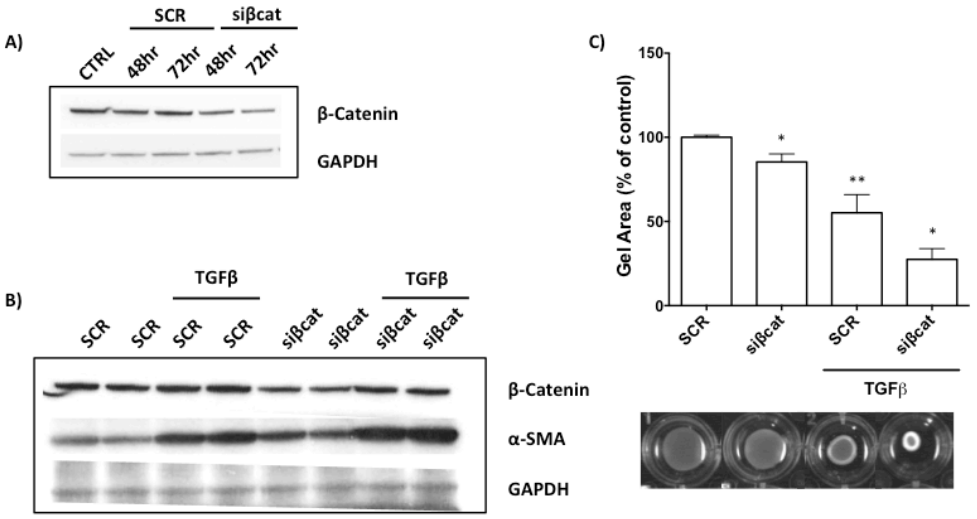

Figure 8.6 β-catenin negatively regulates the profibrotic activation of fibroblasts

β-catenin expression was evaluated in the regulation of TGFβ-mediated profibrotic activity by siRNA-mediated gene silencing. HC fibroblasts were transfected with *β-catenin* siRNA (siβcat) or SCR oligonucleotide. A) β-catenin and GAPDH (loading control) expression were determined by Western blot 48 and 72 hr post-transfection. B) At 72 hr post-transfection, fibroblasts were treated with TGFβ (5 ng/ml) for 72 hr and the expression of β-catenin (+ve), profibrotic marker α-SMA and GAPDH (loading control) were determined by Western blot. C) Relative fibroblast-mediated 3D collagen gel contraction was quantified according to gel surface area under the same condition as in B. Data shown as mean ± SEM, n=3-4; Mann-Whitney test for unpaired samples **P*=0.05, ***P*=0.01.

8.7 DISCUSSION: The consequence of canonical Wnt signalling hyperactivation upon profibrotic activation of fibroblasts

Extensive fibrosis can lead to the destruction of the tissue architecture and ultimately can lead the loss of organ function. While therapies that target immunological, vascular and fibrotic processes are required for the effective treatment of SSc, the development of novel anti-fibrotic treatments may be considered a priority given the morbidity and high risk of mortality associated with fibrosis. Although clinical trials are on-going, there are currently no

treatments available that can lead to the remission of fibrosis (Ong & Denton, 2010). Analogous to activation of the TGFβ pathway in fibroblasts, activation of the canonical Wnt/β-catenin signalling pathway has also been linked pathogenesis of tissue fibrosis (Wei et al., 2011; Beyer et al., 2012; Akhmetshina et al., 2012). Crosstalk between these two pathways is though to be significant and recently the TGFβ-mediated downregulation of DKK-1, a Wnt signalling antagonist, lead to a supposed canonical Wnt signalling-mediated experimental fibrosis (Akhmetshina et al., 2012).

Thus far, this study has elucidated a mechanism whereby canonical Wnt signalling can become hyperactivated in dermal fibroblasts through the TGFβ-mediated downregulation of AXIN2, a critical component of the canonical Wnt signalling pathway. However, in contrast to previous studies, canonical Wnt signalling hyperactivation in HC fibroblasts, mediated by TGFβ-priming, showed no evidence of increased fibrotic activity beyond that of TGFβ (Figure 8.1A-D). These data support the conventional consensus that TGFβ is a potent mediator of fibrotic activity, increasing profibrotic gene expression and facilitating a fibroblast-mediated increase in 3D collagen gel contractile force generation (Figure 8.1A-D) (Desmoulière et al. 1993; Gabbiani 2003; Ho et al. 2014).

Using a complementary approach, hyperactivation of canonical Wnt signalling was achieved siRNA-mediated *AXIN2* depletion in HC fibroblasts (Figure 8.2A, D). Overall, the data from the AXIN2 depletion model are equivalent to those derived form the TGFβ-primed model of canonical Wnt signalling hyperactivation, showing no increase in profibrotic gene

expression, myofibroblast presence or fibroblast-mediated 3D collagen gel contractile force generation (Figure 8.2A-F). While there was a trend towards a reduced myofibroblasts presence in AXIN2 silenced fibroblasts, it was not considered representative of the phenotype due to the lack of any effect upon α-SMA (mRNA/protein) expression or 3D collagen gels contractile force generation (Figure 8.2D-F).

These data provide additional evidence for the absence of canonical Wnt-induced fibrotic activity. This work extends upon the TGFβ-mediated and AXIN2 depletion models of canonical Wnt signalling hyperactivation, and increases the confidence that canonical Wnt signalling does not induce a fundamental increase in dermal fibroblast fibrotic activity.

These independent methods of investigation are in agreement with a comprehensive study in pulmonary fibroblasts, which indicated that adenoviral overexpression of Wnt-3a or β-catenin was not sufficient to activate markers of fibroblast activation, including *COL1A1*, *α-SMA*, *CTGF* and *TGFβ*, and did not increase fibroblast-mediated 3D collagen gel contractile force (Lam et al. 2011). Instead canonical hyperactivation convincingly increased proliferation demonstrated by bromodeoxyuridine incorporation into newly synthesised DNA (Lam et al. 2011). Furthermore, an earlier study also found that β-catenin overexpression had a minimal effect on 3D collagen gel contraction, instead having a more profound effect on fibroblast motility (Poon et al. 2009). Evidently, studies on proliferation and migratory potential would be of significant interest for the completion of this study.

Of interest, and secondary to the aforementioned hypothesis, was the

observation that AXIN2 depletion, by gene silencing or by TGFβ-priming, could be restored following canonical Wnt agonist treatment, which was also observed in the TGFβ-primed model of canonical signalling hyperactivation (Figure 8.2D Vs. Figure 6.4F). This indicated that the increased canonical Wnt signalling response in fibroblasts, as a result of AXIN2 depletion, could be a transient effect. A possible conclusion could be that where there is a high concentration of Wnt agonists an initial increase in canonical Wnt signalling might have a pronounced downstream consequence but, over time, the system compensates through the increased expression AXIN2. It is possible that temporal peaks in the concentrations of TGFβ and canonical agonists, regulated by the ECM, which might have important implications for fibroblast phenotype.

In addition to the function of AXIN2 in the regulation of canonical Wnt signalling, previous studies have suggested that AXIN expression could act to enhance TGFβ signalling activity. Of note, in HEK293 cells AXIN expression has been described to promote TGFβ signalling activation by forming a complex with SMAD7 and Arkadia; a ubiquitin E3 ligase, which leads to the ubiquitin-mediated proteosomal degradation of the inhibitory SMAD7 protein (Wei et al. 2006). In an alternative model, AXIN expression in COS7 cells was found to be inhibitory, forming an inactivating complex with SMAD3 that was only abolished upon TβRI activation (Furuhashi et al. 2001). Therefore the role of AXIN2 in regulating TGFβ signalling is uncertain and was evaluated using both SMAD- and non-SMAD-dependent TGFβ reporter constructs.

In conflict with both of the described models, TGFβ signalling potential was not modified by AXIN2 silencing in HC fibroblasts, consistent with this observation was the absence of a significant effect upon α-SMA expression, myofibroblasts presence or fibroblast-mediated 3D collagen gel contractile force generation (Figure 8.3A-E). These data indicate that AXIN2 does not regulate TGFβ signalling or its concomitant profibrotic activities, but instead is primarily involved in the regulation of canonical Wnt signalling pathway in dermal fibroblasts.

One consequence of reduced AXIN2 expression would be suboptimal destruction complex assembly that results in a reduced ability to negatively regulate β-catenin-mediated activity. As well as nuclear β-catenin staining in SSc dermal tissue, *in vivo*, the stabilisation of β-catenin has been shown to lead to fibrosis including dermal thickening, increased collagen expression and myofibroblast count (Wei et al., 2011; Akhmetshina et al., 2012; Beyer et al., 2012). In this study, two independent models of canonical (β-catenin-mediated) Wnt signalling hyperactivation, achieved by AXIN2 downregulation/depletion, are not in agreement with these studies (Figure 8.1 & Figure 8.2). Hence, the direct effect of β-catenin inhibition upon profibrotic gene expression and canonical Wnt signalling activity were initially determined using in FH535 (β-catenin) inhibitor experiments.

As expected, FH535 co-treatment inhibited the Wnt-3a-induced induction of canonical Wnt signalling and therefore initially validated the activity of the inhibitor (Figure 8.4A-D). Although Wnt-3a did not induce *COL1A1* or *α-SMA* profibrotic gene expression, FH535-mediated β-catenin inhibition reduced the expression of profibrotic genes below control levels thereby

demonstrating the potential requirement of β-catenin for the basal expression of both genes (Figure 8.4C, D).

Included as a positive control, SMAD3 inhibition produced highly similar results to those produced by β-catenin inhibition, namely the negative regulation of the Wnt-3a-induced canonical signalling activity and a coinciding reduction in basal profibrotic gene expression (Figure 8.4E-H). The effect of SMAD3 inhibition on canonical Wnt signalling was supported by previous data, which demonstrated the requirement of SMAD3 for the efficient activation of the canonical Wnt signalling pathway (Figure 7.5E, F).

Independent of canonical Wnt signalling, both β-catenin and SMAD3 inhibitors consistently reduced the basal expression of *α-SMA* and *COL1A1* expression, further supporting the requirement for both SMAD3 and β-catenin in the regulation of their basal expression (Figure 8.4I-K).

Due to these similarities, it is possible that SMAD3 and β-catenin might function as part of a co-dependent mechanism where the affecting the activity of one will reciprocally affect the other. Suggestively, AXIN2 contains both SMAD3 and β-catenin binding domains and could potentially be an intersecting regulator of such a mechanism (Chia & Costantini 2005).

Overall, these augment the view of canonical Wnt signalling activation and extend upon crosstalk between the TGFβ and canonical Wnt signalling pathways, in this instance intersecting through SMAD3.

In addition to SMAD3 crosstalk with the TGFβ pathway, β-catenin was also

implicated in the regulation of the TGFβ signalling pathway. TGFβ signalling, like canonical Wnt signalling, induced the Wnt-independent nuclear translocation of β-catenin, despite hyperactivation of canonical (β-catenin) Wnt signalling not playing an important role in profibrotic activation thus far (Figure 6.4H). Therefore, the consequences of FH535-mediated β-catenin inhibition upon TGFβ-induced profibrotic activities were subsequently determined.

Following FH535-mediated inhibition of β-catenin, TGFβ-induced profibrotic gene expression was dose-dependently inhibited and, in addition, a reduction in TGFβ-induced 3D collagen gel contractile force generation was also evident (Figure 8.5B-E). Indeed, independent FH535 inhibitor treatment also reduced the normal contractile force generated in 3D collagen gels containing resting HC fibroblasts (Figure 8.5E). These data would support the opinion of other studies that β-catenin is central to TGFβ-mediated profibrotic activity in fibroblasts (Akhmetshina et al., 2012; Beyer et al., 2012; Wei et al., 2012). However, those effects assumed to be mediated by β-catenin inhibition, might act in tandem or as a direct result of inhibition of the PPAR pathway, a known alternative target of this inhibitor, which can similarly regulate TGFβ-responsive profibrotic gene targets (Handeli & Simon, 2008).

To confirm the potential involvement of β-catenin in the regulation of TGFβ-mediated profibrotic activity, further experiments were carried out in HC fibroblasts transfected with *β-catenin* siRNA (siβcat). In contrast to those obtained using the FH535-mediated inhibition, depletion of β-catenin

expression increased the TGFβ-induced expression of α-SMA as well as 3D collagen gel contractile force generation (Figure 8.6A-C). These data indicated that β-catenin can act as a negative regulator of the TGFβ signalling pathway, which conflicts with previous reports that have used β-catenin blockade to inhibit experimental fibrosis (Henderson et al. 2010; Kim et al. 2011; Beyer et al. 2012). Instead these data could be used to indirectly support other studies, which have demonstrated, in contrast to fibrotic activity, an important function in proliferation and/or cell motility (Poon et al., 2009; Lam et al. 2011). However, TGFβ acted to mediate the nuclear translocation of β-catenin despite the absence of β-catenin-mediated TOPFlash canonical Wnt signalling reporter activation (Figure 6.2C, D). One hypothesis could be that TGFβ-mediated β-catenin nuclear translocation is independent of canonical Wnt signalling, which is supported by a recent study that identified a β-catenin-dependent YAP1 and the TBX5 transcription factor complex that was important for the cell survival through the upregulation of antiapoptotic genes (Rosenbluh et al. 2012).

Overall, as two independent models of canonical Wnt signalling hyperactivation were unable to significantly influence fibrotic activity in dermal fibroblasts it is likely that this is not the primary consequence. Evidently, evaluation of canonical Wnt signalling hyperactivation on proliferation, migration and cell survival of dermal fibroblasts would be of significant interest for the completion of this study.

9 Conclusion

In SSc, activation of the Wnt/β-catenin signalling pathway, like TGFβ signalling, has been linked to the fibroblast-mediated pathogenesis of tissue fibrosis and the crosstalk between these pathways is considered to be significant. Extending upon this, explanted SSc fibroblasts displayed a clear and consistent differential increase in canonical Wnt signalling response compared to HCs, and also displayed a concomitant decrease in the basal expression of AXIN2, a critical regulator of this pathway. Suggestively, the mean concentration of SFRP4, a putative Wnt antagonist that is increased in SSc tissues, was higher in those patients positive for the Scl-70 autoantibody, which is associated with the fibrotic diffuse-variant of SSc. Indeed, the increased SFRP4 expression observed could be attributable to the fibroblast lineage and its overexpression indicative of either TGFβ or Wnt signalling activation. Given that SFRP4 can potentially function as a Wnt antagonist, it could conceivably be involved in fibrosis through the regulation of the Wnt pathways; however, full-length recombinant SFRP4 protein did not have a measurable effect on Wnt- or even TGFβ-induced pathways. Likewise, expression of CAV-1, a TGFβ-regulated component of the caveolae endocytotic pathway, which can regulate cell surface receptor expression and is known to be downregulated in a subset of SSc fibroblasts, had no evident utility in profibrotic gene expression or canonical Wnt signalling activity characteristic of SSc fibroblasts in this study.

Notably, this study identifies a new mechanism by which TGFβ mediates the increased canonical Wnt signalling response of fibroblasts to canonical Wnt activation without inducing a direct stimulatory effect. Specifically, TGFβ

mediated the downregulation of AXIN2, a critical component of the β-catenin destruction complex, which was sufficient to confer an increased canonical Wnt signalling amplitude equivalent to that observed in SSc fibroblasts. Primarily, this was due to the TGFβ-mediated increase in the rate of *AXIN2* mRNA decay, potentially regulated at its 3'UTR by ARE-binding proteins. Therefore the increased activation of canonical Wnt signalling observed in SSc skin-resident fibroblasts goes beyond the differential expression of secreted Wnt factors and indicates the importance of TGFβ crosstalk in relation to the intracellular expression of AXIN2. Additionally, SMAD3, a known mediator of TGFβ signalling was required for the efficient activation of canonical Wnt signalling but was independent of this mechanism. This suggests that the increased canonical Wnt/β-catenin signalling observed during fibrosis is a consequence of a TGFβ-primed environment and therefore the development of TGFβ-targeted therapies could potentially resolve the aberrant Wnt/β-catenin signalling observed during fibrosis. Indeed, therapies that target immunological, vascular and fibrotic processes are required for the effective treatment of SSc, although the development of novel anti-fibrotic treatments may be considered a priority given the high risk of mortality associated with fibrosis through internal organ involvement.

However, this study provides evidence that the fundamental consequence of canonical Wnt signalling hyperactivation in dermal fibroblasts is independent of profibrotic activation in two independent models. Therefore further evaluation of processes associated with fibrosis, including proliferation, migration and cell survival, might resolve the anti-fibrotic outcomes observed for therapeutics targeting the Wnt/β-catenin pathway in models of experimental fibrosis.

10 Appendix

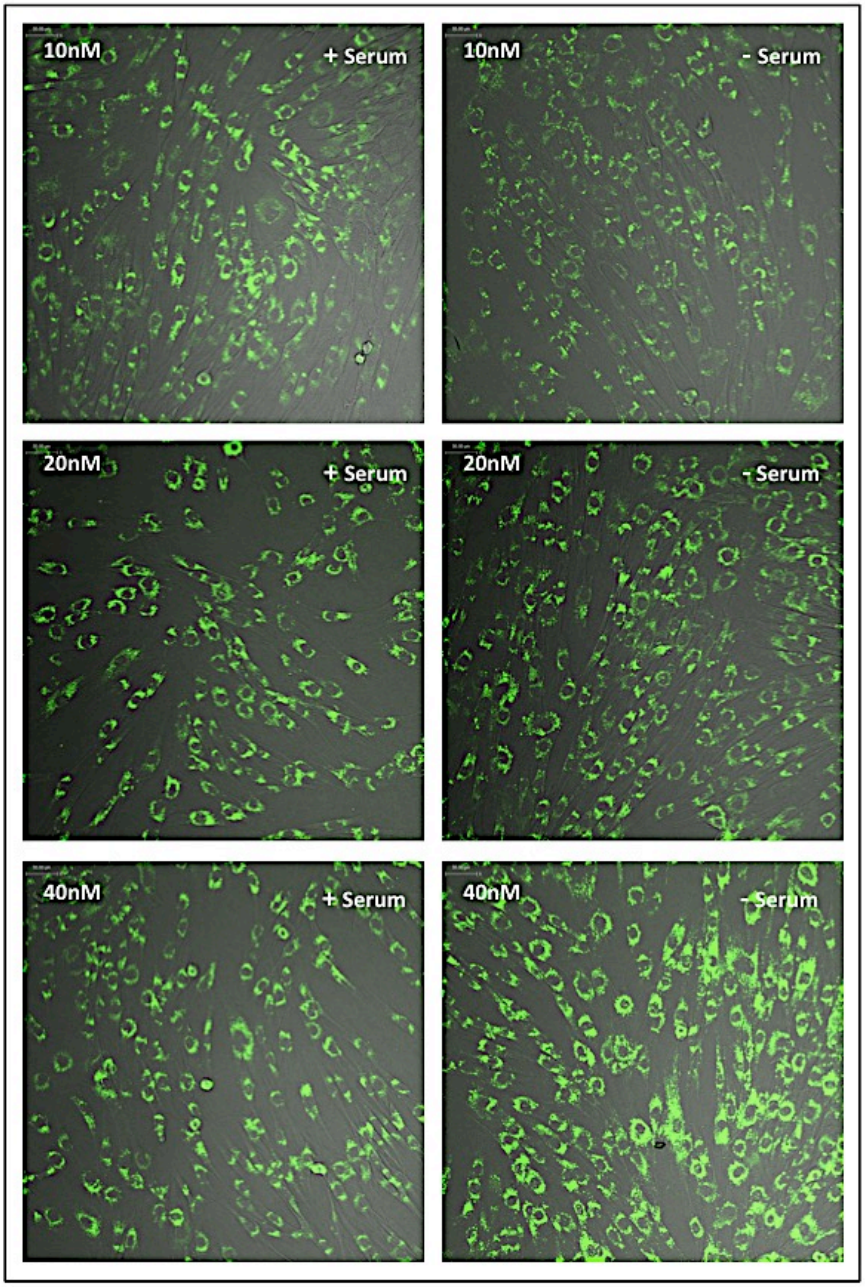

Sup Figure 10.1 siRNA delivery into HC fibroblasts (24 hr)

The AlexaFlour-488 containing oligonucleotide was transfected into HC fibroblasts across at concentrations of 10nM, 20nM and 40nM in the presence and absence of serum. The fluorescent intensity showed a step-wise increase in concentration, which therefore indicated that siRNA transfection across this range could be employed.

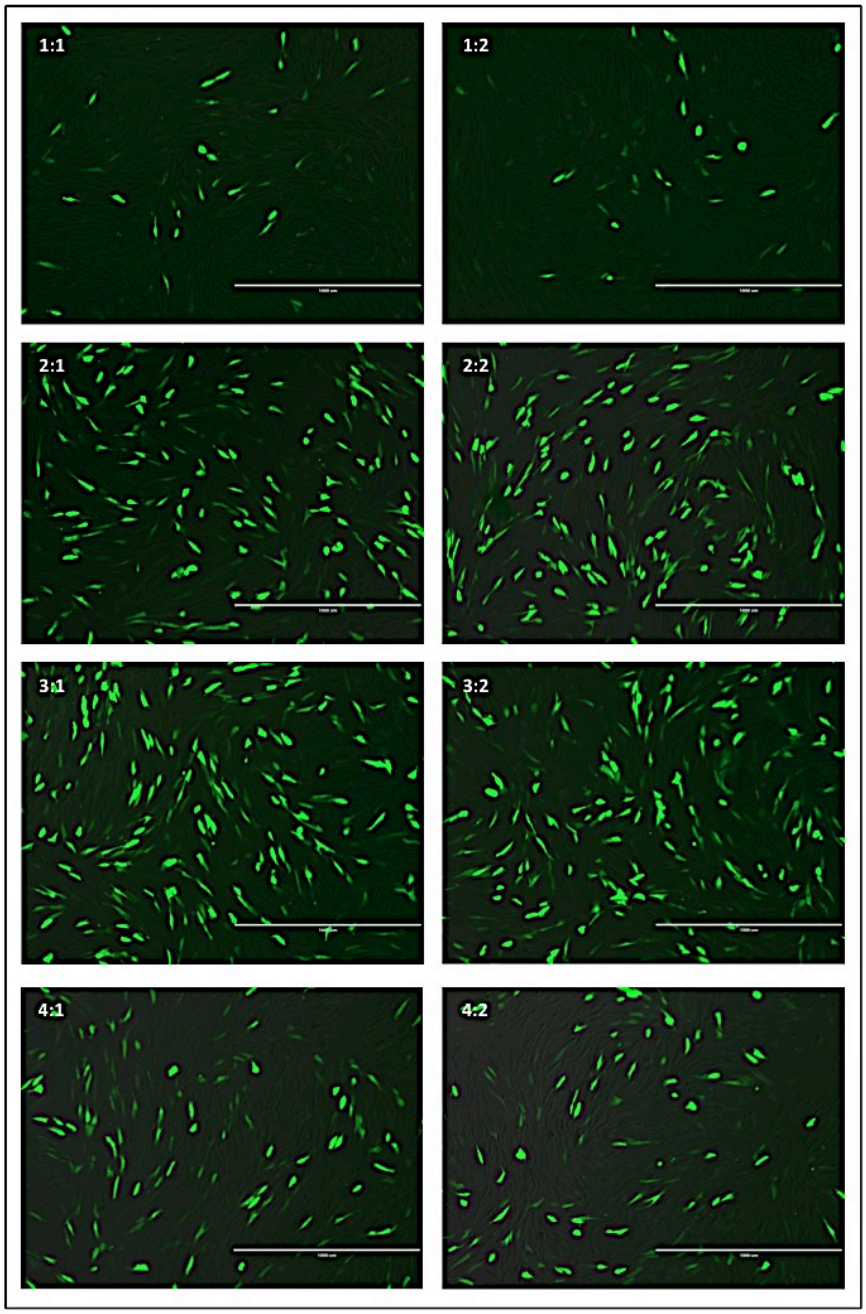

Sup Figure 10.2. Plasmid DNA delivery into HC fibroblasts (24 hr)

Transfection of the IRES-GFP plasmid was used to visualise transfection efficiency at 24 hr post-transfection. Transfection efficiency of HC fibroblasts was determined across with differential combinations of DNA:transfection reagent complexes. At a ratio of 1:1 and 1:2 showed poor transfection efficiency, while efficiency was significantly increased at ratio of 2:1 and 2:2 and at 3:1 and 3:2, which then decreased at higher ratios of 4:1 and 4:2.

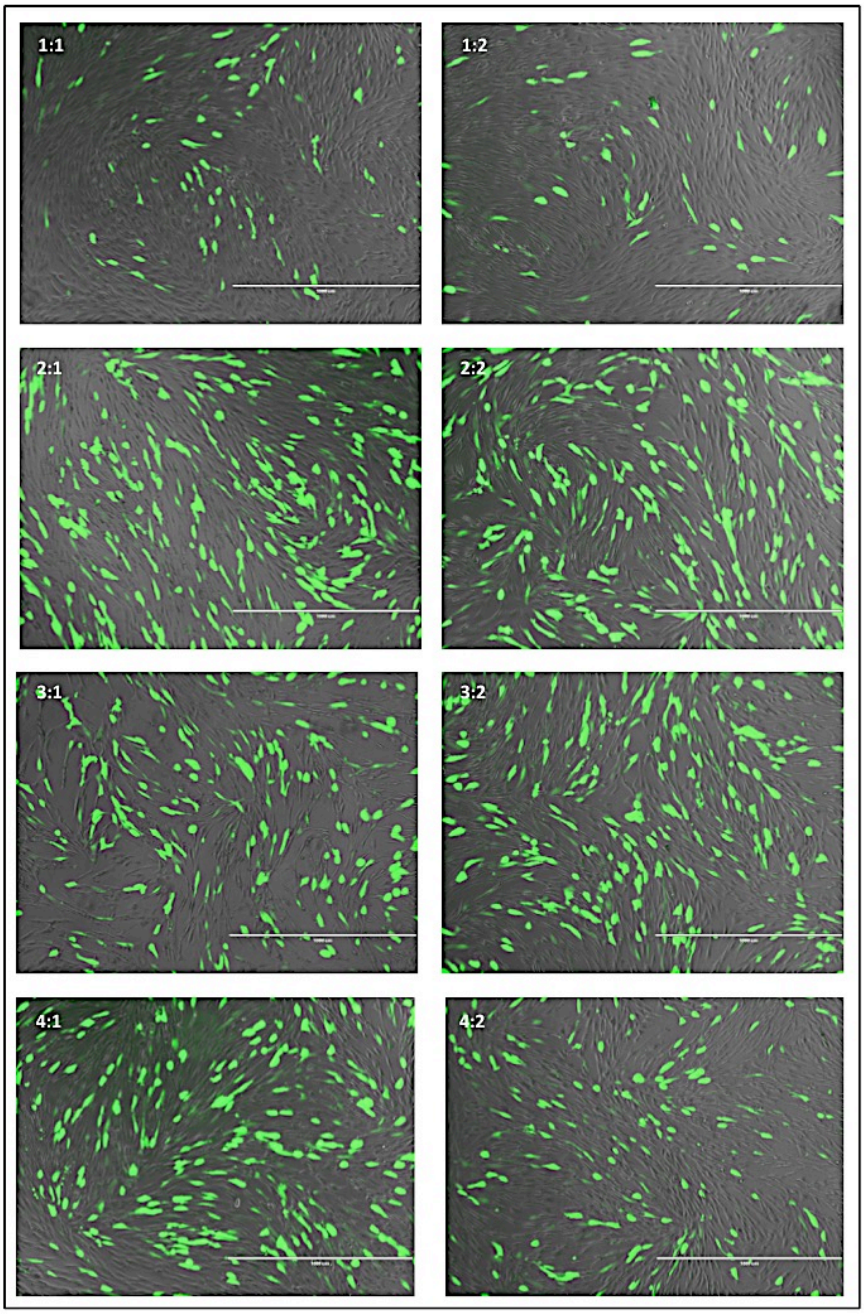

Sup Figure 10.3. Plasmid DNA delivery into HC fibroblasts (48 hr)

48 hr post-transfection of HC fibroblasts with IRES-GFP plasmid. Transfection efficiency was determined across the differential combinations of DNA:transfection reagent complexes. Similar to visualisation at 24 hr, ratios of 1:1 and 1:2 showed poor transfection efficiency, while efficiency was significantly increased at ratio of 2:1 and 2:2 and at 3:1 and 3:2, which then decreased at higher ratios of 4:1 and 4:2.

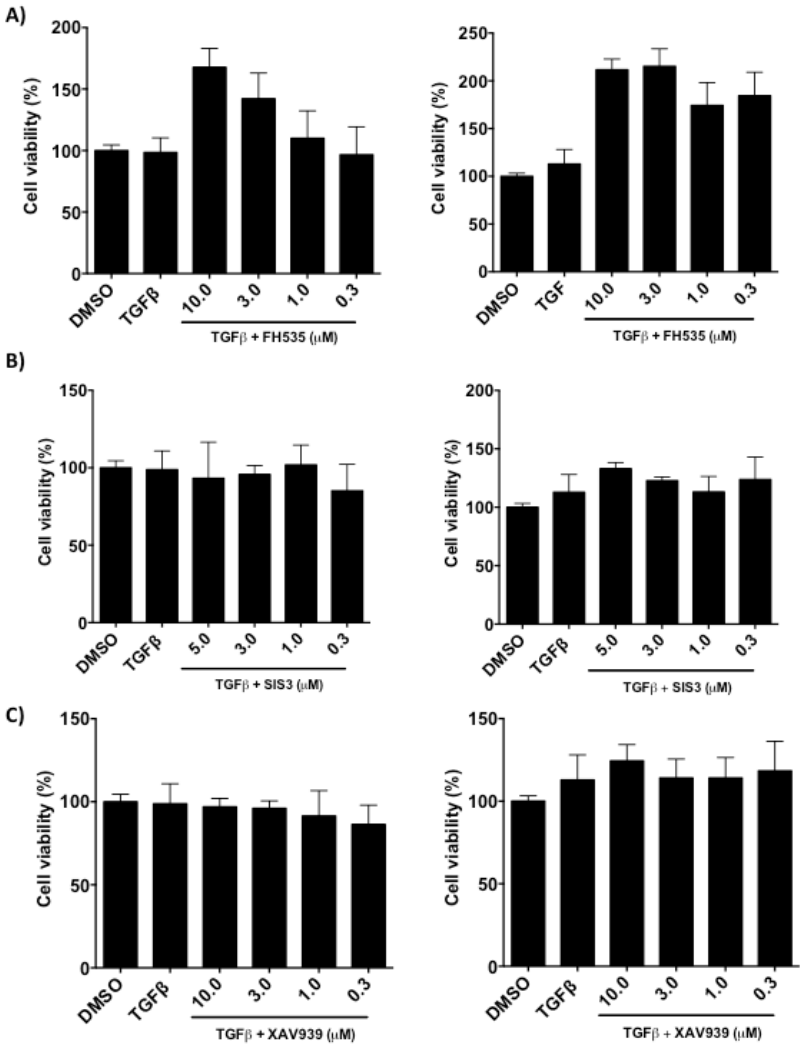

Sup Figure 10.4. MTT fibroblast viability data for small-molecule inhibitors in the presence and absence of TGFβ

HC fibroblasts were treated with TGFβ in the presence or absence of small molecule inhibitors A) FH-535 B) SIS3 and C) XAV-939 at 24 and 72 hr, respectively. MTT cell viability was quantified to determine adverse effects on fibroblast metabolic activity/proliferative potential.

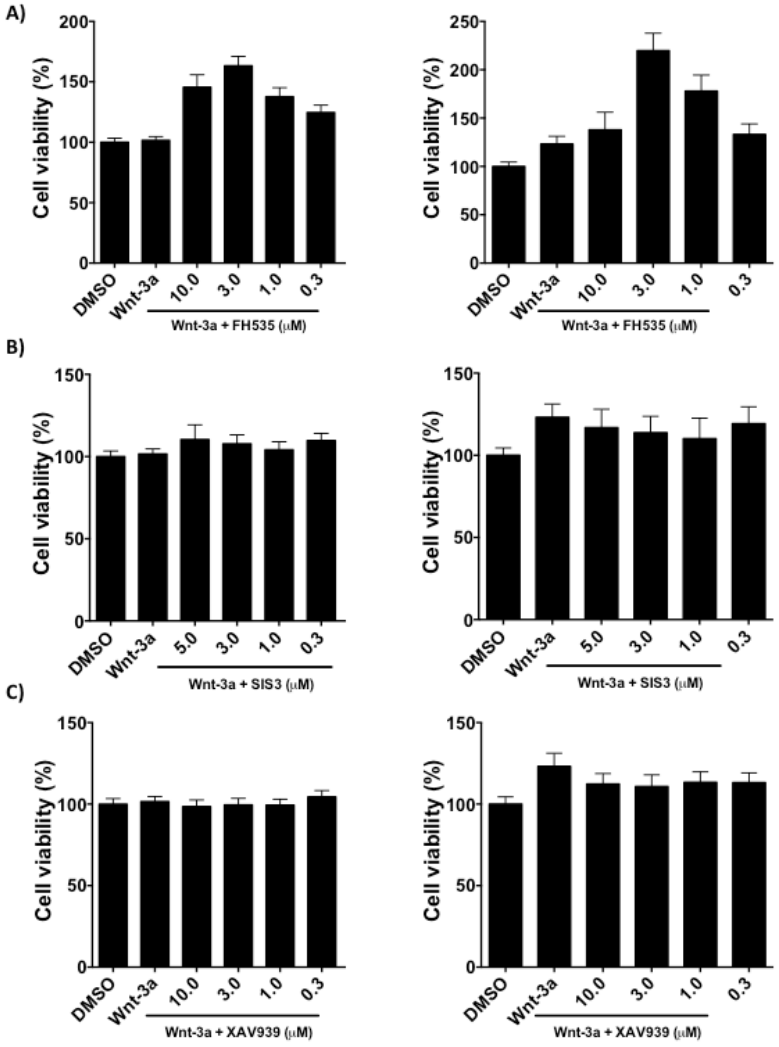

Sup Figure 10.5. MTT fibroblast viability data for small-molecule inhibitors in the presence and absence of Wnt-3a

HC fibroblasts were treated with Wnt-3a in the presence or absence of small molecule inhibitors A) FH-535 B) SIS3 and C) XAV-939 at 24 and 72 hr, respectively. MTT cell viability was quantified to determine adverse effects on fibroblast metabolic activity/proliferative potential.

11 Bibliography

Abraham, D.J., Krieg, T., Distler, J., Distler, O., 2009. Overview of pathogenesis of systemic sclerosis. Rheumatology 48, iii3–7. doi:10.1093/rheumatology/ken481

Akhmetshina, A., Palumbo, K., Dees, C., Bergmann, C., Venalis, P., Zerr, P., Horn, A., Kireva, T., Beyer, C., Zwerina, J., Schneider, H., Sadowski, A., Riener, M.-O., MacDougald, O.A., Distler, O., Schett, G., Distler, J.H.W., 2012. Activation of canonical Wnt signalling is required for TGF-β-mediated fibrosis. Nat. Commun. 3, 735. doi:10.1038/ncomms1734

Akhurst, R.J., Hata, A., 2012. Targeting the TGFβ signalling pathway in disease. Nat. Rev. Drug Discov. 11, 790–811. doi:10.1038/nrd3810

Artlett, C.M., Smith, J.B., Jimenez, S.A., 1998. Identification of Fetal DNA and Cells in Skin Lesions from Women with Systemic Sclerosis. N. Engl. J. Med. 338, 1186–1191. doi:10.1056/NEJM199804233381704

Artlett, C.M., Welsh, K.I., Black, C.M., Jimenez, S.A., 1997. Fetal-maternal HLA compatibility confers susceptibility to systemic sclerosis. Immunogenetics 47, 17–22.

Asano, Y., Ihn, H., Jinnin, M., Tamaki, K., Sato, S., 2011. Altered dynamics of transforming growth factor β (TGF-β) receptors in scleroderma fibroblasts. Ann. Rheum. Dis. 70, 384–387. doi:10.1136/ard.2009.127811

Asano, Y., Ihn, H., Yamane, K., Jinnin, M., Mimura, Y., Tamaki, K., 2005. Involvement of αvβ5 integrin–mediated activation of latent transforming growth factor β1 in autocrine transforming growth factor β signaling in systemic sclerosis fibroblasts. Arthritis Rheum. 52, 2897–2905. doi:10.1002/art.21246

Ask, K., Bonniaud, P., Maass, K., Eickelberg, O., Margetts, P.J., Warburton, D., Groffen, J., Gauldie, J., Kolb, M., 2008. Progressive pulmonary fibrosis is mediated by TGF-beta isoform 1 but not TGF-beta3. Int. J. Biochem. Cell Biol. 40, 484–495. doi:10.1016/j.biocel.2007.08.016

Bányai, L., Patthy, L., 1999. The NTR module: domains of netrins, secreted frizzled related proteins, and type I procollagen C-proteinase enhancer protein are homologous with tissue inhibitors of metalloproteases. Protein Sci. Publ. Protein Soc. 8, 1636–1642.

Bayle, J., Fitch, J., Jacobsen, K., Kumar, R., Lafyatis, R., Lemaire, R., 2008. Increased expression of Wnt2 and SFRP4 in Tsk mouse skin: role of Wnt signaling in altered dermal fibrillin deposition and systemic sclerosis. J. Invest. Dermatol. 128, 871–881. doi:10.1038/sj.jid.5701101

Beanes, S.R., Dang, C., Soo, C., Ting, K., 2003. Skin Repair and Scar Formation: The Central Role of TGF-[beta]. Expert Rev. Mol. Med. 5, 1–22. doi:10.1017/S1462399403005817

Behrens, J., Jerchow, B.A., Würtele, M., Grimm, J., Asbrand, C., Wirtz, R., Kühl, M., Wedlich, D., Birchmeier, W., 1998. Functional interaction of an axin homolog, conductin, with beta-catenin, APC, and GSK3beta. Science 280, 596–599.

Beisang, D., Bohjanen, P.R., 2012. Perspectives on the ARE as it turns 25 years old. Wiley Interdiscip. Rev. RNA 3, 719–731. doi:10.1002/wrna.1125

Bergmann, C., Akhmetshina, A., Dees, C., Palumbo, K., Zerr, P., Beyer, C., Zwerina, J., Distler, O., Schett, G., Distler, J.H.W., 2011. Inhibition of glycogen synthase kinase 3{beta} induces dermal fibrosis by activation of the canonical Wnt pathway. Ann. Rheum. Dis. doi:10.1136/ard.2010.147140

Beyer, C., Distler, O., Distler, J.H.W., 2012a. Innovative antifibrotic therapies in systemic sclerosis. Curr. Opin. Rheumatol. 24, 274–280. doi:10.1097/BOR.0b013e3283524b9a

Beyer, C., Schett, G., Distler, O., Distler, J.H.W., 2010. Animal models of systemic sclerosis: Prospects and limitations. Arthritis Rheum. doi:10.1002/art.27647

Beyer, C., Schramm, A., Akhmetshina, A., Dees, C., Kireva, T., Gelse, K., Sonnylal, S., de Crombrugghe, B., Taketo, M.M., Distler, O., Schett, G., Distler, J.H.W., 2012c. β-catenin is a central mediator of pro-fibrotic Wnt signaling in systemic sclerosis. Ann. Rheum. Dis. 71, 761–767. doi:10.1136/annrheumdis-2011-200568

Blanco, F.F., Sanduja, S., Deane, N.G., Blackshear, P.J., Dixon, D.A., 2014. Transforming Growth Factor Regulates P-Body Formation through Induction of the mRNA Decay Factor Tristetraprolin. Mol. Cell. Biol. 34, 180–195. doi:10.1128/MCB.01020-13

Block, J.A., Sequeira, W., 2001. Raynaud's phenomenon. Lancet 357, 2042–2048. doi:10.1016/S0140-6736(00)05118-7

Bowley, E., Ogorman, D., Gan, B., 2007. β-Catenin Signaling in Fibroproliferative Disease. J. Surg. Res. 138, 141–150. doi:10.1016/j.jss.2006.07.026

Brooks, S.A., Blackshear, P.J., 2013. Tristetraprolin (TTP): Interactions with mRNA and proteins, and current thoughts on mechanisms of action. Biochim. Biophys. Acta BBA - Gene Regul. Mech. 1829, 666–679. doi:10.1016/j.bbagrm.2013.02.003

Broughton, G.I.M.D., Janis, J.E., Attinger, C.E., 2006. Wound Healing: An Overview. [Miscellaneous Article]. Plast. Reconstr. Surg. Curr. Concepts Wound Heal. doi:10.1097/01.prs.0000222562.60260.f9

Brown, J.M., Archer, A.J., Pfau, J.C., Holian, A., 2003. Silica accelerated systemic autoimmune disease in lupus-prone New Zealand mixed mice. Clin. Exp. Immunol. 131, 415–421. doi:10.1046/j.1365-2249.2003.02094.x

Buckley, M.S., Staib, R.L., Wicks, L.M., 2013. Combination therapy in the management of pulmonary arterial hypertension. Int. J. Clin. Pract. Suppl. 13–23. doi:10.1111/ijcp.12136

Cadigan, K.M., Nusse, R., 1997. Wnt signaling: a common theme in animal development. Genes Dev. 11, 3286–3305.

Capozza, F., Trimmer, C., Castello-Cros, R., Katiyar, S., Whitaker-Menezes, D., Follenzi, A., Crosariol, M., Llaverias, G., Sotgia, F., Pestell, R.G., Lisanti, M.P., 2012. Genetic ablation of Cav1 differentially affects melanoma tumor growth and metastasis in mice: role of Cav1 in Shh heterotypic signaling and transendothelial migration. Cancer Res. 72, 2262–2274. doi:10.1158/0008-5472.CAN-11-2593

Carmon, K.S., Loose, D.S., 2008. Secreted Frizzled-Related Protein 4 Regulates Two Wnt7a Signaling Pathways and Inhibits Proliferation in Endometrial Cancer Cells. Mol. Cancer Res. 6, 1017 –1028. doi:10.1158/1541-7786.MCR-08-0039

Carthy, J.M., Garmaroudi, F.S., Luo, Z., McManus, B.M., 2011. Wnt3a Induces Myofibroblast Differentiation by Upregulating TGF-β Signaling Through SMAD2 in a β-Catenin-Dependent Manner. PLoS ONE 6, e19809. doi:10.1371/journal.pone.0019809

Carver, L.A., Schnitzer, J.E., 2003. Caveolae: mining little caves for new cancer targets. Nat. Rev. Cancer 3, 571–581. doi:10.1038/nrc1146

Castor, C.W., Prince, R.K., Dorstewitz, E.L., 1962. Characteristics of human “fibroblasts” cultivated in vitro from different anatomical sites. Lab. Investig. J. Tech. Methods Pathol. 11, 703–713.

Chang, H.Y., Chi, J.-T., Dudoit, S., Bondre, C., van de Rijn, M., Botstein, D., Brown, P.O., 2002. Diversity, topographic differentiation, and positional memory in human fibroblasts. Proc. Natl. Acad. Sci. U. S. A. 99, 12877–12882. doi:10.1073/pnas.162488599

Chen, S., McLean, S., Carter, D.E., Leask, A., 2007a. The gene expression profile induced by Wnt 3a in NIH 3T3 fibroblasts. J. Cell Commun. Signal. 1, 175–183. doi:10.1007/s12079-007-0015-x

Cheon, S.S., Cheah, A.Y.L., Turley, S., Nadesan, P., Poon, R., Clevers, H., Alman, B.A., 2002. beta-Catenin stabilization dysregulates mesenchymal cell proliferation, motility, and invasiveness and causes aggressive fibromatosis and hyperplastic cutaneous wounds. Proc. Natl. Acad. Sci. U. S. A. 99, 6973–6978. doi:10.1073/pnas.102657399

Cheon, S.S., Wei, Q., Gurung, A., Youn, A., Bright, T., Poon, R., Whetstone, H., Guha, A., Alman, B.A., 2006. Beta-catenin regulates wound size and mediates the effect of TGF-beta in cutaneous healing. FASEB J. 20, 692 –701. doi:10.1096/fj.05-4759com

Chia, I.V., Costantini, F., 2005. Mouse axin and axin2/conductin proteins are functionally equivalent in vivo. Mol. Cell. Biol. 25, 4371–4376. doi:10.1128/MCB.25.11.4371-4376.2005

Chong, C.C.W., Stump, R.J.W., Lovicu, F.J., McAvoy, J.W., 2009. TGFβ promotes Wnt expression during cataract development. Exp. Eye Res. 88, 307–313. doi:10.1016/j.exer.2008.07.018

Chrestensen, C.A., Schroeder, M.J., Shabanowitz, J., Hunt, D.F., Pelo, J.W., Worthington, M.T., Sturgill, T.W., 2004. MAPKAP kinase 2 phosphorylates tristetraprolin on in vivo sites including Ser178, a site required for 14-3-3 binding. J. Biol. Chem. 279, 10176–10184. doi:10.1074/jbc.M310486200

Ciani, L., Salinas, P.C., 2007. c-Jun N-terminal kinase (JNK) cooperates with Gsk3β to regulate Dishevelled-mediated microtubule stability. BMC Cell Biol. 8, 27. doi:10.1186/1471-2121-8-27

Cox, T.R., Erler, J.T., 2011. Remodeling and homeostasis of the extracellular matrix: implications for fibrotic diseases and cancer. Dis. Model. Mech. 4, 165–178. doi:10.1242/dmm.004077

Daniels, D.L., Weis, W.I., 2005. β-catenin directly displaces Groucho/TLE repressors from Tcf/Lef in Wnt-mediated transcription activation. Nat. Struct. Mol. Biol. 12, 364–371. doi:10.1038/nsmb912

Dao, D.Y., Yang, X., Chen, D., Zuscik, M., O'Keefe, R.J., 2007. Axin1 and Axin2 Are Regulated by TGF- and Mediate Cross-talk between TGF- and Wnt Signaling Pathways. Ann. N. Y. Acad. Sci. 1116, 82–99. doi:10.1196/annals.1402.082

Deleault, K.M., Skinner, S.J., Brooks, S.A., 2008. Tristetraprolin regulates TNF-alpha mRNA stability via a proteasome dependent mechanism involving the combined action of the ERK and p38 pathways. Mol. Immunol. 45, 13–24. doi:10.1016/j.molimm.2007.05.017

Denton, C.P., Lapadula, G., Mouthon, L., Müller-Ladner, U., 2009. Renal complications and scleroderma renal crisis. Rheumatology 48, iii32–iii35. doi:10.1093/rheumatology/ken483

Denton, C.P., Zheng, B., Evans, L.A., Shi-wen, X., Ong, V.H., Fisher, I., Lazaridis, K., Abraham, D.J., Black, C.M., Crombrugghe, B. de, 2003. Fibroblast-specific Expression of a Kinase-deficient Type II Transforming Growth Factor β (TGFβ) Receptor Leads to Paradoxical Activation of TGFβ Signaling Pathways with Fibrosis in Transgenic Mice. J. Biol. Chem. 278, 25109–25119. doi:10.1074/jbc.M300636200

Derrett-Smith, E.C., Dooley, A., Gilbane, A.J., Trinder, S.L., Khan, K., Baliga, R., Holmes, A.M., Hobbs, A.J., Abraham, D., Denton, C.P., 2013. Endothelial injury in a transforming growth factor β-dependent mouse model of scleroderma induces pulmonary arterial hypertension. Arthritis Rheum. 65, 2928–2939. doi:10.1002/art.38078

Derynck, R., Akhurst, R.J., 2007. Differentiation plasticity regulated by TGF-[beta] family proteins in development and disease. Nat Cell Biol 9, 1000–1004. doi:10.1038/ncb434

Desmoulière, A., Geinoz, A., Gabbiani, F., Gabbiani, G., 1993. Transforming growth factor-beta 1 induces alpha-smooth muscle actin expression in granulation tissue myofibroblasts and in quiescent and growing cultured fibroblasts. J. Cell Biol. 122, 103–111. doi:10.1083/jcb.122.1.103

Dobaczewski, M., Bujak, M., Li, N., Gonzalez-Quesada, C., Mendoza, L.H., Wang, X.-F., Frangogiannis, N.G., 2010. Smad3 signaling critically regulates fibroblast phenotype and function in healing myocardial infarction. Circ. Res. 107, 418–428. doi:10.1161/CIRCRESAHA.109.216101

Dziadzio, M., Smith, R.E., Abraham, D.J., Black, C.M., Denton, C.P., 2005. Circulating levels of active transforming growth factor beta1 are reduced in diffuse cutaneous systemic sclerosis and correlate inversely with the modified Rodnan skin score. Rheumatol. Oxf. Engl. 44, 1518–1524. doi:10.1093/rheumatology/kei088

Eberhardt, W., Doller, A., Akool, E.-S., Pfeilschifter, J., 2007. Modulation of mRNA stability as a novel therapeutic approach. Pharmacol. Ther. 114, 56–73. doi:10.1016/j.pharmthera.2007.01.002

Eisenberg, M.E., Nguyen, B.Y., Karnath, B.M., 2008. Clinical Features of Systemic Sclerosis. Hosp. Physician 33.

Eming, S.A., Krieg, T., Davidson, J.M., 2007. Inflammation in Wound Repair: Molecular and Cellular Mechanisms. J. Invest. Dermatol. 127, 514–525. doi:10.1038/sj.jid.5700701

Endo, Y., Negishi, I., Ishikawa, O., 2002. Possible contribution of microchimerism to the pathogenesis of Sjögren's syndrome. Rheumatol. Oxf. Engl. 41, 490–495.

Esteve, P., Sandonìs, A., Ibañez, C., Shimono, A., Guerrero, I., Bovolenta, P., 2011. Secreted frizzled-related proteins are required for Wnt/β-catenin signalling activation in the vertebrate optic cup. Dev. Camb. Engl. 138, 4179–4184. doi:10.1242/dev.065839

Fagotto, F., Jho, E., Zeng, L., Kurth, T., Joos, T., Kaufmann, C., Costantini, F., 1999. Domains of Axin Involved in Protein-Protein Interactions, Wnt Pathway Inhibition, and Intracellular Localization. J. Cell Biol. 145, 741–756.

Farina, G., Lemaire, R., Pancari, P., Bayle, J., Widom, R.L., Lafyatis, R., 2009. Cartilage oligomeric matrix protein expression in systemic sclerosis reveals heterogeneity of dermal fibroblast responses to transforming growth factor beta. Ann. Rheum. Dis. 68, 435–441. doi:10.1136/ard.2007.086850

Feghali-Bostwick, C., Medsger, T.A., Wright, T.M., 2003. Analysis of systemic sclerosis in twins reveals low concordance for disease and high concordance for the presence of antinuclear antibodies. Arthritis Rheum. 48, 1956–1963. doi:10.1002/art.11173

Frantz, C., Stewart, K.M., Weaver, V.M., 2010. The extracellular matrix at a glance. J. Cell Sci. 123, 4195–4200. doi:10.1242/jcs.023820

Fujimoto, T., Kogo, H., Nomura, R., Une, T., 2000. Isoforms of caveolin-1 and caveolar structure. J. Cell Sci. 113, 3509–3517.

Furuhashi, M., Yagi, K., Yamamoto, H., Furukawa, Y., Shimada, S., Nakamura, Y., Kikuchi, A., Miyazono, K., Kato, M., 2001. Axin Facilitates Smad3 Activation in the Transforming Growth Factor β Signaling Pathway. Mol. Cell. Biol. 21, 5132–5141. doi:10.1128/MCB.21.15.5132-5141.2001

Gabbiani, G., 2003. The myofibroblast in wound healing and fibrocontractive diseases. J. Pathol. 200, 500–503. doi:10.1002/path.1427

Gabrielli, A., Avvedimento, E.V., Krieg, T., 2009. Scleroderma. N. Engl. J. Med. 360, 1989–2003. doi:10.1056/NEJMra0806188

Gabrielli, A., Di Loreto, C., Taborro, R., Candela, M., Sambo, P., Nitti, C., Danieli, M.G., DeLustro, F., Dasch, J.R., Danieli, G., 1993. Immunohistochemical Localization of Intracellular and Extracellular Associated TGFβ in the Skin of Patients with Systemic Sclerosis (Scleroderma) and Primary Raynaud's Phenomenon. Clin. Immunol. Immunopathol. 68, 340–349. doi:10.1006/clin.1993.1136

Galbiati, F., Volonte', D., Brown, A.M.C., Weinstein, D.E., Ben-Ze'ev, A., Pestell, R.G., Lisanti, M.P., 2000. Caveolin-1 Expression Inhibits Wnt/β-Catenin/Lef-1 Signaling by Recruiting β-Catenin to Caveolae Membrane Domains. J. Biol. Chem. 275, 23368–23377. doi:10.1074/jbc.M002020200

Galdo, F.D., Sotgia, F., de Almeida, C., Jasmin, J.-F., Musick, M., Lisanti, M., Jimenez, S.A., 2008. Decreased expression of caveolin-1 in Systemic Sclerosis: crucial role in the pathogenesis of tissue fibrosis. Arthritis Rheum. 58, 2854–2865. doi:10.1002/art.23791

Gao, X., Hannoush, R.N., 2014. Single-cell imaging of Wnt palmitoylation by the acyltransferase porcupine. Nat. Chem. Biol. 10, 61–68. doi:10.1038/nchembio.1392

George, J., Roulot, D., Koteliansky, V.E., Bissell, D.M., 1999. In vivo inhibition of rat stellate cell activation by soluble transforming growth

factor beta type II receptor: a potential new therapy for hepatic fibrosis. Proc. Natl. Acad. Sci. U. S. A. 96, 12719–12724.
Gilbane, A.J., Denton, C.P., Holmes, A.M., 2013a. Scleroderma pathogenesis: a pivotal role for fibroblasts as effector cells. Arthritis Res. Ther. 15, 215. doi:10.1186/ar4230
Gilbane, A.J., Denton, C.P., Holmes, A.M., 2013b. Scleroderma pathogenesis: a pivotal role for fibroblasts as effector cells. Arthritis Res. Ther. 15, 215. doi:10.1186/ar4230
Gillespie, J., Tinazzi, I., Colato, C., Benedetti, F., Biasi, D., Caramaschi, P., Emery, P., Galdo, F.D., 2011. Epithelial cells undergoing epithelial mesenchymal transition (EMT) in systemic sclerosis lack caveolin-1 and modulate WNT signaling in the dermis by secreting SFRP4. Ann. Rheum. Dis. 70, A31–A32. doi:10.1136/ard.2010.149104.18
Gold, L.S., Ward, M.H., Dosemeci, M., De Roos, A.J., 2007. Systemic autoimmune disease mortality and occupational exposures. Arthritis Rheum. 56, 3189–3201. doi:10.1002/art.22880
Gregersen, P.K., Behrens, T.W., 2006. Genetics of autoimmune diseases — disorders of immune homeostasis. Nat. Rev. Genet. 7, 917–928. doi:10.1038/nrg1944
Grumolato, L., Liu, G., Mong, P., Mudbhary, R., Biswas, R., Arroyave, R., Vijayakumar, S., Economides, A.N., Aaronson, S.A., 2010. Canonical and noncanonical Wnts use a common mechanism to activate completely unrelated coreceptors. Genes Dev. 24, 2517–2530. doi:10.1101/gad.1957710
Guglielmo, G.M.D., Roy, C.L., Goodfellow, A.F., Wrana, J.L., 2003. Distinct endocytic pathways regulate TGF-|[beta]| receptor signalling and turnover. Nat. Cell Biol. 5, 410–421. doi:10.1038/ncb975
Gu, L., Zhu, Y.-J., Yang, X., Guo, Z.-J., Xu, W.-B., Tian, X.-L., 2007. Effect of TGF-beta/Smad signaling pathway on lung myofibroblast differentiation. Acta Pharmacol. Sin. 28, 382–391. doi:10.1111/j.1745-7254.2007.00468.x
Guo, X., Ramirez, A., Waddell, D.S., Li, Z., Liu, X., Wang, X.-F., 2008. Axin and GSK3- control Smad3 protein stability and modulate TGF- signaling. Genes Dev. 22, 106–120. doi:10.1101/gad.1590908
Handeli, S., Simon, J.A., 2008. A small-molecule inhibitor of Tcf/beta-catenin signaling down-regulates PPARgamma and PPARdelta activities. Mol. Cancer Ther. 7, 521–529. doi:10.1158/1535-7163.MCT-07-2063
Hart, M.J., de los Santos, R., Albert, I.N., Rubinfeld, B., Polakis, P., 1998. Downregulation of β-catenin by human Axin and its association with the APC tumor suppressor, β-catenin and GSK3β. Curr. Biol. 8, 573–581. doi:10.1016/S0960-9822(98)70226-X
Hassan, G.S., Williams, T.M., Frank, P.G., Lisanti, M.P., 2006. Caveolin-1-deficient aortic smooth muscle cells show cell autonomous abnormalities in proliferation, migration, and endothelin-based signal transduction. Am. J. Physiol. Heart Circ. Physiol. 290, H2393–2401. doi:10.1152/ajpheart.01161.2005
Hayashida, T., Decaestecker, M., Schnaper, H.W., 2003. Cross-talk between ERK MAP kinase and Smad signaling pathways enhances TGF-beta-dependent responses in human mesangial cells. FASEB J. Off. Publ. Fed. Am. Soc. Exp. Biol. 17, 1576–1578. doi:10.1096/fj.03-0037fje

Hayashi, H., Abdollah, S., Qiu, Y., Cai, J., Xu, Y.Y., Grinnell, B.W., Richardson, M.A., Topper, J.N., Gimbrone, M.A., Wrana, J.L., Falb, D., 1997. The MAD-related protein Smad7 associates with the TGFbeta receptor and functions as an antagonist of TGFbeta signaling. Cell 89, 1165–1173.

Henderson, W.R., Chi, E.Y., Ye, X., Nguyen, C., Tien, Y., Zhou, B., Borok, Z., Knight, D.A., Kahn, M., 2010. Inhibition of Wnt/beta-catenin/CREB binding protein (CBP) signaling reverses pulmonary fibrosis. Proc. Natl. Acad. Sci. U. S. A. 107, 14309–14314. doi:10.1073/pnas.1001520107

Hinz, B., 2010. The myofibroblast: Paradigm for a mechanically active cell. J. Biomech. 43, 146–155. doi:10.1016/j.jbiomech.2009.09.020

Hinz, B., Celetta, G., Tomasek, J.J., Gabbiani, G., Chaponnier, C., 2001. Alpha-smooth muscle actin expression upregulates fibroblast contractile activity. Mol. Biol. Cell 12, 2730–2741.

Hinz, B., Phan, S.H., Thannickal, V.J., Galli, A., Bochaton-Piallat, M.-L., Gabbiani, G., 2007. The myofibroblast: one function, multiple origins. Am. J. Pathol. 170, 1807–1816. doi:10.2353/ajpath.2007.070112

Ho, K.T., Reveille, J.D., 2003. The clinical relevance of autoantibodies in scleroderma. Arthritis Res. Ther. 5, 80–93.

Hough, C., Radu, M., Doré, J.J.E., 2012. TGF-Beta Induced Erk Phosphorylation of Smad Linker Region Regulates Smad Signaling. PLoS ONE 7, e42513. doi:10.1371/journal.pone.0042513

Houseley, J., Tollervey, D., 2009. The Many Pathways of RNA Degradation. Cell 136, 763–776. doi:10.1016/j.cell.2009.01.019

Ho, Y.Y., Lagares, D., Tager, A.M., Kapoor, M., 2014. Fibrosis—a lethal component of systemic sclerosis. Nat. Rev. Rheumatol. 10, 390–402. doi:10.1038/nrrheum.2014.53

Huang, C. -l., 2005. Wnt5a Expression Is Associated With the Tumor Proliferation and the Stromal Vascular Endothelial Growth Factor--An Expression in Non-Small-Cell Lung Cancer. J. Clin. Oncol. 23, 8765–8773. doi:10.1200/JCO.2005.02.2871

Huang, F., Chen, Y.-G., 2012. Regulation of TGF-Beta receptor activity. Cell Biosci. 2, 9. doi:10.1186/2045-3701-2-9

Huang, S.-M.A., Mishina, Y.M., Liu, S., Cheung, A., Stegmeier, F., Michaud, G.A., Charlat, O., Wiellette, E., Zhang, Y., Wiessner, S., Hild, M., Shi, X., Wilson, C.J., Mickanin, C., Myer, V., Fazal, A., Tomlinson, R., Serluca, F., Shao, W., Cheng, H., Shultz, M., Rau, C., Schirle, M., Schlegl, J., Ghidelli, S., Fawell, S., Lu, C., Curtis, D., Kirschner, M.W., Lengauer, C., Finan, P.M., Tallarico, J.A., Bouwmeester, T., Porter, J.A., Bauer, A., Cong, F., 2009. Tankyrase inhibition stabilizes axin and antagonizes Wnt signalling. Nature 461, 614–620. doi:10.1038/nature08356

Hu, B., Wu, Z., Phan, S.H., 2003. Smad3 mediates transforming growth factor-beta-induced alpha-smooth muscle actin expression. Am. J. Respir. Cell Mol. Biol. 29, 397–404. doi:10.1165/rcmb.2003-0063OC

Hudson, M., Assayag, D., Caron, M., Fox, B.D., Hirsch, A., Steele, R., Gaudreau-Taillefer, R., Tatibouet, S., Rudski, L., Baron, M., 2013. Comparison of different measures of diffusing capacity for carbon monoxide (DLCO) in systemic sclerosis. Clin. Rheumatol. 32, 1467–1474. doi:10.1007/s10067-013-2301-8

Humbert, M., Morrell, N.W., Archer, S.L., Stenmark, K.R., MacLean, M.R., Lang, I.M., Christman, B.W., Weir, E.K., Eickelberg, O., Voelkel, N.F., Rabinovitch, M., 2004. Cellular and molecular pathobiology of pulmonary arterial hypertension. J. Am. Coll. Cardiol. 43, 13S–24S. doi:10.1016/j.jacc.2004.02.029

Humphreys, B.D., Lin, S.-L., Kobayashi, A., Hudson, T.E., Nowlin, B.T., Bonventre, J.V., Valerius, M.T., McMahon, A.P., Duffield, J.S., 2010. Fate tracing reveals the pericyte and not epithelial origin of myofibroblasts in kidney fibrosis. Am. J. Pathol. 176, 85–97. doi:10.2353/ajpath.2010.090517

Ihn, H., Yamane, K., Kubo, M., Tamaki, K., 2001. Blockade of endogenous transforming growth factor beta signaling prevents up-regulated collagen synthesis in scleroderma fibroblasts: association with increased expression of transforming growth factor beta receptors. Arthritis Rheum. 44, 474–480. doi:10.1002/1529-0131(200102)44:2<474::AID-ANR67>3.0.CO;2-#

Jho, E., Zhang, T., Domon, C., Joo, C.-K., Freund, J.-N., Costantini, F., 2002. Wnt/beta-catenin/Tcf signaling induces the transcription of Axin2, a negative regulator of the signaling pathway. Mol. Cell. Biol. 22, 1172–1183.

Jiang, F., Parsons, C., Stefanovic, B., 2006. Gene expression profile of quiescent and activated rat hepatic stellate cells implicates Wnt signaling pathway in activation. J. Hepatol. 45, 401–409. doi:10.1016/j.jhep.2006.03.016

Jian, H., 2006. Smad3-dependent nuclear translocation of beta-catenin is required for TGF-beta1-induced proliferation of bone marrow-derived adult human mesenchymal stem cells. Genes Dev. 20, 666–674. doi:10.1101/gad.1388806

Jinnin, M., Ihn, H., Tamaki, K., 2006. Characterization of SIS3, a novel specific inhibitor of Smad3, and its effect on transforming growth factor-beta1-induced extracellular matrix expression. Mol. Pharmacol. 69, 597–607. doi:10.1124/mol.105.017483

Joseph, C.G., Darrah, E., Shah, A.A., Skora, A.D., Casciola-Rosen, L.A., Wigley, F.M., Boin, F., Fava, A., Thoburn, C., Kinde, I., Jiao, Y., Papadopoulos, N., Kinzler, K.W., Vogelstein, B., Rosen, A., 2014. Association of the Autoimmune Disease Scleroderma with an Immunologic Response to Cancer. Science 343, 152–157. doi:10.1126/science.1246886

Kaidi, A., Williams, A.C., Paraskeva, C., 2007. Interaction between β-catenin and HIF-1 promotes cellular adaptation to hypoxia. Nat. Cell Biol. 9, 210–217. doi:10.1038/ncb1534

Kang, S., Min, A., Im, S.-A., Song, S.-H., Kim, S.G., Kim, H.-A., Kim, H.-J., Oh, D.-Y., Jong, H.-S., Kim, T.-Y., Bang, Y.-J., 2015. TGF-β Suppresses COX-2 Expression by Tristetraprolin-Mediated RNA Destabilization in A549 Human Lung Cancer Cells. Cancer Res. Treat. Off. J. Korean Cancer Assoc. 47, 101–109. doi:10.4143/crt.2013.192

Kapoun, A.M., Gaspar, N.J., Wang, Y., Damm, D., Liu, Y.-W., O'young, G., Quon, D., Lam, A., Munson, K., Tran, T.-T., Ma, J.Y., Murphy, A., Dugar, S., Chakravarty, S., Protter, A.A., Wen, F.-Q., Liu, X., Rennard, S.I., Higgins, L.S., 2006. Transforming growth factor-beta

receptor type 1 (TGFbetaRI) kinase activity but not p38 activation is required for TGFbetaRI-induced myofibroblast differentiation and profibrotic gene expression. Mol. Pharmacol. 70, 518–531. doi:10.1124/mol.105.021600

Katsumoto, T.R., Whitfield, M.L., Connolly, M.K., 2011. The pathogenesis of systemic sclerosis. Annu. Rev. Pathol. 6, 509–537. doi:10.1146/annurev-pathol-011110-130312

Kawano, Y., Kypta, R., 2003. Secreted antagonists of the Wnt signalling pathway. J. Cell Sci. 116, 2627–2634. doi:10.1242/jcs.00623

Kikuchi, A., Yamamoto, H., Sato, A., 2009. Selective activation mechanisms of Wnt signaling pathways. Trends Cell Biol. 19, 119–129. doi:10.1016/j.tcb.2009.01.003

Kim, K.H., Kim, J.M., Choi, Y.-L., Shin, Y.K., Lee, H., Seong, I.O., Kim, B.K., Chae, S.W., Chung, Y.-S., Kim, S.-H., 2009. Expression of sonic hedgehog signaling molecules in normal, hyperplastic and carcinomatous endometrium. Pathol. Int. 59, 279–287. doi:10.1111/j.1440-1827.2009.02366.x

Kim, S.-H., Turnbull, J., Guimond, S., 2011. Extracellular matrix and cell signalling: the dynamic cooperation of integrin, proteoglycan and growth factor receptor. J. Endocrinol. 209, 139–151. doi:10.1530/JOE-10-0377

Kim, T.H., Kim, S.-H., Seo, J.-Y., Chung, H., Kwak, H.J., Lee, S.-K., Yoon, H.J., Shin, D.H., Park, S.S., Sohn, J.W., 2011a. Blockade of the Wnt/β-catenin pathway attenuates bleomycin-induced pulmonary fibrosis. Tohoku J. Exp. Med. 223, 45–54.

Klingberg, F., Hinz, B., White, E.S., 2013. The myofibroblast matrix: implications for tissue repair and fibrosis. J. Pathol. 229, 298–309. doi:10.1002/path.4104

Ko, K.S., Arora, P.D., Bhide, V., Chen, A., McCulloch, C.A., 2001. Cell-cell adhesion in human fibroblasts requires calcium signaling. J. Cell Sci. 114, 1155–1167.

Krüger, R., Heinrich, R., 2004. Model reduction and analysis of robustness for the Wnt/beta-catenin signal transduction pathway. Genome Inform. Int. Conf. Genome Inform. 15, 138–148.

Kubiczkova, L., Sedlarikova, L., Hajek, R., Sevcikova, S., 2012. TGF-β - an excellent servant but a bad master. J. Transl. Med. 10, 183. doi:10.1186/1479-5876-10-183

Kubo, M., Ihn, H., Yamane, K., Tamaki, K., 2002. Upregulated expression of transforming growth factor-beta receptors in dermal fibroblasts of skin sections from patients with systemic sclerosis. J. Rheumatol. 29, 2558–2564.

Labbe, E., Letamendia, A., Attisano, L., 2000. Association of Smads with lymphoid enhancer binding factor 1/T cell-specific factor mediates cooperative signaling by the transforming growth factor-beta and Wnt pathways. Proc. Natl. Acad. Sci. 97, 8358–8363. doi:10.1073/pnas.150152697

Laeremans, H., Rensen, S.S., Ottenheijm, H.C.J., Smits, J.F.M., Blankesteijn, W.M., 2010. Wnt/frizzled signalling modulates the migration and differentiation of immortalized cardiac fibroblasts. Cardiovasc. Res. 87, 514 –523. doi:10.1093/cvr/cvq067

Lam, A.P., Flozak, A.S., Russell, S., Wei, J., Jain, M., Mutlu, G.M., Budinger, G.R.S., Feghali-Bostwick, C.A., Varga, J., Gottardi, C.J., 2011. Nuclear beta-Catenin Is Increased in Systemic Sclerosis Pulmonary Fibrosis and Promotes Lung Fibroblast Migration and Proliferation. Am. J. Respir. Cell Mol. Biol. 45, 915–922. doi:10.1165/rcmb.2010-0113OC

Lammi, L., Arte, S., Somer, M., Jarvinen, H., Lahermo, P., Thesleff, I., Pirinen, S., Nieminen, P., 2004. Mutations in AXIN2 cause familial tooth agenesis and predispose to colorectal cancer. Am. J. Hum. Genet. 74, 1043–1050. doi:10.1086/386293

Lapébie, P., Borchiellini, C., Houliston, E., 2011a. Dissecting the PCP pathway: One or more pathways?: Does a separate Wnt-Fz-Rho pathway drive morphogenesis? BioEssays 33, 759–768. doi:10.1002/bies.201100023

Laurent, M.N., Blitz, I.L., Hashimoto, C., Rothbächer, U., Cho, K.W., 1997. The Xenopus homeobox gene twin mediates Wnt induction of goosecoid in establishment of Spemann's organizer. Dev. Camb. Engl. 124, 4905–4916.

Leask, A., 2010. Potential Therapeutic Targets for Cardiac Fibrosis TGFβ, Angiotensin, Endothelin, CCN2, and PDGF, Partners in Fibroblast Activation. Circ. Res. 106, 1675–1680. doi:10.1161/CIRCRESAHA.110.217737

Leask, A., Abraham, D.J., 2004. TGF-β signaling and the fibrotic response. FASEB J. 18, 816–827. doi:10.1096/fj.03-1273rev

Leask, A., Abraham, D.J., Finlay, D.R., Holmes, A., Pennington, D., Shi-Wen, X., Chen, Y., Venstrom, K., Dou, X., Ponticos, M., Black, C., Jackman, J.K., Findell, P.R., Connolly, M.K., 2002. Dysregulation of transforming growth factor β signaling in scleroderma: Overexpression of endoglin in cutaneous scleroderma fibroblasts. Arthritis Rheum. 46, 1857–1865. doi:10.1002/art.10333

LeBleu, V.S., Taduri, G., O'Connell, J., Teng, Y., Cooke, V.G., Woda, C., Sugimoto, H., Kalluri, R., 2013. Origin and function of myofibroblasts in kidney fibrosis. Nat. Med. 19, 1047–1053. doi:10.1038/nm.3218

Lee, J.-L., Lin, C.-T., Chueh, L.-L., Chang, C.-J., 2004. Autocrine/Paracrine Secreted Frizzled-related Protein 2 Induces Cellular Resistance to Apoptosis: A POSSIBLE MECHANISM OF MAMMARY TUMORIGENESIS. J. Biol. Chem. 279, 14602–14609. doi:10.1074/jbc.M309008200

LeRoy, E.C., Black, C., Fleischmajer, R., Jablonska, S., Krieg, T., Medsger, T.A., Jr, Rowell, N., Wollheim, F., 1988. Scleroderma (systemic sclerosis): classification, subsets and pathogenesis. J. Rheumatol. 15, 202–205.

Leung, J.Y., Kolligs, F.T., Wu, R., Zhai, Y., Kuick, R., Hanash, S., Cho, K.R., Fearon, E.R., 2002. Activation of AXIN2 expression by beta-catenin-T cell factor. A feedback repressor pathway regulating Wnt signaling. J. Biol. Chem. 277, 21657–21665. doi:10.1074/jbc.M200139200

Levänen, B., Wheelock, A.M., Eklund, A., Grunewald, J., Nord, M., 2011. Increased pulmonary Wnt (wingless/integrated)-signaling in patients with sarcoidosis. Respir. Med. 105, 282–291. doi:10.1016/j.rmed.2010.11.018

Levine, J.H., Moses, H.L., Gold, L.I., Nanney, L.B., 1993. Spatial and temporal patterns of immunoreactive transforming growth factor beta 1, beta 2, and beta 3 during excisional wound repair. Am. J. Pathol. 143, 368–380.

Leyns, L., Bouwmeester, T., Kim, S.-H., Piccolo, S., De Robertis, E.M., 1997. Frzb-1 Is a Secreted Antagonist of Wnt Signaling Expressed in the Spemann Organizer. Cell 88, 747–756. doi:10.1016/S0092-8674(00)81921-2

Liang, H., Chen, Q., Coles, A.H., Anderson, S.J., Pihan, G., Bradley, A., Gerstein, R., Jurecic, R., Jones, S.N., 2003. Wnt5a inhibits B cell proliferation and functions as a tumor suppressor in hematopoietic tissue. Cancer Cell 4, 349–360. doi:10.1016/S1535-6108(03)00268-X

Li, C., Bapat, B., Alman, B.A., 1998. Adenomatous polyposis coli gene mutation alters proliferation through its beta-catenin-regulatory function in aggressive fibromatosis (desmoid tumor). Am. J. Pathol. 153, 709–714.

Li, S., Couet, J., Lisanti, M.P., 1996. Src tyrosine kinases, Galpha subunits, and H-Ras share a common membrane-anchored scaffolding protein, caveolin. Caveolin binding negatively regulates the auto-activation of Src tyrosine kinases. J. Biol. Chem. 271, 29182–29190.

Li, T.-F., Chen, D., Wu, Q., Chen, M., Sheu, T., Schwarz, E.M., Drissi, H., Zuscik, M., O'Keefe, R.J., 2006. Transforming Growth Factor-β Stimulates Cyclin D1 Expression through Activation of β-Catenin Signaling in Chondrocytes. J. Biol. Chem. 281, 21296–21304. doi:10.1074/jbc.M600514200

Liu, C., Li, Y., Semenov, M., Han, C., Baeg, G.-H., Tan, Y., Zhang, Z., Lin, X., He, X., 2002a. Control of β-Catenin Phosphorylation/Degradation by a Dual-Kinase Mechanism. Cell 108, 837–847. doi:10.1016/S0092-8674(02)00685-2

Liu, W., Dong, X., Mai, M., Seelan, R.S., Taniguchi, K., Krishnadath, K.K., Halling, K.C., Cunningham, J.M., Qian, C., Christensen, E., Roche, P.C., Smith, D.I., Thibodeau, S.N., 2000. Mutations in AXIN2 cause colorectal cancer with defective mismatch repair by activating β-catenin/TCF signalling. Nat. Genet. 26, 146–147. doi:10.1038/79859

Liu, W., Rui, H., Wang, J., Lin, S., He, Y., Chen, M., Li, Q., Ye, Z., Zhang, S., Chan, S.C., Chen, Y.-G., Han, J., Lin, S.-C., 2006. Axin is a scaffold protein in TGF-beta signaling that promotes degradation of Smad7 by Arkadia. EMBO J. 25, 1646–1658. doi:10.1038/sj.emboj.7601057

Lopez-Rios, J., Esteve, P., Ruiz, J.M., Bovolenta, P., 2008. The Netrin-related domain of Sfrp1 interacts with Wnt ligands and antagonizes their activity in the anterior neural plate. Neural Develop. 3, 19. doi:10.1186/1749-8104-3-19

Lukashev, M.E., Werb, Z., 1998. ECM signalling: orchestrating cell behaviour and misbehaviour. Trends Cell Biol. 8, 437–441. doi:10.1016/S0962-8924(98)01362-2

Luna-Ulloa, L.B., Hernández-Maqueda, J.G., Castañeda-Patlán, M.C., Robles-Flores, M., 2011. Protein kinase C in Wnt signaling: implications in cancer initiation and progression. IUBMB Life 63, 915–921. doi:10.1002/iub.559

Luo, W., Lin, S.-C., 2004. Axin: a master scaffold for multiple signaling pathways. Neurosignals 13, 99–113. doi:10.1159/000076563

Lu, P., Takai, K., Weaver, V.M., Werb, Z., 2011. Extracellular Matrix Degradation and Remodeling in Development and Disease. Cold Spring Harb. Perspect. Biol. 3. doi:10.1101/cshperspect.a005058

Marderosian, M., Sharma, A., Funk, A.P., Vartanian, R., Masri, J., Jo, O.D., Gera, J.F., 2006. Tristetraprolin regulates Cyclin D1 and c-Myc mRNA stability in response to rapamycin in an Akt-dependent manner via p38 MAPK signaling. Oncogene 25, 6277–6290. doi:10.1038/sj.onc.1209645

Martires, K.J., Baird, K., Steinberg, S.M., Grkovic, L., Joe, G.O., Williams, K.M., Mitchell, S.A., Datiles, M., Hakim, F.T., Pavletic, S.Z., Cowen, E.W., 2011. Sclerotic-type chronic GVHD of the skin: clinical risk factors, laboratory markers, and burden of disease. Blood 118, 4250–4257. doi:10.1182/blood-2011-04-350249

Massagué, J., Seoane, J., Wotton, D., 2005. Smad transcription factors. Genes Dev. 19, 2783–2810. doi:10.1101/gad.1350705

Mazumdar, J., O'Brien, W.T., Johnson, R.S., LaManna, J.C., Chavez, J.C., Klein, P.S., Simon, M.C., 2010. O2 regulates stem cells through Wnt/β-catenin signalling. Nat. Cell Biol. 12, 1007–1013. doi:10.1038/ncb2102

Mazzoni, S.M., Fearon, E.R., 2014. AXIN1 and AXIN2 variants in gastrointestinal cancers. Cancer Lett. 355, 1–8. doi:10.1016/j.canlet.2014.09.018

McCrea, P.D., Turck, C.W., Gumbiner, B., 1991. A homolog of the armadillo protein in Drosophila (plakoglobin) associated with E-cadherin. Science 254, 1359–1361.

Melkonyan, H.S., Chang, W.C., Shapiro, J.P., Mahadevappa, M., Fitzpatrick, P.A., Kiefer, M.C., Tomei, L.D., Umansky, S.R., 1997. SARPs: A family of secreted apoptosis-related proteins. Proc. Natl. Acad. Sci. 94, 13636 –13641.

Mestas, J., Hughes, C.C.W., 2004. Of mice and not men: differences between mouse and human immunology. J. Immunol. Baltim. Md 1950 172, 2731–2738.

Milano, A., Pendergrass, S.A., Sargent, J.L., George, L.K., McCalmont, T.H., Connolly, M.K., Whitfield, M.L., 2008. Molecular subsets in the gene expression signatures of scleroderma skin. PloS One 3, e2696. doi:10.1371/journal.pone.0002696

Mimura, Y., Ihn, H., Jinnin, M., Asano, Y., Yamane, K., Tamaki, K., 2005. Constitutive thrombospondin-1 overexpression contributes to autocrine transforming growth factor-beta signaling in cultured scleroderma fibroblasts. Am. J. Pathol. 166, 1451–1463.

Moinzadeh, P., Fonseca, C., Hellmich, M., Shah, A.A., Chighizola, C., Denton, C.P., Ong, V.H., 2014. Association of anti-RNA polymerase III autoantibodies and cancer in scleroderma. Arthritis Res. Ther. 16, R53. doi:10.1186/ar4486

Mori, L., Bellini, A., Stacey, M.A., Schmidt, M., Mattoli, S., 2005. Fibrocytes contribute to the myofibroblast population in wounded skin and originate from the bone marrow. Exp. Cell Res. 304, 81–90. doi:10.1016/j.yexcr.2004.11.011

Morin, P.J., Sparks, A.B., Korinek, V., Barker, N., Clevers, H., Vogelstein, B., Kinzler, K.W., 1997. Activation of beta-catenin-Tcf signaling in colon

cancer by mutations in beta-catenin or APC. Science 275, 1787–1790.

Morrone, S., Cheng, Z., Moon, R.T., Cong, F., Xu, W., 2012. Crystal structure of a Tankyrase-Axin complex and its implications for Axin turnover and Tankyrase substrate recruitment. Proc. Natl. Acad. Sci. U. S. A. 109, 1500–1505. doi:10.1073/pnas.1116618109

Moulin, V., Tam, B.Y., Castilloux, G., Auger, F.A., O'Connor-McCourt, M.D., Philip, A., Germain, L., 2001. Fetal and adult human skin fibroblasts display intrinsic differences in contractile capacity. J. Cell. Physiol. 188, 211–222. doi:10.1002/jcp.1110

Muley, A., Majumder, S., Kolluru, G.K., Parkinson, S., Viola, H., Hool, L., Arfuso, F., Ganss, R., Dharmarajan, A., Chatterjee, S., 2010. Secreted Frizzled-Related Protein 4. Am. J. Pathol. 176, 1505–1516. doi:10.2353/ajpath.2010.090465

Nakajima, H., Ito, M., Morikawa, Y., Komori, T., Fukuchi, Y., Shibata, F., Okamoto, S., Kitamura, T., 2009. Wnt modulators, SFRP-1, and SFRP-2 are expressed in osteoblasts and differentially regulate hematopoietic stem cells. Biochem. Biophys. Res. Commun. 390, 65–70. doi:10.1016/j.bbrc.2009.09.067

Nemoto, S., Xiang, J., Huang, S., Lin, A., 1998. Induction of apoptosis by SB202190 through inhibition of p38beta mitogen-activated protein kinase. J. Biol. Chem. 273, 16415–16420.

Nihtyanova, S.I., Denton, C.P., 2010. Autoantibodies as predictive tools in systemic sclerosis. Nat. Rev. Rheumatol. 6, 112–116. doi:10.1038/nrrheum.2009.238

Nishita, M., Hashimoto, M.K., Ogata, S., Laurent, M.N., Ueno, N., Shibuya, H., Cho, K.W.Y., 2000. Interaction between Wnt and TGF-β signalling pathways during formation of Spemann's organizer. Nature 403, 781–785. doi:10.1038/35001602

Ogawa, K., Chen, F., Kim, Y.-J., Chen, Y., 2003. Transcriptional Regulation of Tristetraprolin by Transforming Growth Factor- in Human T Cells. J. Biol. Chem. 278, 30373–30381. doi:10.1074/jbc.M304856200

Ong, V.H., Denton, C.P., 2010. Innovative therapies for systemic sclerosis. Curr. Opin. Rheumatol. 22, 264–272. doi:10.1097/BOR.0b013e328337c3d6

Otranto, M., Sarrazy, V., Bonte, F., Hinz, B., Gabbiani, G., Desmouliere, A., 2012. The role of the myofibroblast in tumor stroma remodeling. Cell Adhes. Migr. 6, 203–219. doi:10.4161/cam.20377

Park, D.S., Cohen, A.W., Frank, P.G., Razani, B., Lee, H., Williams, T.M., Chandra, M., Shirani, J., De Souza, A.P., Tang, B., Jelicks, L.A., Factor, S.M., Weiss, L.M., Tanowitz, H.B., Lisanti, M.P., 2003. Caveolin-1 null (-/-) mice show dramatic reductions in life span. Biochemistry (Mosc.) 42, 15124–15131. doi:10.1021/bi0356348

Penn, H., Howie, A. j., Kingdon, E. j., Bunn, C. c., Stratton, R. j., Black, C. m., Burns, A., Denton, C. p., 2007. Scleroderma renal crisis: patient characteristics and long-term outcomes. QJM 100, 485–494. doi:10.1093/qjmed/hcm052

Perry-III, W.L., Vasicek, T.J., Lee, J.J., Rossi, J.M., Zeng, L., Zhang, T., Tilghman, S.M., Costantini, F., 1995. Phenotypic and Molecular Analysis of a Transgenic Insertional Allele of the Mouse Fused Locus. Genetics 141, 321–332.

Pfau, J.C., Serve, K.M., Noonan, C.W., 2014. Autoimmunity and Asbestos Exposure. Autoimmune Dis. 2014. doi:10.1155/2014/782045

Phelan, C.M., Borg, A., Cuny, M., Crichton, D.N., Baldersson, T., Andersen, T.I., Caligo, M.A., Lidereau, R., Lindblom, A., Seitz, S., Kelsell, D., Hamann, U., Rio, P., Thorlacius, S., Papp, J., Olah, E., Ponder, B., Bignon, Y.J., Scherneck, S., Barkardottir, R., Borresen-Dale, A.L., Eyfjörd, J., Theillet, C., Thompson, A.M., Larsson, C., 1998. Consortium study on 1280 breast carcinomas: allelic loss on chromosome 17 targets subregions associated with family history and clinical parameters. Cancer Res. 58, 1004–1012.

Piera-Velazquez, S., Li, Z., Jimenez, S.A., 2011. Role of Endothelial-Mesenchymal Transition (EndoMT) in the Pathogenesis of Fibrotic Disorders. Am. J. Pathol. 179, 1074–1080. doi:10.1016/j.ajpath.2011.06.001

Poon, R., Nik, S.A., Ahn, J., Slade, L., Alman, B.A., 2009. Beta-catenin and transforming growth factor beta have distinct roles regulating fibroblast cell motility and the induction of collagen lattice contraction. BMC Cell Biol. 10, 38. doi:10.1186/1471-2121-10-38

Qian, D., Jones, C., Rzadzinska, A., Mark, S., Zhang, X., Steel, K.P., Dai, X., Chen, P., 2007. Wnt5a functions in planar cell polarity regulation in mice. Dev. Biol. 306, 121–133. doi:10.1016/j.ydbio.2007.03.011

Quillinan, N.P., Denton, C.P., 2009. Disease-modifying treatment in systemic sclerosis: current status. Curr. Opin. Rheumatol. 21, 636–641. doi:10.1097/BOR.0b013e3283310d57

Radstake, T.R.D.J., Gorlova, O., Rueda, B., Martin, J.-E., Alizadeh, B.Z., Palomino-Morales, R., Coenen, M.J., Vonk, M.C., Voskuyl, A.E., Scheurwegh, A.J., Broen, J.C., van Riel, P.L.C.M., van 't Slot, R., Italiaander, A., Ophoff, R.A., Riemekasten, G., Hunzelmann, N., Simeon, C.P., Ortego-Centeno, N., Gonzalez-Gay, M.A., Gonzalez-Escribano, M.F., Airo, P., van Laar, J., Herrick, A., Worthington, J., Hesselstrand, R., Smith, V., de Keyser, F., Houssiau, F., Chee, M.M., Madhok, R., Shiels, P., Westhovens, R., Kreuter, A., Kiener, H., de Baere, E., Witte, T., Padykov, L., Klareskog, L., Beretta, L., Scorza, R., Lie, B.A., Hoffman-Vold, A.-M., Carreira, P., Varga, J., Hinchcliff, M., Gregersen, P., Lee, A.T., Ying, J., Han, Y., Weng, S.-F., Amos, C.I., Wigley, F.M., Hummers, L., Nelson, J.L., Agarwal, S.K., Assassi, S., Gourh, P., Tan, F.K., Koeleman, B.P.C., Arnett, F.C., Martin, J., Mayes, M.D., 2010. Genome-wide association study of systemic sclerosis identifies CD247 as a novel susceptibility locus. Nat. Genet. 42, 426–429. doi:10.1038/ng.565

Rao, D.D., Vorhies, J.S., Senzer, N., Nemunaitis, J., 2009. siRNA vs. shRNA: Similarities and differences. Adv. Drug Deliv. Rev. 61, 746–759. doi:10.1016/j.addr.2009.04.004

Razani, B., Engelman, J.A., Wang, X.B., Schubert, W., Zhang, X.L., Marks, C.B., Macaluso, F., Russell, R.G., Li, M., Pestell, R.G., Di Vizio, D., Hou, H., Kneitz, B., Lagaud, G., Christ, G.J., Edelmann, W., Lisanti, M.P., 2001. Caveolin-1 null mice are viable but show evidence of hyperproliferative and vascular abnormalities. J. Biol. Chem. 276, 38121–38138. doi:10.1074/jbc.M105408200

Razani, B., Zhang, X.L., Bitzer, M., Von Gersdorff, G., Böttinger, E.P., Lisanti, M.P., 2001. Caveolin-1 Regulates Transforming Growth

Factor (TGF)-B/SMAD Signaling Through an Interaction with the TGF-B Type I Receptor. J. Biol. Chem. 276, 6727–6738. doi:10.1074/jbc.M008340200

Roberts, A.B., Sporn, M.B., 1992. Differential expression of the TGF-beta isoforms in embryogenesis suggests specific roles in developing and adult tissues. Mol. Reprod. Dev. 32, 91–98. doi:10.1002/mrd.1080320203

Rodnan, G.P., Benedek, T.G., Medsger, J. Thomas A., Cammarata, R.J., 1967. The Association of Progressive Systemic Sclerosis (Scleroderma) with Coal Miners' Pneumoconiosis and Other Forms of Silicosis. Ann. Intern. Med. 66, 323–334. doi:10.7326/0003-4819-66-2-323

Rodnan, G.P., Lipinski, E., Luksick, J., 1979. Skin thickness and collagen content in progressive systemic sclerosis and localized scleroderma. Arthritis Rheum. 22, 130–140.

Roose, J., Molenaar, M., Peterson, J., Hurenkamp, J., Brantjes, H., Moerer, P., van de Wetering, M., Destrée, O., Clevers, H., 1998. The Xenopus Wnt effector XTcf-3 interacts with Groucho-related transcriptional repressors. Nature 395, 608–612. doi:10.1038/26989

Rosenbluh, J., Nijhawan, D., Cox, A.G., Li, X., Neal, J.T., Schafer, E.J., Zack, T.I., Wang, X., Tsherniak, A., Schinzel, A.C., Shao, D.D., Schumacher, S.E., Weir, B.A., Vazquez, F., Cowley, G.S., Root, D.E., Mesirov, J.P., Beroukhim, R., Kuo, C.J., Goessling, W., Hahn, W.C., 2012. β-Catenin-driven cancers require a YAP1 transcriptional complex for survival and tumorigenesis. Cell 151, 1457–1473. doi:10.1016/j.cell.2012.11.026

Rubinfeld, B., Robbins, P., El-Gamil, M., Albert, I., Porfiri, E., Polakis, P., 1997. Stabilization of beta-catenin by genetic defects in melanoma cell lines. Science 275, 1790–1792.

Rubio-Rivas, M., Royo, C., Simeón, C.P., Corbella, X., Fonollosa, V., 2014. Mortality and survival in systemic sclerosis: systematic review and meta-analysis. Semin. Arthritis Rheum. 44, 208–219. doi:10.1016/j.semarthrit.2014.05.010

Russell, S.B., Russell, J.D., Trupin, K.M., Gayden, A.E., Opalenik, S.R., Nanney, L.B., Broquist, A.H., Raju, L., Williams, S.M., 2010. Epigenetically altered wound healing in keloid fibroblasts. J. Invest. Dermatol. 130, 2489–2496. doi:10.1038/jid.2010.162

Sakanaka, C., Weiss, J.B., Williams, L.T., 1998. Bridging of beta-catenin and glycogen synthase kinase-3beta by axin and inhibition of beta-catenin-mediated transcription. Proc. Natl. Acad. Sci. U. S. A. 95, 3020–3023.

Salic, A., Lee, E., Mayer, L., Kirschner, M.W., 2000. Control of β-Catenin Stability: Reconstitution of the Cytoplasmic Steps of the Wnt Pathway in Xenopus Egg Extracts. Mol. Cell 5, 523–532. doi:10.1016/S1097-2765(00)80446-3

Sargent, J.L., Milano, A., Bhattacharyya, S., Varga, J., Connolly, M.K., Chang, H.Y., Whitfield, M.L., 2009b. A TGFβ-Responsive Gene Signature Is Associated with a Subset of Diffuse Scleroderma with Increased Disease Severity. J. Invest. Dermatol. 130, 694–705. doi:10.1038/jid.2009.318

Schaller, M.D., 2010. Cellular functions of FAK kinases: insight into molecular mechanisms and novel functions. J. Cell Sci. 123, 1007–1013. doi:10.1242/jcs.045112

Schoenberg, D.R., Maquat, L.E., 2012. Regulation of cytoplasmic mRNA decay. Nat. Rev. Genet. doi:10.1038/nrg3160

Schor, S.L., Schor, A.M., Rushton, G., Smith, L., 1985. Adult, foetal and transformed fibroblasts display different migratory phenotypes on collagen gels: evidence for an isoformic transition during foetal development. J. Cell Sci. 73, 221–234.

Schubert, W., Sotgia, F., Cohen, A.W., Capozza, F., Bonuccelli, G., Bruno, C., Minetti, C., Bonilla, E., DiMauro, S., Lisanti, M.P., 2007. Caveolin-1(−/−)- and Caveolin-2(−/−)-Deficient Mice Both Display Numerous Skeletal Muscle Abnormalities, with Tubular Aggregate Formation. Am. J. Pathol. 170, 316–333. doi:10.2353/ajpath.2007.060687

Sfikakis, P.P., McCune, B.K., Tsokos, M., Aroni, K., Vayiopoulos, G., Tsokos, G.C., 1993. Immunohistological Demonstration of Transforming Growth Factor-β Isoforms in the Skin of Patients with Systemic Sclerosis. Clin. Immunol. Immunopathol. 69, 199–204. doi:10.1006/clin.1993.1170

Shand, L., Lunt, M., Nihtyanova, S., Hoseini, M., Silman, A., Black, C.M., Denton, C.P., 2007. Relationship between change in skin score and disease outcome in diffuse cutaneous systemic sclerosis: application of a latent linear trajectory model. Arthritis Rheum. 56, 2422–2431. doi:10.1002/art.22721

Shi, M., Zhu, J., Wang, R., Chen, X., Mi, L., Walz, T., Springer, T.A., 2011. Latent TGF-β structure and activation. Nature 474, 343–349. doi:10.1038/nature10152

Sivova, N., Launay, D., WÃ©meau-Stervinou, L., De Groote, P., Remy-Jardin, M., Denis, G., Lambert, M., Lamblin, N., Morell-Dubois, S., Fertin, M., Lefevre, G., Sobanski, V., Le Rouzic, O., Hatron, P.-Y., Wallaert, B., Hachulla, E., Perez, T., 2013. Relevance of Partitioning DLCO to Detect Pulmonary Hypertension in Systemic Sclerosis. PLoS ONE 8, e78001. doi:10.1371/journal.pone.0078001

Slusarski, D.C., Yang-Snyder, J., Busa, W.B., Moon, R.T., 1997. Modulation of embryonic intracellular Ca2+ signaling by Wnt-5A. Dev. Biol. 182, 114–120. doi:10.1006/dbio.1996.8463

Smith, E.A., LeRoy, E.C., 1990. A possible role for transforming growth factor-beta in systemic sclerosis. J. Invest. Dermatol. 95, 125S–127S.

Sonnylal, S., Denton, C.P., Zheng, B., Keene, D.R., He, R., Adams, H.P., Vanpelt, C.S., Geng, Y.J., Deng, J.M., Behringer, R.R., de Crombrugghe, B., 2007. Postnatal induction of transforming growth factor beta signaling in fibroblasts of mice recapitulates clinical, histologic, and biochemical features of scleroderma. Arthritis Rheum. 56, 334–344. doi:10.1002/art.22328

Stamos, J.L., Weis, W.I., 2013. The β-catenin destruction complex. Cold Spring Harb. Perspect. Biol. 5, a007898. doi:10.1101/cshperspect.a007898

Steen, V.D., Medsger, T.A., 2001. Improvement in skin thickening in systemic sclerosis associated with improved survival. Arthritis Rheum. 44, 2828–2835.

Stoecklin, G., Stubbs, T., Kedersha, N., Wax, S., Rigby, W.F.C., Blackwell, T.K., Anderson, P., 2004. MK2-induced tristetraprolin:14-3-3 complexes prevent stress granule association and ARE-mRNA decay. EMBO J. 23, 1313–1324. doi:10.1038/sj.emboj.7600163

Sun, L., Stoecklin, G., Van Way, S., Hinkovska-Galcheva, V., Guo, R.-F., Anderson, P., Shanley, T.P., 2007. Tristetraprolin (TTP)-14-3-3 complex formation protects TTP from dephosphorylation by protein phosphatase 2a and stabilizes tumor necrosis factor-alpha mRNA. J. Biol. Chem. 282, 3766–3777. doi:10.1074/jbc.M607347200

Tan, C.W., Gardiner, B.S., Hirokawa, Y., Layton, M.J., Smith, D.W., Burgess, A.W., 2012. Wnt Signalling Pathway Parameters for Mammalian Cells. PLoS ONE 7, e31882. doi:10.1371/journal.pone.0031882

Taniguchi, K., Roberts, L.R., Aderca, I.N., Dong, X., Qian, C., Murphy, L.M., Nagorney, D.M., Burgart, L.J., Roche, P.C., Smith, D.I., Ross, J.A., Liu, W., 2002. Mutational spectrum of beta-catenin, AXIN1, and AXIN2 in hepatocellular carcinomas and hepatoblastomas. Oncogene 21, 4863–4871. doi:10.1038/sj.onc.1205591

Tejpar, S., Nollet, F., Li, C., Wunder, J.S., Michils, G., dal Cin, P., Van Cutsem, E., Bapat, B., van Roy, F., Cassiman, J.J., Alman, B.A., 1999. Predominance of beta-catenin mutations and beta-catenin dysregulation in sporadic aggressive fibromatosis (desmoid tumor). Oncogene 18, 6615–6620. doi:10.1038/sj.onc.1203041

Tian, X., Zhang, J., Tan, T.K., Lyons, J.G., Zhao, H., Niu, B., Lee, S.R., Tsatralis, T., Zhao, Y., Wang, Y., Cao, Q., Wang, C., Wang, Y., Lee, V.W.S., Kahn, M., Zheng, G., Harris, D.C.H., 2013. Association of β-catenin with P-Smad3 but not LEF-1 dissociates in vitro profibrotic from anti-inflammatory effects of TGF-β1. J. Cell Sci. 126, 67–76. doi:10.1242/jcs.103036

Torres, M.A., Yang-Snyder, J.A., Purcell, S.M., DeMarais, A.A., McGrew, L.L., Moon, R.T., 1996. Activities of the Wnt-1 class of secreted signaling factors are antagonized by the Wnt-5A class and by a dominant negative cadherin in early Xenopus development. J. Cell Biol. 133, 1123 –1137. doi:10.1083/jcb.133.5.1123

Toualbi, K., Güller, M.C., Mauriz, J.-L., Labalette, C., Buendia, M.-A., Mauviel, A., Bernuau, D., 2007. Physical and functional cooperation between AP-1 and beta-catenin for the regulation of TCF-dependent genes. Oncogene 26, 3492–3502. doi:10.1038/sj.onc.1210133

Tourkina, E., Richard, M., Gööz, P., Bonner, M., Pannu, J., Harley, R., Bernatchez, P.N., Sessa, W.C., Silver, R.M., Hoffman, S., 2008. Antifibrotic properties of caveolin-1 scaffolding domain in vitro and in vivo. Am. J. Physiol. Lung Cell. Mol. Physiol. 294, L843–861. doi:10.1152/ajplung.00295.2007

Uemura, M., Swenson, E.S., Gaça, M.D.A., Giordano, F.J., Reiss, M., Wells, R.G., 2005. Smad2 and Smad3 play different roles in rat hepatic stellate cell function and alpha-smooth muscle actin organization. Mol. Biol. Cell 16, 4214–4224. doi:10.1091/mbc.E05-02-0149

Uhl, M., 2004. SD-208, a Novel Transforming Growth Factor Receptor I Kinase Inhibitor, Inhibits Growth and Invasiveness and Enhances Immunogenicity of Murine and Human Glioma Cells In vitro and In

vivo. Cancer Res. 64, 7954–7961. doi:10.1158/0008-5472.CAN-04-1013

Uren, A., Reichsman, F., Anest, V., Taylor, W.G., Muraiso, K., Bottaro, D.P., Cumberledge, S., Rubin, J.S., 2000. Secreted frizzled-related protein-1 binds directly to Wingless and is a biphasic modulator of Wnt signaling. J. Biol. Chem. 275, 4374–4382.

Valenta, T., Hausmann, G., Basler, K., 2012. The many faces and functions of β-catenin. EMBO J. 31, 2714–2736. doi:10.1038/emboj.2012.150

van den Hoogen, F., Khanna, D., Fransen, J., Johnson, S.R., Baron, M., Tyndall, A., Matucci-Cerinic, M., Naden, R.P., Medsger, T.A., Carreira, P.E., Riemekasten, G., Clements, P.J., Denton, C.P., Distler, O., Allanore, Y., Furst, D.E., Gabrielli, A., Mayes, M.D., van Laar, J.M., Seibold, J.R., Czirjak, L., Steen, V.D., Inanc, M., Kowal-Bielecka, O., Müller-Ladner, U., Valentini, G., Veale, D.J., Vonk, M.C., Walker, U.A., Chung, L., Collier, D.H., Ellen Csuka, M., Fessler, B.J., Guiducci, S., Herrick, A., Hsu, V.M., Jimenez, S., Kahaleh, B., Merkel, P.A., Sierakowski, S., Silver, R.M., Simms, R.W., Varga, J., Pope, J.E., 2013. 2013 classification criteria for systemic sclerosis: an American college of rheumatology/European league against rheumatism collaborative initiative. Ann. Rheum. Dis. 72, 1747–1755. doi:10.1136/annrheumdis-2013-204424

Varallo, V.M., Gan, B.S., Seney, S., Ross, D.C., Roth, J.H., Richards, R.S., McFarlane, R.M., Alman, B., Howard, J.C., 2003. Beta-catenin expression in Dupuytren's disease: potential role for cell-matrix interactions in modulating beta-catenin levels in vivo and in vitro. Oncogene 22, 3680–3684. doi:10.1038/sj.onc.1206415

Varga, J., Abraham, D., 2007. Systemic sclerosis: a prototypic multisystem fibrotic disorder. J. Clin. Invest. 117, 557–567. doi:10.1172/JCI31139

Varga, J., Pasche, B., 2009. Transforming growth factor-ss as a therapeutic target in systemic sclerosis. Nat. Rev. Rheumatol. 5, 200–206. doi:10.1038/nrrheum.2009.26

Verrecchia, F., Chu, M.L., Mauviel, A., 2001. Identification of novel TGF-beta /Smad gene targets in dermal fibroblasts using a combined cDNA microarray/promoter transactivation approach. J. Biol. Chem. 276, 17058–17062. doi:10.1074/jbc.M100754200

Vuga, L.J., Ben-Yehudah, A., Kovkarova-Naumovski, E., Oriss, T., Gibson, K.F., Feghali-Bostwick, C., Kaminski, N., 2009. WNT5A is a regulator of fibroblast proliferation and resistance to apoptosis. Am. J. Respir. Cell Mol. Biol. 41, 583–589. doi:10.1165/rcmb.2008-0201OC

Wang, Q., Wang, Y., Hyde, D.M., Gotwals, P.J., Koteliansky, V.E., Ryan, S.T., Giri, S.N., 1999. Reduction of bleomycin induced lung fibrosis by transforming growth factor beta soluble receptor in hamsters. Thorax 54, 805–812.

Wang, S., Krinks, M., Lin, K., Luyten, F.P., Moos, M., 1997. Frzb, a Secreted Protein Expressed in the Spemann Organizer, Binds and Inhibits Wnt-8. Cell 88, 757–766. doi:10.1016/S0092-8674(00)81922-4

Wang, X.M., Zhang, Y., Kim, H.P., Zhou, Z., Feghali-Bostwick, C.A., Liu, F., Ifedigbo, E., Xu, X., Oury, T.D., Kaminski, N., Choi, A.M.K., 2006. Caveolin-1: a critical regulator of lung fibrosis in idiopathic pulmonary fibrosis. J. Exp. Med. 203, 2895–2906. doi:10.1084/jem.20061536

Wawrzak, D., Métioui, M., Willems, E., Hendrickx, M., Genst, E. de, Leyns, L., 2007. Wnt3a binds to several sFRPs in the nanomolar range. Biochem. Biophys. Res. Commun. 357, 1119–1123. doi:10.1016/j.bbrc.2007.04.069

Weeraratna, A.T., Jiang, Y., Hostetter, G., Rosenblatt, K., Duray, P., Bittner, M., Trent, J.M., 2002. Wnt5a signaling directly affects cell motility and invasion of metastatic melanoma. Cancer Cell 1, 279–288. doi:10.1016/S1535-6108(02)00045-4

Wei, J., Bhattacharyya, S., Tourtellotte, W.G., Varga, J., 2011. Fibrosis in systemic sclerosis: Emerging concepts and implications for targeted therapy. Autoimmun. Rev. 10, 267–275. doi:10.1016/j.autrev.2010.09.015

Wei, J., Fang, F., Lam, A.P., Sargent, J.L., Hamburg, E., Hinchcliff, M.E., Gottardi, C.J., Atit, R., Whitfield, M.L., Varga, J., 2012. Wnt/β-catenin signaling is hyperactivated in systemic sclerosis and induces Smad-dependent fibrotic responses in mesenchymal cells. Arthritis Rheum. 64, 2734–2745. doi:10.1002/art.34424

Wei, J., Melichian, D., Komura, K., He, T.-C., Lafyatis, R., MacDougald, O.A., Varga, J., 2011b. Canonical Wnt signaling induces skin fibrosis and subcutaneous lipoatrophy: a novel mouse model for scleroderma? Arthritis Rheum. 63, 1707–1717. doi:10.1002/art.30312

Wells, A.U., Denton, C.P., 2014. Interstitial lung disease in connective tissue disease—mechanisms and management. Nat. Rev. Rheumatol. 10, 728–739. doi:10.1038/nrrheum.2014.149

Whitfield, M.L., Finlay, D.R., Murray, J.I., Troyanskaya, O.G., Chi, J.-T., Pergamenschikov, A., McCalmont, T.H., Brown, P.O., Botstein, D., Connolly, M.K., 2003. Systemic and cell type-specific gene expression patterns in scleroderma skin. Proc. Natl. Acad. Sci. U. S. A. 100, 12319–12324. doi:10.1073/pnas.1635114100

Willert, K., Shibamoto, S., Nusse, R., 1999. Wnt-induced dephosphorylation of axin releases beta-catenin from the axin complex. Genes Dev. 13, 1768–1773.

Williams, M.H., Das, C., Handler, C.E., Akram, M.R., Davar, J., Denton, C.P., Smith, C.J., Black, C.M., Coghlan, J.G., 2006. Systemic sclerosis associated pulmonary hypertension: improved survival in the current era. Heart 92, 926–932. doi:10.1136/hrt.2005.069484

Winstone, T.A., Assayag, D., Wilcox, P.G., Dunne, J.V., Hague, C.J., Leipsic, J., Collard, H.R., Ryerson, C.J., 2014. Predictors of mortality and progression in scleroderma-associated interstitial lung disease: a systematic review. Chest 146, 422–436. doi:10.1378/chest.13-2626

Wong, N.A.C.S., Pignatelli, M., 2002. ?-Catenin--A Linchpin in Colorectal Carcinogenesis? Am. J. Pathol. 160, 389–401.

Woodman, S.E., Ashton, A.W., Schubert, W., Lee, H., Williams, T.M., Medina, F.A., Wyckoff, J.B., Combs, T.P., Lisanti, M.P., 2003. Caveolin-1 knockout mice show an impaired angiogenic response to exogenous stimuli. Am. J. Pathol. 162, 2059–2068. doi:10.1016/S0002-9440(10)64337-4

Wu, R., Zhai, Y., Fearon, E.R., Cho, K.R., 2001. Diverse mechanisms of beta-catenin deregulation in ovarian endometrioid adenocarcinomas. Cancer Res. 61, 8247–8255.

Wynn, T., 2008. Cellular and molecular mechanisms of fibrosis. J. Pathol. 214, 199–210. doi:10.1002/path.2277

Xu, H.-T., Wang, L., Lin, D., Liu, Y., Liu, N., Yuan, X.-M., Wang, E.-H., 2006. Abnormal beta-catenin and reduced axin expression are associated with poor differentiation and progression in non-small cell lung cancer. Am. J. Clin. Pathol. 125, 534–541. doi:10.1309/0MDY-02KH-EW1F-6RT6

Yamamoto, H., Komekado, H., Kikuchi, A., 2006. Caveolin Is Necessary for Wnt-3a-Dependent Internalization of LRP6 and Accumulation of β-Catenin. Dev. Cell 11, 213–223. doi:10.1016/j.devcel.2006.07.003

Yamamoto, H., Oue, N., Sato, A., Hasegawa, Y., Yamamoto, H., Matsubara, A., Yasui, W., Kikuchi, A., 2010. Wnt5a signaling is involved in the aggressiveness of prostate cancer and expression of metalloproteinase. Oncogene 29, 2036–2046.

Yamamoto, S., Nishimura, O., Misaki, K., Nishita, M., Minami, Y., Yonemura, S., Tarui, H., Sasaki, H., 2008. Cthrc1 Selectively Activates the Planar Cell Polarity Pathway of Wnt Signaling by Stabilizing the Wnt-Receptor Complex. Dev. Cell 15, 23–36. doi:10.1016/j.devcel.2008.05.007

Yang, Y.-C., Piek, E., Zavadil, J., Liang, D., Xie, D., Heyer, J., Pavlidis, P., Kucherlapati, R., Roberts, A.B., Böttinger, E.P., 2003. Hierarchical model of gene regulation by transforming growth factor β. Proc. Natl. Acad. Sci. 100, 10269–10274. doi:10.1073/pnas.1834070100

Yin, C., Ciruna, B., Solnica-Krezel, L., 2009. Convergence and extension movements during vertebrate gastrulation. Curr. Top. Dev. Biol. 89, 163–192. doi:10.1016/S0070-2153(09)89007-8

Yu, L., Border, W.A., Huang, Y., Noble, N.A., 2003. TGF-beta isoforms in renal fibrogenesis. Kidney Int. 64, 844–856. doi:10.1046/j.1523-1755.2003.00162.x

Zeng, L., Fagotto, F., Zhang, T., Hsu, W., Vasicek, T.J., Perry, W.L., Lee, J.J., Tilghman, S.M., Gumbiner, B.M., Costantini, F., 1997. The mouse Fused locus encodes Axin, an inhibitor of the Wnt signaling pathway that regulates embryonic axis formation. Cell 90, 181–192.

Zhang, H.Y., Phan, S.H., 1999. Inhibition of myofibroblast apoptosis by transforming growth factor beta(1). Am. J. Respir. Cell Mol. Biol. 21, 658–665. doi:10.1165/ajrcmb.21.6.3720

Zhang, M., Wang, M., Tan, X., Li, T.-F., Zhang, Y.E., Chen, D., 2010. Smad3 Prevents β-Catenin Degradation and Facilitates β-Catenin Nuclear Translocation in Chondrocytes. J. Biol. Chem. 285, 8703–8710. doi:10.1074/jbc.M109.093526

Zhang, P., Cai, Y., Soofi, A., Dressler, G.R., 2012. Activation of Wnt11 by TGF-β drives mesenchymal gene expression through non-canonical Wnt signaling in renal Epithelial cells. J. Biol. Chem. doi:10.1074/jbc.M112.357202